

**MEASUREMENT AND ANALYSIS OF THE THERMAL  
PROPERTIES OF THE GROUND FOR GROUND HEAT  
EXCHANGER APPLICATIONS IN CYPRUS**

A thesis submitted for the degree of Doctor of Philosophy

by

Iosifina I. Stylianou

Department of Mechanical and Aerospace Engineering  
Brunel University London

October 2019

## Abstract

Geothermal energy is a renewable resource and is attracting increasing attention for heating but also for cooling of domestic and commercial buildings in warm climates. Successful utilization of geothermal energy requires knowledge of the geothermal properties of the ground. In Cyprus only very limited research has been carried out to-date on the use of ground source heat pumps, and information is needed to enable engineers to size correctly Ground Heat Exchangers (GHE) for Ground Source Heat Pump applications. To address this, the main objective of the research presented in this thesis was to investigate the thermal properties of the ground at a number of locations in Cyprus and use the results to develop data and easy to use tools to enable engineers and researchers to evaluate the potential and design Ground Heat Exchangers (GHEs) for specific locations and thermal loads.

The research involved an extended geological sampling on the island and measurements of the thermal properties of 148 ground samples in the laboratory in their dry and water saturated states. Thermal conductivity values for dry samples were found to be in the range between 0.4 and 4.2 W m<sup>-1</sup> K<sup>-1</sup>, thermal diffusivity values between 0.3 and 1.9×10<sup>-6</sup> m<sup>2</sup> s<sup>-1</sup> and specific heat capacity between 0.5 and 1.5 J K<sup>-1</sup> kg<sup>-1</sup>. Results also showed thermal conductivity and thermal diffusivity to increase with water content for most of the ground samples investigated.

To understand and visualize all measured data, Geographic Information System (GIS) software was used to generate maps of ground density, thermal conductivity, and thermal diffusivity. From the maps, the Troodos Ophiolite terrane which dominates the central part of Cyprus, was found to offer the best thermal properties for the utilization of geothermal energy on the Island.

Geothermal modeling was carried out to investigate the effect of (a) summer and winter mode of operation, (b) ground temperature variation with depth to consider the effects of daily and seasonal ambient temperature variations on ground temperature, (c) borehole radius, (d) borehole grout properties, (e) U-tube diameter, (f) U-tube leg and distance from the centre of the borehole, and (g) ground water level and flow velocity, on the performance of GHEs.

For the prediction of the heat injection rate of a GHE, a tool was developed with the use of FlexPDE software (PDE Solutions Inc). The tool considers GHE characteristics, the installation area and ground properties and groundwater flow. Twenty-two boreholes located in Nicosia were simulated to determine their geothermal performance. GIS software was employed to develop, for the first time, maps that provide information on the geothermal properties of the ground in Cyprus per meter depth to enable easy evaluation of the suitability of the ground for the installation of GHEs. All geothermal maps compiled in the framework of this research, are now available online, in a web application at <https://amc-cy.maps.arcgis.com/apps/ImageryViewer/index.html?appid=d81a63acc03c4c35a80c65e8c1689c77> to facilitate easy accessibility by engineers working in the GHE design and installation field, for the use of engineers and designers of GHEs and ground source heat pump systems.

## **Statement of Copyright**

The copyright of this thesis is reserved with the author, Mrs. Iosifina I. Stylianou. No part of the thesis can be reproduced without her prior written consent and any information used from the thesis should be duly acknowledged.

## **Declaration**

The work described in this thesis has not been previously submitted for a degree in this or any other university and unless otherwise referenced it is the author's own work.

## Publications for this PhD research

- **Stylianou, I.I.**, Tassou, S., Florides, G., Christodoulides, P. and Aresti, L. (2019). Modeling of Vertical Ground Heat Exchangers in the Presence of Groundwater Flow and Underground Temperature Gradient. *Energy & Buildings*, 192 (2019) 15–30, <https://doi.org/10.1016/j.enbuild.2019.03.020>.
- **Stylianou, I.I.**, Christodoulides, P., Aresti, L. Tassou, S. and Florides, G. (2018). Borehole Ground Heat Exchangers and The Flow of Underground Water. *International Journal of Industrial Electronics and Electrical Engineering*, ISSN(p): 2347-6982, ISSN(e): 2349-204X, Volume-6, Issue-9, Sep.-2018, <http://ijiee.org.in>.
- **Stylianou, I.I.**, Florides, G., Tassou, S., Tsiolakis, E. and Christodoulides, P. (2017). Methodology for Estimating the Ground Heat Absorption Rate of Ground Heat Exchangers. *Energy*, 127 (2017) 258-270.
- **Stylianou I.I.**, Tassou S., Christodoulides P., Panayides I., Florides G. (2016). Measurement and analysis of thermal properties of rocks for the compilation of geothermal maps of Cyprus. *Renewable Energy*, 88 (2016) 418-429.
- **Stylianou, I.I.**, Christodoulides, P., Aresti, L., Tassou, S. and Florides, G. (2018) “Borehole Ground Heat Exchangers and the Flow of Groundwater”. *Conference International Society for Engineers and Researchers*, Sydney, Australia 24–25 October, 2018.
- **Stylianou, I.I.**, Florides, G., Tassou, S., Tsiolakis, E. and Christodoulides, P. (2018) “GeoThermal Maps” [StoryMap Presentation]. Marathon Data Systems, *26th Pan-Hellenic ArcGIS Users Meeting*, Athens, Greece, 10-11 May 2018. Available at: <https://arcg.is/1LumOT> [8 May 2018]
- **Stylianou, I.I.**, Florides, G., Tassou, S., Tsiolakis, E. and Christodoulides, P. (2017) “Methodology for Estimating the Ground Heat Absorption Rate” [PowerPoint presentation]. *4th International Conference on Energy, Sustainability and Climate Change Energy, Sustainability & Climate Change*, Santorini, Greece, 12-14 June, 2017.
- **Stylianou, I.I.**, Florides, G., Tassou, S., Tsiolakis, E. and Christodoulides, P. (2017) “Geothermal Maps of the Greater Lefkosia Area, Cyprus” [Poster Presentation]. Marathon Data Systems, *25th Pan-Hellenic ArcGIS Users Meeting*, Athens, Greece, 11-12 May 2017.

## Other publications related to the research

- Florides, A.G., Theofanous, E., **Stylianou, I.I.**, Christodoulides, P., Kalogirou, S., Messarites, V., Zomeni, Z., Tsiolakis, E., Pouloupatis, D.P., Panayiotou, P.G. (2014). Thermal properties of the ground in Cyprus and their correlations and effect on the efficiency of Ground Heat Exchangers. *World Academy of Science, Engineering and Technology*, 86 (2014).
- Florides, G., Pouloupatis, P.D., Kalogirou, S., Messaritis, V., Panayides, I., Zomeni, Z., Koutsoumpas, K. (2013). Geothermal properties of the ground in Cyprus and their effect on the efficiency of ground coupled heat pumps. *Renewable Energy*, 49, 85-89.
- Kalogirou, S.A., Florides, G.A., Pouloupatis, P.D., Panayides, I., **Joseph-Stylianou, J.** and Zomeni, Z. (2012). Artificial neural networks for the generation of geothermal maps of ground temperature at various depths by considering land configuration. *Energy*, 48(1), 233-240.
- Florides, G.A., Pouloupatis, P. D., Kalogirou, S., Messaritis, V., Panayides, I., Zomeni, Z., and Koutsoumpas, K. (2011). The geothermal characteristics of the ground and the potential of using ground coupled heat pumps in Cyprus. *Energy*, 36(8), 5027-5036.
- Pouloupatis, P.D., Florides, G., and Tassou, S. (2011). Measurements of ground temperatures in Cyprus for ground thermal applications. *Renewable Energy*, 36(2), 804-814.
- Florides, G.A., Christodoulides, P., and Pouloupatis, P. (2012). An analysis of heat flow through a borehole heat exchanger validated model. *Applied Energy*, 92, 523-533.
- Florides, A.G., Theofanous, E., **Stylianou, I.I.**, Tassou, S., Christodoulides, P., Zomeni, Z., Kalogirou, S., Messarites, V., Pouloupatis, P. and Panayiotou, G. (2013). Vertical and Horizontal Ground Heat Exchanger Modelling. Murdoch University, *World Renewable Energy Congress*, Perth Australia, 14-18 July 2013.

## **Acknowledgements**

I wish to express my sincere thanks to my supervisors, Prof. Savvas Tassou and Prof. Georgios Florides, since without their support and guidance, the implementation of this project would not be possible.

I would also like to acknowledge the financial support from the Research Promotion Foundation of Cyprus (RPF), as a part of this work was carried out in the framework of a research project co-funded by the RPF under Contract: ΤΕΧΝΟΛΟΓΙΑ/ΕΝΕΡΓ/0311(BIE)/01 and all collaborators for their dedication to the project and all their support and assistance. Also, the late geologist Ioannis Panayides, who inspired me by his dedication and support.

Finally, my husband and family, which without their support and understanding, my dream to pursue doctoral level research could not come true.

## List of Contents

Abstract.....	1
Chapter 1: Introduction.....	15
1.1    Main Aim and Objectives.....	17
1.2    Structure of Thesis .....	19
Chapter 2: Background.....	21
2.1    Introduction .....	21
2.2    Ground Heat Exchangers and Heat Pumps.....	22
2.3    Geology of Cyprus .....	28
2.4    Geothermal Background of Cyprus.....	33
2.5    Summary .....	39
Chapter 3: Modeling Vertical Ground Heat Exchangers .....	38
3.1    Introduction .....	40
3.2    Computational Model.....	42
3.3    Programming with FlexPDE.....	47
3.3.1    Properties and Geometry of the Proposed Model.....	49
3.3.2    Simulation Results.....	54
3.4    Summary .....	58
Chapter 4: Model Validation.....	59
4.1    Introduction .....	59
4.2    Model Validation and Results.....	60
4.2.1    Study Case at the Prodromi Area .....	60
4.2.2    Study Case at the Lakatameia Area.....	70
4.3    Summary.....	90
Chapter 5: Measurement and Analysis of the Thermal Properties of Rocks for the Compilation of Geothermal Maps .....	91
5.1    Introduction .....	91
5.2    Geological Sampling and Sample Preparation.....	92
5.3    Laboratory Tests .....	94
5.4    Laboratory Results .....	98
5.4.1    Thermal conductivity and thermal diffusivity of geological formations .....	98
5.4.2    Thermal conductivity and thermal diffusivity of lithotypes.....	102



5.4.3	Comparison with thermal conductivity values of lithologies for other countries .....	108
5.4.4	Relation of the thermal conductivity and the geological age of rock samples .....	109
5.5	Geothermal Maps .....	110
5.5.1	Map Compilation .....	111
5.5.2	Map Results .....	111
5.6	Summary .....	118
Chapter 6:	Estimation of ground heat absorption rate of a GHE at a particular location .....	120
6.1	Introduction .....	120
6.2	3D Geological Modeling of the Study Area .....	120
6.3	Thermal Properties of Nicosia Lithologies .....	122
6.3.1	Geological sampling.....	122
6.3.2	Thermal properties of the ground.....	122
6.3.3	Test Results.....	123
6.3.4	Thermal Conductivity and Specific Heat Capacity Maps of the Greater Nicosia Area ..	128
6.4	Application of Ground Heat Exchangers in the Greater Nicosia Area.....	128
6.4.1	Mathematical model.....	128
6.4.2	Results .....	132
6.4.3	GHE Suitability Map for the Greater Nicosia Area .....	134
6.5	Summary .....	134
Chapter 7:	Conclusions and recommendations for future work.....	135
7.1	Introduction .....	135
7.2	Main Conclusions .....	135
7.3	Recommendations for Future Work.....	138
Reference	.....	139
APPENDIX I	.....	149
APPENDIX II	.....	160
APPENDIX III	.....	192

## List of Figures

Figure 2- 1: Schematic diagram of heat flow from earth's core.....	21
Figure 2- 2: GHE principle of operation.....	22
Figure 2- 3: Horizontal-type Ground Heat Exchanger configurations .....	23
Figure 2- 4: Common ground heat exchanger pipe designs.....	24
Figure 2- 5: (a) Single well standing column configuration, (b) two wells standing column configuration (c) Borehole heat exchanger configuration .....	25
Figure 2- 6: (a) Heat pump principle .....	26
Figure 2- 7: Geothermal heat cycle .....	27
Figure 2- 8: (a) Schematic presentation of the formation and evolution of the lithology of Cyprus, (b) schematic presentation of the stratigraphy Troodos–Mesaoria–Cape Greco area.....	29
Figure 2- 9: The island of Cyprus is divided into four geological Terranes. ....	30
Figure 2-10: Geological Map of Cyprus 1:250,000.....	30
Figure 2-11: Maps of Ground Temperature and Thermal Conductivity of Cyprus.....	36
Figure 2-12: Boreholes location of Crustal Study .....	37
Figure 3- 1: Positions of the 8 geothermal boreholes in Cyprus .....	41
Figure 3- 2: Geothermal borehole filled with bentonite .....	43
Figure 3- 3: Cylindrical model representing a part of a tube of a geothermal heat exchanger .....	45
Figure 3- 4: Meshes created with FlexPDE Software .....	48
Figure 3- 5: A cross section of the Borehole.....	50
Figure 3- 6: Explanatory diagram of the study area, as used in the FlexPDE.....	52
Figure 3- 7: Final 3D Mesh created by FlexPDE software.....	53
Figure 3- 8: 3D Domain created by FlexPDE software.....	53
Figure 3- 9: Input fluid temperature (Tfluidin), output fluid temperature and temperature at the centre of the domain vs Time .....	54
Figure 3- 10: Temperature distribution around the borehole at the surface, after 50 h of operation....	55
Figure 3- 11: Temperature distribution around the borehole at the level of the aquifer, after 50 h of operation .....	56
Figure 3- 12: Temperature distribution around the borehole at the end of the tubes, after 50 h of operation .....	56
Figure 3- 13: Temperature distribution along the center of the right tube, after 50 h of operation.....	57

Figure 3- 14: Temperature distribution along the center of the left tube, after 50 h of operation.....	57
Figure 3- 15: Temperature distribution around the borehole along the center of the domain, after 50 h of operation .....	58
Figure 4 - 1: Positions of 8 geothermal boreholes in Cyprus.....	60
Figure 4 - 2: Output graph showing inlet (Tfluidin) and outlet (Tfluidout) fluid temperature .....	62
Figure 4 - 3: Comparison of numerical model results with measured TRT data .....	63
Figure 4 - 4: Output Temperatures for different values of the distance between the centre of each tube and the centre of the borehole .....	64
Figure 4 - 5: Effect of centre to centre tube distance on the output fluid temperature, after 50 h of operation.....	66
Figure 4 - 6: Input fluid temperature for different values of fluid velocity and constant heat injected into the borehole.....	68
Figure 4 - 7: Output fluid temperatures of for different values of fluid velocity and constant heat injected into the borehole.....	68
Figure 4 - 8: Graph showing the effect of GHE fluid velocity on the mean temperature of GHE .....	69
Figure 4 - 9: Effect of fluid velocity in the GHE on the inlet and outlet fluid temperature after 50 h of operation. ....	70
Figure 4 - 10: Temperatures recorded in BHs located in different geographical locations in Cyprus	71
Figure 4 - 11: December, February and July recorded underground temperature at the Lakatameia BH Shallow Zone (0–7m).....	72
Figure 4 - 12: December, February and July recorded underground temperature at the Lakatameia BH Deep Zone (7–160m) .....	72
Figure 4 - 13: The FlexPDE model for the energy analysis of the Lakatameia BH.....	74
Figure 4 - 14: Initial ground temperature on the vertical borehole axis .....	75
Figure 4 - 15: Recorded temperatures (December) at the Lakatameia BH in comparison with the FlexPDE script calculated values .....	76
Figure 4 - 16: Thermal energy per m of GHE rejected to the ground in relation to the three layers of the borehole .....	76
Figure 4 - 17: Temperature distribution at the initial stages of the simulation (top) and at the end of the 50 h (bottom).....	78
Figure 4 - 18: GHE exiting fluid temperature plotted against time steady temperature fluid entering the GHE of 45, 35 and 28 °C .....	80

Figure 4 - 19: fluid temperature exiting GHE plotted against time for three cases of steady temperature fluid entering the GHE, of 0, 9 and 18°C. ....	80
Figure 4 - 20: Input and output circulating fluid temperatures for different radius of a BH, after 25 and 50 h of continuous operation of the GHE.....	81
Figure 4 - 21: Plot of the absorbed thermal energy per m against the BH radius in the three types of layers of the BH .....	82
Figure 4 - 22: Temperature evolution of the GHE for various values of the grout thermal conductivity .....	82
Figure 4 - 23: Effect of the grout thermal conductivity on the fluid temperature of the U-tube, after 25 and 50 h continuous operation.....	83
Figure 4 - 24: Effect of the U-tube diameter on the fluid temperature of the U-tube, after 25 and 50 h continuous operation.....	85
Figure 4 - 25: Comparison of input and output circulating fluid temperatures for different distances between the leg center and the BH center of the GHE, after 25 and 50 h continuous operation .....	86
Figure 4 - 26: Circulating fluid temperatures in the GHE for different underground water velocities, after 25 and 50 h continuous operation.....	86
Figure 4 - 27: Heat per m of GHE rejected to the ground in relation to the GHE exiting fluid temperature (which also corresponds to the pump input fluid temperature).....	88
Figure 4 - 28: Characteristics of a typical heat pump, showing the heat pump entering fluid temperature against the ratio of pump capacity over power input.....	88
Figure 5 - 1: Sampling points .....	93
Figure 5 - 2: Cutting samples with the use of a circular saw.....	94
Figure 5 - 3: Samples ready for testing.....	94
Figure 5 - 4: Isomet 2104 portable Heat Transfer Analyzer.....	95
Figure 5 - 5: Sample covered with paraffin.....	97
Figure 5 - 6: Sample covered with nylon foil.....	97
Figure 5 - 7: Mean values of thermal conductivity ( $\lambda$ ), thermal diffusivity ( $\alpha$ ), specific heat capacity ( $c_p$ ) and density ( $\rho$ ) for dry samples grouped by geological formation.....	100
Figure 5 - 8: Mean values of thermal conductivity ( $\lambda$ ), thermal diffusivity ( $\alpha$ ), specific heat capacity ( $c_p$ ) and density ( $\rho$ ) for water saturated samples grouped by geological formation.....	101
Figure 5 - 9: Mean values of thermal diffusivity $\alpha$ per lithology: dry samples and water saturated samples .....	106

Figure 5 - 10: Mean values of thermal conductivity $\lambda$ per lithology: dry samples and water saturated samples .....	106
Figure 5 - 11: Thermal conductivity values measured on samples with different geological age .....	109
Figure 5 - 12: Thermal Conductivity Map of Cyprus (Dry).....	113
Figure 5 - 13: Thermal Conductivity Map of Cyprus (Water Saturated).....	114
Figure 5 - 14: Thermal Diffusivity Map of Cyprus (Dry).....	115
Figure 5 - 15: Thermal Diffusivity Map of Cyprus (Water Saturated).....	116
Figure 5 - 16: Density Maps of Cyprus (Bulk Density).....	117
Figure 6 - 1: Map of the four major tectonic-stratigraphic terranes of Cyprus .....	121
Figure 6 - 2: 3D Geological Model .....	123
Figure 6 - 3: Range of values measured in the laboratory for thermal conductivity $\lambda$ grouped by the geological formation/member of sample .....	124
Figure 6 - 4: Range of values for specific heat capacity $c_p$ grouped by the geological formation/member of sample .....	125
Figure 6 - 5: Thermal Conductivity Map of the Greater Nicosia Area .....	126
Figure 6 - 6: Specific Heat Capacity Map of the Greater Nicosia Area.....	127
Figure 6 - 7: Location map of boreholes used as study cases and cross section.....	129
Figure 6 - 8: Geological borehole logs of the twenty-two study cases as used in FlexPDE software	131
Figure 6 - 9: GHE heat loss (kW) for each study case as calculated by FlexPDE software.....	132
Figure 6 - 10: GHE Suitability Map for the Greater Nicosia Area.....	133

## List of Tables

Table 2 - 1: Geological Formations studied and their lithological composition as presented in the Geological Map of Cyprus.....	32
Table 3 - 1: Borehole properties.....	50
Table 4 - 1: Thermal properties of the Prodromi borehole .....	61
Table 4 - 2: Temperature values calculated with the use of the Flex software and temperature values measured with the TRT carried out at the Prodromi BH .....	63
Table 4 - 3: Outlet Temperature values calculated for different values of D_cpc .....	65
Table 4 - 4: Temperature of fluid exiting GHE after 50h of operation.....	66
Table 4 - 5: Values of inlet and outlet temperature after 50 h of operation for different fluid velocities .....	69
Table 4 - 6: Soil/rock thermal properties used in the simulation .....	73
Table 4 - 7: GHE properties .....	74
Table 4 - 8: Input data for different U-tube sizes .....	84
Table 4 - 9: Heat Pump manufacturer specification.....	89
Table 5 - 1: Laboratory measured values of thermal conductivity ( $\lambda$ ), thermal diffusivity ( $\alpha$ ), specific heat capacity ( $c_p$ ) and density ( $\rho$ ) grouped by geological formation as presented in the Geological Map of Cyprus .....	104
Table 5 - 2: Laboratory measured values of thermal conductivity ( $\lambda$ ), thermal diffusivity ( $\alpha$ ), specific heat capacity ( $c_p$ ) and density ( $\rho$ ) grouped by geological formation. ....	105
Table 5 - 3: Laboratory measured values of thermal conductivity ( $\lambda$ ), thermal diffusivity ( $\alpha$ ) and specific heat capacity ( $c_p$ ) per lithology.....	107
Table 5 - 4: Thermal conductivity mean values measured on dry samples in various countries .....	108
Table 6 - 1: Mean values of measured thermal conductivity $\lambda$ , thermal diffusivity $\alpha$ , density $\rho$ and calculated specific heat capacity $c_p$ per geological unit.....	125
Table 6 - 2: GHE parameters used in the simulation.....	130
Table 6 - 3: GHE heat loss per meter after 12, 18 and 24 working hours.....	132

**List of accompanying materials included in the DVD accompanying this thesis.**

APPENDIX I

Script used in FLEX software

APPENDIX II

1. Sample list and sampling locations
2. Analytical laboratory results of dry samples
3. Analytical laboratory results of water saturated samples
4. Analytical laboratory results of density of dry and water saturated samples

APPENDIX III

Sample Catalog Gallery

APPENDIX IV

Series of Geothermal Maps of Cyprus

1. DensityMapOfCyprus Dry\_46.5x30cm
2. DesignLoad MapOfGHEForTheGreaterNicosiaAreaCyprus\_A3
3. DiffusivityMapOfCyprus Dry\_46.5x30cm
4. DiffusivityMapOfCyprus Wet\_46.5x30cm
5. SpecificHeatCapacityMapForTheGreaterNicosiaArea\_A3
6. ThermalConductivityMapForTheGreaterNicosiaArea\_A3
7. ThermalConductivityOfCyprus Dry\_46.5x30cm
8. ThermalConductivityOfCyprus Wet\_46.5x30cm

## Chapter 1: Introduction

The word "Geothermal" comes from the Greek words "Geo" that means "earth" and "therme" that means "heat", i.e. geothermal refers to heat flowing inside the earth. This heat is continuously flowing outwards, traveling to the surrounding rock, the mantle. Humanity has been taking advantage of this free energy in many ways for more than two thousand years (Cataldi et al., 1999).

Renewable energy is a growing field and geothermal energy although still not very extensively employed, is gaining increasing attention as it can offer a wide range of applications in the field of both electricity, and heating and cooling, and it has a great potential for further development. It is a local energy solution for local communities, industry, and domestic consumers bearing in mind that heating and cooling represents around 50% of the EU's final energy consumption. Buildings consume more than two thirds of the thermal energy in Europe, and geothermal energy offers the potential for wide application of renewable energy that can contribute to the decarbonization of the EU economy (ReGeoCities Project, 2015). For shallow geothermal energy (up to 200 m), the overall installation growth is steady. It is estimated that at the end of 2013 the installed capacity was 17,700 MWth distributed over more than 1.3 million GSHP installations. The countries with the highest amount of geothermal heat pumps are Sweden, Germany, France and Switzerland. These four countries alone account for 64% of all installed capacity for shallow geothermal energy in Europe. In the period 2010-2015, Italy, Poland and the Czech Republic have been the countries with the highest growth rate (ReGeoCities Project, 2015) unlike Cyprus, which has fallen far behind in the use of GHE. For this reason, the dissemination of knowledge about GHEs in Cyprus has become essential, in order to empower engineers to introduce geothermal energy in the country.

Geothermal resources can be classified as low, medium and high enthalpy resources according to their ability to perform thermodynamic work (Lee, 2001). Shallow geothermal energy constitutes a renewable energy source with high energy savings potential for heating and cooling in residential and commercial buildings. Over the past few decades, different techniques have been established to extract geothermal heat from shallow to deep subsurface



levels. The closed-loop borehole, also called vertical Ground Heat Exchanger (GHE), is a standard approach for lower and mid-depth applications and achieves up to 70% energy savings compared to traditional heating/cooling systems (ReGeoCities Project, 2015).

Using the term traditional air-conditioning systems, we refer to systems utilizing fossil fuels. Both systems, GHE and traditional air-conditioning, are based on the principle of the refrigeration cycle. In the case of the GHE heat rejection takes place in the ground whereas in air conditioning systems in the majority of cases heat is rejected to the ambient air.

The underground environment provides lower temperature for cooling and higher temperature for heating and experiences less temperature fluctuation than ambient air. From studies undertaken in areas with no tectonic activity, the mean annual ground temperature of the surface zone equals to the mean annual air temperature of the area  $\pm 1^{\circ}\text{C}$ . In a study undertaken in the UK in urban and nearby rural locations, the underground temperature was found to be higher than the mean annual air temperature by between 0.5 and 2.0 $^{\circ}\text{C}$  with the average being 0.9 $^{\circ}\text{C}$  (Busby, 2015). The higher ground temperatures lead to higher efficiencies for the GHE system and lower operating costs due to the reduced temperature across the condenser and evaporator of the heat pump compared to air source systems (Casasso et al., 2018). The only additional energy that a GHE system requires over an air source system is a small amount of electricity that is employed for the circulation of the secondary fluid in the ground heat exchanger.

The performance of GHEs is a function of the equipment involved i.e. the tubes and the grouting material of the GHE (Christodoulides et al., 2012), the velocity of the circulating liquid (Bidarmaghz et al., 2013), the thermal conductivity of the subsurface (Stylianou et al., 2016; Christodoulides et al., 2016; Florides et al., 2013; Svec et al., 1983), the depth of the borehole (Holmberg et al., 2015), and the presence of underground water (Fujii et al., 2013; Fan et al., 2007). Therefore, it is of great importance to develop methodologies for the technical and economic optimisation of GHE systems.

The thermal properties of the ground is the key parameter that influences the performance of all geothermal projects. It is well known that thermal conductivity and other thermophysical

properties of the ground are affected by various factors like the temperature (Abdulagatova, 2009; Miao, 2014), pressure (Gorgulu et al., 2008; Abdulagatova, 2009), mineralogical composition (Vasseur, 1995; Woodside and Messmer, 1961; Vasseur, 1995; Gegenhuber, 2012) and water content (Canakci, 2007; Jorand, 2011). The variation of the ground properties is also a function of the geological age of the lithology (Liu et al., 2011).

Studies undertaken in Cyprus in the last four decades, provided some data on the ground temperature of the island which showed that the temperature varies with depth (Kalogirou et al., 2012; Pouloupatis, 2014; Morgan, 1975). In deeper depths, below 7 or 8 m depending on the geographic location, the temperature remains almost constant throughout the year and is higher than that of the ambient air during the winter and lower during the summer.

Only limited work on the thermal properties of the ground in Cyprus existed prior to this thesis. The current work adds substantially to previous work through the analysis of 148 samples collected from different locations and ground depths. Both dry and wet analysis was carried out to establish the impact of water on the properties of the ground.

This research, focuses on a new methodology for modeling the thermal response of vertical GHEs, when imposing underground water flow and a temperature gradient on the numerical model to represent the temperature of the depth profile, Data from boreholes located in Nicosia (capital city of Cyprus) were used with the geothermal model to establish the thermal performance of the ground over time, and a heat load per meter depth map was established for the first time to aid GHE design.

In order to understand and visualize all measured data, detailed Geothermal Maps have been compiled for the first time for Cyprus to be available to engineers and researchers as a powerful tool for use in the design of GHE systems.

## **1.1 Main Aim and Objectives**

The main objective of this research was to develop methodologies, tools and guides that can be used by engineers and designers for the appropriate sizing of vertical GHEs for different

thermal loads and to use the knowledge gained to provide understanding of the geothermal properties of the ground in Cyprus. This was achieved through the investigation of the influence of:

- i. the thermal properties of the ground i.e. thermal conductivity, thermal diffusivity, specific heat capacity, temperature, and the variation of these properties in the presence of underground water,
- ii. the geometry of the GHE i.e. U-tube pipe diameter, distance between the centre of each tube and the centre of the borehole, borehole diameter, circulating fluid velocity and underground water flow velocity,
- iii. summer and winter mode of operation,

on the performance of GHEs for different locations in Cyprus. Modelling was performed using the FlexPDE software (FlexPDE, 1995).

The methodology was based on measuring and analyzing the thermal properties of the ground in Cyprus, the development of tools that can be used for the optimisation of the thermal response of a vertical GHE system and the use of these tools for the prediction of heat injection rates of the GHE, depending on its characteristics, the installation area ground properties and groundwater flow.

To achieve the main aim of the study, the following specific objectives were set:

- Carry out geological sampling and measure in the laboratory the thermal properties of lithotypes present in the area.
- Investigate the impact of (a) water in samples, (b) the mineralogical composition and (c) the geological age of rocks on the thermal properties of the geological samples.
- Develop and validate simulation tools with actual data of Thermal Response Tests (TRT) carried out in Cyprus and use the tools to investigate the effect of (a) borehole radius, (b) borehole grout properties, (c) U-tube diameter, (d) U-tube leg and borehole centre distance, and (e) groundwater flow velocity, on GHE performance.

- With the use of Geographical Information Systems (GIS) software, compile and analyze GeoThermal Maps to enable easy evaluation of the suitability of the ground for GHE applications.

## **1.2 Structure of Thesis**

Following the Chapter 1: Introduction which gives a small introduction to the main aim and objectives of this research, in Chapter 2: Background, a general review of the geothermal energy and its exploitation is presented. The operational principle of Ground Heat Exchangers is explained and the Chapter closes with an analysis of the geological conditions of the island, and the presentation of other relevant studies undertaken in Cyprus.

Chapter 3 focuses on geothermal modeling with emphasis given to heat transfer parameters and equations, and introduction to the FlexPDE software (PDE Solutions Inc) which was used for geothermal design and energy analysis. Based on the methodology described in Chapter 3, Chapter 4, includes the results of investigations of the effect of (a) summer and winter mode of operation, (b) underground temperature variation, (c) borehole radius, (d) borehole grout properties, (e) U-tube diameter, (f) U-tube leg and borehole center distance, and (g) groundwater flow velocity.

Chapter 5 describes the geological sampling, and presents the results of the analysis of the thermal properties of each sample carried out in the laboratory. The results were subsequently used to develop geothermal maps of Cyprus with the use of GIS software.

Chapter 6 focuses on the methodology for the prediction of heat injection rates of a GHE, depending on its characteristics, the properties of the ground in the installation area, and groundwater flow. A tool was created with the use of FlexPDE software (PDE Solutions Inc), and a study case was chosen in order to validate the results. Twenty-two boreholes located in Nicosia were tested through simulation for their geothermal performance over time. Subsequently the estimated heat load for the boreholes was used as an input to the GIS software

and a map of thermal load that can be transferred to or from the ground per meter depth map was compiled for the area.

Chapter 7: Conclusions and recommendations for future work presents the overall conclusions of the work and suggestions for further research on the subject.

## Chapter 2: Background

### 2.1 Introduction

At earth's inner core, approximately 6,400 km deep, temperatures reach  $6100 \pm 100$  °C (Alfe, 2009). Heat is continuously flowing outwards, traveling to the surrounding rock, the mantle. When temperatures and pressures become high enough, some mantle rock melts, creating magma which is lighter than the surrounding rocks and it starts moving towards the earth's crust. If the magma finds a way to the surface, then we have lava flows, otherwise magma stays under the earth's crust heating the surroundings (Figure 2-1). It is estimated that thermal energy in the earth's core can provide humanity with heat for the next million years at predictable rates (Pollack et al., 1993).

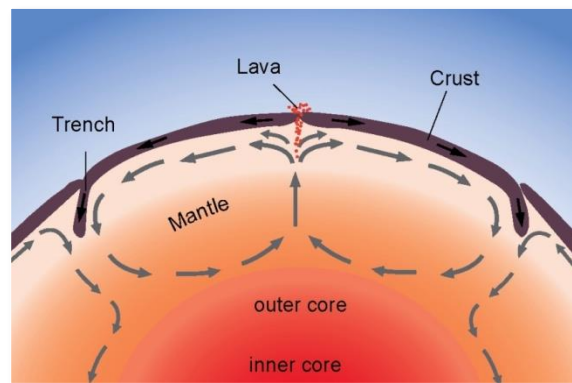


Figure 2-1: Schematic diagram of heat flow from earth's core (modified from Kious and Tilling, 1996)

In GHE systems heat transfer takes place primarily by conduction and convection and the thermal properties of the ground play a very important role in determining how effectively heat can be extracted or stored in the ground for heating and cooling purposes.

This chapter provides a review of GHE systems and of previous work carried out to facilitate the utilization of geothermal energy in Cyprus for heating and cooling.

## 2.2 Ground Heat Exchangers and Heat Pumps

To take advantage of all the ground properties and to exploit effectively the heat capacity of the ground, Ground Heat Exchangers (GHE) or Earth Heat Exchangers (EHE) are used. These systems use the ground as a heat source when operating in the heating mode and as a heat sink when operating in the cooling mode. Knowing that ground temperature below a certain depth remains relatively constant throughout the year (Popiel, 2001; Hepbasli et al., 2003; Florides et al., 2011), using a circulating medium in the summer, heat can be extracted from the hot environment of a building and rejected to the ground. In winter, reversing the process, the cold environment of a building will draw heat, though the circulating air or liquid, from the relative warm ground (Figure 2-2). GHEs can be used for water heating, air conditioning of buildings or for improving the efficiency of a heat pump.

GHEs can be categorized as ground coupled (closed loop) systems or as groundwater (open loop) systems (Mands and Sanner, 2005), and as miscellaneous systems (Kalogirou and Florides, 2007). The type chosen for a certain application depends on the geometrical characteristics of the system, the ground thermal characteristics, the thermal characteristics of the pipe used and the undisturbed ground temperature during the operation of the system (Kalogirou and Florides, 2007).

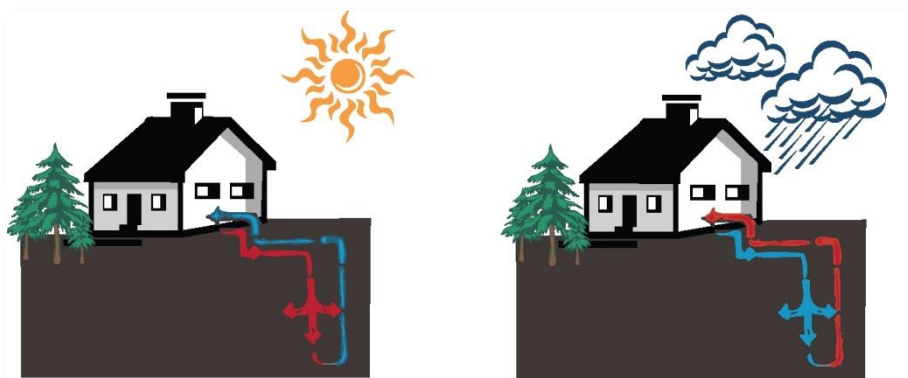


Figure 2-2: GHE principle of operation

GHEs are usually constructed with vertical or horizontal pipes buried in the ground through which a heat transfer medium such as water, antifreeze solution or air circulates to exchange heat between the ground and the building. In an open system heat is transferred with air. This is achieved by passing air through pipes buried in the ground for pre-heating or pre-cooling the building directly.

Close loop systems operate on the same principle as open loop systems with the heat transferred from/to the water or antifreeze solution of the GHE.

The pipes, where the heat exchange takes place, are buried horizontally (Figure 2- 3), obliquely or vertically in the ground. Most commonly, plastic pipes are used due to their low cost and long lifetime. In a horizontal configuration, pipes must be placed at a depth of 1-2 m and they can provide 1 KW of heating or cooling capacity every 35-60 m length (Geothermal Heat Pump Consortium, 2015). They have a number of tubes connected, either in series or in parallel. It is usually the most cost-effective when adequate yard area is available and trenches are easy to dig, especially when the building is under construction. The tube is sometimes curled into a slinky shape (Figure 2- 3 (d)). In this way more piping can be placed into shorter trenches in order to reduce the amount of land space needed. These collectors are also affected by the seasonal weather conditions because they are placed in small depths.

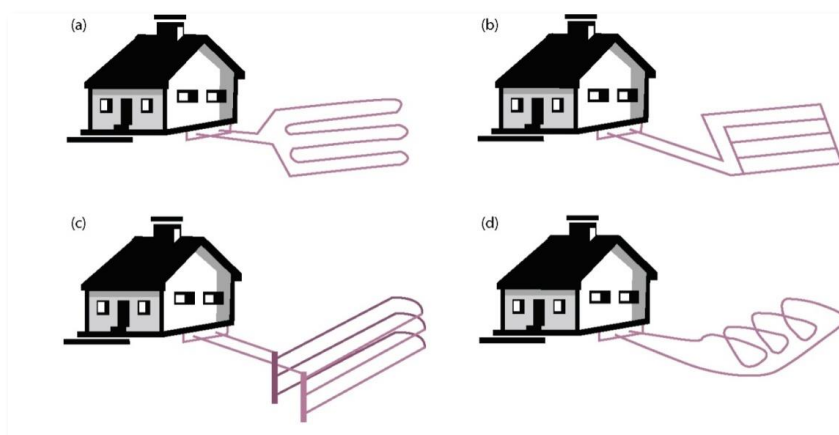


Figure 2- 3: Horizontal-type Ground Heat Exchanger configurations, (a) connection in series (b) parallel connection (c) trench connection and (d) “Slinky”-type



Vertical GHE or borehole heat exchangers are more widely used as they can be installed in almost every ground type, and only a small installation surface area is needed. A typical borehole used for geothermal purposes can be from 20 to 300 m deep with a diameter of 10-15 cm (Pahud and Matthey, 2001). The space between the GHE pipes and the borehole must be filled with a material that ensures good thermal contact between the pipe and the undisturbed ground to reduce as much as possible the thermal resistance (Geothermal Heat Pump Consortium, [www.geoexchangers.org](http://www.geoexchangers.org)). A good material for this purpose is bentonitic clay (Fabien et al., 2011; Christodoulides et al., 2012).

According to the type of pipe that is used, borehole heat exchangers are classified in two groups (Kalogirou and Florides, 2007):

- U-pipes, which are designed by a pair of straight pipes connected with a U-turn at the bottom of the borehole (Figure 2- 4(a), (b))

Coaxial or concentric pipes which contain a straight pipe inside a larger diameter pipe (Figure 2- 4(c)) or are joined in other more complex configurations Figure 2- 4(d). Coaxial pipes, in most cases, can contain a larger amount of water and offer higher fluid flows (Raymond, 2015).

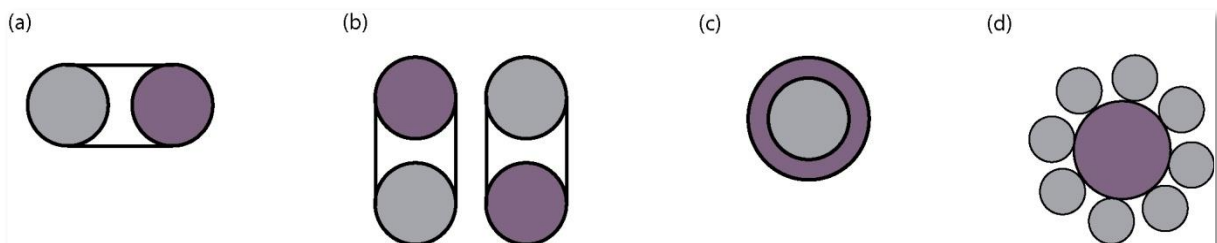


Figure 2- 4: Common ground heat exchanger pipe designs,  
(a) single U-pipe, (b) double U-pipe, (c) simple coaxial, (d) complex coaxial

The miscellaneous systems consist of a standing column well, where water is pumped from the bottom of the well to a heat pump and returns either to the top of the same well (Figure 2-5(a)) or in another well some distance away (Figure 2-5(b)).

Ground Coupled Heat Pumps (GCHP) or Geothermal Heat Pumps (GHP) are systems combining a heat pump with a Ground Heat Exchanger (GHE) for the heat exchange process. A Ground Coupled Heat Pump (GCHP) is a central heating and/or cooling system that transfers heat to or from the ground. It uses the earth as a heat source in the winter or a heat sink in the summer. This design takes advantage of the moderate temperatures in the ground to boost efficiency and reduce the operational costs of heating and cooling systems.

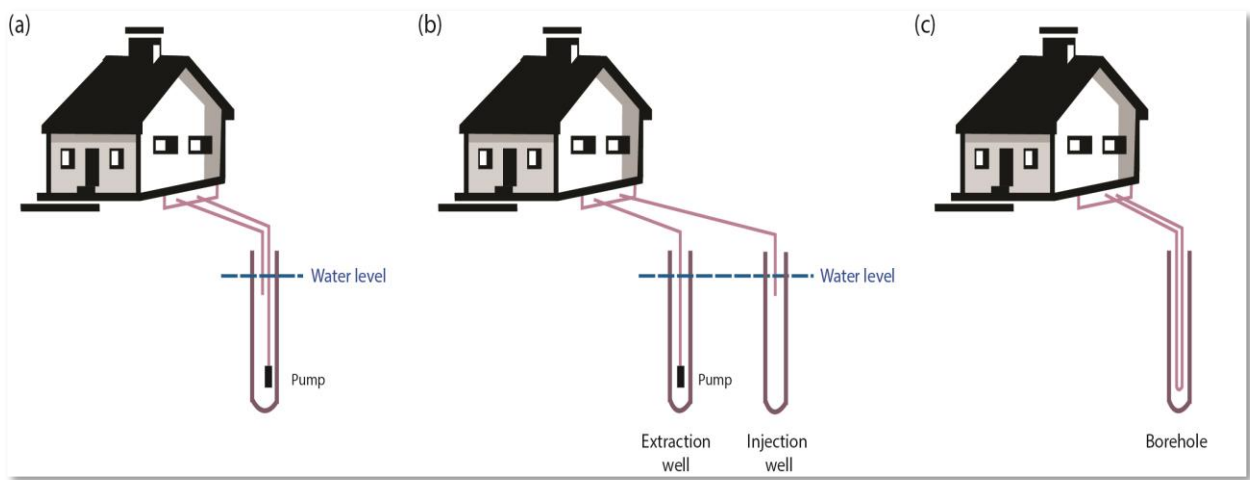


Figure 2-5: (a) Single well standing column configuration, (b) two wells standing column configuration (c) Borehole heat exchanger configuration

GHPs consist of three parts: the GHE, the heat pump unit, and the air or water delivery system. In the case of a GCHP in the winter, the heat pump removes heat from the GHE and pumps it into the indoor heat delivery system. In the summer, the process is reversed and the condenser and evaporator reverse their roles, with the use of the reversing valve, so that the heat pump moves heat from the indoor air into the GHE (Figure 2- 6 (a)).

The vast majority of GCHPs work on the principle of the vapor compression cycle. The main components of the system in this case, are a compressor, an expansion valve, the reversing valve and two heat exchangers referred to as the evaporator and condenser. The components are connected to form a closed circuit, as shown in Figure 2- 6 (b).

In Figure 2-7 (a) shows a diagram of a GCHP system during the heating cycle. The fluid circulates through the loop absorbing heat from the ground and the heat energy is transferred to the heat pump unit. Then the heat pump delivers the heat for space heating through the ducting system. For cooling, the process is simply reversed (Figure 2-7(b)) with the use of reversing valve.

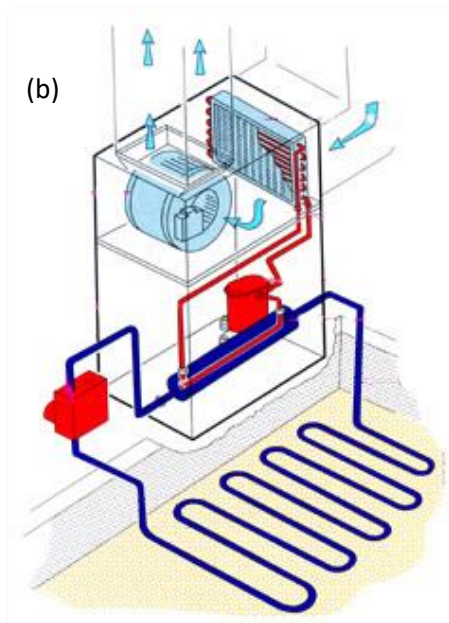
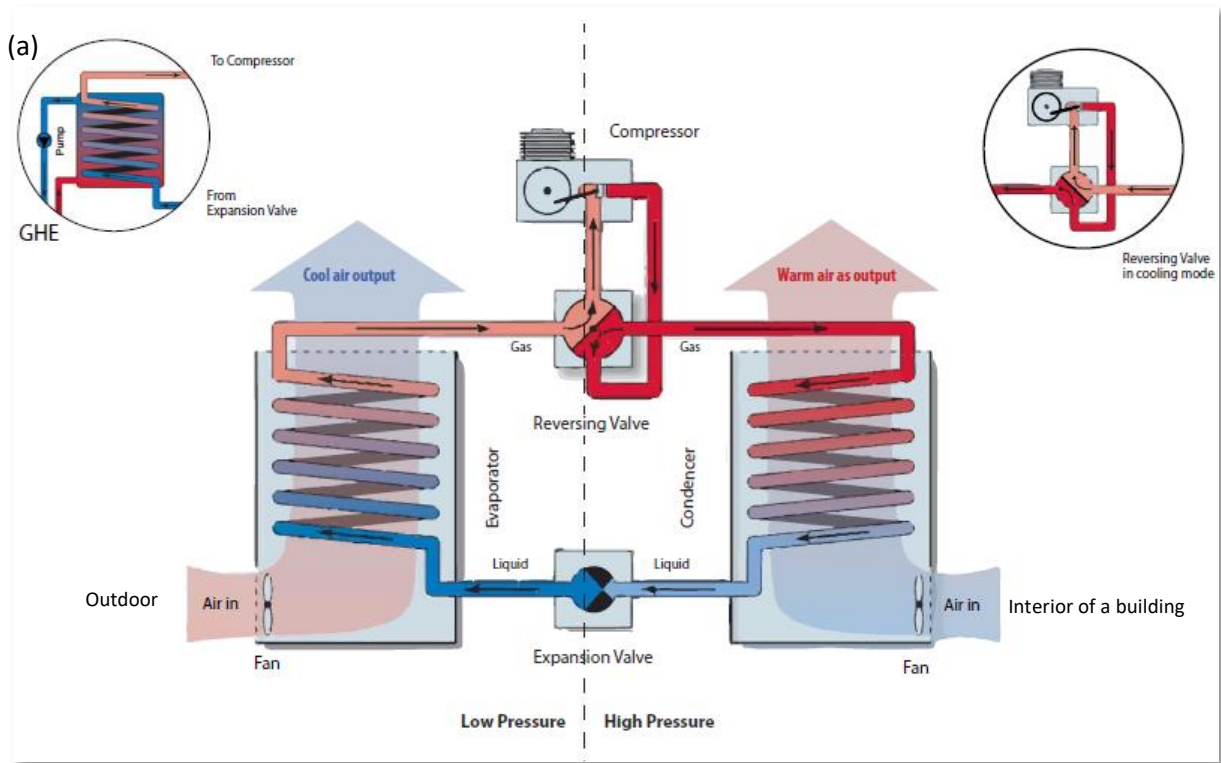
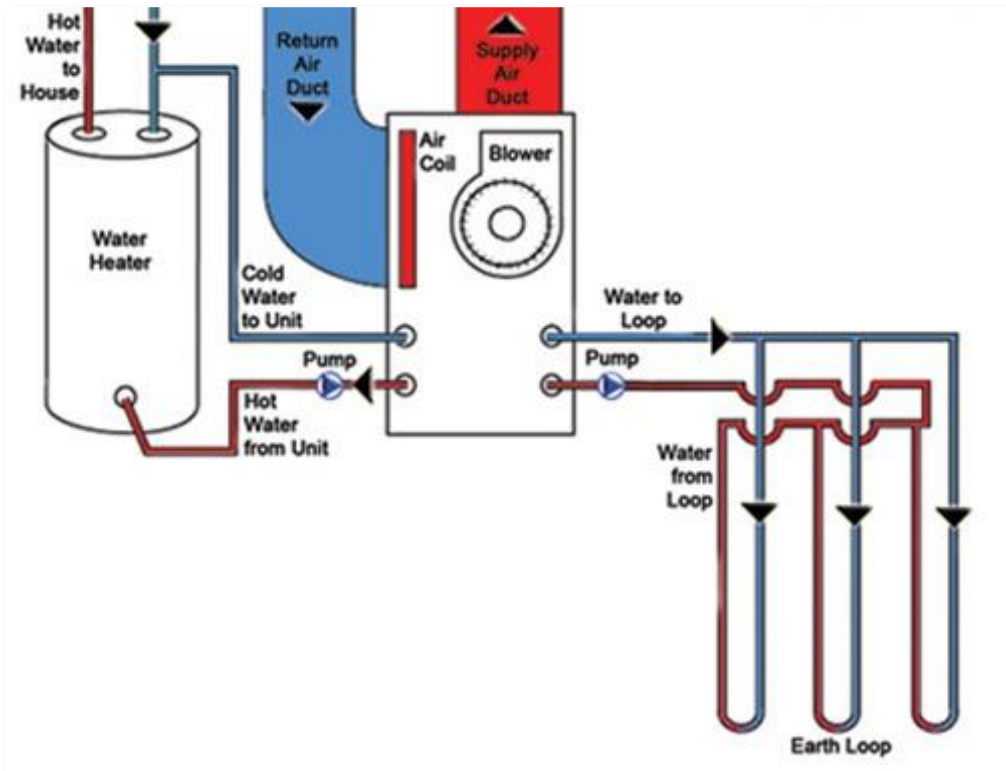


Figure 2- 6: (a) Heat pump principle (modified from warewolf-cluster.org) in heating and cooling mode (b) Diagram of a real GHPS system (modified from www.dteenergy.com)

(a)



(b)

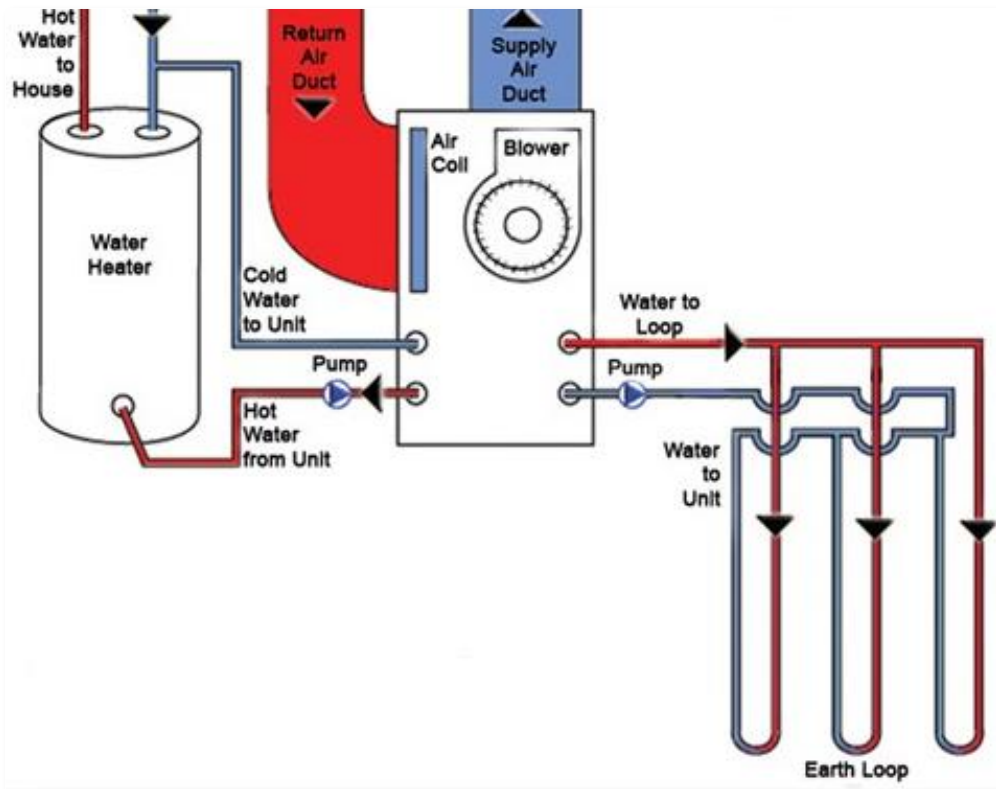


Figure 2-7: Geothermal heat cycle principle (a) cooling mode (b) heating mode  
([www.drkohlman.com](http://www.drkohlman.com))

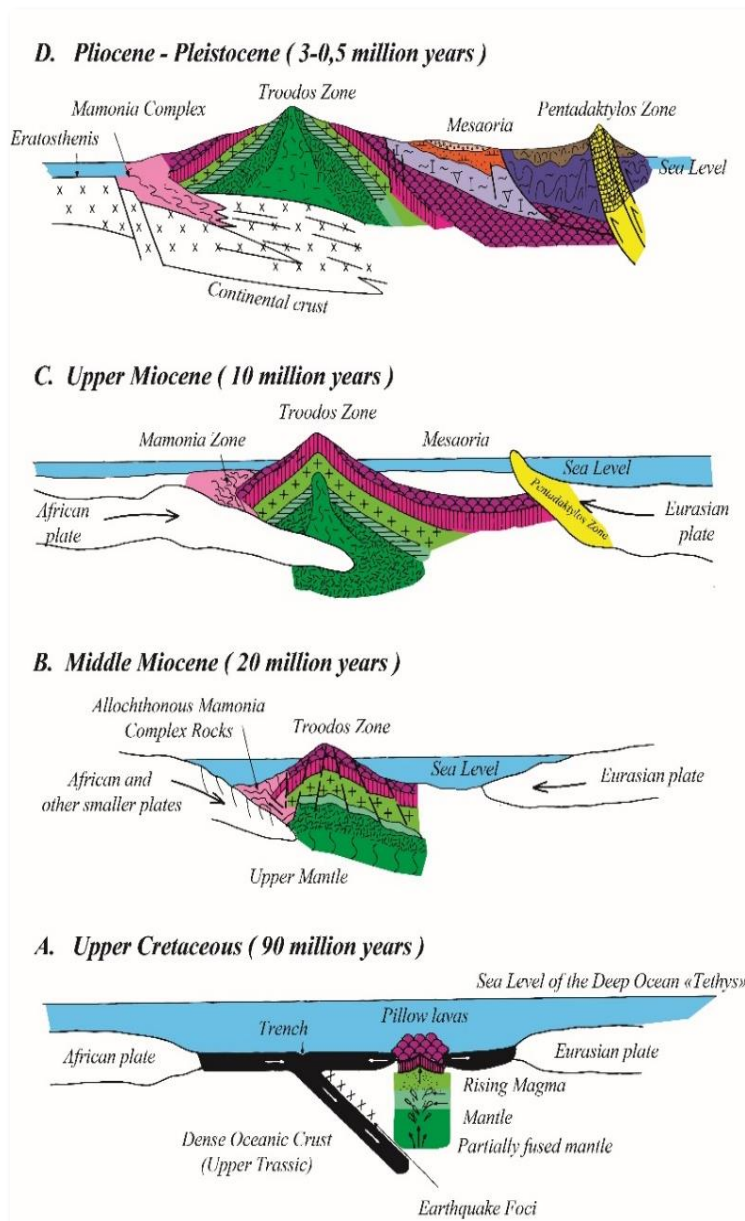
## 2.3 Geology of Cyprus

Cyprus is the third largest island in the Mediterranean Sea. It lies in the north-east corner, latitude 35° N and longitude 33° E, and covers an area of 9,251 km<sup>2</sup>. The climate is Mediterranean, with long, warm, dry summers from June to October and mild winters with occasional rain, lasting from December to April (Meteorological Service of the Republic of Cyprus, <http://www.moa.gov.cy/ms>). These climatic conditions, are suitable for the application of GHEs in conjunction with ground source heat pump for both heating and cooling (Florides, 2011; Pouloupatis et al., 2010).

In Ground Source Heat Pump systems, the heat exchange rate is an important factor with regards to the initial cost of the system. When the Ground Heat Exchanger (GHE) is installed in a lithology with good thermal properties, the thermal performance of the GHE exchanger is improved. So, it is of importance to have knowledge of the thermal properties of the ground in installation area.

The geological formation of Cyprus took place through a series of tectonic episodes (Figure 2-8(a)) that were initiated with the collision of the African and the Eurasian Plate, which formed the Troodos Ophiolite (Robinson and Malpas, 1990). A schematic presentation of the stratigraphy Troodos–Mesaoria–Cape Greco area is shown in Figure 2-8(b).

When geologists describe the geology of an area they group regions with the same geological structure, evolution and age together, calling them geotectonic zones. The descriptions of rocks on the basis of characteristics such as colour, mineralogic composition, and grain size are called lithologies (Neuendorf et al., 2011).



(a)

GEOLOGICAL TIME	FORMATION	LITHOLOGY
Pleistocene	Fanglomerate	Conglomerates & Sandstones
	Apalos	Clays, Silts, Sands & Conglomerates
Pliocene	Nicosia	Fossiliferous Marls
	Kalavassos	Saccharoidal Gypsum Laminated Gypsum
Miocene	Koronia Mem.	Reefal Bioclastic Limestones
	Pakhna	Pale Yellow Chalks
	Terraz Mem.	Reefal Bioclastic Limestones
Oligocene		
Eocene	Lefkara	White Chalks
Palaeocene		
Upper Cretaceous		

(b)

Figure 2-8: (a) Schematic presentation of the formation and evolution of the lithology of Cyprus, (b) schematic presentation of the stratigraphy Troodos–Mesaoria–Cape Greco area (adapted from the Cyprus Geological Survey Department, [www.moa.gov.cy/gsd](http://www.moa.gov.cy/gsd))

Cyprus from a geological point of view is divisible into four trending geological terranes (Figure 2- 9), namely (a) the Troodos Ophiolite Complex (Range), (b) the Mesaoria Plain (or Circum Troodos Sedimentary Succession), (c) the Keryneia or Pentadactylos Range and (d)

the Mamonia Complex (Xenophontos and Malpas, 1987; Panayides, 2009). The topography of the island is characterised by the tectonic structure of these four geological terranes.

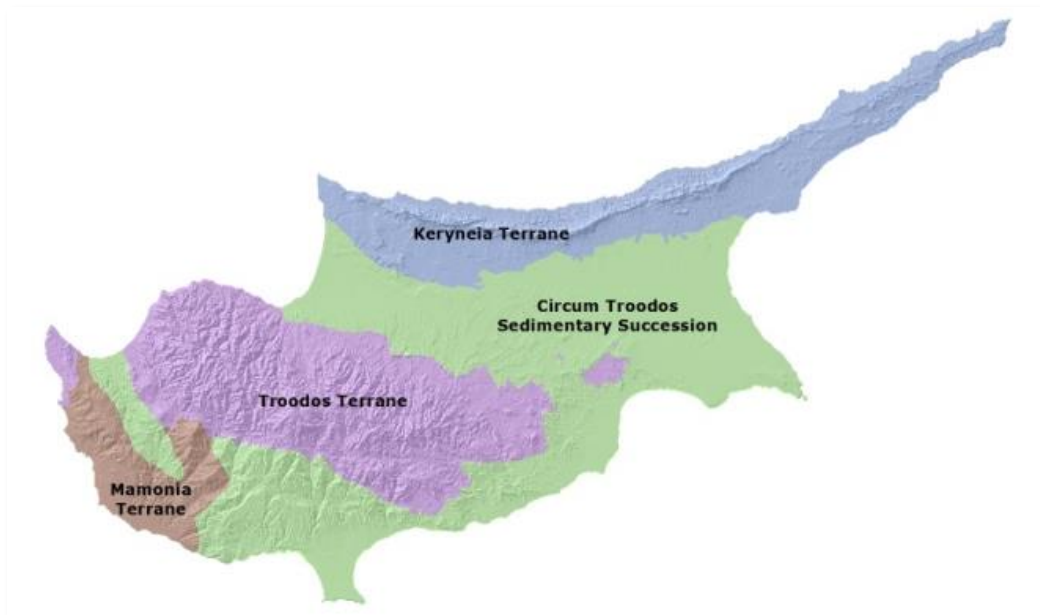


Figure 2- 9: The island of Cyprus is divided into four geological Terranes (Cyprus Geological Survey Department, [www.moa.gov.cy/gsd](http://www.moa.gov.cy/gsd))

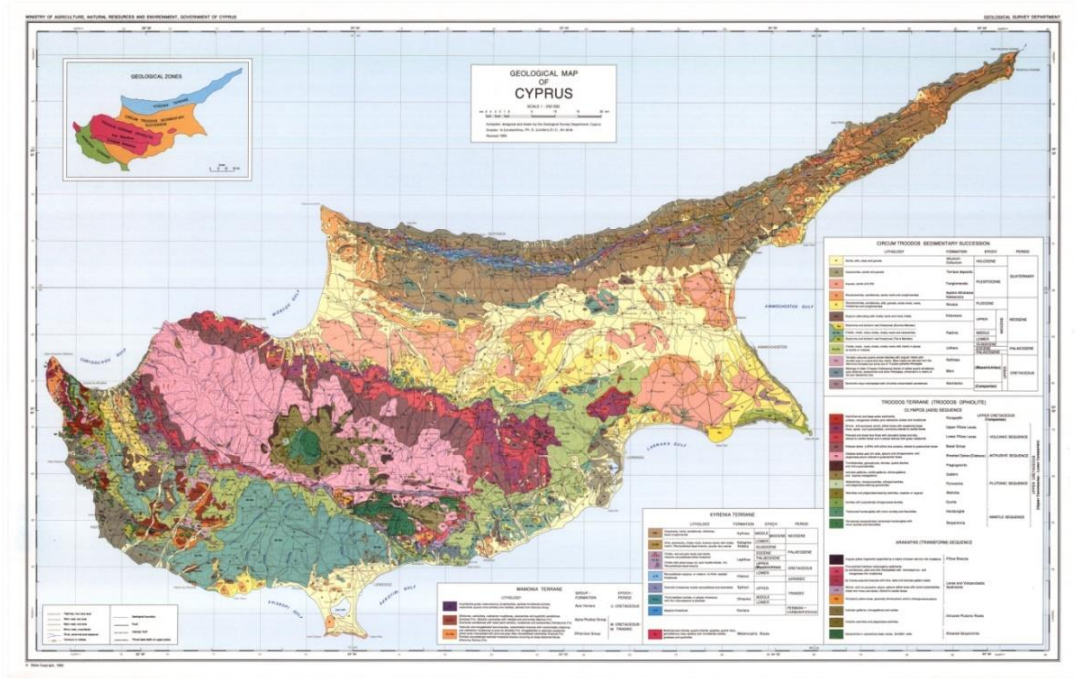


Figure 2-10: Geological Map of Cyprus 1:250,000 (Cyprus Geological Survey Department, [www.moa.gov.cy/gsd](http://www.moa.gov.cy/gsd))

The first terrane, the Troodos Terrane (Troodos Ophiolite Complex), is one of the most intensively studied ophiolites in the world. It dominates the central part of the island and it covers an area of 2,368 km<sup>2</sup>, i.e. the 25.4 % of the total area of the island. The Ophiolite sequence features in two separate areas within the Troodos Range, in the central Troodos and the Lemesos Forest in the southeastern part of the range (Arakapas Sequence as presented on the Geological Map of Cyprus), (Robertson, 2000). The Troodos Range is the most impressive topographic feature on the island of Cyprus. Its highest peak, Olympus, has an elevation of 1,951 m. The Troodos Ophiolite, as is more widely known to geologists, is a portion of an ancient oceanic lithosphere, created 90 million years ago (Robertson, 2000). Troodos therefore presents the stratigraphy of the ocean crust plus the underlying upper mantle (Malpas et al., 1990). The Troodos along with the Oman Ophiolite are the only ophiolites in the world with undisrupted rock sequences (Gass, 1989).

The second terrane, the Circum Troodos Sedimentary Succession, is a succession of Upper Cretaceous to Pleistocene sedimentary rocks that appears in the Mesaoria Plain as well as in the southern part of the island (Figure 2- 9). The Mesaoria Plain is a topographically low, rather flat area, which occupies the central part of the island between the Troodos Range to the south and the Pentadaktylos Range to the north. Its area is 5,649 km<sup>2</sup> and represents 60.7 % of the total area of the island. It consists of bentonitic clays, volcanoclastics, melange, marls, chalks, cherts, limestones, calcarenites, evaporites and clastic sediments.

The third terrane, Kyreneia Terrane, forms a narrow chain of mountains at the northern part of the island. It runs from the west to the east making a very open curvature. The crest of the range for most of its length varies in altitude between 800 and 1,000 m with its highest point at just over 1,000 m.

The geology that constitutes the fourth terrane, the Mamonia Terrane, is referred to us as the Mamonia Complex in most of the earlier geological literature of the island. Rocks belonging to this zone are extensively found in the western and southwestern Cyprus. Smaller occurrences are found at the tip of the Akrotiri peninsula and in the southeastern part of the island.



Note that lithologies in the Arakapas Sequence, the Mamonia terrane and the Keryneia or Pentadactylos Range (except the Kythrea Formation) have not been considered in the present study due to the occupation of these areas of the island by Turkey.

The most recent Geological map covering the whole island is the Geological Map of Cyprus 1:250,000 revised in 1995 (Geological Map of Cyprus, 1995). It was prepared by the Geological Survey Department of Cyprus and it separates the geology of the island into 44 geological units (Figure 2-10), (Table 2 - 1).

Table 2 - 1: Geological Formations studied and their lithological composition as presented in the Geological Map of Cyprus.

<b>FORMATION</b>	<b>Lithology</b>	<b>Geological age</b>
<b>Circum Troodos Sedimentary Succession</b>		
Alluvium – Colluvium	Sands, silts clays and gravels	Holocene - Pleistocene
Terrace Deposits	Calcarenites, sands and gravels	Quaternary - Pleistocene
Franglomerate	Gravels, sands and silts	
Apalos– Athalassa– Kakkaristra	Biocalcarenites, sandstones, gravels, marls, limestone and conglomerates	Quaternary - Pleistocene Neogene - Pliocene
Nicosia	Biocalcarenites, sandstones, silts, gravels, marls, limestones and conglomerates	Neogene - Pliocene
Kalavastos	Gypsum alternating with chalky marls and marly chinks	Neogene - Upper Miocene
Pakhna	Biostrome and bioherm reef limestones (Koronia Member)	Neogene - Upper Miocene
	Chinks, marls, marly chinks, chalky marls and calcarenites	Neogene - Middle Miocene
	Biostrome and bioherm reef limestone (Terra Member)	Neogene - Lower Miocene
Lefkara	Chinks, marls, marly chinks with cherts in places as bands or nodules	Palaeogene
Kathikas	Variably coloured, poorly sorted debrites with angular clasts upto boulder size in a sand and clay matrix. Most clasts are derived from the Mamonia Complex but some are of Troodos ophiolite lithologies	Upper cretaceous – Maastrichtian
Moni	Melange of older (Triassic - Cretaceous) blocks of yellow quartz sandstone, grey siltstone, serpentinite and other lithologies, entrained in a matrix of silt and bentonitic clay	
Kannaviou	Bentonitic clays interbedded with off-white volcanoclastic sandstones	Upper cretaceous – Maastrichtian/Campanian

Troodos Ophiolite		
Perapedhi	Hydrothermal and deep water sediments: umbers, manganoan shales, pink radiolarian shales and mudstones	Upper cretaceous - Upper Cenomanian/Lower Campanian
Upper Pillow Lavas	Olivine- and pyroxene-phyric, pillow lavas with occasional sheet flows, dykes and hyaloclastites, commonly altered to zeolite facies	
Lower Pillow Lavas	Pillowed and sheet lava flows with abundant dykes and silts, altered to zeolite facies and in places stained with green celadonite	
Basal Group	Diabase dykes (>50%) with pillow lava screens, altered to greenschist facies	
Sheeted Dykes (Diabase)	Diabase dykes upto 3m wide, aphyric and clinopyroxene- and plagioclase-phyric, altered to greenschist facies	
Plagiogranite	Trondhjemites, granophyres, diorites, quartz-diorites and micro granodiorites	
Gabbro	Isotropic gabbros, uralite gabbros, olivine gabbros and layered melagabbros	
Pyroxenite	Websterites, clinopyroxenites, orthopyroxenites and plagioclase bearing pyroxenites	
Wehrlite	Wehrlites and plagioclase-bearing wehrlites, massive or layered	
Dunite	Dunites and subordinate clinopyroxene-dunites	
Harzburgite	Tectonized harzburgites with minor dunites and lherzolites	
Serpentinite	Pervasively serpentinized, tectonized harzburgites with minor dunites and lherzolites	
Keryneia Terrane		
Kythrea	Greywacke, marls, sandstones, siltstones, basal conglomerate.	Neogene - MiddleMiocene

## 2.4 Geothermal Background of Cyprus

A first geothermal study related to Cyprus was reported in 1973 in a thesis by Paul Morgan with the title “Terrestrial heat flow studies in Cyprus and Kenya”. The primary aim of the study was to measure thermal conductivity, porosity, bulk and grain volume on chip samples and the temperature in boreholes (Morgan, 1973).

Totally 33 boreholes (BH) were included in the research and the highest conductivity value was recorded in a borehole drilled for mining purposes at the Limni Mine. Porosity, bulk density and grain density were also measured on core and chip samples taken from different lithologies. It was reported that there was a large difference in the values measured in solid samples compared to the values obtained from the chip samples.

A second study took place in Cyprus in 2010-2011 funded by the Research Promotion Foundation and undertaken by the Cyprus University of Technology and the Cyprus Geological Survey Department (GSD) and funded by the Research Promotion Foundation of Cyprus (ΤΕΧΝΟΛΟΓΙΑ/ ΕΝΕΡΓ/ 0308(BIE)/ 15). The results indicated that there is potential for the efficient use of Ground Coupled Heat Pumps (GCHP) in Cyprus that could lead to significant savings in heating and cooling energy consumption (Florides, 2011, Pouloupatis et al., 2010). All results are presented in the PhD thesis of P. Pouloupatis published in 2014 (Pouloupatis, 2014).

The project included drilling boreholes in 8 locations, at Lakatameia, Kivides, Meneou, Ayia Napa, Lemesos, Saitas, Geroskipou and Prodromi (Polis Chrysochous). Rock samples were collected from every different geological formation for each borehole and a vertical profile showing the lithology was drawn. The thermal conductivity of indicative specimens was determined using a heat transfer analyser.

U-tube heat exchangers made of polyethylene pipe were subsequently installed in the boreholes and thermocouples were used to measure the ground temperature at different depths for an entire year. The data were then used to draw temperature and thermal conductivity maps for the ground at depths of 20 m, 50 m and 100 m at the 8 locations (Figure 2-11) presents the published maps based for 50 m depth based on the data from the project ([www.moa.gov.cy/gsd/projects](http://www.moa.gov.cy/gsd/projects)).

The temperatures measured in the 8 BHs located in different geographical locations show that ground is divided into three zones, namely (a) the surface zone, (b) the shallow zone and (c) the deep zone. In general, the surface zone is affected by short-term weather conditions, changing to seasonal variations as the depth increases (shallow zone), and for depth bigger than 8 m approximately (deep zone) the ground temperature remains almost constant throughout the

year (Florides et al., 2010). Similar statements were made by Vijdea et al. (2014) presenting the ThermoMap project of Constanta (Romania), by Sliwa and Rosen (2015) studying the Natural and Artificial Methods for Regeneration of Heat Resources for borehole GHEs in Kraków, Poland and by Correia et al. (2012) studying Livingston Island (Antarctica). All the above projects, although they refer to different geographical locations, they all verify the presence of the three underground zones and that the ground temperature in deep underground layers (approximately below 8 m) remains constant during the year.

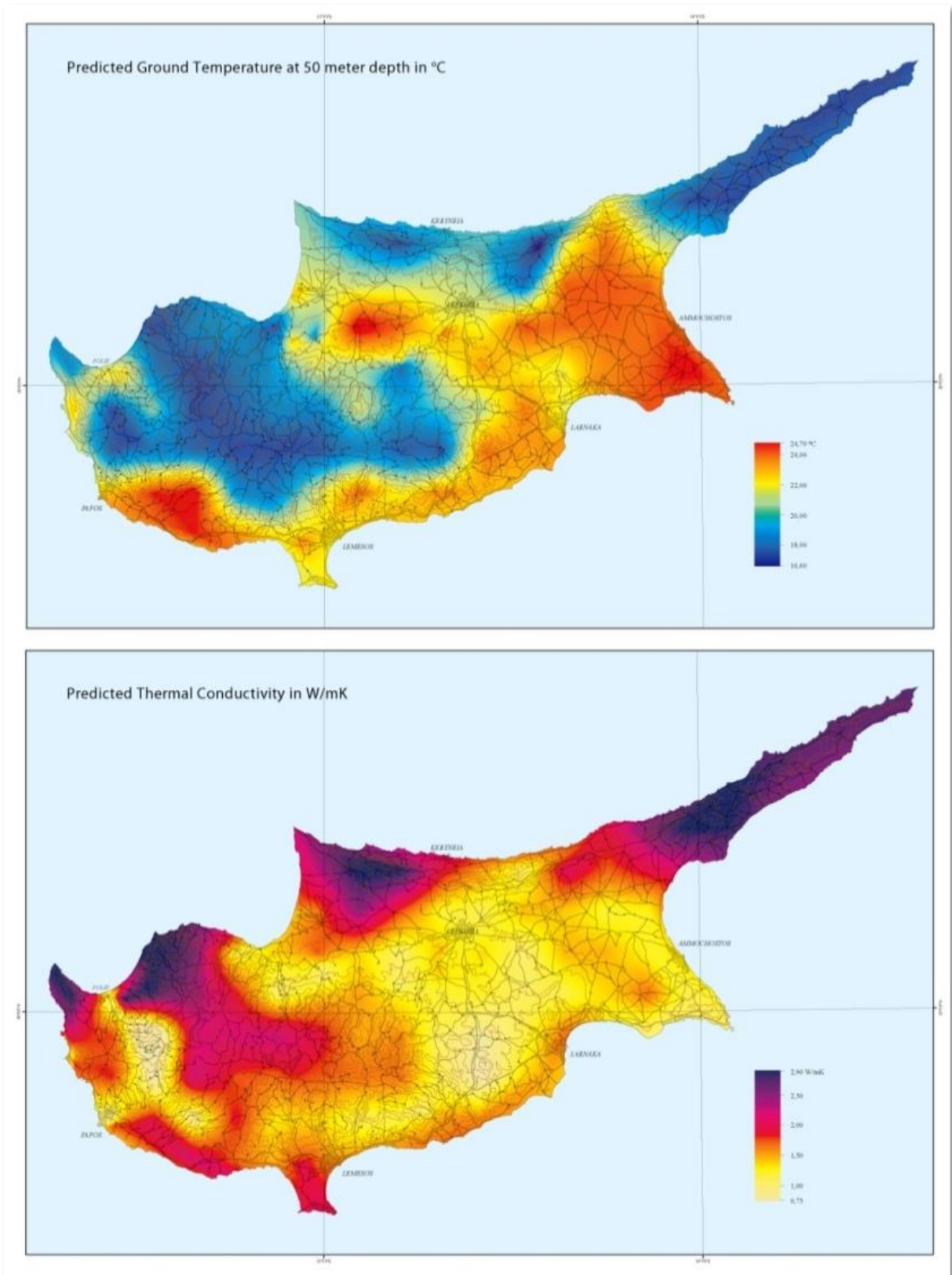


Figure 2-11: Maps of Ground Temperature and Thermal Conductivity of Cyprus  
 (www.moa.gov.cy/gsd/ projects)

Except these two projects, we have additional geothermal information concerning the underground of the island from other sources, such as the Cyprus Crustal Study Project (Gibson et al., 1989) and a thesis undertaken by Constantinou (2004) investigating the hydrogeological conditions of the island (Constantinou, 2004).

In 1978, an international consortium of scientists from Canada, Denmark, the United Kingdom, Iceland, the United States, and West Germany successfully completed a research deep drilling project in Iceland. These scientists subsequently formed the International Crustal Research Drilling Group (ICRDG), to organize further deep drilling investigations and to compare the results with those from the Deep Sea and Ocean Drilling Projects. It was hoped, in this way, to better understand the structure and composition of the ocean crust. Having this in mind, ICRDG started the Cyprus Crustal Study Project in 1980 (Gibson et al., 1989) which proceeded to investigate the Troodos ophiolite in Cyprus and gave important information about the bedrock of Cyprus. Its' framework included deep borehole drilling in different places in Europe. In Cyprus, five deep boreholes were drilled at the Ophiolite near Palaichory, Mitsero, Ayio Epiphanio and Klirou (two boreholes) with 2,263m, 701m, 689m, 485m and 226m depth respectively (Figure 2-12). An integrated petrological, structural, and geophysical study of the ophiolite, involving both field mapping and diamond drilling was therefore performed.

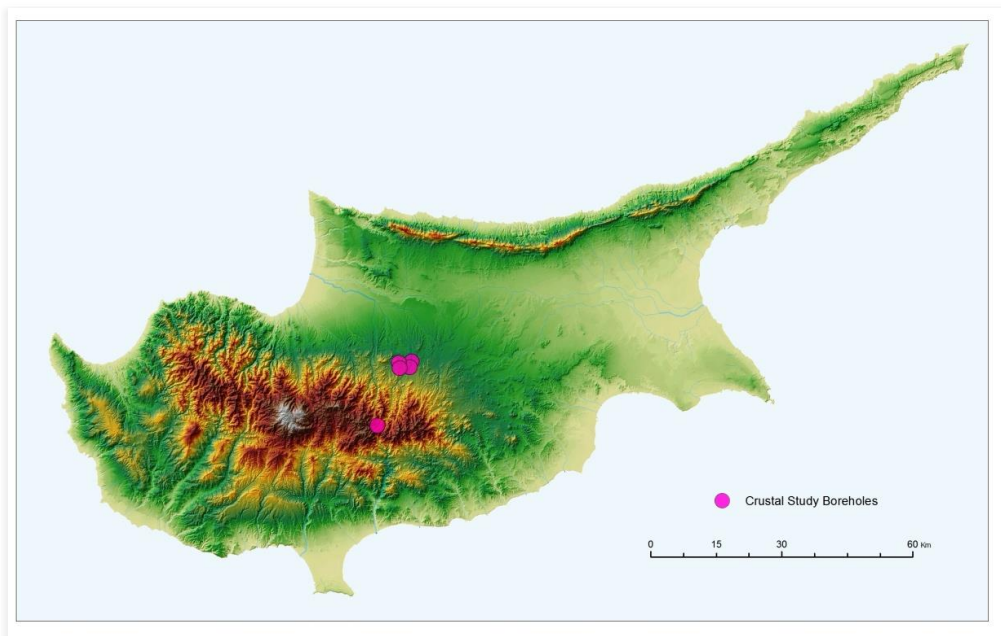


Figure 2-12: Boreholes location of Crustal Study (3D model data supplied by Cyprus GSD)

A temperature sensor was used for the measurement of underground temperature increasing with depth. Borehole (BH) at Palaichory is of great interest as the BH was drilled at the center of the Troodos Ophiolite and the depth reached was 2,263 m. Temperature recorded at 2.075 m depth was 45°C. Temperature recorded at the surface of the BH was 19.3 °C, but at water level (80m depth) it was decreased to 15.9 °C. This is an important observation, verifying that at the transition point from air into water, in all the boreholes regardless of depth, there is a change at measured temperature, an increase or decrease range from 1.5°C to 4°C. This could be justified if we adopt the theory suggesting that when drilling a BH, different water strata are connected at different levels, causing water flow from lower and more warm points to upper levels. In addition, air compared with water is a bad heat conductor with higher thermal resistance and therefore in the borehole air is heated to a lower temperature than water.

By further analysis of the BHs temperature logbooks and having in mind the temperature change due to transition from air to water, we used the project data to calculate the underground temperature gradient, using temperature values measured below water level. Calculated values range from 1.2 to 1.6 °C per 100 m. Only exception was at Klirou1 BH with underground temperature gradient equal to 2.2 °C per 100 m.

In more detail, Ayios Epiphanius BH water level was found at 13.5 m depth and average temperature gradient is equal to 1.2 °C per 100 m, using recorded values for depth 13.5 to 212 m (max temperature at 212 m equal to 22.2 °C). At Mitsero BH water level was located at BH's surface and average temperature gradient is equal to 1.6 °C per 100m, using recorded values for depth 0 to 193 m (max temperature at 193 m equal to 22.0 °C). At Palaichory BH water level was found at 80 m depth and average temperature gradient is calculated to 1.46 °C per 100 m, using recorded values for depth 80 to 2075 m (max temperature at 2075 m equal to 45.0 °C). Finally, near Klirou village, at Klirou4 BH water level was found at 10 m depth and temperature gradient is equal to 1.6 °C per 100 m (using recorded values for depth 10 to 105 m and max temperature at 105 m equal to 22.0 °C) and at Klirou1 BH temperature gradient is equal to 2.2 °C per 100 m, using recorded values for depth 8.5 to 283 m (max temperature at 283 m equal to 23.5 °C).

## 2.5 Summary

Thermal properties of the ground are of importance in many engineering applications, including geothermal energy. They depend on many factors, such as type of rock, particle size distribution, rock structure, porosity, degree of water saturation etc. Additionally, the presence of underground aquifers influence the thermal properties and can play an important role in the design of Ground Heat Exchanger systems.

A large number of GHE systems are today in use all over the world for residential and commercial heating and cooling applications. A very small number of studies undertaken in Cyprus in the last 45 years provided some data on temperatures of the ground in different parts of the island. However, this data is not sufficient to enable the design of GHEs and heat pumps with any degree of confidence, hence the work in this project which aims to provide more comprehensive information not only on the ground thermal properties but also the influence of water on these properties.



## Chapter 3: Modeling Vertical Ground Heat Exchangers

### 3.1 Introduction

Over the past few decades, different techniques have been established to extract geothermal heat from shallow to deep subsurface levels. Ground Heat Exchangers are systems used widely for exploit effectively the heat capacity of the ground and the closed-loop borehole, also called vertical Ground Heat Exchanger (GHE), is a standard approach for lower and mid-depth applications (see Chapter 2: Background).

In this Chapter, we will deal with the analysis a computational model constructed to simulate the heat transfer in the borehole GHE. In more detail, in Section 3.2 the computational model is presented and in Section 3.3, based on the model and using the FlexPDE software (PDE Solutions Inc), a script was created and the importance of various parameters was tested. Finally, in Section 3.4 the conclusions of the study are presented. The validation of the model is presented in Chapter 4: Model Validation.

The created model for the GHE system, is based on the principle of energy conservation. The fluid circulates through tubes that are located inside a borehole (BH), resulting in indirect thermal contact between the fluid and the subsurface. For the calculation of the temperature of the heat carrier fluid, which is circulated in the U-tubes of the GHE, various analytical and numerical models have been developed over the years. Classic analytical solutions used for dimensioning vertical GHE include the line- and the cylindrical-source models (Yang et al., 2010; Kavanaugh, 1995; Bernier, 2001). On the other hand, numerical models are based on Finite Element Methods (FEM) (Lee, 2011; Zeng et al., 2002). The main difference between analytical and numerical methods lies in setting up the initial and boundary values.

A number of commercial and freeware software programs designed by companies and research centers, suitable for GHE system design can be found in the market. These include the (a) GS2000 designed by Natural Resources Canada-Caneta Research Inc., (b) CLGS Software by IGSHPA, (c) GshpCalc by Energy Information Services, (d) Ground Loop Design (GLD) by

Thermal Dynamics, (e) GeoLink Design Studio by WaterFurnace, (f) HYDROTHERM by US Geological Survey, (g) SVHeat by SoilVision Systems Ltd, (h) TEMP/W by GEO-SLOPE International Ltd, (i) FlexPDE designed by PDE Solutions Inc., (j) COMSOL Software by COMSUL, (k) GLHEPRO by the International Ground Source Heat Pump Association, (l) CLGS by Oklahoma State and (m) GeoT\*SOL by Valentin Software GmbH. Most of them are user-friendly and they can offer powerful tools for the designer. Design comparisons and multiple scenarios or projects can be handled easily in vertical or horizontal structures with real-world shapes.

In this study, the FlexPDE software (PDE Solutions Inc) was used to reach an accurate numerical solution to a Partial Differential Equations (PDEs) model, with the use of FEM, for the energy flow and temperature change in and around a borehole (BH). FlexPDE offers the opportunity for a detailed description of the geometry and boundary conditions. FlexPDE is a general-purpose software, and it was chosen as it can solve steady-state or time-dependent problems and three-dimensional free boundary problems. It is a script-driven program that users enter equations, boundary conditions and domain description. FlexPDE builds a mesh, constructs a system FEM, solves it, and presents an easy to use graphical output. The software also includes Arbitrary Lagrange/Eulerian (ALE) moving-mesh capabilities (FlexPDE 6 Manual). In general, it can be used for solving PDEs involving heat flow, electric and magnetic fields or stress analysis (Zhang and Li, 2010; Tariq et al., 2012; Heng et al., 2009; Fernando et al., 2011).

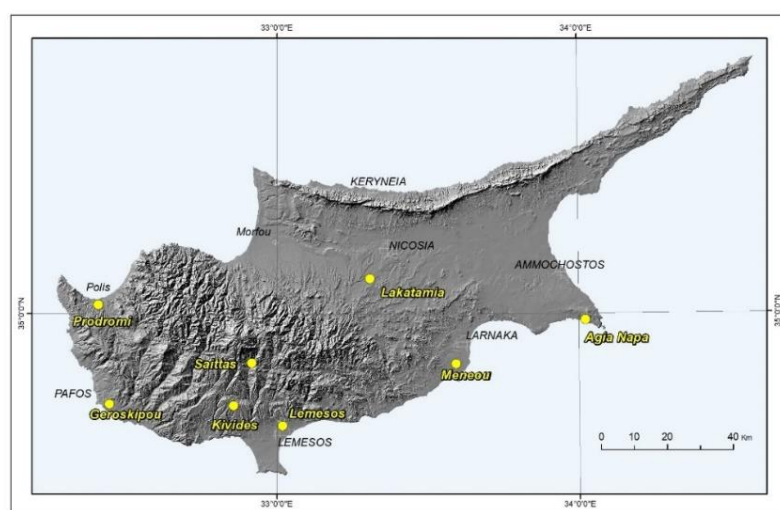


Figure 3- 1: Positions of the 8 geothermal boreholes in Cyprus

The temperature of the ground in Cyprus was recorded in eight BHs, in the framework of a project undertaken by the Cyprus University of Technology and funded by the Research Promotion Foundation of Cyprus (ΤΕΧΝΟΛΟΓΙΑ/ ΕΝΕΠΓ/ 0308(BIE)/ 15), for the efficient use of Ground Coupled Heat Pumps in Cyprus (Florides et al., 2011; Pouloupatis et al., 2010). The temperatures measured in the eight BHs located in different geographical locations (Figure 3- 1), show that ground is divided into zones and for depth bigger than 8 m approximately (deep zone), the ground temperature remains almost constant throughout the year (Florides et al., 2010) (see Chapter 2: Background).

### **3.2 Computational Model**

Our study cases refer to a geothermal system combining a borehole GHE and the surrounding rock mass crossed by an aquifer. The designed model was created using the FlexPDE software (PDE Solutions Inc) to test the response of the GHE and the effect of heat transfer inside and around the borehole. To address the heat transfer across the GHE, it was necessary to consider that the heat flow in a shallow geothermal system involves coupled heat conduction and convection, occurring in the borehole GHE and the surrounding ground. Heat conduction in the ground occurs as a result of thermal energy transfer due to temperature gradients between the layers of the earth and the borehole GHE. Heat convection occurs as a result of diffusion and advection of heat due to the liquid flow in the tubes and the motion of water in porous layers.

Due to the underground aquifer crossing the BH, the area around the borehole could be separated into two phases, namely (a) a fully saturated porous material, consisting of solid particles and water and (b) a completely dry material (Al-Khoury et al., 2010). An aquifer is defined as a body of rock that contains sufficient saturated permeable material to absorb groundwater and transfer it to wells and springs (Neuendorf et al., 2011). The impact of the porosity of rocks in underground layers was also considered in this investigation.

In a GHE system, plastic tubes (polyethylene or polypropylene) are installed in the ground and the space between the tube and the hole is filled with an appropriate material (grout) to ensure

good contact between the tube and the undisturbed ground and to reduce the thermal resistance. The grout is often a bentonite-clay mixture which is sometimes enhanced with additives of higher thermal conductivity in order to match the higher thermal conductivity of the surrounding ground (Figure 3- 2). The heat transfer rate between the circulating fluid and the surrounding ground depends upon the local overall heat transfer resistance composed by the fluid traveling in the tube, the wall, the bentonite filler and the resistance of the ground. The overall heat transfer resistance is rather difficult to estimate as in most cases we can only guess the structure and the other parameters that should be taken into account for the surrounding soils/rocks. In addition, bentonite is going to work as an insulator, stopping an aquifer intruding the borehole.

A vertical heat exchanger is usually drilled to a depth of 20–300 m with a diameter of 10–20 cm. A borehole system can comprise a number of individual boreholes (multiple boreholes). In our study a single borehole is used with a single U-tube connection.

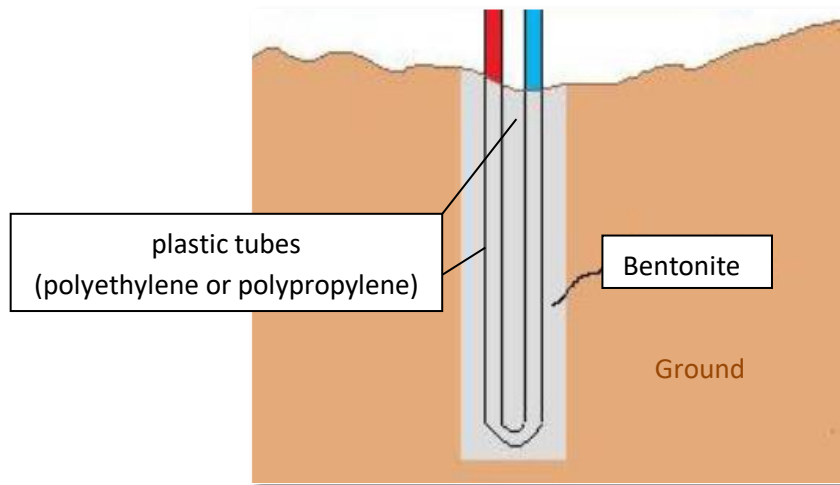


Figure 3- 2: Geothermal borehole filled with bentonite

The conduction equation (Fourier's law) is:

$$q = -\lambda A \frac{\Delta T}{\Delta x} \quad (1)$$

where,  $A$  = heat transfer area ( $m^2$ ),  $\lambda$  = thermal conductivity of the material ( $W/m K$ ),  $\Delta T$  = temperature difference across the material ( $^{\circ}C$ ) and  $\Delta x$  = material thickness ( $m$ ).

The negative sign in Equation (1) is necessary because temperature decreases in the direction of the flux flow. In 3D form, Equation (1) becomes:

$$\vec{q} = q_x \vec{i} + q_y \vec{j} + q_z \vec{k} \quad (2)$$

The heat exchange in a cylinder was described in detail by Carslaw and Jaeger and a mathematical solution was given with the use of a one dimensional heat conservation model as shown below, Carslaw and Jaeger (1993):

$$\frac{\partial \varphi}{\partial t} + u \frac{\partial \varphi}{\partial x} - \frac{\partial}{\partial x} \left( D \frac{\partial \varphi}{\partial x} \right) = S \quad (3)$$

where,  $D$ = mass diffusion coefficient,  $u$ = horizontal velocity,  $\varphi$ = object of interest and  $S$ = source of heat.

Having in mind that in a shallow geothermal borehole we have transfer of heat from the tubes to the surroundings only by conduction and convection, then a one-dimensional heat conservation equation for an incompressible fluid of volume  $V_f = A_f dz$  (where  $A_f$  is the fluid cross-sectional area) flowing in the tube with a velocity  $u = dz/dt$  (Figure 3- 3) is described by:

$$A_f \rho_f c_f \frac{\partial T}{\partial t} + A_f \rho_f c_f u \frac{\partial T}{\partial z} + A_f \frac{\partial}{\partial z} \left( -\lambda_f \frac{\partial T}{\partial z} \right) + \pi d_{in} h (T_f - T_p) = 0 \quad (4)$$

where,  $A_f$  = fluid cross-sectional area ( $m^2$ ),  $u$  = fluid velocity ( $m s^{-1}$ ),  $h$  = convection heat transfer coefficient ( $W m^{-2} K^{-1}$ ),  $\lambda$  = thermal conductivity ( $W m^{-1} K^{-1}$ ),  $\rho_f$  = density of the fluid ( $kg m^{-3}$ ),  $c_f$  = specific heat capacity of fluid ( $J kg^{-1} K^{-1}$ ),  $T$  = temperature ( $^{\circ}C$ ),  $T_p$  = temperature on tube ( $^{\circ}C$ ),  $T_f$  = fluid temperature ( $^{\circ}C$ ),  $\partial T$  = steady temperature difference between the inlet and outlet tube temperature ( $^{\circ}C$ ),  $d_{in}$  = internal diameter ( $m$ ) and  $t$  = time ( $s$ ).

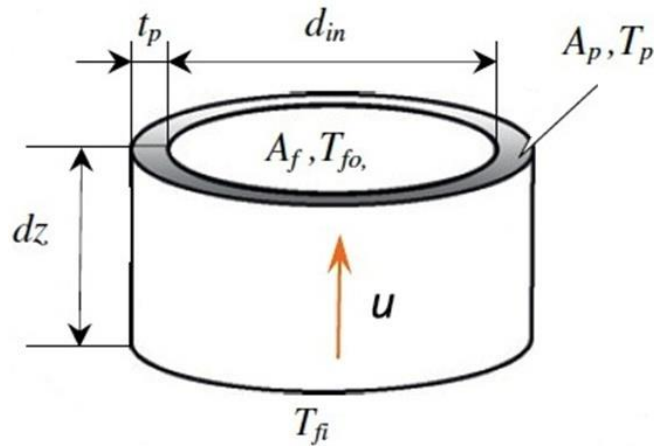


Figure 3- 3: Cylindrical model representing a part of a tube of a geothermal heat exchanger

Equation 4 can be used for the fluid in both sides of the tubes of a geothermal heat exchanger by changing the sign of velocity  $u$ , which in the upward-flow leg is positive (Figure 3- 3) and in the downward-flow leg is negative.

Note that at the boundary between the fluid and the tubes the convective heat flux is  $h\Delta T$ , where  $h$  is the convective heat transfer coefficient of the process ( $\text{W m}^{-2} \text{K}^{-1}$ ) and  $\Delta T$  is the temperature difference at the boundary.

The convection heat transfer coefficient  $h$  can be estimated to be (Florides et al., 2008):

$$h = \lambda \frac{\text{Nu}}{D_H} \quad (5)$$

where  $D_H$  is the hydraulic diameter (in this case the tube-inside diameter) and  $\text{Nu}$  is the Nusselt number. The Nusselt number in this case can be expressed through the Dittus–Boelter correlation as

$$\text{Nu} = 0.023\text{Re}^{0.8}\text{Pr}^n, \quad (6)$$

where  $Pr = \mu c_p / \lambda$  is the Prandtl number,  $Re = \rho c_p d_{in} / \mu$  is the Reynolds number,  $\mu$  is the dynamic viscosity, and  $n = 0.4$  for heating (wall hotter than the bulk fluid) and 0.33 for cooling (wall cooler than the bulk fluid).

Taking into consideration that for the cylindrical model conduction can take place in all three directions and convection takes place only in one direction i.e. the direction of the movement of the water in tubes then a 3-D space heat conservation equation per unit volume may be written as:

$$\rho_f c_f \frac{\partial T}{\partial t} + \rho_f c_f u \frac{\partial T}{\partial z} + \left[ \frac{\partial}{\partial x} \left( -\lambda_f \frac{\partial T}{\partial x} \right) + \frac{\partial}{\partial y} \left( -\lambda_f \frac{\partial T}{\partial y} \right) + \frac{\partial}{\partial z} \left( -\lambda_f \frac{\partial T}{\partial z} \right) \right] + \frac{4}{d_{in}} h (T_f - T_p) = 0 \quad (7)$$

In addition, the energy conservation equation for the tube becomes:

$$\rho_p c_p \frac{\partial T}{\partial t} + \left[ \frac{\partial}{\partial x} \left( -\lambda_p \frac{\partial T}{\partial x} \right) + \frac{\partial}{\partial y} \left( -\lambda_p \frac{\partial T}{\partial y} \right) + \frac{\partial}{\partial z} \left( -\lambda_p \frac{\partial T}{\partial z} \right) \right] + \frac{h}{t_p} (T_p - T_f) = 0 \quad (8)$$

and for the ground (per unit volume):

$$\rho_g c_g \frac{\partial T}{\partial t} + \left[ \frac{\partial}{\partial x} \left( -\lambda_g \frac{\partial T}{\partial x} \right) + \frac{\partial}{\partial y} \left( -\lambda_g \frac{\partial T}{\partial y} \right) + \frac{\partial}{\partial z} \left( -\lambda_g \frac{\partial T}{\partial z} \right) \right] = 0 \quad (9)$$

In the presence of aquifer groundwater ground mass can be considered as a saturated two-phase porous material consisting of solid particles and water. Dry soil/rock is considered as one phase material, Al-Khoury et al. (2010).

In a state of thermodynamic equilibrium, i.e.  $T_s = T_w = T$  ( $s$  and  $w$  refer to the solid and fluid-water phases respectively) assuming that there is no heat transfer from one phase to another, the energy balance equation is written as (Al-Khoury et al., 2010):

$$\rho c \frac{\partial T}{\partial t} + \rho c_w v \Delta T + \left[ \frac{\partial}{\partial x} \left( -\lambda \frac{\partial T}{\partial x} \right) + \frac{\partial}{\partial y} \left( -\lambda \frac{\partial T}{\partial y} \right) + \frac{\partial}{\partial z} \left( -\lambda \frac{\partial T}{\partial z} \right) \right] = 0 \quad (10)$$

where,

$\lambda = (1-n) \lambda_s + n \lambda_w$  - thermal conductivity of the porous matrix (W/m K)

$\rho c = (1-n) \rho c_s + n \rho c_w$  - volume heat capacity of the soil matrix (J/m<sup>3</sup> K)

$v$  = the flow velocity considered anisotropic along the principal axis (m/s)

$T$  = temperatures,  $T_s$  for dry soil and  $T_w$  for saturated soil (K)

$c$  = volume heat capacity,  $c_s$  for dry soil and  $c_w$  for saturated soil (J/kg K)

$\rho$  = mass density of the porous matrix (kg/m<sup>3</sup>)

$n$  = porosity

The fluid properties necessary for the application of the equations above are evaluated at the bulk temperature, thus mitigating the need of an iterative process. The formulas calculating the temperature gradient in Chapter 4 for shallow and deep zones were introduced in the software for summer and winter operation.

The basic equation governing the heat flow in a BH and the surrounding area, used in FlexPDE (PDE Solutions Inc) use is:

$$Q = \rho c_p \frac{\partial T}{\partial t} + \rho_f c_{pf} u_{in} \cdot \nabla T + \rho_w c_{pw} u_p \cdot \nabla T + \nabla \cdot (-\lambda \nabla T) \quad (12)$$

where  $\rho$  denotes the density (kg m<sup>-3</sup>),  $u$  the velocity (m s<sup>-1</sup>),  $T$  the temperature (K),  $c_p$  the specific heat capacity (J kg<sup>-1</sup> K<sup>-1</sup>),  $\lambda$  the thermal conductivity (W m<sup>-1</sup> K<sup>-1</sup>),  $Q$  the power density of the heat source (W m<sup>-3</sup>). Subscript  $f$  denotes fluid,  $w$  denotes water,  $in$  denotes inside tube and  $p$  denotes porous media.

The full validation of the model is shown in section 3.4 where underground temperature profile is implemented in the basic formula.

### 3.3 Programming with FlexPDE

FlexPDE (PDE Solutions Inc) is a script-driven program which based on user inputs constructs a system finite-element model, solves it, and presents graphical outputs (Figure 3- 4).



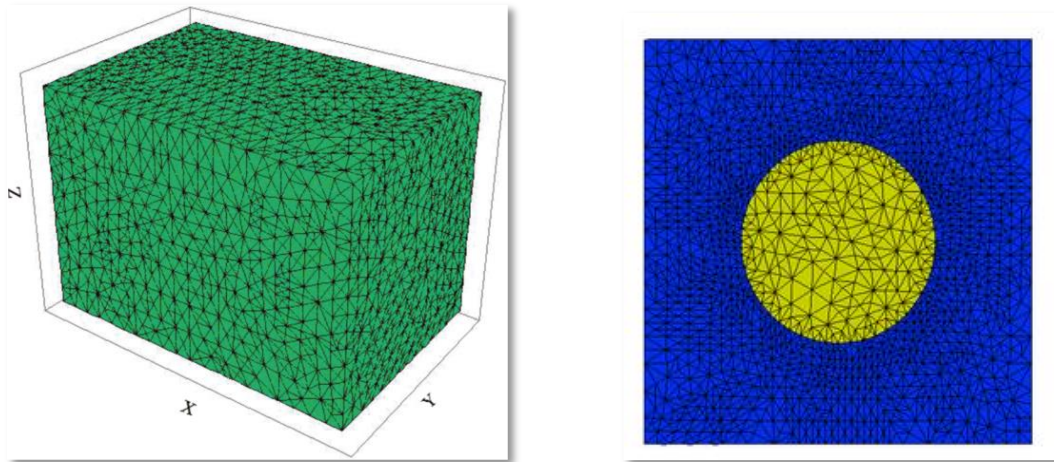


Figure 3- 4: Meshes created with FlexPDE Software

A script written in FlexPDE software (PDE Solutions Inc) is a readable text file consisting of a number of sections, each identified by a header. The main sections are:

- TITLE – a label for the output
- SELECT – user controls over the default behaviour of FlexPDE
- VARIABLES – name dependent variables
- DEFINITIONS – definitions of useful parameters, relationships or functions
- EQUATIONS –association of partial differential equations and variable
- BOUNDARIES – definition of the perimeter of the domain, description of the geometry of each part, joining together line or arc segments
- MONITORS and PLOTS – desired graphical output and any combination of CONTOUR, SURFACE, ELEVATION or VECTOR plots are listed
- END – completes the script
- Comments can be placed anywhere in a script.

The easiest way to setup a problem is by defining the following in the following order: variables and equations, domain, material parameters, boundary conditions and finally specifying the graphical output.

An example of the model/script for the needs of FlexPDE (PDE Solutions Inc) in order to solve a typical energy analysis problem of a vertical U-tube GHE, crossed by an aquifer, is shown in APPENDIX I. The script is explained in great detail with comments and can be used for any GHE by adjusting the relevant parameters.

### **3.3.1 Properties and Geometry of the Proposed Model**

The script written for the needs of FlexPDE (Appendix I) refers to a geothermal system combining a borehole heat exchanger and the surrounding soil mass crossed by an aquifer. The GHE domain is illustrated in Figure 3- 5 and Figure 3- 6.

Because of the difference in scales of the tube length compared to the diameter, there is a need for a large number of cells for adequate modeling. As FlexPDE (PDE Solutions Inc) tries to make mesh cells as nearly equilateral as possible, severely distorted cells increase the numerical difficulty of the matrix solution, especially for thin cylindrical shells. Therefore, a linear transformation was applied by using a scale factor in the z direction, in order to reduce calculation time. Several tests were made to ensure that the scale factor employed, (zscale) of 1% did not affect the accuracy of modelling.

The GHE domain is consists of five horizontal layers, with different thermal parameters and properties and the study area is a cylinder with radius (L) equal to 0.5 m. The center of the BH and study area is located at 0.0 (x,y). A single borehole is used, 102 m long ( $D_{total}$ ) with radius ( $D_{Rb}$ ) 0.1 m. The heat exchangers are of the single U-tube connection. The tubes used are 100 m in length ( $D_a$ ), 0.0285 m inner diameter ( $D_{in}$ ) and wall thickness 3.5 mm ( $D_{pthick}$ ). The distance between the centre of the tube and the centre of borehole ( $D_{cpc}$ ) is 0.048 cm and the borehole is filled with bentonite. The initial temperature of the ground and the underground water temperature was set to 23.2° C. All the GHE characteristics used in the simulation are shown in Table 3 - 1.

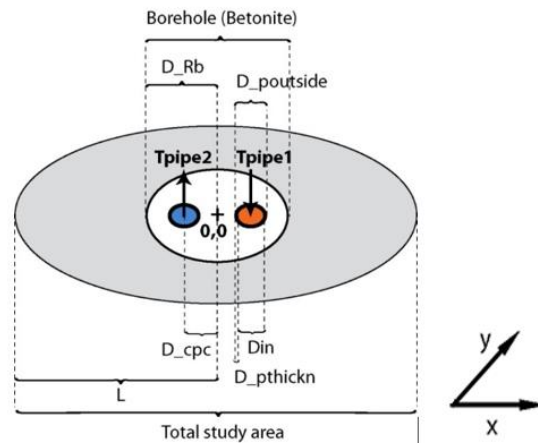


Figure 3- 5: A cross section of the Borehole

Table 3 - 1: Borehole properties

Property	Value	Unit	Symbol used in software
Fluid velocity in tubes	0.5	$\text{m s}^{-1}$	upipe
Fluid density	1000	$\text{Kgm}^{-3}$	ro
Fluid specific heat	4182	$\text{J Kg}^{-1} \text{K}^{-1}$	cp
Fluid thermal conductivity	0.58	$\text{W m}^{-1}\text{K}^{-1}$	K
Inner diameter of tube	0.025	m	Din
External diameter heat exchanger tube	0.032	m	D_poutside
Wall thickness of heat exchanger tube	0.0035	m	D_pthick
Distance between center of borehole to center of each heat exchanger tube	0.048	m	D_cpc
Temperature of ground	23.2	$^{\circ} \text{C}$	Temp initial
Rock density (Region 1)	1800	$\text{Kgm}^{-3}$	ro
Rock specific heat (Region 1)	780	$\text{J Kg}^{-1} \text{K}^{-1}$	cp
Rock thermal conductivity (Region 1)	1.5	$\text{W m}^{-1}\text{K}^{-1}$	K
Rock density (Region 2)	1290	$\text{Kgm}^{-3}$	ro
Rock specific heat (Region 2)	780	$\text{J Kg}^{-1} \text{K}^{-1}$	cp
Rock thermal conductivity (Region 2)	1.7	$\text{W m}^{-1}\text{K}^{-1}$	K
Rock density (Region 3)	2234	$\text{Kgm}^{-3}$	rsw

Property	Value	Unit	Symbol used in software
Rock specific heat (Region 3)	780	J Kg <sup>-1</sup> K <sup>-1</sup>	cp
Rock thermal conductivity for dry soil (Region 3)	0.9	W m <sup>-1</sup> K <sup>-1</sup>	K_dry
Rock thermal conductivity for saturated soil (Region 3)	1.1	W m <sup>-1</sup> K <sup>-1</sup>	K_satur
Specific heat for dry soil (Region 3)	718	J Kg <sup>-1</sup> K <sup>-1</sup>	cs
Specific heat for saturated soil (Region 3)	4180	J Kg <sup>-1</sup> K <sup>-1</sup>	cw
Rock density (Region 4)	2000	Kgm <sup>-3</sup>	ro
Rock specific heat (Region 4)	880	J Kg <sup>-1</sup> K <sup>-1</sup>	cp
Rock thermal conductivity (Region 4)	1.7	W m <sup>-1</sup> K <sup>-1</sup>	K
Rock density (Region 5)	1000	Kgm <sup>-3</sup>	ro
Rock specific heat (Region 5)	780	J Kg <sup>-1</sup> K <sup>-1</sup>	cp
Rock thermal conductivity (Region 5)	0.8	W m <sup>-1</sup> K <sup>-1</sup>	K
Borehole radius	0.1	m	D_Rb
Thermal conductivity of Borehole fill- dry	0.8	W m <sup>-1</sup> K <sup>-1</sup>	K
Thermal conductivity of Borehole fill- saturated	0.8	W m <sup>-1</sup> K <sup>-1</sup>	K
Borehole fill density	1000	Kgm <sup>-3</sup>	ro
Specific heat of borehole dry fill	780	J Kg <sup>-1</sup> K <sup>-1</sup>	cp
Specific heat of borehole saturated fill	2000	J Kg <sup>-1</sup> K <sup>-1</sup>	cp
Length of heat exchanger	100	m	D_a
Convection heat transfer coefficient	2145	Wm <sup>-2</sup> K <sup>-1</sup>	ho
Scaling factor	0.01		zscale

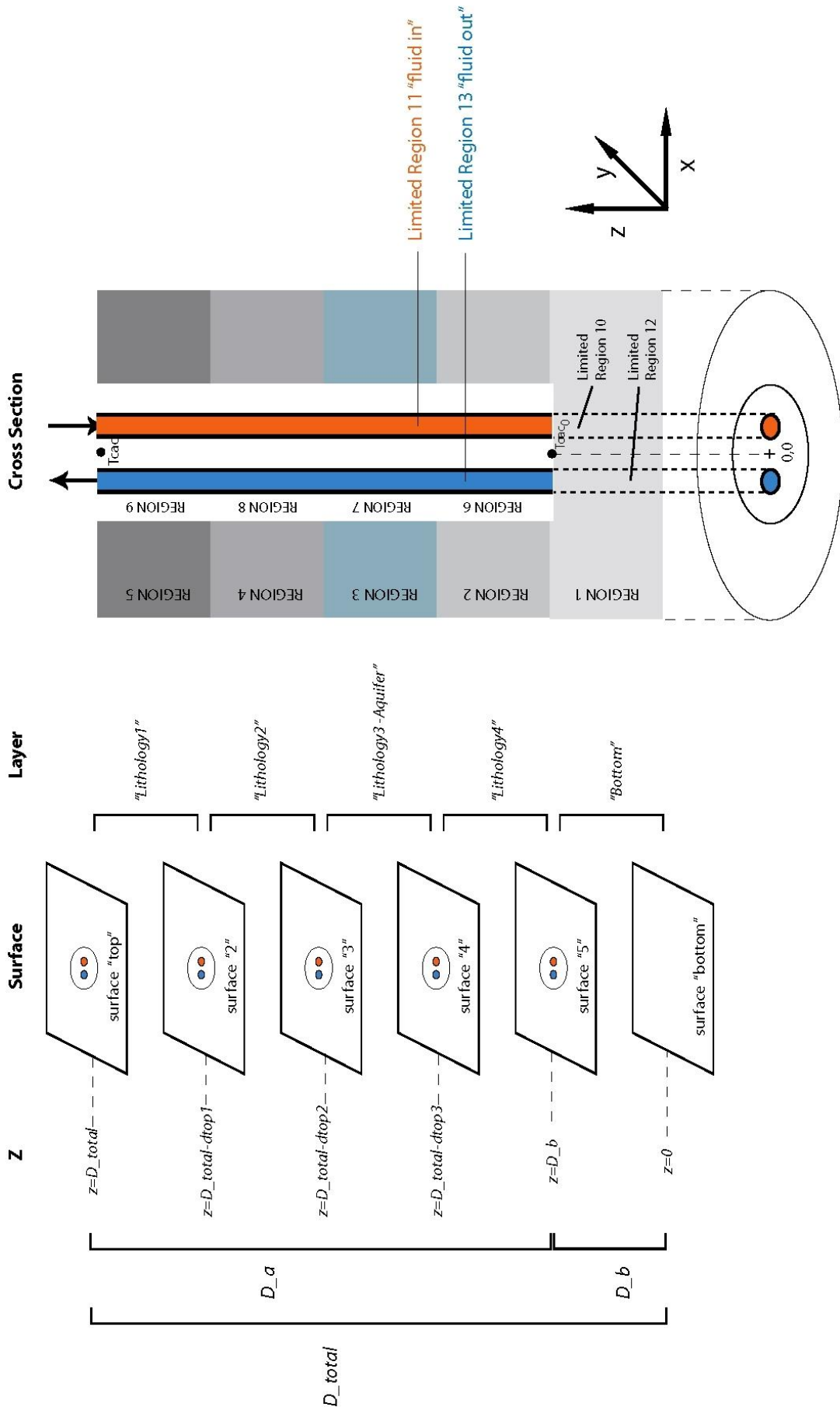


Figure 3- 6: Explanatory diagram of the study area, as used in the FlexPDE (not in scale)

The final 3D mesh and the 3D domain created by the software are shown in Figure 3- 7 and Figure 3- 8 respectively. The figures also illustrate the scaled geometry of the GHE.

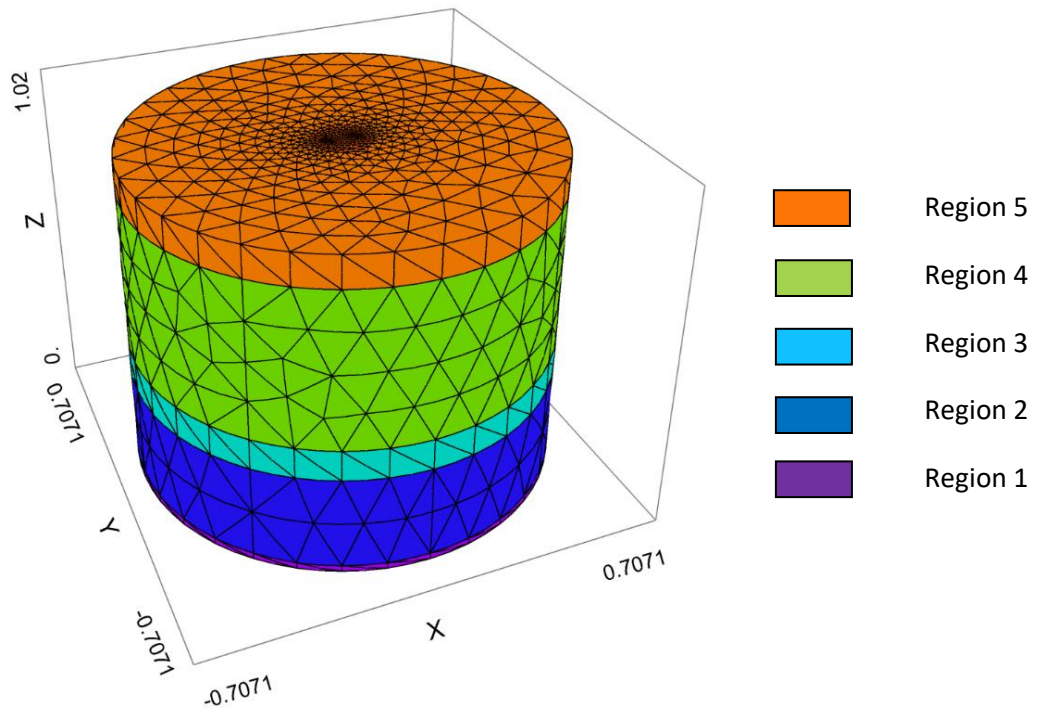


Figure 3- 7: Final 3D Mesh created by FlexPDE software

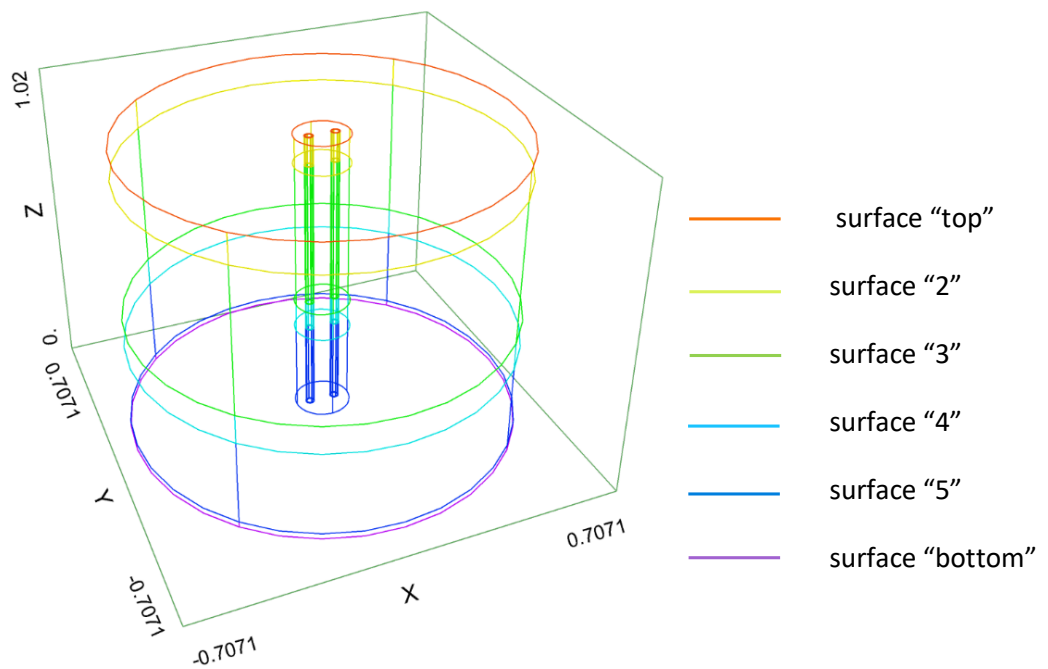


Figure 3- 8: 3D Domain created by FlexPDE software

### 3.3.2 Simulation Results

The results of FlexPDE (PDE Solutions Inc) simulations are obtained by using the commands HISTORY and CONTOUR under the section “PLOTS” of the software. HISTORY plots display the variation of temperature across the stages of a problem and CONTOUR creates contour lines for temperature at any point of the study area (more details in Appendix I).

Figure 3- 9 illustrates the output graphs displaying temperature values, after 50 hours of operation, for:

- 1) Input fluid temperature (Tfluidin)
- 2) Output fluid temperature (Tfluidout)
- 3) The temperature at the center of the domain at point Tcac (see Figure 3- 6).

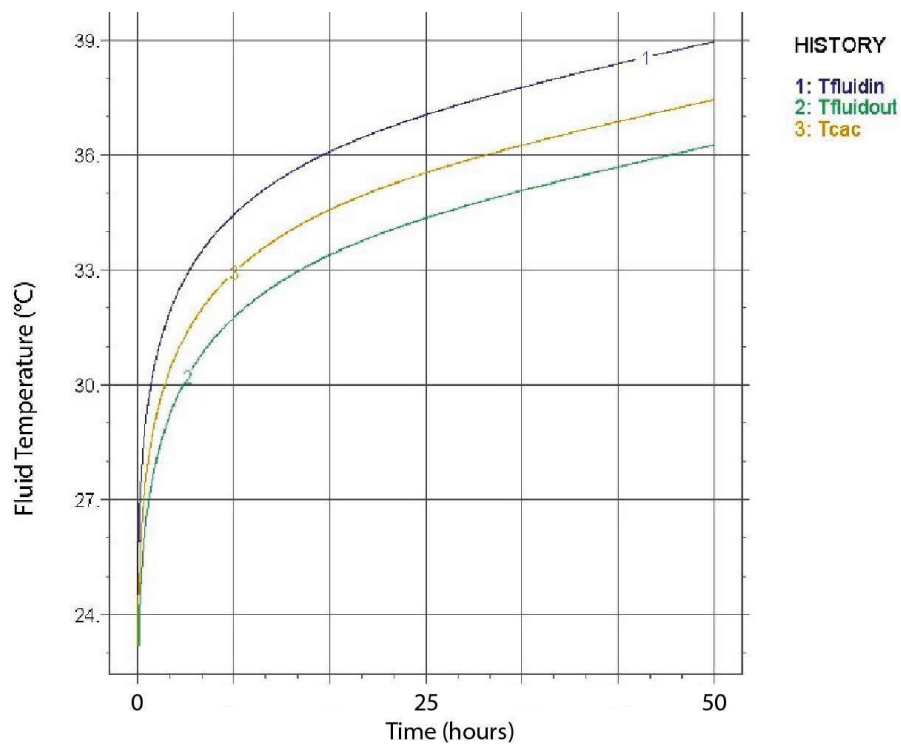


Figure 3- 9: Input fluid temperature (Tfluidin), output fluid temperature (Tfluidout) and temperature at the center of the domain (at point Tcac) vs Time

Figure 3- 10, Figure 3- 11 and Figure 3- 12 illustrate a cross section of temperature distribution around the borehole at different z levels after 50 hours of operation; Figure 3- 10 at the top surface of the GHE ( $z = D\_Total$ ), Figure 3- 11 at level 0.35 i.e. at the level where the aquifer is crossing the BH and Figure 3- 12 at the end of the tubes at the point of U-tube connection.

The GHE is working in summer mode and as we can observe from the isothermal ellipse lines, the temperature of the input side (right side) is higher, therefore the ground temperature around the tube is higher than that on the left side. Ground, at this point, is working as a sink by absorbing heat from the input fluid. In this way, lower temperature values at the left tube i.e. output fluid are observed. Also, isothermal lines illustrated at the point where the aquifer is crossing the borehole show lower values (Figure 3- 11). Temperature distribution along the center of the input and output tube, after 50 h of operation, is shown in Figure 3- 13 and Figure 3- 14 respectively. Isothermal lines created around the right tube have higher values than those of the left tube, confirming the results of Figure 3- 10, Figure 3- 11 and Figure 3- 12.

Finally, in Figure 3- 15 the temperature distribution along the center of the GHE tubes is presented. The right tube with the higher temperature is the input side and the left tube the output side.

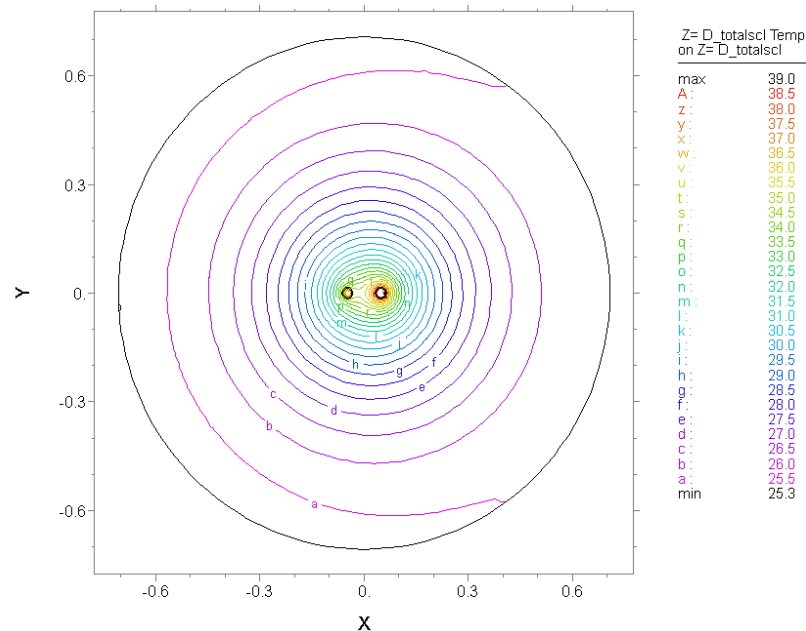


Figure 3- 10: Temperature distribution around the borehole at the surface, after 50 h of operation



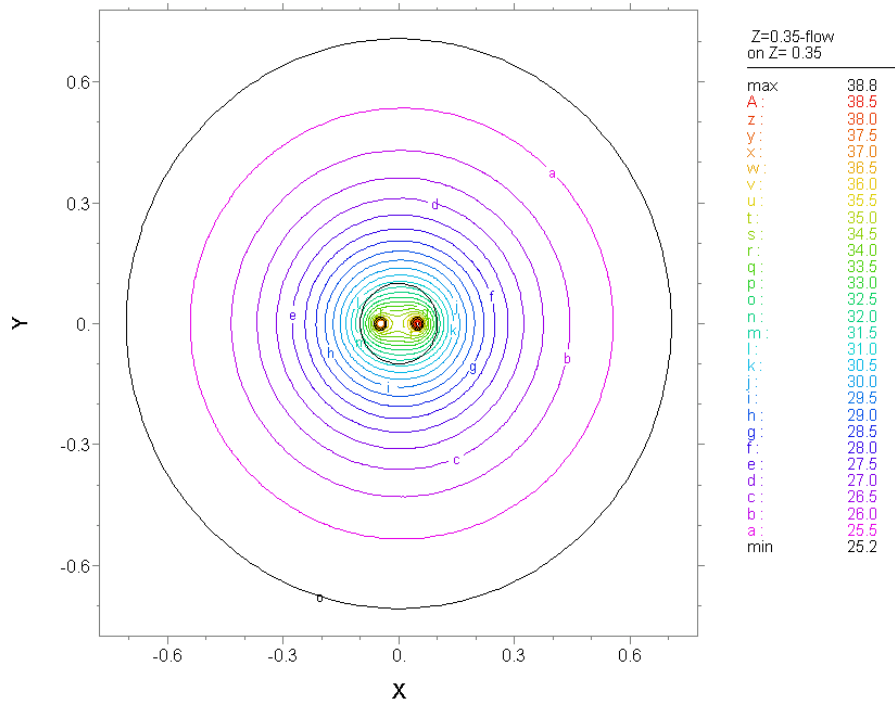


Figure 3- 11: Temperature distribution around the borehole at the level of the aquifer, after 50 h of operation

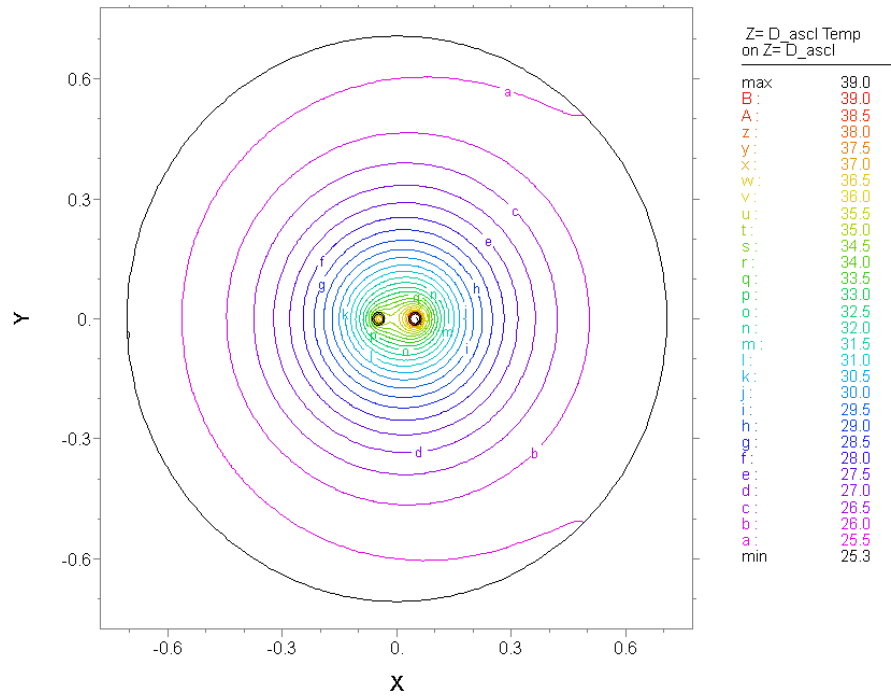


Figure 3- 12: Temperature distribution around the borehole at the end of the tubes, after 50 h of operation

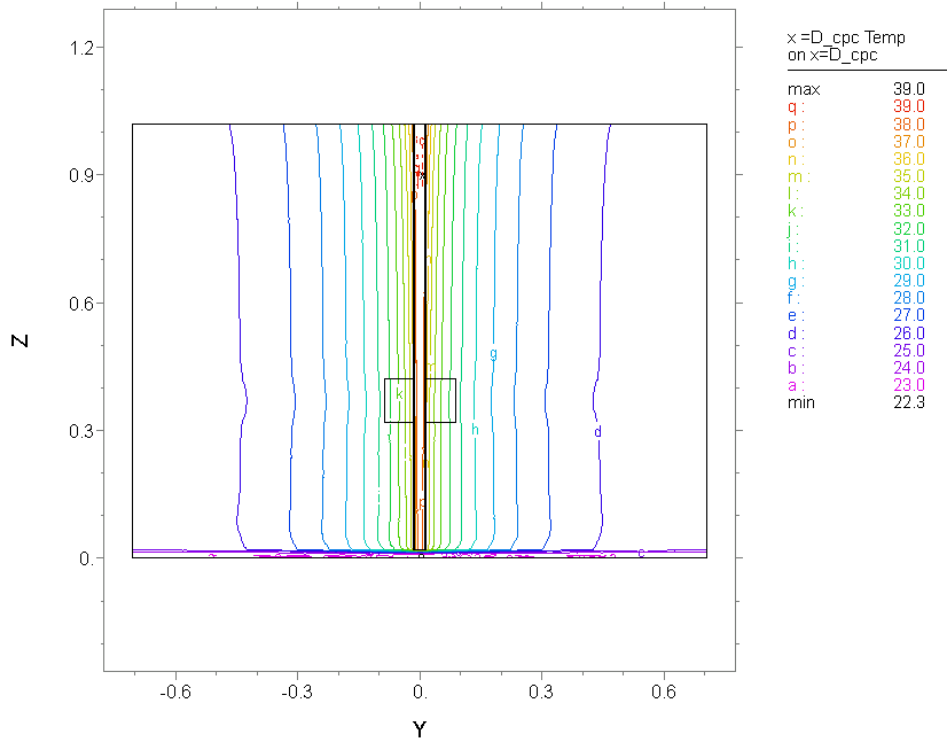


Figure 3- 13: Temperature distribution along the center of the right tube (inlet), after 50 h of operation

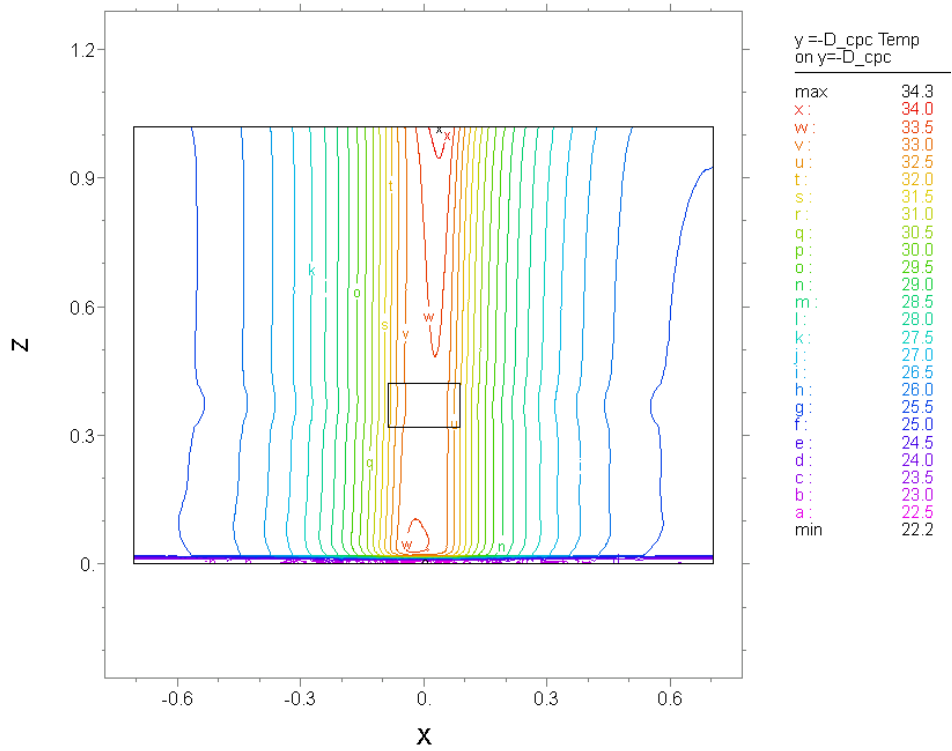


Figure 3- 14: Temperature distribution along the center of the left tube (outlet), after 50 h of operation

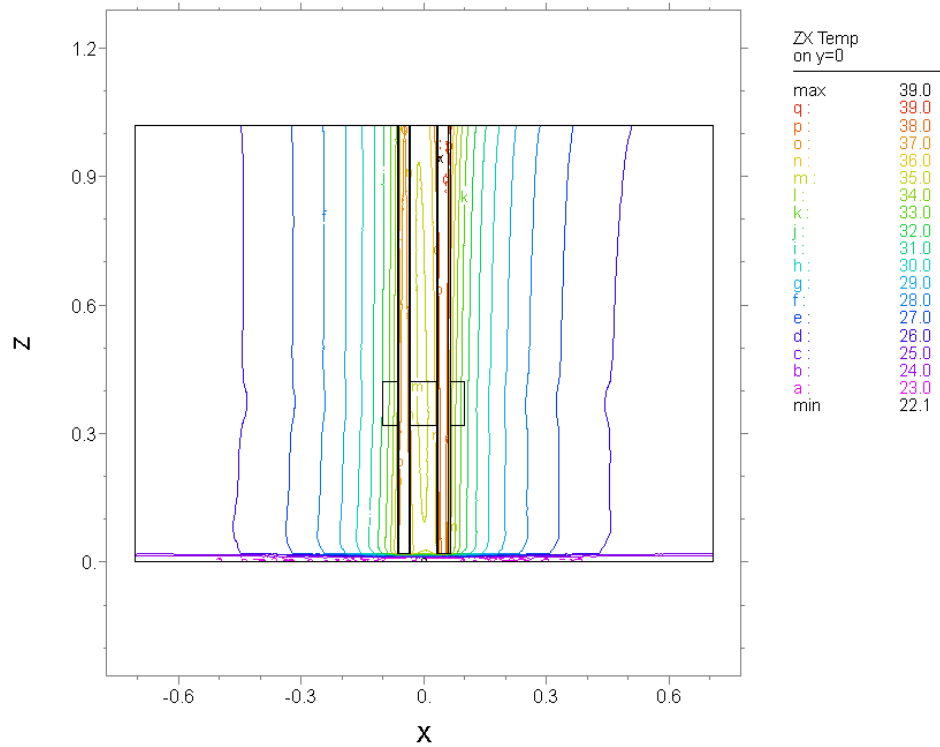


Figure 3- 15: Temperature distribution around the borehole along the center of the domain, after 50 h of operation

### 3.4 Summary

In this chapter, the mathematical model that governs the heat transfer in vertical GHEs in dry and water saturated rocks/soils with or without groundwater flow were presented. A computational model was constructed in the FlexPDE software (PDE Solutions Inc) environment and the thermal response of the GHE was investigated.

Temperature distribution in the ground along the centre of the BH, after 50 h of operation, was plotted. Isothermal lines created around the input tube have higher values than those of the output tube due to the temperature loss to the ground in the cooling mode operation.

## Chapter 4: Model Validation

### 4.1 Introduction

In a GHE system, fluid circulates through tubes that are located inside a borehole (BH), resulting in indirect thermal contact between the fluid and the subsurface. This method is controlled by the effective heat exchange area of the GHE and can be limited by the equipment involved, i.e. the tubes, the grouting material of the GHE (Christodoulides et al., 2012), the velocity of circulating liquid (Bidarmaghz et al., 2013), the thermal conductivity of the subsurface (Stylianou et al., 2016; Christodoulides et al., 2016; Florides et al., 2013; Svec et al., 1983) and the presence of underground water (Fujii et al., 2013; Fan et al., 2007). It is therefore important to identify ways and use validated tools for the technical and economic optimisation of the GHE system.

The chapter focuses on a methodology of calculating the heat injection rates of GHEs, depending on the borehole characteristics. The effect of the (a) summer and winter mode of operation, (b) U-tube tube diameter, (c) U-tube leg and borehole center distance, (d) borehole diameter, (e) circulating water velocity and (f) groundwater flow velocity was investigated. To validate the proposed methodology, two study cases were set up in areas with high potential for geothermal usage.

The first area considered was the coastal area, at the west part of the island and the second area very close to Nicosia, the capital city of Cyprus. The seasonal difference of environmental temperature in Cyprus between mid-summer and mid-winter is quite large, being about 18 °C inland and about 14 °C in the coastline. Differences between day maximum and night minimum temperatures are also quite large, especially inland in the summer. The aforementioned differences in winter are between 8 to 10 °C at the lowlands and 5 to 6 °C on the mountains, increasing in summer to 16 °C at the central plain of the island (capital city) and 9 to 12 °C elsewhere (Meteorological Service Cyprus, [www.moa.gov.cy/ms](http://www.moa.gov.cy/ms)).

The temperature of the ground in Cyprus was recorded in eight Boreholes, in the framework of a project undertaken by the Cyprus University of Technology and funded by the Research Promotion Foundation of Cyprus (ΤΕΧΝΟΛΟΓΙΑ/ ΕΝΕΡΓ/ 0308(BIE)/ 15), for the efficient use of Ground Coupled Heat Pumps in Cyprus (Florides et al., 2011; Pouloupatis et al., 2010). Among them were the Prodromi and Lakatameia BH, which were used as study cases in this Chapter of the thesis (Figure 4 - 1).

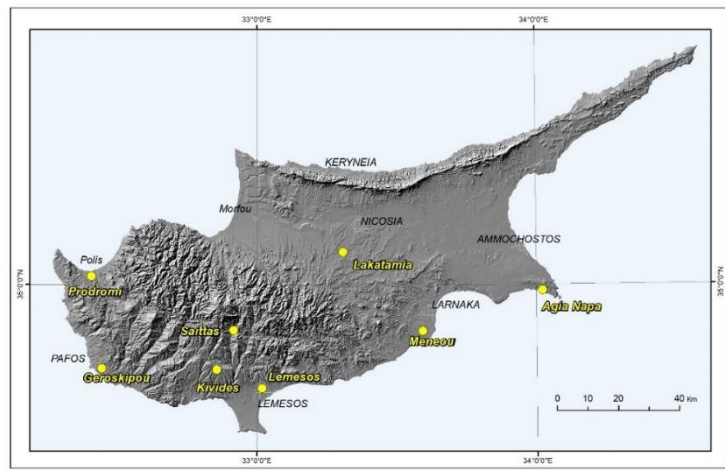


Figure 4 - 1: Positions of 8 geothermal boreholes in Cyprus (Florides et al., 2011; Pouloupatis et al., 2010)

The temperatures measured in February, July and December at the two Boreholes chosen as study cases, were used to fit correlations of the variation of ground temperature with depth. These correlations Boreholes were used in the FlexPDE software (PDE Solutions Inc) to investigate the behavior of the GHE to changes in design and input parameters.

## 4.2 Model Validation and Results

### 4.2.1 Study Case at the Prodromi Area

#### 4.2.1.1 Experimental Data

The BH drilled at Prodromi village, near Polis Chrysochou in Cyprus (Figure 4 - 1) is 100 m deep and has a diameter of 0.2 m. The distance from the center of the borehole to the center of

each tube is 0.05 m. The GHEs were of the U type with plastic tubes (polyethylene) of 3 mm thickness, 32 mm external diameter,  $0.51 \text{ W m}^{-1} \text{ K}^{-1}$  thermal conductivity,  $950 \text{ kg m}^{-3}$  density and  $1800 \text{ W m}^{-1} \text{ K}^{-1}$  specific heat capacity. The space between the tubes and the hole was filled with bentonitic clay to ensure good contact between the tube and the undisturbed ground and reduce the thermal resistance. The initial ground temperature during the Thermal Response Test (TRT) was  $21^\circ\text{C}$ . The TRT is a method used to determine the ground thermal characteristics (Mogensen, 1983) and is based on the injection of constant thermal energy into the BH ( $2,780 \text{ W}$  at  $21^\circ\text{C}$  in this case) while recording the mean borehole temperature during the test. The geological log of the BH, with the measured thermal properties of each underground layer, are shown in Table 4 - 1. For the direct measurement of the thermophysical properties of the different types of Lithology, the Isomet 2104 (Applied Precision, Inc) portable heat transfer analyzer was used (see Chapter 5: Measurement and Analysis of the Thermal Properties of Rocks for the Compilation of Geothermal Maps).

Table 4 - 1: Thermal properties of the Prodromi borehole (thermal conductivity, specific heat capacity, density)

Layer	Depth (m)		Type of Lithology	Thermal conductivity $\lambda$ ( $\text{W m}^{-1} \text{ K}^{-1}$ )	Specific heat capacity $c_p$ ( $\text{W kg}^{-1} \text{ K}^{-1}$ )	Density $\rho$ ( $\text{kg m}^{-3}$ )
	From	To				
top	0	9	Pale yellow chalk	1.64	731	2,353
1	9	50	White very hard limestone	1.73	780	2,290
2	50	80				
3	80	100	Light bluish-grey very hard limestone with some bands of white very hard limestone	1.94	840	2,330
bottom	100	105				

### 4.2.1.2 Validation

To validate the numerical model, the script written in FlexPDF software was adjusted for the geometry and the thermal properties of the Prodromi BH. The velocity of the (PDE Solutions Inc) underground water was set to zero, as no underground water was present in the BH. The output graphs of the resulted model are illustrated in Figure 4 - 2. A comparison of the output data with the in-situ TRT results obtained for the Prodromi borehole is shown in Table 4 - 2 and Figure 4 - 3.

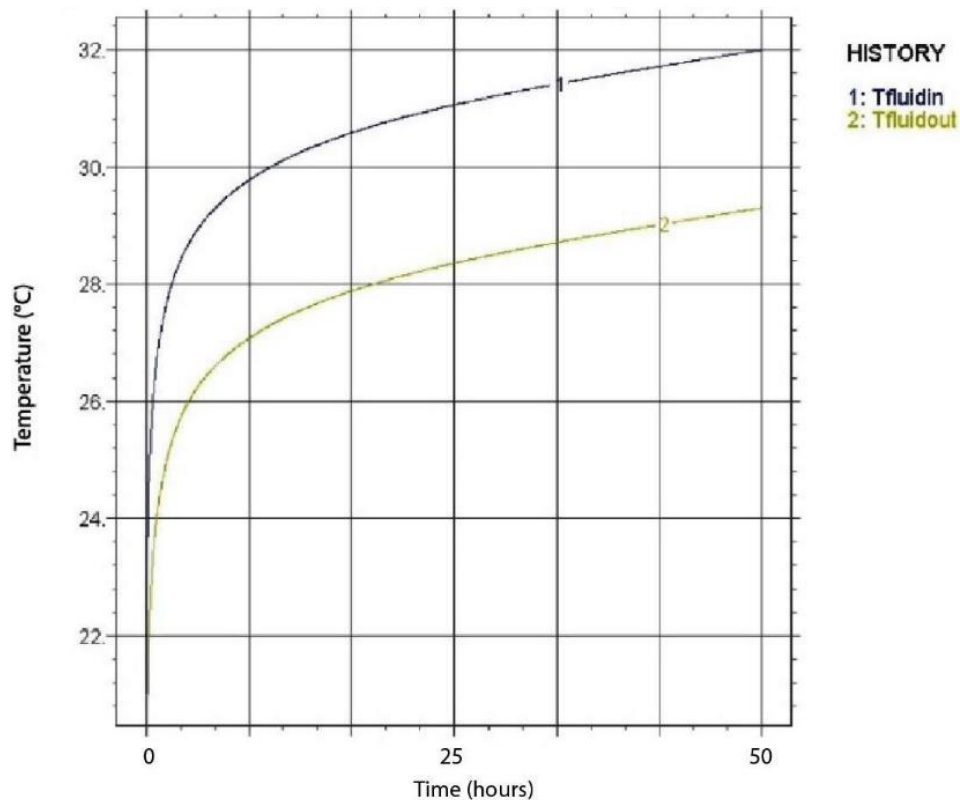


Figure 4 - 2: Output graph showing inlet (Tfluidin) and outlet (Tfluidout) fluid temperature

As observed there is a good agreement allowing one to confidently use the numerical model to extract realistic conclusions for the conditions specified.

Table 4 - 2: Temperature values calculated with the use of the Flex software and temperature values measured with the TRT carried out at the Prodromi BH

Time (h)	Fluid INLET Temperature at Prodromi BH TRT <b>Tin TRT (°C)</b>	Fluid INLET Temperature <b>Tin calculated (°C)</b>	Fluid OUTLET Temperature at Prodromi BH TRT <b>Tout TRT (°C)</b>	Fluid OUTLET Temperature <b>Tout calculated (°C)</b>
0	21.0	21.0	21.0	21.0
2.0	28.8	28.2	26.2	25.7
5.0	29.4	29.0	27.0	26.5
9.0	29.9	29.9	27.5	27.3
16.5	30.8	30.6	28.0	27.9
25.0	31.0	31.0	28.6	28.4
34.0	31.2	31.4	29.2	28.8
41.5	31.9	31.8	29.5	29.2
50.0	32.0	32.0	29.7	29.5

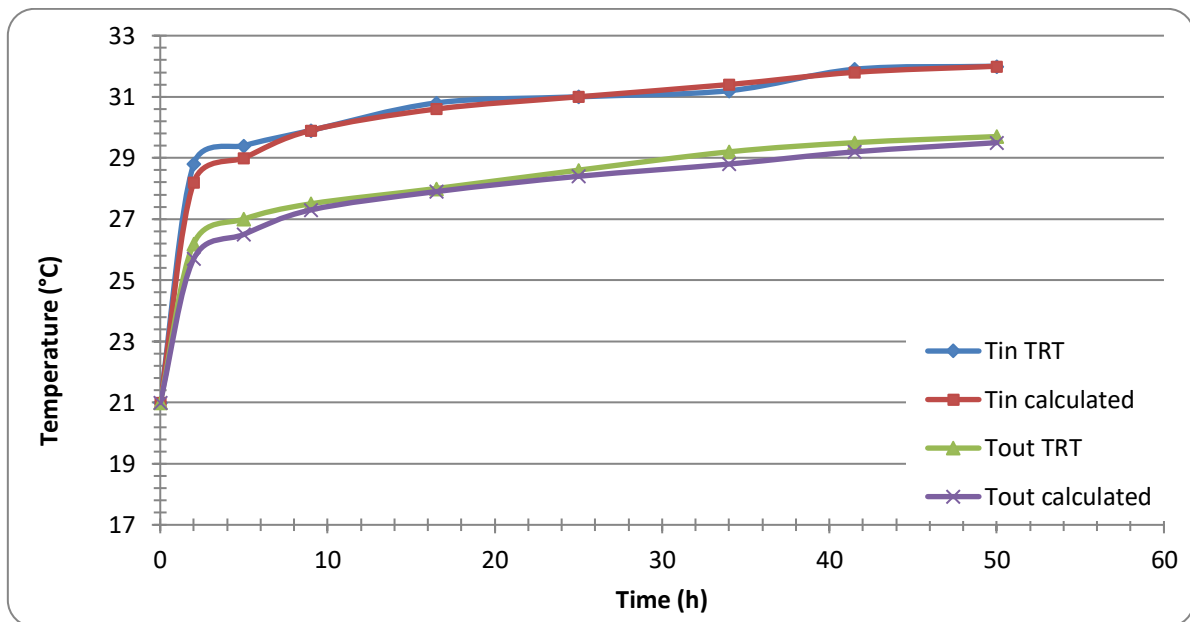


Figure 4 - 3: Comparison of numerical model results with measured TRT data (GHE at Prodromi area)



### 4.2.1.3 Parameterization of the GHE

This section presents the evaluation of the thermal response of the BH by changing its main features: (a) the distance between GHE legs and BH centre and (b) the circulating fluid velocity. These are important design parameters for GHEs.

#### A. Distance between the centre of each tube and the centre of the borehole

The Flex PDE script was set up to examine the effect of varying the distance between the centre of each tube and the center of the borehole ( $D_{cpc}$ ). GHE was working in summer mode, i.e. heat was injected into the ground and runs were performed for  $D_{cpc}$  equal to 0.045, 0.048, 0.060, 0.070, 0.080 and 0.090 m.

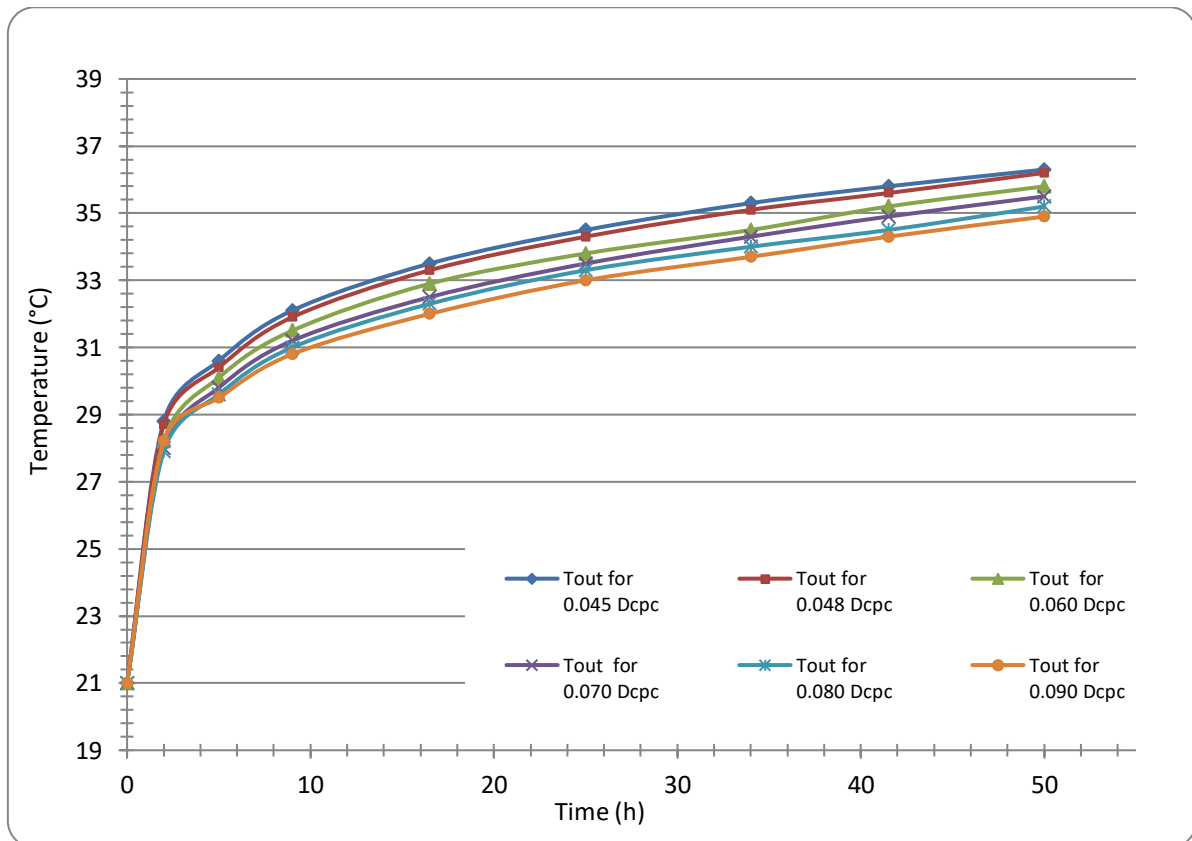


Figure 4 - 4: Output Temperatures for different values of the distance between the centre of each tube and the centre of the borehole ( $D_{cpc}$ )

Results are illustrated in Table 4 - 3 and Figure 4 - 4 and prove that the tubes in-between distance is of great importance. The closer the tubes are, the higher the outlet fluid temperature is, i.e. the lower the performance of the GHE. This is because only the one side of each tube can exchange heat directly with the ground, since a part of each tube is blocked by the other tube. In Figure 4 - 4, where the temperatures of fluid exiting the GHE are illustrated, it is clearly indicated that by increasing the distance between the two tubes, the temperature of the exiting fluid is reduced and the performance of the GHE, when working in summer mode, is increased.

Comparing the results of GHE output temperature after 50 hours of operation (Table 4 - 4), it can be seen that there is almost a linear relationship between the centre distance of the two tubes and the outlet temperature of the GHE (Figure 4 - 5).

Table 4 - 3: Outlet Temperature values calculated for different values of D\_cpc (distance between the centre of each pipe and the centre of the borehole)

Time (h)	Outlet temperature for D_cpc <b>0.045 m</b> (°C)	Outlet temperature D_cpc <b>0.048 m</b> (°C)	Outlet temperature for D_cpc <b>0.060 m</b> (°C)	Outlet temperature for D_cpc <b>0.070 m</b> (°C)	Outlet temperature for D_cpc <b>0.080 m</b> (°C)	Outlet temperature for D_cpc <b>0.090 m</b> (°C)
0	21.0	21.0	21.0	21.0	21.0	21.0
2.0	28.8	28.7	28.2	28.0	27.9	28.2
5.0	30.6	30.4	30.1	29.8	29.6	29.5
9.0	32.1	31.9	31.5	31.2	31.0	30.8
16.5	33.5	33.3	32.9	32.5	32.3	32.0
25.0	34.5	34.3	33.8	33.5	33.3	33.0
34.0	35.3	35.1	34.5	34.3	34.0	33.7
41.5	35.8	35.6	35.2	34.9	34.5	34.3
50.0	36.3	36.2	35.8	35.5	35.2	34.9

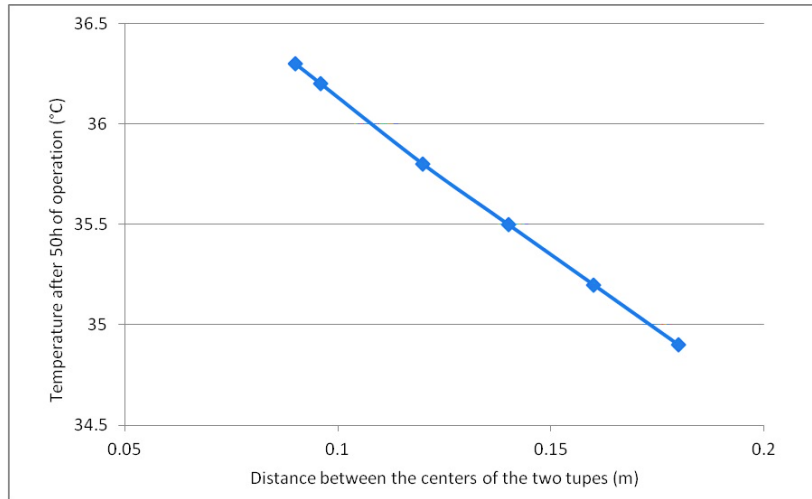


Figure 4 - 5: Effect of centre to centre tube distance on the output fluid temperature, after 50 h of operation

Table 4 - 4: Temperature of fluid exiting GHE after 50h of operation

Distance between the centers of the two tubes (m) - Dcpc	Temperature of output fluid after 50h operation (°C)
0.090	36.3
0.096	36.2
0.120	35.8
0.140	35.5
0.160	35.2
0.180	34.9

## B. Influence of circulating fluid velocity

To investigate the effect of fluid velocity, seven different models were set up for seven different GHE circulating fluid velocities. In all FlexPDE runs, it was assumed that constant thermal energy (Q) 2780 W was injected into the borehole continuously for 50 hours.

Having in mind that heat load ( $Q$ ) equals:

$$Q = \frac{m \cdot c_p \cdot dT}{dt} \quad (1)$$

where  $m$  = mass (kg),  $c_p$  = specific heat capacity (J/K),  $dT$  = temperature difference (°C) and  $dt$  = time duration (s)

then, by changing the fluid velocity in the heat exchanger, we also must consider in our calculations that the total mass of the fluid also changes as:

$$m = A \cdot u \cdot \rho \quad (2)$$

where,  $m$  = fluid mass (kg),  $A$  = cross section area of tube (m<sup>2</sup>),  $\rho$  = density (kg/m<sup>3</sup>) and  $u$  = fluid velocity (m/s). This change also affects the value of heat transfer coefficient ( $h$ ) (Chapter 3, Equation 5), which depends on Reynolds and Prandtl number (Chapter 3, Equation 6).

The results of GHE input and output fluid temperature are illustrated in Figure 4 - 6 and Figure 4 - 7 respectively. It can be seen that for a constant heat input, increasing the fluid velocity reduces both the input but also the output temperature of the GHE.

Figure 4 - 8 shows the effect of circulating fluid velocity on the mean temperature ( $(T_{out} - T_{in})/2$ ) of the GHE, after 50 h of operation. Comparing the mean fluid temperature for different values of fluid velocity, we observe that the GHE has an outlet fluid temperature of 35.5°C after 50 h of operation for 1.5 m/s as opposed to 36.4°C for 0.4 m/s.

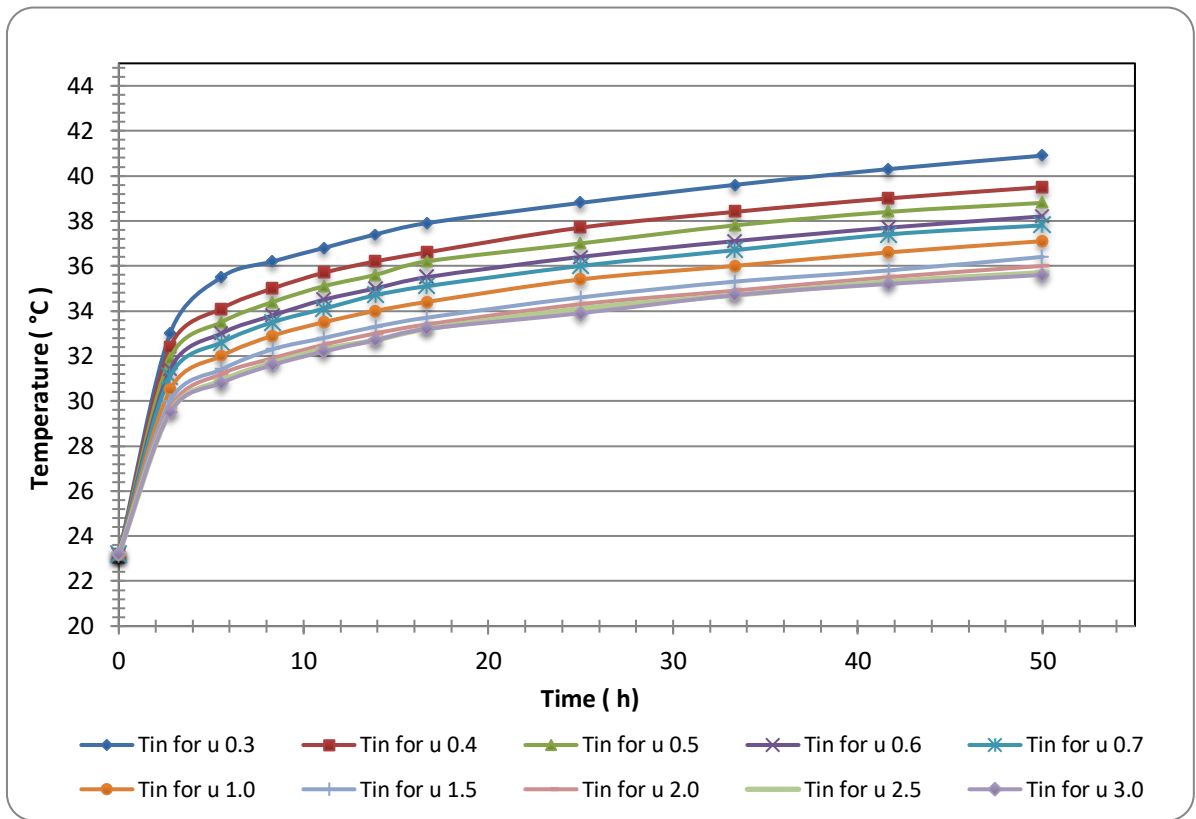


Figure 4 - 6: Input fluid temperature for different values of fluid velocity and constant heat injected into the borehole

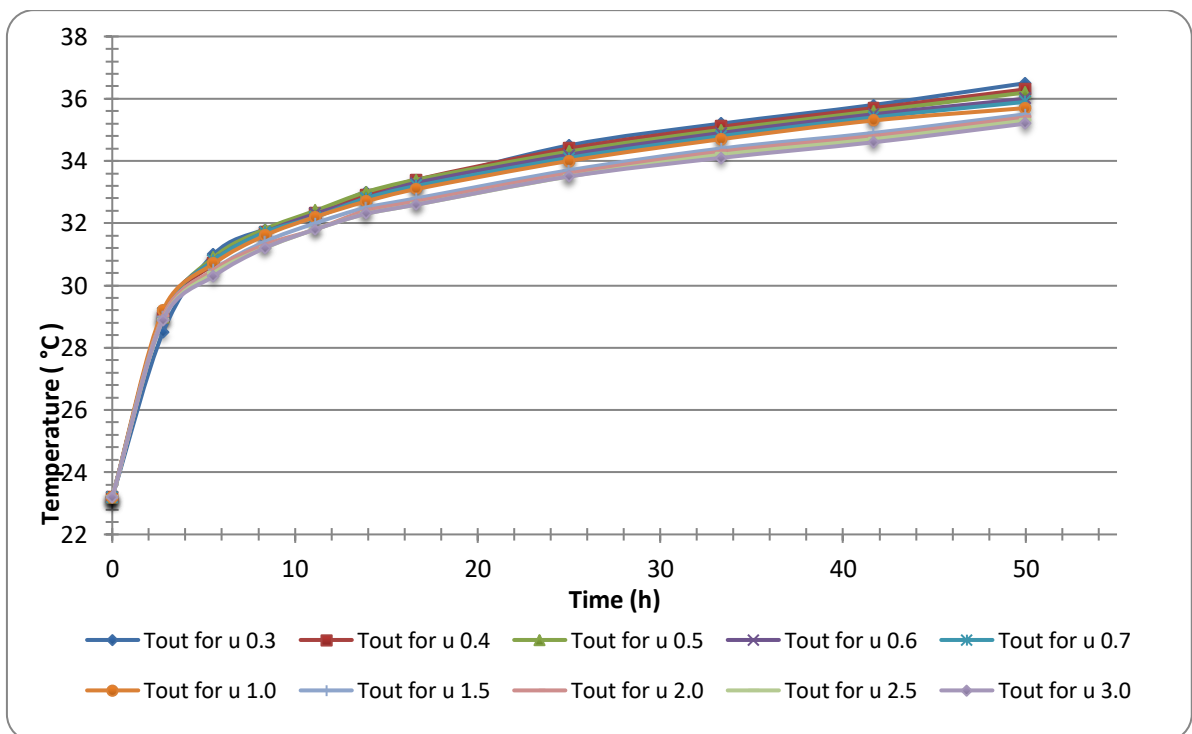


Figure 4 - 7: Output fluid temperatures of for different values of fluid velocity and constant heat injected into the borehole

Table 4 - 5: Values of inlet and outlet temperature after 50 h of operation for different fluid velocities

Fluid velocity (m/s)	Temperature of INPUT fluid (°C) (after 50 h of operation)	Temperature of OUTPUT fluid (°C) (after 50 h of operation)
0.3	40.9	36.5
0.4	39.5	36.3
0.5	38.8	36.2
0.6	38.2	36.0
0.7	37.8	35.9
1.0	37.1	35.7
1.5	36.4	35.5
2.0	36.0	35.4
2.5	35.7	35.3
3.0	35.6	35.2

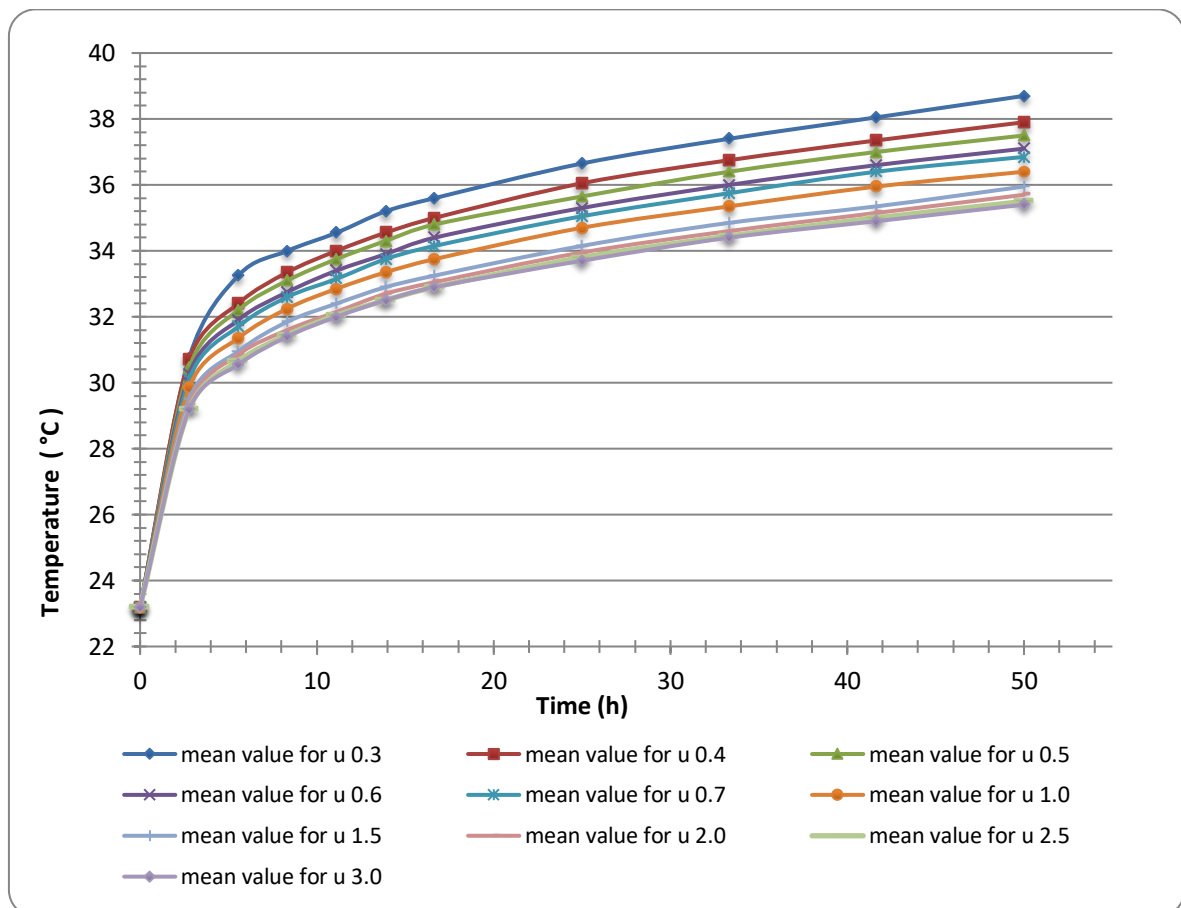


Figure 4 - 8: The effect of GHE fluid velocity on the mean temperature of GHE ((T<sub>out</sub>-T<sub>in</sub>)/2)

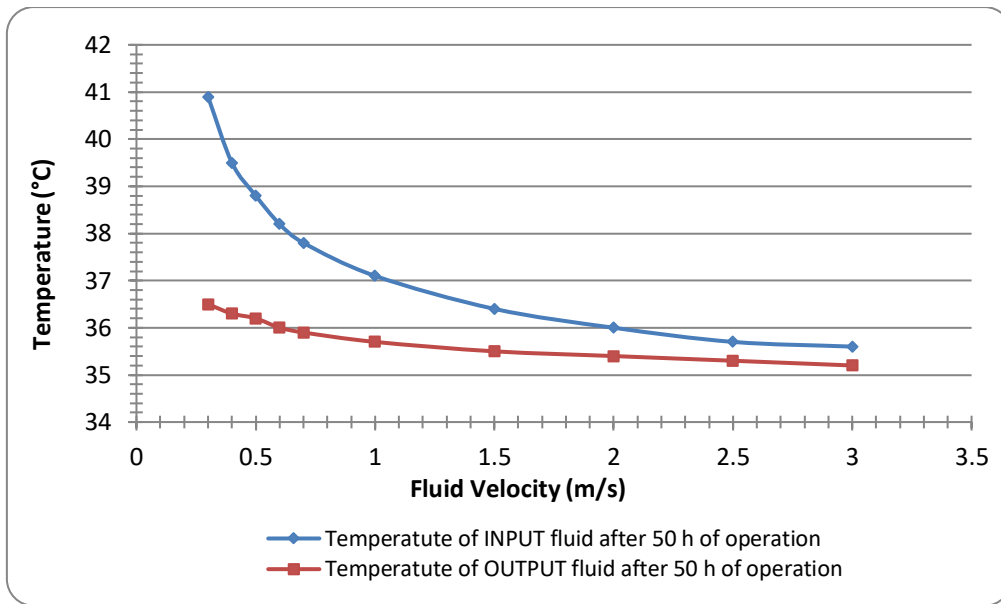


Figure 4 - 9: The effect of fluid velocity in the GHE on the inlet and outlet fluid temperature after 50 h of operation.

Figure 4 - 9 shows the values of inlet and outlet temperature after 50 h of operation. Here it is observed that after a certain velocity the difference between the inlet and outlet temperature diminishes. If we supply Equation 1 with this data, it is observed that the heat load transferred to the ground, above this critical velocity, is increasing only in small steps. This will also have a negative effect on the performance of a heat pump coupled to the GHE as by increasing the fluid velocity, the power consumption of the pump will be increasing too (Porwal, 2015).

## 4.2.2 Study Case at the Lakatameia Area

### 4.2.2.1 Experimental Data

At the Lakatameia BH (Figure 4 - 1), measured underground temperature for depths larger than 7m up to 100 m was approximately equal to 22 °C, increasing to 23 °C at the depth of 160 m. Recorded temperatures over a period of a year are shown in Figure 4 - 10.

The recorded temperatures at the Lakatameia BH shallow zone, at the most representative months of the year for heating and cooling, February, July, and December are shown in Figure

4 - 11 (Pouloupatis, 2014). The variation of the temperatures for the deep zone for the same months is shown in Figure 4 - 12. To input the variation of these temperatures in FlexPDE, best-fit polynomial equations were fitted to data as shown in Figure 4 - 11 and Figure 4 - 12. At the Lakatameia area, the vertical GHE was drilled to a depth of 160 m with a 20 cm diameter of drill. The study area is a circle with radius equal to 1.4 m and the heat exchanger is of the single U-tube configuration (see Figure 4 - 13). The tube material was polyethylene. The space between the tubes and the hole was filled with an appropriate grout material (bentonitic clay with cement) to ensure good contact between the tube and the undisturbed ground and to reduce the thermal resistance. The tube length was 160 m, the tube inner diameter 0.032 m and the wall thickness 0.003 m. The distance between the center of the tube and the center of the borehole was 0.06 m. The underground water level was at 80 m depth, measured from the surface (Florides et al., 2011). From the geological point of view, the BH consists of Marls (Nicosia Formation). The thermal conductivity of the ground was measured to be  $\lambda = 1.45 \text{ W m}^{-1} \text{ K}^{-1}$ . The soil/rock thermal properties of the area used in the simulations are given in Table 4 - 6 and the characteristics of the GHE in Table 4 - 7.

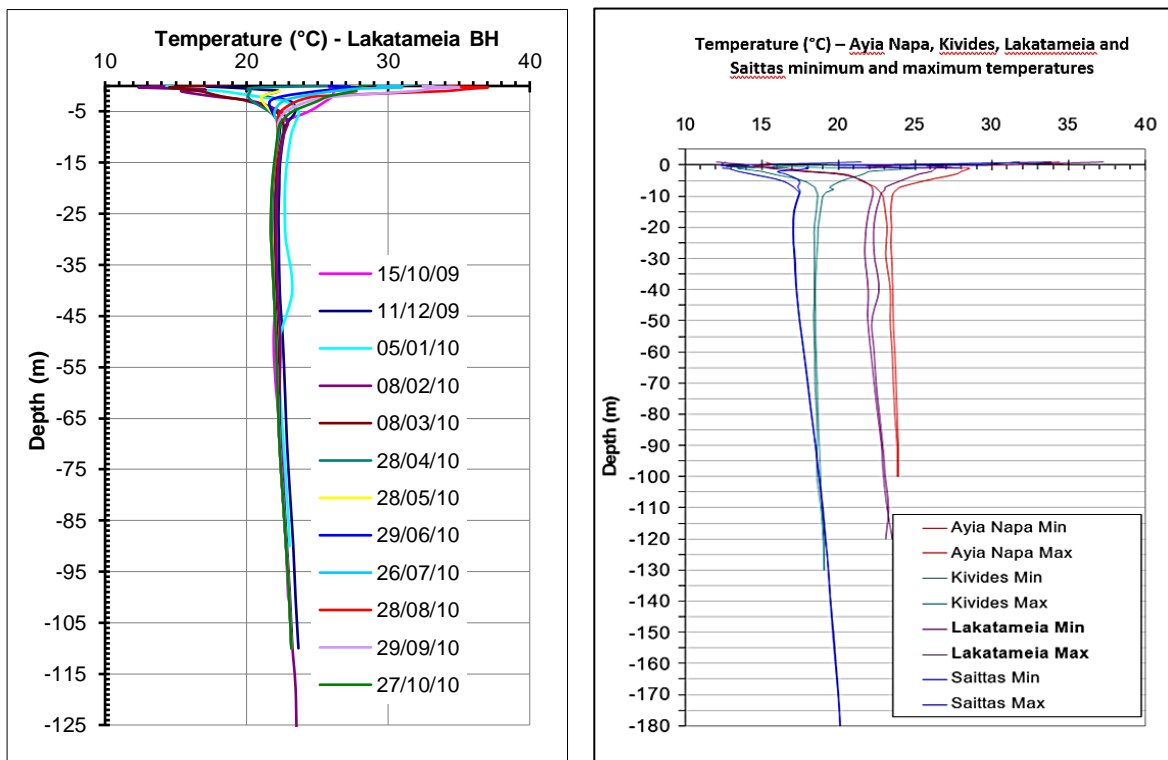


Figure 4 - 10: Temperatures recorded in 4 BHs located in different geographical locations in Cyprus, throughout a whole year (Pouloupatis, 2014)



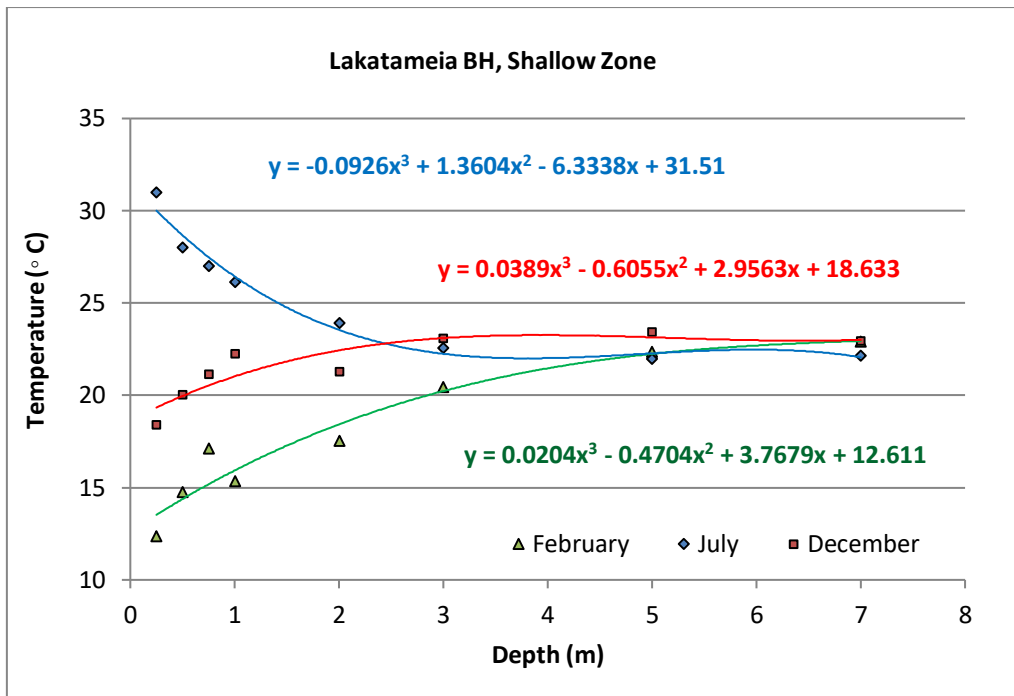


Figure 4 - 11: December, February and July recorded underground temperature at the Lakatameia BH Shallow Zone (0–7m). Also shown is the best-fit equation in each case.

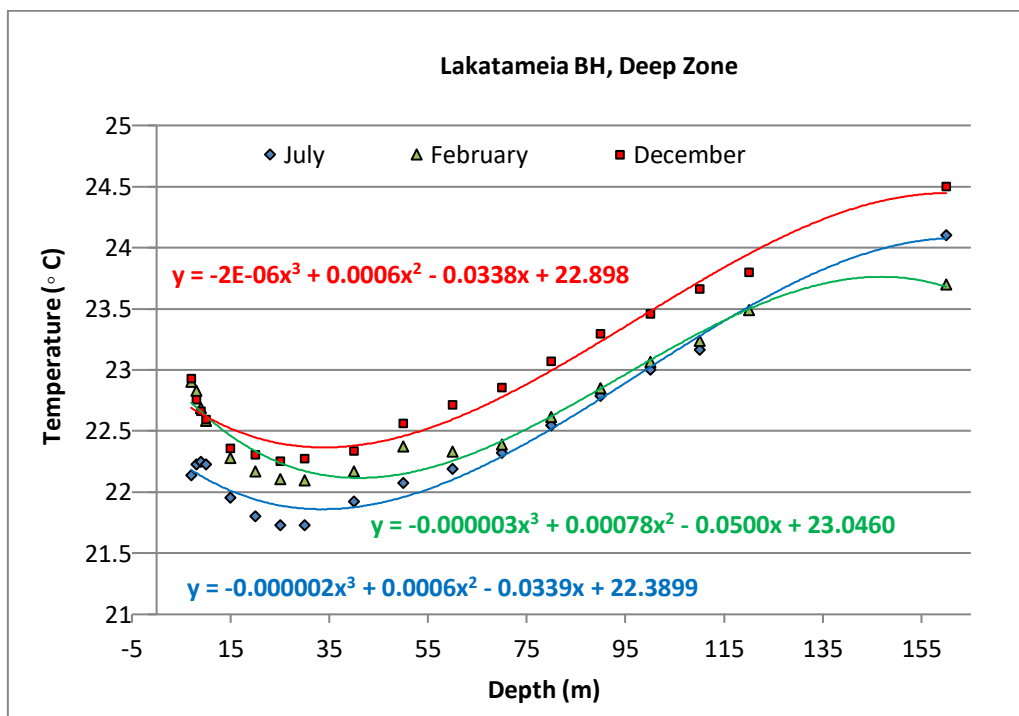


Figure 4 - 12: December, February and July recorded underground temperature at the Lakatameia BH Deep Zone (7–160m). Also shown is the best fit equation in each case.

In addition, two groundwater flow velocities were recorded in the water bearing layers, a nearly insignificant one in the majority of them of about  $0.000000012 \text{ m s}^{-1}$  and a higher one of  $0.00005 \text{ m s}^{-1}$  over a depth of about 25 m where the ground composed of Marly Sand. Groundwater velocities were based on observations of the Geological Survey Department of Cyprus.

Table 4 - 6: Soil/rock thermal properties used in the simulation

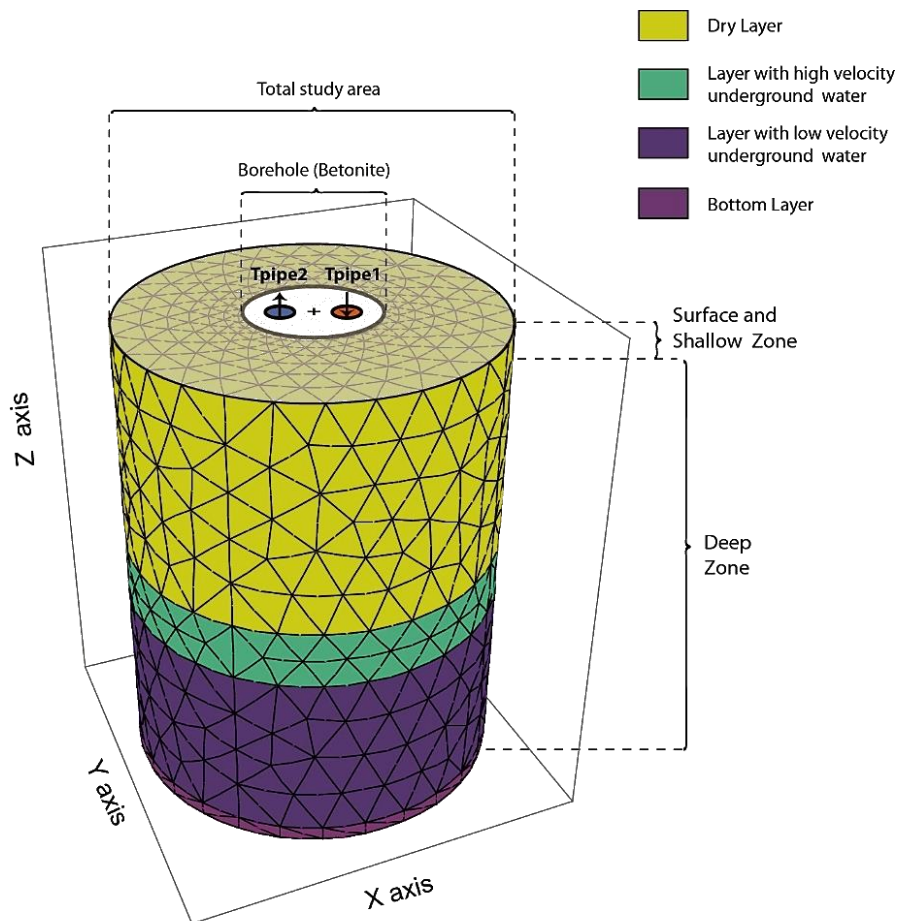
		Properties (Thermal conductivity $\lambda$ , density $\rho$ , specific heat capacity $c_p$ )
Ground	Dry	$\lambda = 1.4 \text{ W m}^{-1} \text{ K}^{-1}$ $\rho = 2,300 \text{ kg m}^{-3}$ $c_p = 950 \text{ J kg}^{-1} \text{ K}^{-1}$
	100% saturated	$\lambda = 1.5 \text{ W m}^{-1} \text{ K}^{-1}$ $\rho = 2,600 \text{ kg m}^{-3}$ $c_p = 1,000 \text{ J kg}^{-1} \text{ K}^{-1}$
Grout	Dry	$\lambda = 0.9 \text{ W m}^{-1} \text{ K}^{-1}$ $\rho = 1,500 \text{ kg m}^{-3}$ $c_p = 800 \text{ J kg}^{-1} \text{ K}^{-1}$
	100% saturated	$\lambda = 1.1 \text{ W m}^{-1} \text{ K}^{-1}$ $\rho = 1,700 \text{ kg m}^{-3}$ $c_p = 850 \text{ J kg}^{-1} \text{ K}^{-1}$

#### 4.2.2.2 Calibration of the Model

The temperature gradients for December in Figure 4 - 11 and Figure 4 - 12 for the depth profile were programmed into the model with the ground properties and characteristics of the GHE in Tables 4-6 and 4-7. Calculated initial ground temperatures on the vertical borehole axis are illustrated in Figure 4 - 14 which correspond to the actual measured values of the ground. This was achieved by setting GHE geometry (Figure 4 – 13) and boundary conditions of the actual BH to the corresponding parameters in FlexPDE software (PDE Solutions Inc). It is worth mentioning that the ground temperature measured in the BH increases up to a depth of 5 m reaching  $23.4 \text{ }^\circ\text{C}$  and then decreases by tiny steps up to 30 m. Then ground temperature increases again, reaching  $24.5 \text{ }^\circ\text{C}$  at 160 m depth from the surface.

Table 4 - 7: GHE properties

Property	Unit
Tube type	Polyethylene single U-tube connection
Tube length	160 m
Tube size (diameter)	0.032 m
Distance between the center of each tube and the center of the borehole	0.06 m
Grout	Bentonite clay with cement (radius 0.1 m)
Initial inlet fluid temperature	22.85 °C
Input and output temperature difference	5.2 °C
Input thermal energy	5,710 W



3D Mesh Lakatameia BH

Figure 4 - 13: The FlexPDE model for the energy analysis of the Lakatameia BH: 80 m dry well area shown in yellow; 25 m high water velocity area shown in green; 55 m low water velocity area shown in blue; 5 m base area shown in purple (sketch not to scale).

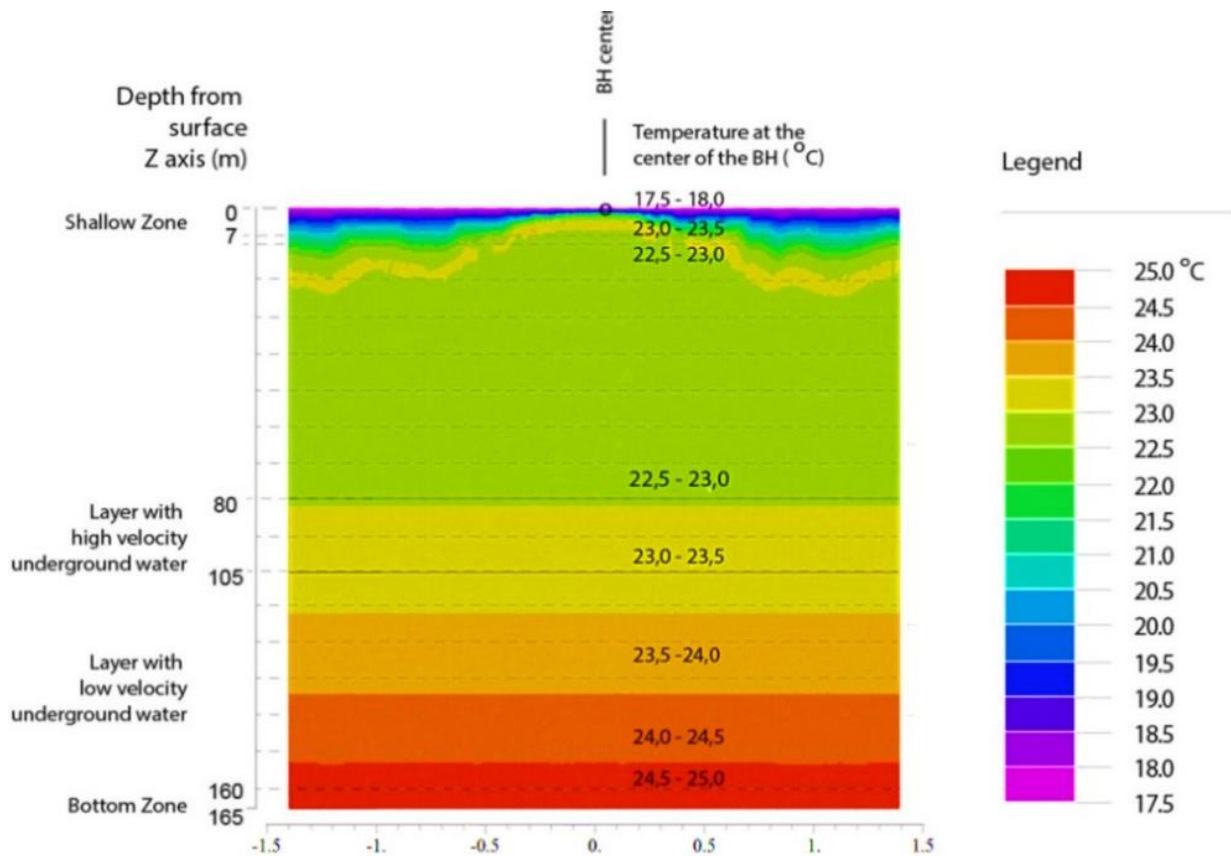


Figure 4 - 14: Initial ground temperature on the vertical borehole axis (initial model was scaled in the z coordinate by 0.00385)

By meshing the model with equilateral cells, high computational memory and time would be required, since the  $z$  dimension has an enormous difference in relation to the other dimensions. For this reason, the geometry of the Lakatameia BH was scaled in the  $z$ -coordinate by a factor of 0.00385, which is the maximum factor that the computer could handle. The final results for the model calibration show a good agreement with TRT measured values (Figure 4 - 15), allowing one to confidently use the model to extract realistic conclusions for the specified ground conditions.

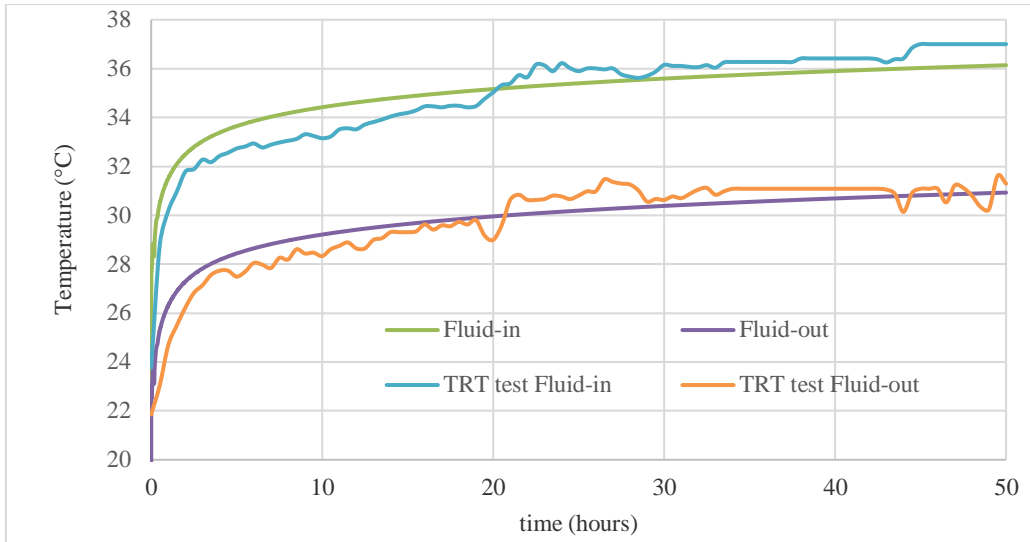


Figure 4 - 15: Recorded temperatures (December) at the Lakatameia BH (denoted by TRT Fluid-in/out), in comparison with the FlexPDE script calculated values (denoted by Fluid-in/out)

At this stage it is of interest to observe how the heat is absorbed by the various layers of the ground. Through the process of TRT heat is injected into the ground, but the rejection of heat is not only related to the velocity of the fluid flowing around the GHE (see comparison of high to low velocity layer in Figure 4 - 16) but also the difference between the temperature of the circulating fluid and the ground. For this reason, at the beginning of the operation of the GHE system, more heat is rejected to the ground at the top dry layer than the heat rejected in the layer with low underground water velocity.

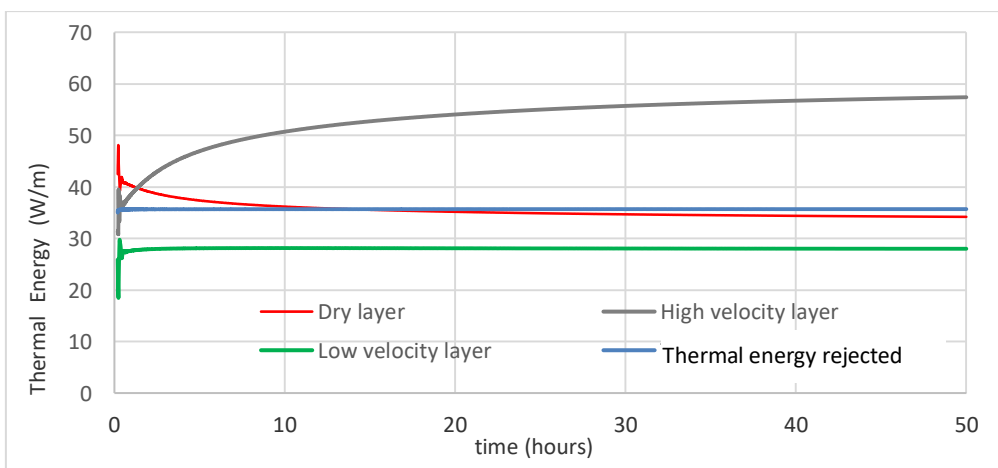
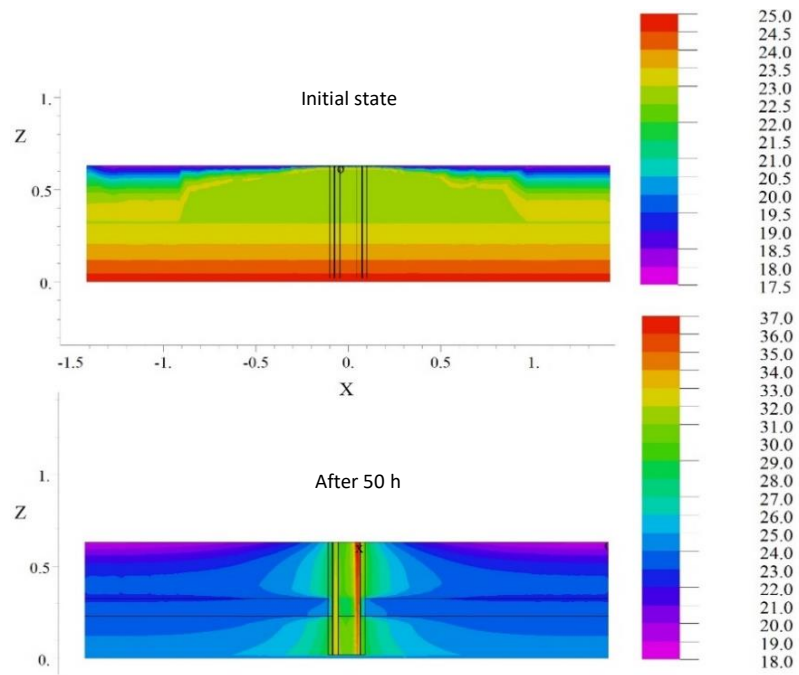


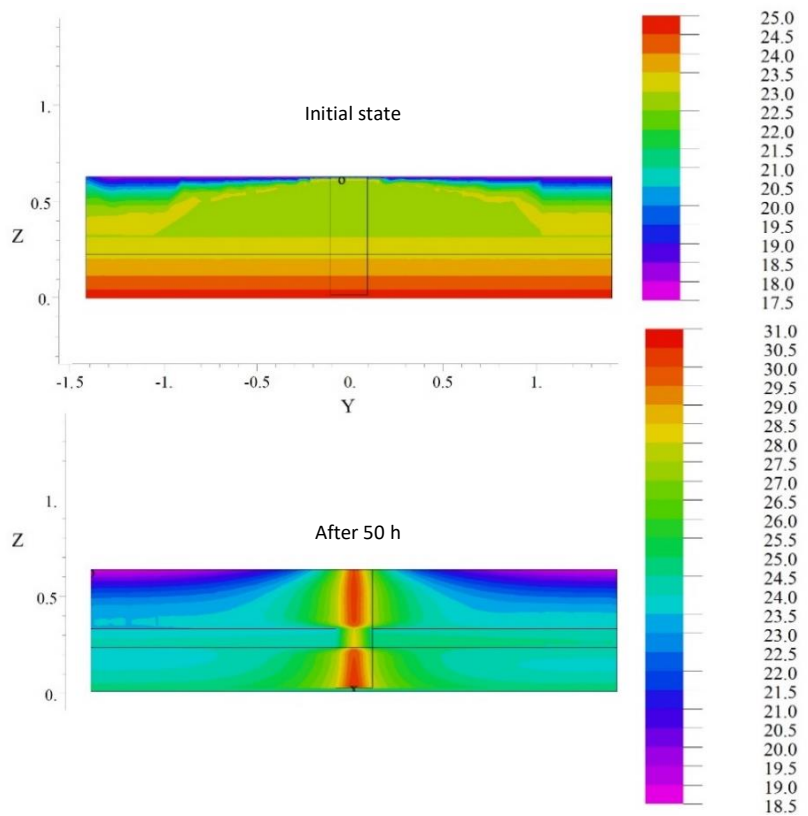
Figure 4 - 16: Thermal energy per m of GHE rejected to the ground in relation to the three layers of the borehole

Figure 4 - 17 (a) shows the temperature distribution at the initial stages of the simulation and at the end of the 50 h, in the  $x$ -direction. At 50 h, it is seen that the grout in the borehole has attained a uniform higher temperature than the surroundings, of about 31 °C, due to its lower thermal conductivity than the ground (Table 4 - 6). The middle layer, where higher velocity flow is presented, attains a lower temperature of about 24 °C. It can also be observed that the heat in the low velocity layer spreads wider than in the top dry layer, remaining a few degrees cooler (the geometry of the borehole is presented in Figure 4 -13 and Figure 4 - 14).

A similar pattern is presented in Figure 4 - 17 (b) in the  $y$ -direction, but the grout in the high velocity layer is cooled at a higher rate and the heat is transferred along the  $y$ -direction. Here it should be mentioned that underground water flow is in the  $y$  direction.



(a)



(b)

Figure 4 - 17: Temperature distribution at the initial stages of the simulation (top) and at the end of the 50 h (bottom), (a) in the  $x$ -direction, (b) in the  $y$ -direction

### 4.2.2.3 GHE modeling for the summer and the winter season

The thermal response of the GHE was investigated for the maximum and the minimum load months of the year in Cyprus, i.e. July and February (Pouloupatis, 2014). The best-fit equations for temperature gradients (for the shallow and deep zones), derived in 4.2.2.1, were again used for the simulations.

Calculated values for summer are illustrated in Figure 4 - 18, where the GHE fluid temperature exiting GHE is plotted against time. It can be seen that after 50 h of operation, for the steady input temperature of 45 °C, the fluid outlet temperature from the GHE is approximately 36.5 °C, i.e. 8.5 °C lower than the input temperature. For a steady input temperature of 35 °C, the output temperature is 30.5 °C, lower by 4.5 °C compared to the input, and for a steady input temperature of 28 °C, the outlet temperature is 26 °C, i.e. only 2 °C lower than the input.

For the winter operation the process is simply reversed and the GHE absorbs heat from the ground. Calculated values for winter are illustrated in Figure 4 - 19. It can be seen that for a 50 h of operation, when the steady fluid input temperature is 18 °C, the steady-state outlet temperature is 19.8 °C. For a steady input temperature of 9 °C, the steady-state temperature outlet temperature is 14.5 °C, and for an input temperature of 0 °C, the outlet temperature is 9 °C. Increasing the temperature difference between the inlet fluid and the ground, increases the heat removed from the ground as is expected.



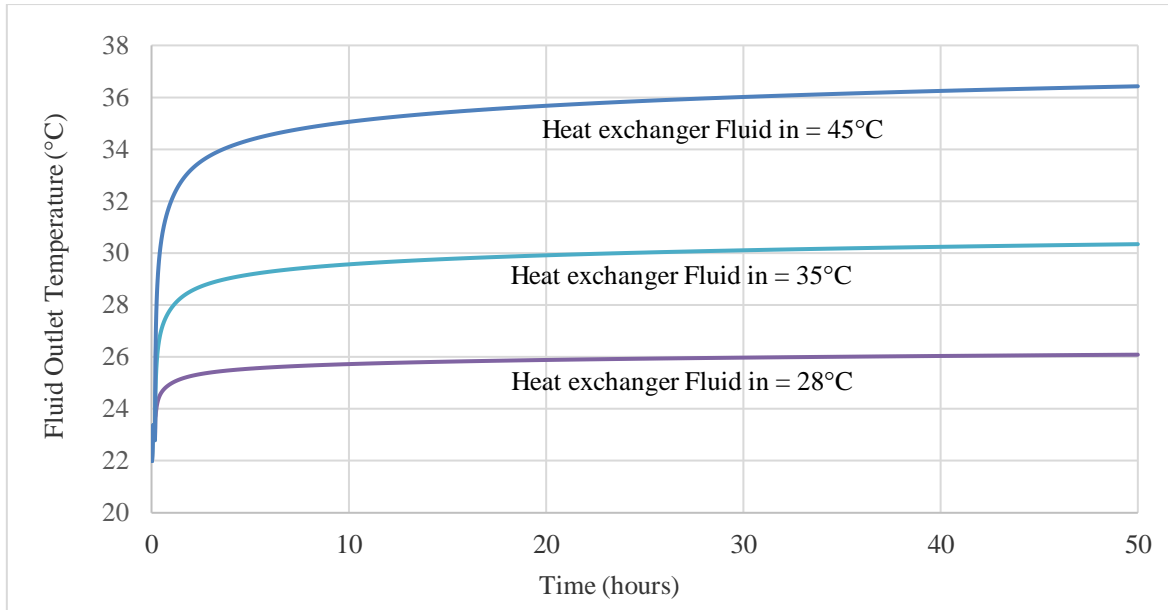


Figure 4 - 18: GHE exiting fluid temperature plotted against time steady temperature fluid entering the GHE of 45, 35 and 28 °C

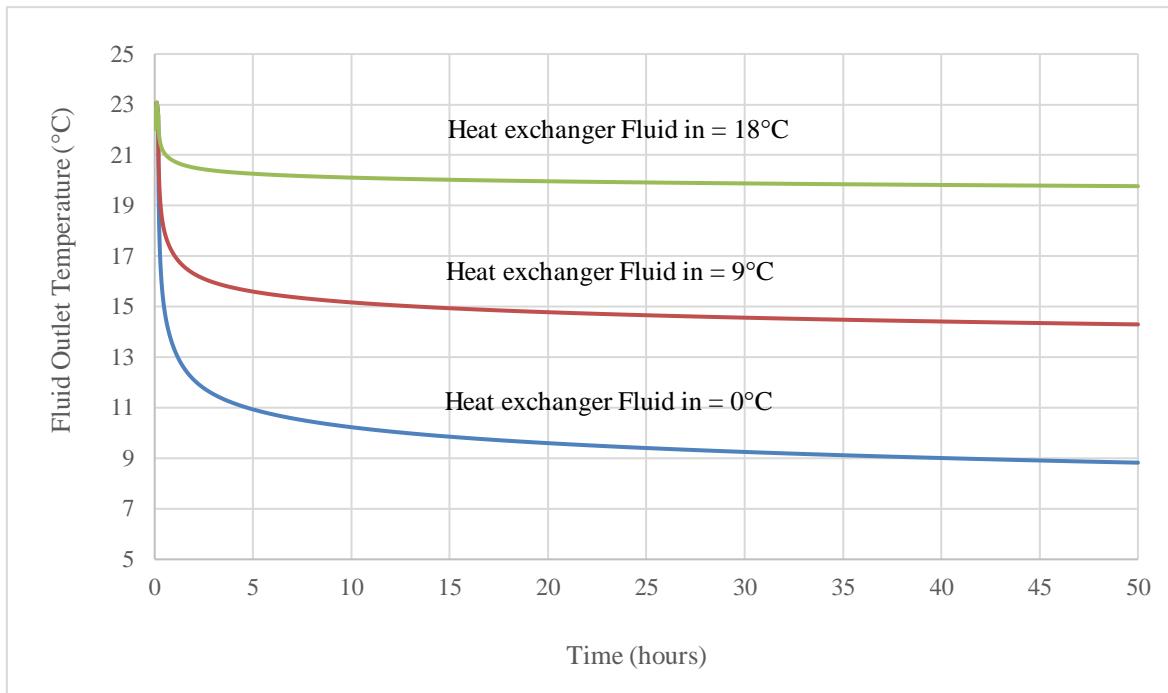


Figure 4 - 19: Fluid temperature exiting GHE plotted against time for three cases of steady temperature fluid entering the GHE, of 0, 9 and 18°C

#### 4.2.2.4 Parameterisation of the GHE

In this section, a parametric analysis of the Lakatameia GHE working in the summer mode is provided.

##### A. Borehole radius

Four different borehole radiuses were used, 0.08, 0.100, 0.125, 0.15 m in the GHE modeling, to evaluate their impact on the thermal response of the GHE. The results are shown in Figure 4 - 20 where it can be seen that a smaller borehole radius, in this case, results in a lower fluid outlet temperature from the GHE i.e for smaller radius the GHE has better performance. This is due to the thermal properties of the grout (see Table 4 - 6) which are poorer than the thermal properties of the surrounding rocks/soil. In more detail, the geological formation of the Lakatameia location have a higher thermal diffusivity than the grout used in the GHE.

Also, the higher input and output fluid temperature presented in bigger borehole radius is due to the accumulation of heat in the bigger radius grout, because of its higher resistance as it is sealing the borehole and blocking the flow of underground water, which is working in benefit of heat diffusion in the ground.

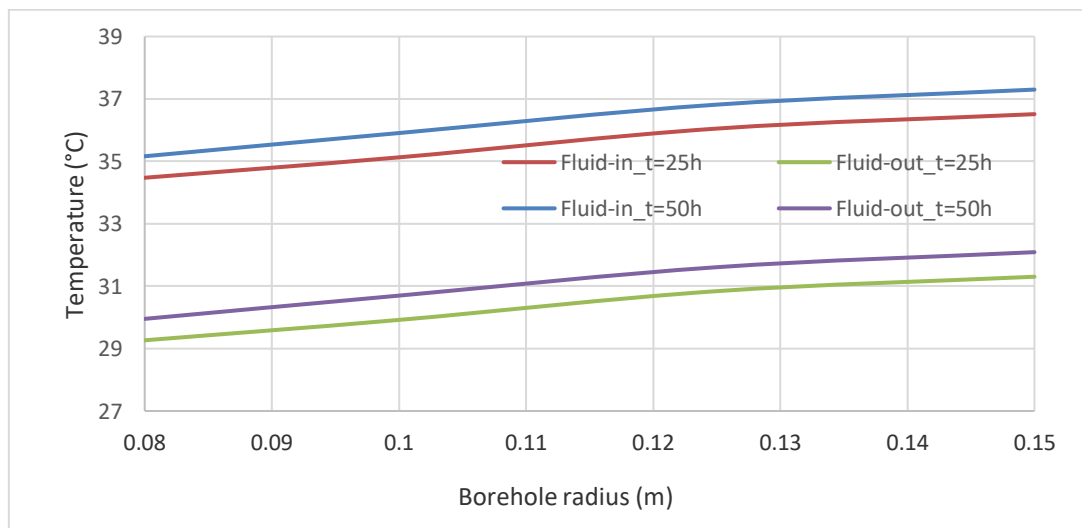


Figure 4 - 20: Input and output circulating fluid temperatures for different radius of a BH, after 25 and 50 h of continuous operation of the GHE

Plotting the absorbed heat per m of the borehole length against the radius of the borehole shown in Figure 4 - 21 it can be observed that heat transfer to the ground is higher for the wet layer with the higher ground water velocity. For the dry layers and very low ground water velocity the heat transfer to the ground remains fairly constant with the borehole radius.

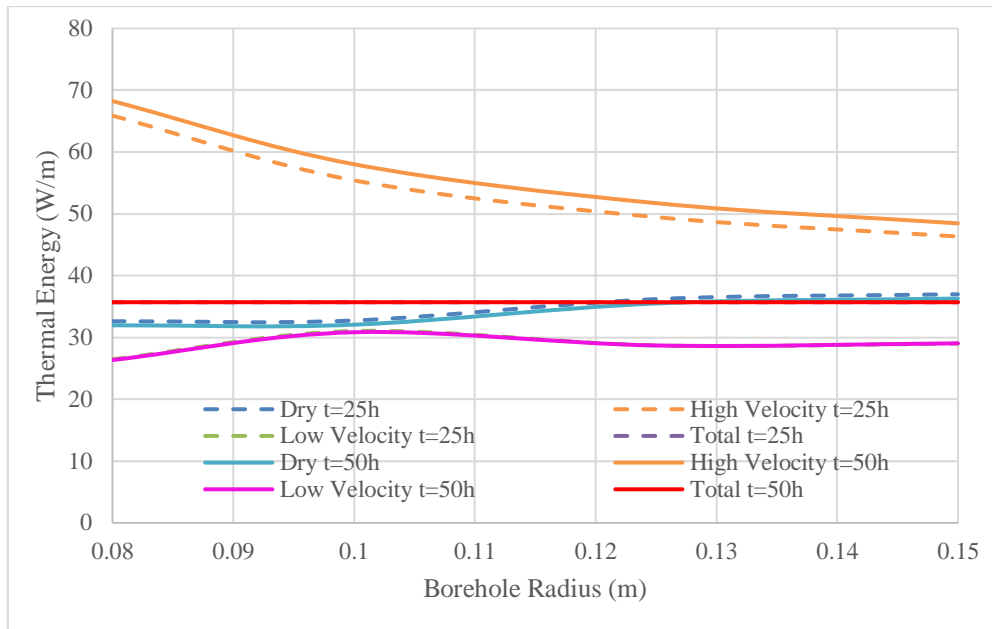


Figure 4 - 21: The absorbed thermal energy per m against the BH radius in the three types of layers of the BH (the graph of “Total t=25h” and “Low Velocity t=25h” are being overlapped by “Total t=50h” and “Low Velocity t=50h” graphs respectively)

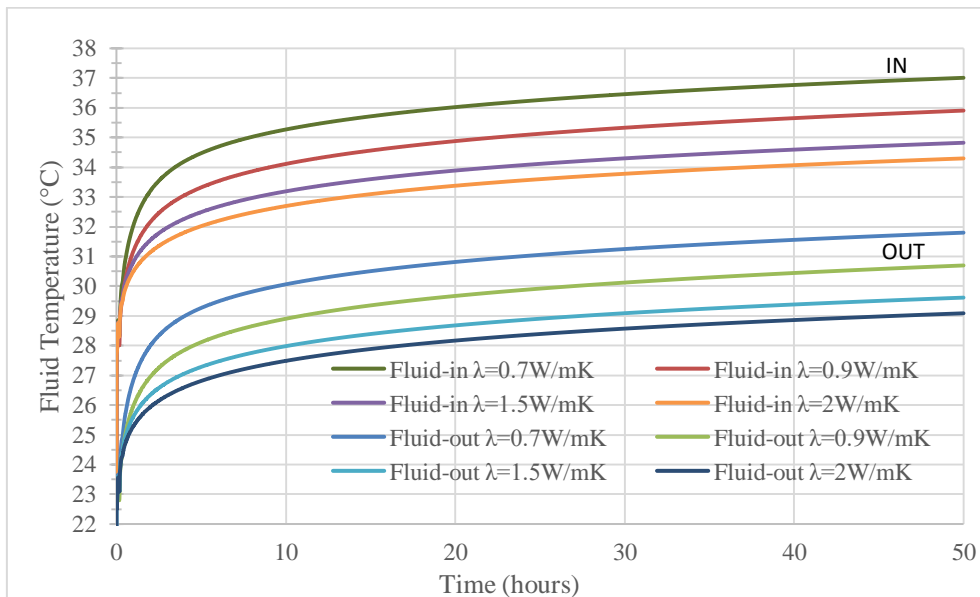


Figure 4 - 22: Temperature evolution of the GHE for various values of the grout thermal conductivity  $\lambda$

## B. Grout thermal conductivity

Figure 4 - 22 and Figure 4 -23 show the influence of grout thermal conductivity on the temperature of the fluid exiting the GHE in the summer period. It can be seen that the higher the thermal conductivity of the grout, the higher is the heat rejection to the ground and the lower the exit fluid temperature. This will have a positive effect on the performance of a heat pump coupled to the GHE.

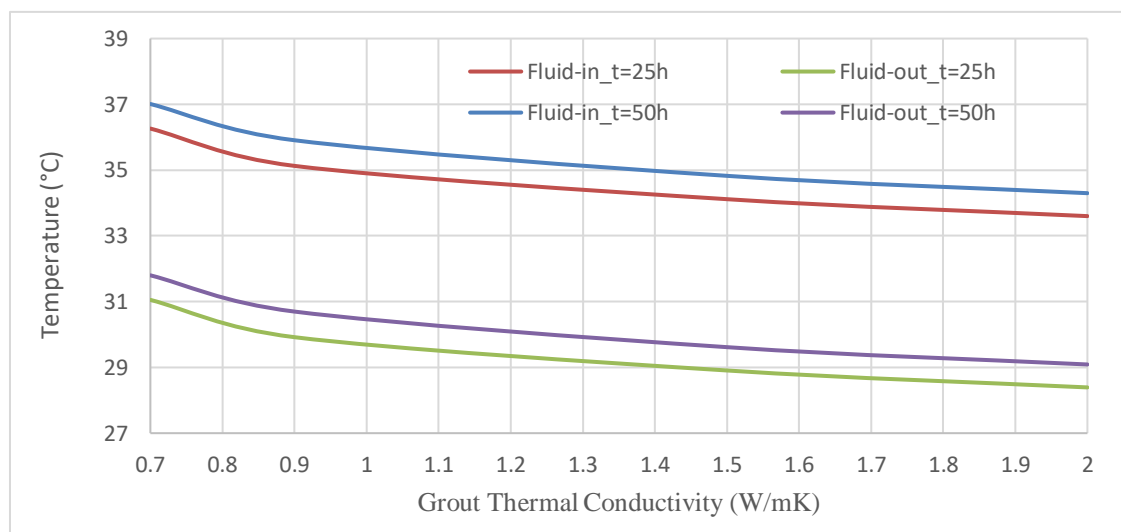


Figure 4 -23: Effect of the grout thermal conductivity on the fluid temperature of the U-tube, after 25 and 50 h continuous operation

## C. Influence of U-tube diameter

Different commercial sizes of tube were considered in order to identify the importance of the tube diameter on the GHE design in the summer mode. For the simulations the heat rejection was kept constant at 5,710 W with the temperature difference between input and output circulating water being 5.2 °C. Input data are shown in Table 4 - 8.

Table 4 - 8: Input data for different U-tube sizes

Outside diameter (mm)	Inside diameter (mm)	Wall thickness (mm)	Heat transfer coefficient (W/(m <sup>2</sup> K))	Circulating Fluid Velocity (m/s)
20	16.1	1.95	4,627	1.293
25	20.1	2.45	3,103	0.829
32	25.9	3.05	1,950	0.495
40	32.3	3.85	1,321	0.321

The results show that increasing the internal U-tube inside diameter from 16.1 to 32.3 mm results in a reduction in the outlet fluid temperature by approximately 1 °C (Figure 4 - 24).

This result is a function of many parameters which include the properties of the ground, the heat transfer coefficient and the residence time in the GHE. For example, increasing the tube diameter reduces the fluid velocity and heat transfer coefficient but increases the residence time of the fluid in the heat exchanger which can lead to an overall increase in the total heat transferred to the ground.

#### **D. Distance between GHE legs and BH centre**

In order to investigate the influence of the distance between the leg centre to the borehole centre of the GHE, simulations were carried out for distances between 0.035 to 0.065 m.

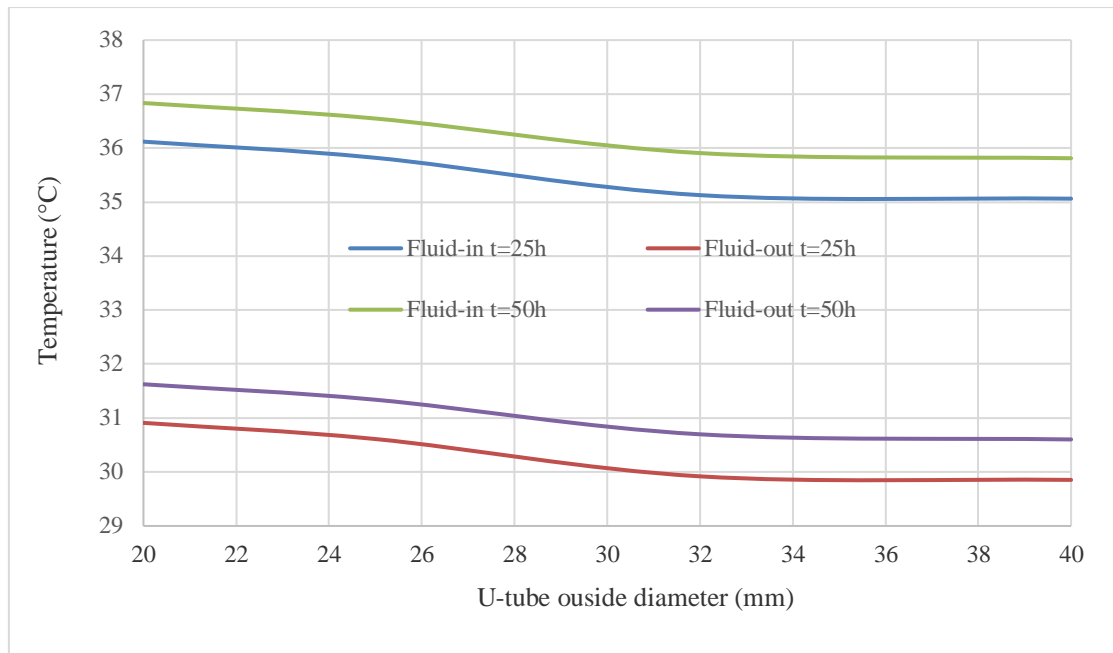


Figure 4 - 24: Effect of the U-tube diameter on the fluid temperature of the U-tube, after 25 and 50 h continuous operation

Results confirm that the larger the distance between the tubes and the BH centre, the better the thermal response of the GHE in the summer mode, i.e. the lower the temperature of the output fluid and the higher the energy rejected to the ground (Figure 4 - 25).

### E. Underground water velocity

It is known that the presence of underground water improves the heat exchange of the GHE with the ground (Fujii et al., 2013; Fan et al., 2007). In this study different ground water velocities were investigated and the results are presented in Figure 4 - 26. It can be seen that

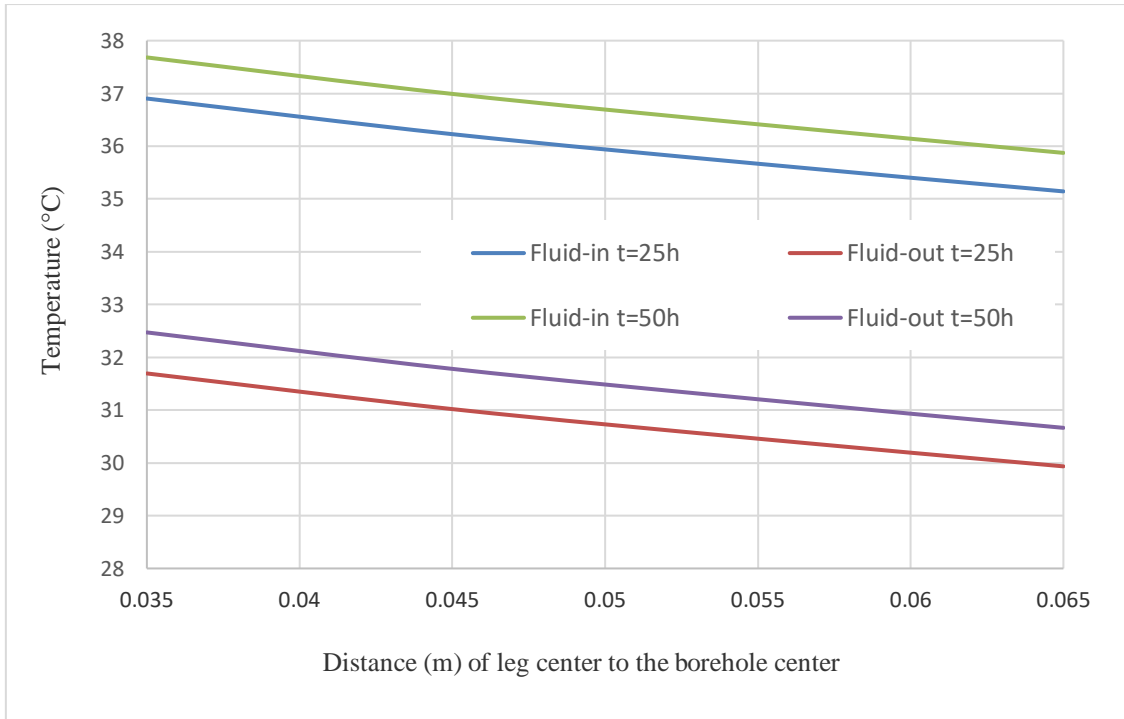


Figure 4 - 25: Comparison of input and output circulating fluid temperatures for different distances between the leg center and the BH center of the GHE, after 25 and 50 h continuous operation

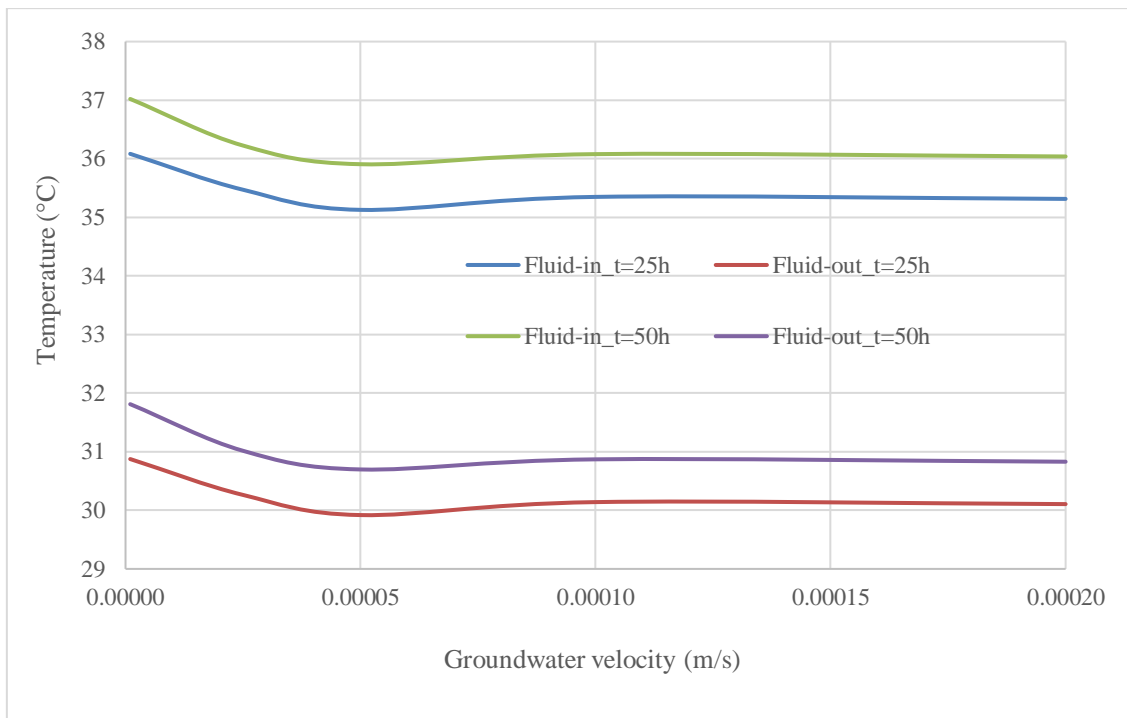


Figure 4 - 26: Circulating fluid temperatures in the GHE for different underground water velocities, after 25 and 50 h continuous operation

the efficiency of the GHE increases as the ground water velocity increases, reaching a maximum value at a velocity of approximately  $0.000045\text{m s}^{-1}$ .

#### **4.2.2.5 Geothermal Heat Pumps**

In order to increase the heating and cooling load delivered by a GHE system, a Ground Coupled Heat Pump (GCHP) should be used. The GCHP will be coupled to the GHE and the characteristics of the borehole and the ground will determine the heat pump specification.

The selection of the GCHP should also be made based on the data collected from the Thermal Response Test (TRT) in each location investigated. The GCHP to be selected should have inlet temperatures similar to TRT exiting fluid temperatures in order to perform efficiently. In the case of Lakatameia, the calculated temperature of the water exiting the GHE, for a single U-tube GHE, did not exceed  $38.4\text{ }^{\circ}\text{C}$  (Pouloupatis, 2017) (Figure 4 - 18).

Figure 4 – 27, shows the heat per meter of the Lakatameia GHE that is rejected to the ground (in summer mode) in relation to the GHE exiting water temperature for the cases of 25 h and 50 h continuous operation. GHE's exiting fluid temperature also corresponds to the heat pump input fluid temperature), but an engineer should consult all the pump specifications in order to decide about the GHE design temperature. The characteristics of such a heat pump are given in Pouloupatis et al. (2017), where Figure 4 – 28 is extracted from. It can be seen that, in summer mode, the heat pump capacity over the input power is nearly doubled from a pump entering fluid temperature of  $44\text{ }^{\circ}\text{C}$  to one entering at  $20\text{ }^{\circ}\text{C}$ . This means that to achieve lower temperatures a bigger number of BHs are needed, meaning a higher initial cost. Therefore, the designer should consider the benefits of a higher heat pump efficiency to the disadvantage of the higher initial cost, so as to come to an economical decision.



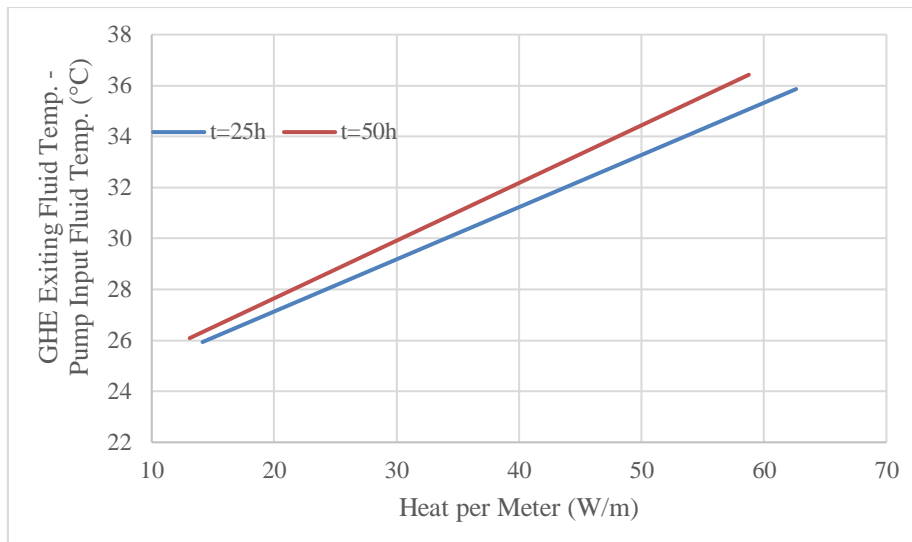


Figure 4 – 27: Heat per m of GHE rejected to the ground in relation to the GHE exiting fluid temperature (which also corresponds to the pump input fluid temperature), for cases of 25 h and 50 h continuous operation

For the winter operation, the process is simply reversed and the heat pump absorbs heat from the ground. Calculated values for winter were illustrated in Figure 4 - 19, where the GHE exiting fluid temperature is plotted against time.

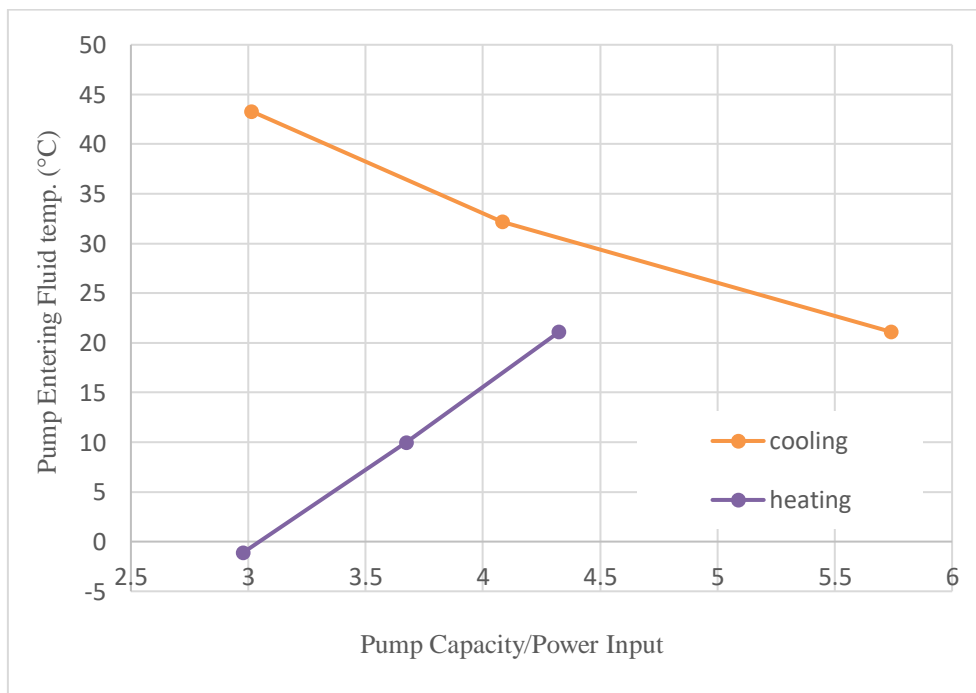


Figure 4 – 28: Characteristics of a typical heat pump, showing the heat pump entering fluid temperature against the ratio of pump capacity over power input, for cooling and heating mode of operation

For design purposes, the heating load of a typical house in Cyprus is required. As a typical house in Cyprus was assumed a two storey house with three bedrooms and a total useful floor area of 190 m<sup>2</sup>. The typical monthly heating load in February was calculated to 1622 kWh and the typical cooling load for a whole month in summer mode (July) to 1508 kWh (Pouloupatis, 2014). Table 4 - 9 shows the Capacity and Power of the selected GCHP in kW based on the entering water temperature at the specified flow rate. The water flow rate in the GHEs during the TRTs was between 10.5 – 12 L/min. Therefore, in a geothermal system of about 5 to 7 GHEs the nominal system flow should to be between 52.5 – 84 L/min. These specifications are given by the GCHP manufacturers.

Table 4 – 9: Heat Pump Manufacturer Specification

Flow rate (L/min)	Cooling mode			Heating mode		
	Entering Water Temp. (°C)	Capacity (kW)	Power input (kW)	Entering Water Temp. (°C)	Capacity (kW)	Power input (kW)
30.3	21.1	18.2	3.17	-1.1	12.6	4.23
	32.2	16.5	4.04	10	15.8	4.3
	43.3	14.8	4.91	21.1	18.9	4.37
56.8	21.1	17.9	2.88	-1.1	13.1	4.27
	32.2	16.6	3.72	10	16.5	4.32
	43.3	15.2	4.57	21.1	19.9	4.38

Based on the selected heat pump and its specifications and assuming a system flow rate of 11.4 L/min/3.5 kW of peak cooling load and a 100 m fixed borehole length, the minimum number of boreholes to be drilled in each of the locations in order to satisfy the heating and cooling loads of the house is calculated. In Lakatameia area, 700 m total GHE length is required, in order to satisfy to load required for a single house.

### **4.3 Summary**

In this Chapter the computational model presented in Chapter 3 was calibrated using data from a Thermal Response Test, carried out in Lakatameia, Cyprus. By using the validated model, the heat injection rate of the GHE was investigated.

Increasing the distance between the tubes of the GHE improves performance. A limitation, however, is the cost of drilling a larger diameter borehole and the larger quantity of grout that needs to be used.

All design and operating parameters have an optimum with respect to performance and cost and these factors need to be taken into consideration in the design of GHEs for heat pump applications.

## Chapter 5: Measurement and Analysis of the Thermal Properties of Rocks for the Compilation of Geothermal Maps

### 5.1 Introduction

Previous studies in Cyprus have classified the island in the category of low enthalpy with high potential for the usage of geothermal energy for space air-conditioning (Kalogirou et al., 2012; Pouloupatis, 2014; Morgan, 1975). In addition, there are data showing that ground temperature variation depends on depth from the ground surface. In more detail, the surface zone in Cyprus reaches a depth of 0.5 m where the ground is affected by short term weather variations, changing to seasonal variations as the depth increases. The shallow zone penetrates to 7–8 m. At deeper layers, the ground temperature remains almost constant throughout the year within a range between 18–23°C depending on the area (Pouloupatis, 2014; Florides et al., 2010). Similar studies were undertaken in other countries verifying the presence of the three underground zones, and the fact that the ground temperature in deep underground layers (below 8 m) remains constant during the year. For example, Livingston Island in Antarctica, (Correia et al., 2012), Romania (Vijdea et al., 2014) and Kraków, Poland (Sliwa and Rosen, 2015).

Thermal conductivity is a parameter that describes how easily heat is transmitted through a material. The thermal conductivity of rocks is a key parameter that affects the final performance of all geothermal projects. Additionally, it is well known that thermal conductivity and other thermophysical properties of rocks are affected by various factors: temperature (Abdulagatova, 2009; Miao, 2014), pressure (Gorgulu et al., 2008; Abdulagatova, 2009), mineralogical composition (Neuendorf et al., 2011), porous and cracks (Gegenhuber, 2012), and water content (Canakci, 2007; Jorand, 2011). It can also be affected by the burial depth (Liu et al., 2011; Correia, 2012) and the geological age of the lithology (Stylianou et al., 2016; Liu et al., 2011).

In this Chapter, results of a study to define a range of values for thermal conductivity  $\lambda$  ( $\text{W m}^{-1} \text{K}^{-1}$ ), density  $\rho$  ( $\text{kg m}^{-3}$ ) and specific heat capacity  $c_p$  ( $\text{J K}^{-1} \text{kg}^{-1}$ ) for each type of rock found

in Cyprus are presented. The relation between the properties is expressed by the thermal diffusivity  $\alpha$  ( $\text{m}^2 \text{s}^{-1}$ ) (Chapter 4, Equation 1) which measures the material's ability to respond to changes in its thermal environment and is equal to the thermal conductivity divided by density  $\rho$  and specific heat capacity at constant pressure.

$$\alpha = \frac{\lambda}{\rho \cdot c_p} \quad (1)$$

The impact on thermal conductivity of (a) water in samples, (b) the mineralogical composition, and (c) the geological age of rocks is also presented in this Chapter.

## 5.2 Geological Sampling and Sample Preparation

Due to the little information on the thermal properties of the ground in Cyprus, geological sampling was carried out. The sites were selected according to the geological formation, the lithology and their geographical location in order to take representative samples from the formations shown on the Geological Map of Cyprus (1995). Information about the geology of Cyprus was presented in Chapter 2. Part of this sampling was carried out under the research project funded by the Research Promotion Foundation (RPF) of Cyprus under contract TEXNOΛΟΓΙΑ/ΕΝΕΡΓ/0311(BIE)/01 and the European Regional Development Fund (ERDF) of the EU.

Samples were collected from outcrops and to overcome the lack of samples from some formations, samples were also obtained from the drill core archive of the Cyprus Geological Survey Department. Sampling mainly covered the area of the two biggest in size terranes of the island, the Troodos Ophiolite and Circum Troodos Sedimentary Succession. The two terranes cover the most densely populated areas and the 86.2% of the total area of the island. Sampling was not executed in the north part of Cyprus, which is under the control of Turkish troops since 1974. The complete list of samples with the coordinates of their collection point is shown in Appendix II. Totally 148 samples were collected (Figure 5 - 1).

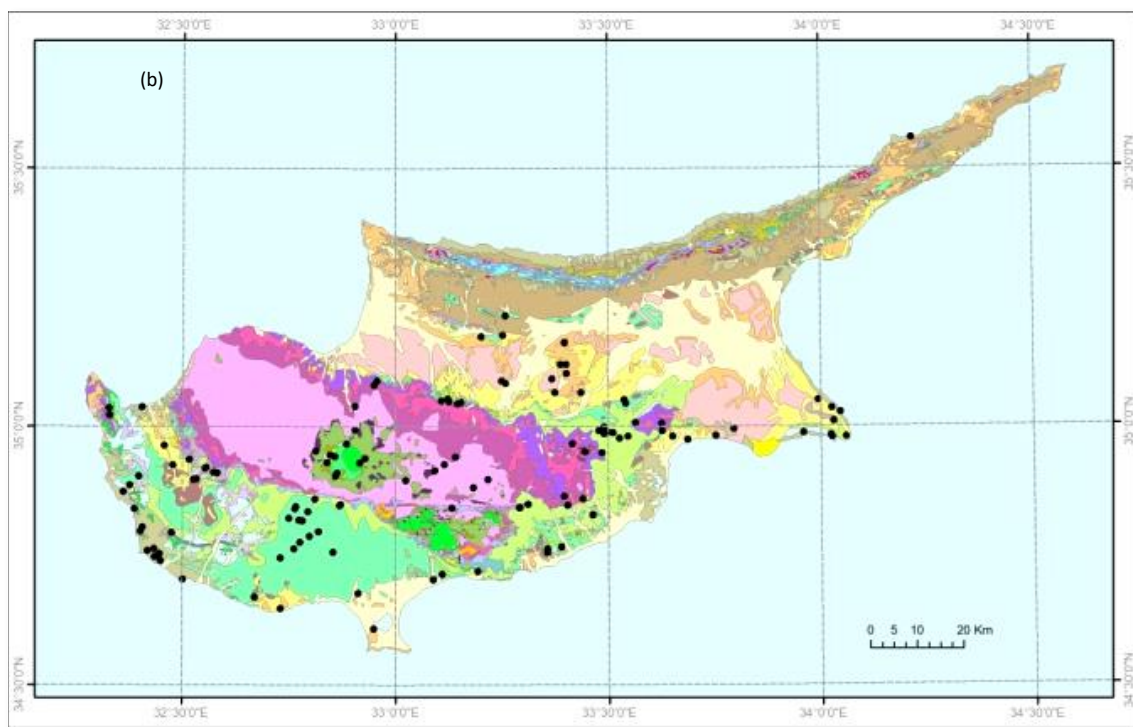
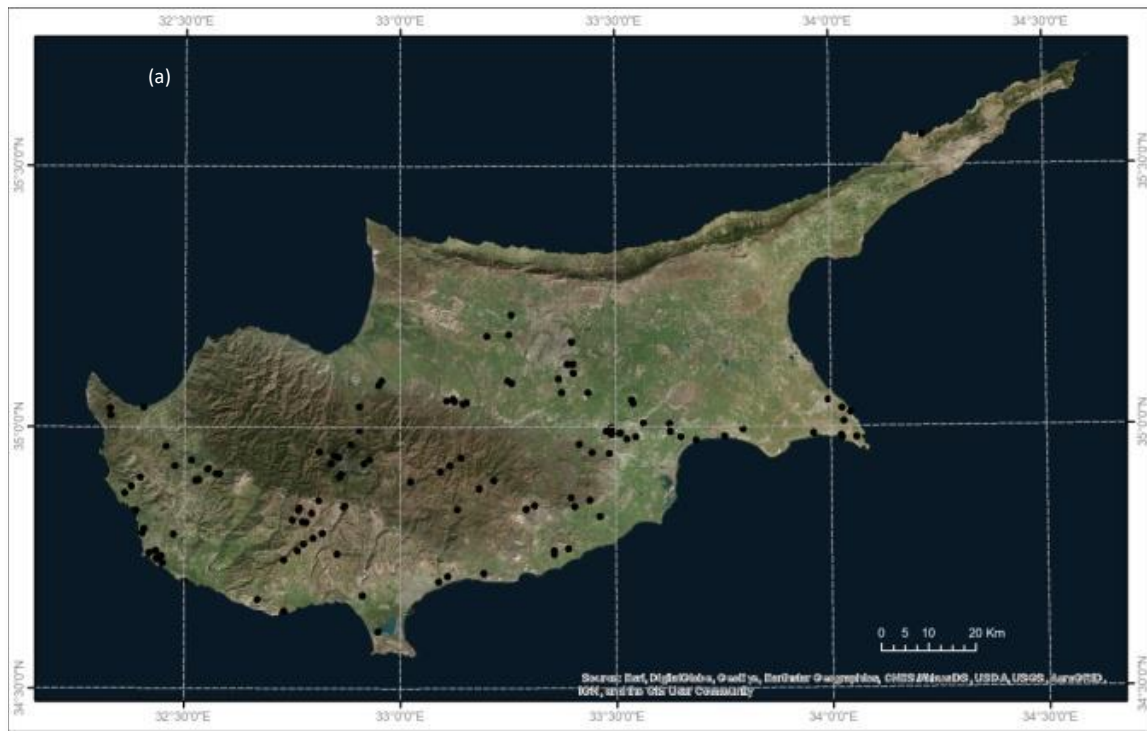


Figure 5 -1: Sampling points (Background: (a) Satellite Image, Source: Esri, Digital Globe, GeoEye, Earthstar Geographics, CNES/AirbusDS, USGS, AeroGRID, IGN and the GIS User Community (b) Geological Map of Cyprus (1995))

Thermal properties of the collected samples were measured with the use of Isomet 2104 Heat Transfer Analyzer (Applied Precision, Inc). For conducting measurements with the surface probe, a smooth flat surface was required. In order to create the testing surface, the samples were cut by means of a diamond disk and a circular saw (Figure 5 - 2). After slitting, the sample faces were polished and lapped. The samples were prepared in the shape of a rectangular prism with at least two flat testing surfaces of  $7 \times 7 \text{ cm}^2$  and 4 cm thickness, to be suitable for the testing (Figure 5 - 3).



Figure 5 -2: Cutting samples with the use of a circular saw



Figure 5 -3: Samples ready for testing

It is worth to mention that most of the samples located on Troodos Mountain have presented a high degree of difficulty in cutting. The hardest to cut were the samples of Sheeted Dykes (Diabase), Plagiogranite, Gabbro, Pyroxenite, Serpentinite, Wehrlite, Dunite and Harzburgite. These lithologies are primarily present on the Troodos Mountain.

### 5.3 Laboratory Tests

Due to the difficulty of measuring thermal properties in situ, results of the collected geological samples were obtained from measurements in the laboratory, at room temperature.

The Isomet 2104 (Applied Precision, Inc) portable heat transfer analyzer was used for the measurements (Figure 5 - 4). Isomet 2104 is a multifunctional portable instrument, equipped

with various probes; needle probes are for porous, fibrous or soft material, and surface probes are suitable for hard materials. In this research mainly surface probes were used. The measurements were based on the analysis of the temperature response of the sample material to heat flow impulses.

The measurement method applied by Isomet complies with the standards ASTM-D-5334-08 and ASTM-D-5930-09. According to these methods, constant electric power is applied to an electric heater having a direct thermal contact with the surface of the sample. Measuring errors in the determination of thermal conductivity were in the range  $\pm 5\%$  for the measuring range  $0.015\text{--}0.7 \text{ W m}^{-1} \text{ K}^{-1}$  and  $\pm 10\%$  for the measuring range  $0.7\text{--}6.0 \text{ W m}^{-1} \text{ K}^{-1}$ .



Figure 5 - 4: Isomet 2104 portable Heat Transfer Analyzer

The measurements of thermal properties were performed on samples in their dry (oven dry) and water-saturated state in order to fulfill the objective of this research, to determine the impact of moisture content on the thermal response of the underground. For each of the collected samples the following properties were recorded:

1. Volumetric heat capacity  $VCH$  (Density x specific heat capacity ( $\rho.c_p$ ))
2. Diffusivity  $\alpha$
3. Thermal conductivity  $\lambda$



The first measurement, volumetric heat capacity  $VCH$  was divided by the density (determined in the laboratory) in order to calculate the specific heat capacity. A complete list with laboratory results can be found in APPENDIX II.

As explained above (paragraph 4.1), thermal properties of rocks are affected by various factors, among them the temperature (Miao, 2014; Abdulagatova, 2009), pressure (Abdulagatova, 2009; Gorgulu et al., 2008; Tong et al., 2009) and the burial depth (Correia, 2012; Liu et al., 2011). In Cyprus ground temperature below 8 m remains almost constant throughout the year, in a range between 18–23°C depending on the area of interest (Pouloupatis, 2014; Florides et al., 2010). This range of temperature is very close to the room temperature that tests have performed. Concerning the impact of pressure/burial depth on the thermal properties of rocks in our case, i.e. at the installations of geothermal heat exchangers up to 200 m, it is assumed to be negligible due to the small depth variation. Although pressure may be a key parameter that affects the final thermal performance of rocks and soil, the effect of pressure on thermal conductivity is small at pressures below 100 MPa (1000 bar) (Abdulagatova et al., 2009; Sweet, 1979). In more detail, Abdulagatova et al. (2009) presented the results of thermal conductivity measurements for dry porous sandstone rock (porosity of 13%). Pressure dependence up to 100 MPa did not exceed 8% of the value measured under atmospheric pressure. In addition, Sweet (1979) presented measured values for Pyrex Glass, Basalt, Limestone, Teflon, Halite and Quartz. Values presented increased by only 3% at pressures of 100 MPa.

For calculating a borehole's overall thermal properties using the properties of collected samples there are various automated routines. Such a routine is the layer calculator of the Ground Loop Design (GLD, 2012) program that allows designers to use data from a drilling log to produce a quick weighted-average calculation for thermal conductivity, thermal diffusivity and borehole thermal resistance. The thickness of each type of soil/rock forming the borehole is required along with the thermal conductivity and diffusivity as measured in the laboratory.

For the measurements, samples were dried in an oven at  $110 \pm 10$  °C for 24 h (ASTM-C-332). This temperature ensures the retention of crystalline or inherent moisture ( $H_2O^+$ ) from almost all mineral phases, and the complete loss of hygroscopic moisture ( $H_2O^-$ ).

Samples were fully saturated by staying immersed in water at room temperature for a period of 24 h (ASTM-C-127-93). Difficulties were faced with soluble in water samples. In those cases, samples were sprayed with water until they were fully saturated. This method was chosen trying to keep the structure of the sample as close as it is found in nature. Additionally, Isomet flat probe electric signal does not penetrate deep inside the sample, but only to some centimeters below the surface of the sample, where fully saturated material was obtained.

Frost weathering processes were not investigated in this research. Only conditions for vertical geothermal boreholes were investigated and as we know from previous researches in Cyprus, temperature below 8 m stays constant at approximate 18-23° C (Pouloupatis, 2014; Florides et al., 2010). It is also rather uncommon in Cyprus that temperature decreases below 0° C in winter time (Meteorological Service of Cyprus).

Densities were required for calculating the specific heat capacity of the samples as the measurement of Isomet, measures only volumetric heat capacity *VHC*. Volume and density were defined by laboratory tests based on CYS-EN-13383-2:2011. The volume of small in size or soluble in water samples were measured using the *Displacement Method (Archimedes Principle)*, after they were tightly covered in nylon foil (Figure 5 - 6) or paraffin (Figure 5 - 5). These methods were chosen as most of our samples were of irregular size. For dry samples bulk densities were used in order to calculate the specific heat capacity of each sample.



Figure 5 -5: Sample covered with paraffin



Figure 5 -6: Sample covered with nylon foil

Difficulties were also faced when measuring samples of the Alluvium – Colluvium and Fanglomerate Formations. These samples were composed of a mixture of soil and gravels, most times uncemented. In these cases, several measurements were taken on gravels and soils and an average value was calculated.

## 5.4 Laboratory Results

Laboratory results of each rock type were found to be within a range of values for each thermo physical property. In brief, thermal conductivity  $\lambda$  values for dry samples vary from 0.1 to 4.2  $\text{Wm}^{-1}\text{K}^{-1}$ , thermal diffusivity  $\alpha$  values range between  $0.2 \times 10^{-6}$  and  $1.9 \times 10^{-6} \text{ m}^2 \text{ s}^{-1}$  and specific heat capacity values  $c_p$  range from 0.5 to 1.5  $\text{J K}^{-1}\text{kg}^{-1}$ . For water-saturated samples thermal conductivity measured values vary from 0.6 to 4.5  $\text{W m}^{-1}\text{K}^{-1}$ , thermal diffusivity values from  $0.3 \times 10^{-6}$  to  $1.9 \times 10^{-6} \text{ m}^2 \text{ s}^{-1}$  and specific heat capacity from 0.6 to 1.7  $\text{J K}^{-1}\text{kg}^{-1}$ .

Recorded values for each thermo-physical property were first grouped according to the geological formation of the sample and then by lithology.

### 5.4.1 Thermal conductivity and thermal diffusivity of geological formations

In this study 11 geological formations of the Circum Troodos Sedimentary Succession and 11 formations of the Troodos Ophiolite were considered (Table 5 - 1). From the 148 collected samples the 140 were examined with respect to rock formation; 41 samples pertain to Pachna and 25 to Nicosia, which are the most commonly found formations in Cyprus, 14 samples pertain to Lefkara formation, 9 samples to Pillow Lavas and 9 to Terrace Deposits, 7 to Sheeted Dykes (Diabase), 5 to Kalavastos, 5 to Alluvium – Colluvium, 4 to Basal Group, 4 to Fanglomerate, 3 to Gabbro, 3 to Apalos – Athalassa - Kakkaristra, 3 to Harzburgite, 2 to Wehrlite, 2 to Serpentine, 1 to Kannaviou, 1 to Plagiogranite, 1 to Pyroxenite and 1 to Dunite formation respectively.

Laboratory results give a range of values for each property and mean values were calculated for thermal conductivity  $\lambda$ , diffusivity  $\alpha$  and specific heat capacity  $c_p$ . The column “min” shown in Table 5 - 1 is the minimum actual measured value of the tested samples, “max” is the

maximum actual measured value and “average” is the mean value of the actual measured values.

Results are also illustrated in Figure 5 - 7 and Figure 5 - 8 which show the mean values of thermal conductivity ( $\lambda$ ), thermal diffusivity ( $\alpha$ ), specific heat capacity ( $c_p$ ) and density ( $\rho$ ) for dry samples and water saturated samples respectively. Samples are grouped by geological formation as shown on the Geological Map of Cyprus (Table 5 - 1). Measured values taken for 100% moisture conditions (Figure 5 - 8) for most of the geological formations are higher than or about the same as measurements taken for oven-dry samples. The increasing effect of moisture content is due to the thermal conductivity of water, which is considerably higher than the thermal conductivity of air that fills the pores of rocks in dry conditions (Momose and Kasubuchi, 2002). The thermal conductivity of air at 20 °C is  $0.026 \text{ W m}^{-1} \text{ K}^{-1}$  (Montgomery,

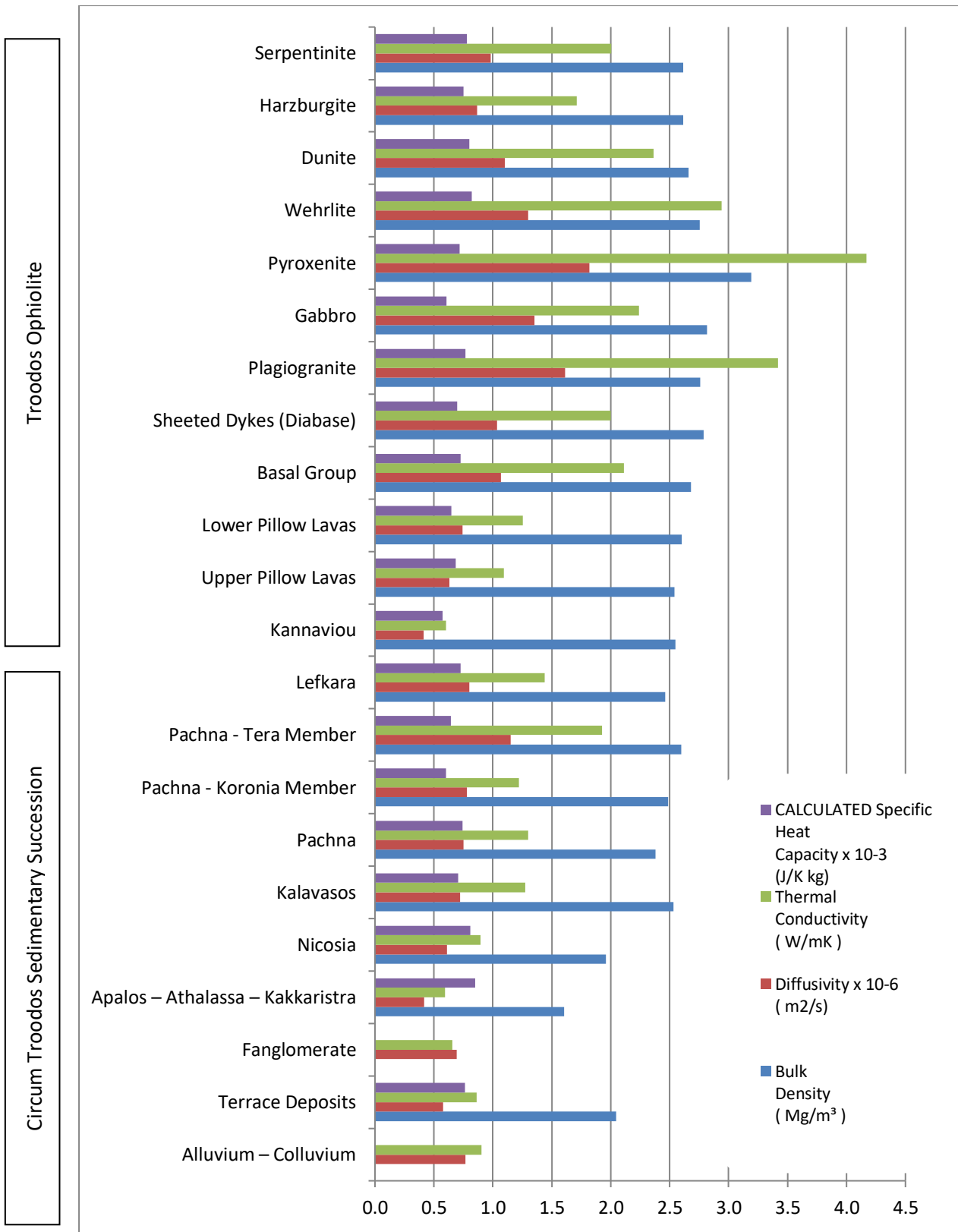


Figure 5 - 7: Mean values of thermal conductivity ( $\lambda$ ), thermal diffusivity ( $\alpha$ ), specific heat capacity ( $c_p$ ) and density ( $\rho$ ) for dry samples grouped by geological formation

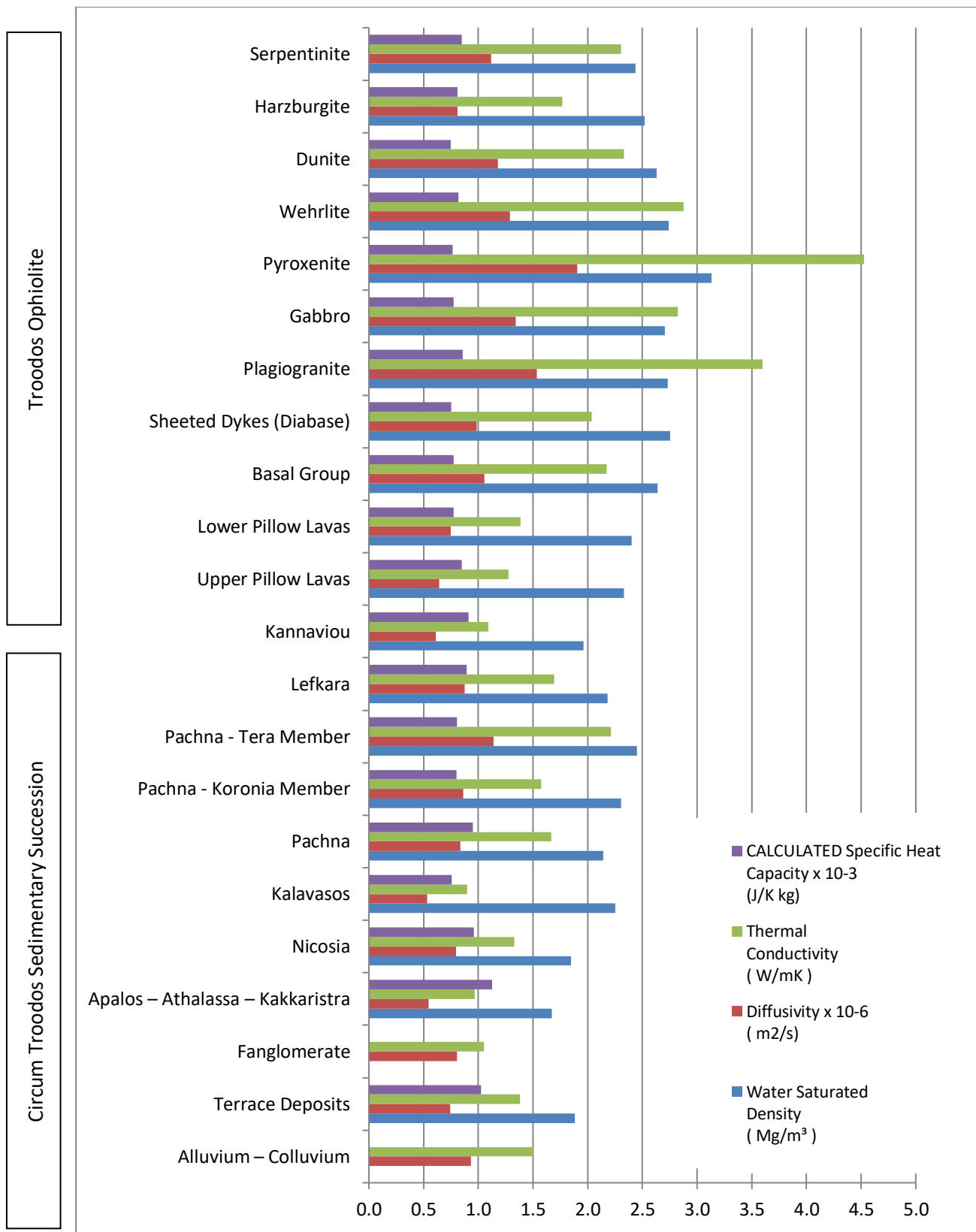


Figure 5 - 8: Mean values of thermal conductivity ( $\lambda$ ), thermal diffusivity ( $\alpha$ ), specific heat capacity ( $c_p$ ) and density ( $\rho$ ) for water saturated samples grouped by geological formation

1947), as opposed to the thermal conductivity of water at 23 °C, which is  $0.06 \text{ W m}^{-1} \text{ K}^{-1}$  (Venart and Prasad, 1980). Kalavastos Formation shows an exception, where considerably higher values were measured on the 5 dry test samples. The lithological composition of

Kalavastos Formation, as presented in Chapter 2, is Gypsum alternating with Chalky Marls and Marly Chalks. Note that those differences of the order of  $0.1 \text{ W m}^{-1} \text{ K}^{-1}$  for thermal conductivity  $\lambda$  and  $0.1 \times 10^{-6} \text{ m}^2 \text{ s}^{-1}$  for thermal diffusivity  $\alpha$  are not significant due to the small number of tested samples and to the measuring error of Isomet 2104 (Applied Precision, Inc). It is worth noting that thermal properties of the lithologies of the Circum Troodos Sedimentary Succession exhibit higher rates of increase under moisture conditions in comparison to lithologies found on the Troodos Mountain.

Highest mean thermal conductivities are observed for lithologies of the Troodos Ophiolite: Plagiogranite, Gabbro, Pyroxenite, Wehrlite, Dunite (which are all classified as lithologies of the plutonic sequence), and Harzburgite, Serpentinite (which are classified as lithologies of the mantle sequence) (Gass, 1990). The Troodos Ophiolite is a fully developed and representative piece of ocean crust (Malpas et al., 1990) but geographically, the lithologies are located at the top of the Troodos Mountain. The reason for having higher thermal conductivities may be found in the chemical composition of these lithologies which is very rich in minerals; the Geochemical Atlas of Cyprus shows much higher concentrations of metals and minerals at the Troodos Mountain than the rest of the island (Cohen et al., 2011).

#### **5.4.2 Thermal conductivity and thermal diffusivity of lithotypes**

Each geological formation may contain more than one lithotype, as explained in Chapter 2. For data sorted by their lithology, laboratory results again gave a range of values for each measured property and mean values were calculated for thermal conductivity  $\lambda$ , thermal diffusivity  $\alpha$  and specific heat capacity  $c_p$  (Table 5 - 3). The column “min” in the Table 5 - 3 shows the minimum measured values of the tested samples, “max” refers to maximum measured values and “average” is the mean of the measured values.

Figure 5 - 9 and Figure 5 - 10 show the mean values of thermal diffusivity  $\alpha$  and thermal conductivity  $\lambda$  respectively as presented in Table 5 - 3. Dry samples are illustrated with red colour and water saturated samples with blue colour. Mean values of thermal conductivity  $\lambda$  taken at 100% moisture conditions are equal or higher than those for dry samples for all lithologies, with the only exception of Gypsum, which has higher thermal conductivity under dry conditions (Figure 5 - 10). This is due to the molecular structure of Gypsum with water present ( $\text{CaSO}_4 \cdot 2\text{H}_2\text{O}$ ).



Table 5 – 1 (continue in Table 5-2): Laboratory measured values of thermal conductivity ( $\lambda$ ), thermal diffusivity ( $\alpha$ ), specific heat capacity ( $c_p$ ) and density ( $\rho$ ) grouped by geological formation as presented in the Geological Map of Cyprus (1995).

Geological formation	Thermal Conductivity $\lambda$ (W m <sup>-1</sup> K <sup>-1</sup> )						Thermal Diffusivity $\alpha$ $\times 10^{-6}$ (m <sup>2</sup> s <sup>-1</sup> )						Specific Heat Capacity $c_p$ $\times 10^{-3}$ (J K <sup>-1</sup> kg <sup>-1</sup> )						Density $\rho$ $\times 10^{-3}$ (kg m <sup>-3</sup> )						No. of samples	
	DRY			WATER SATURATED			DRY			WATER SATURATED			DRY			WATER SATURATED			DRY			WATER SATURATED				
	max	min	average	max	min	average	max	min	average	max	min	average	max	min	average	max	min	average	max	min	average	max	min	average		max
<b>Circum Troodos Sedimentary Succession</b>																										
<b>Alluvium – Colluvium</b>	2.2	0.3	0.9	2.3	0.9	1.5	1.5	0.3	0.8	1.6	0.5	0.9	Could not be calculated						Could not be calculated						5	
<b>Terrace Deposits</b>	1.4	0.5	0.9	1.8	1.0	1.4	0.9	0.4	0.6	1.0	0.5	0.7	1.0	0.6	0.8	1.5	0.8	1.0	2.6	1.4	2.1	2.4	1.4	1.9	9	
<b>Fanglomerate</b>	1.1	0.1	0.7	1.3	0.6	1.0	1.0	0.2	0.7	0.9	0.6	0.8	Could not be calculated						Could not be calculated						4	
<b>Apalos– Athalassa– Kakkaristra</b>	0.7	0.4	0.6	1.1	0.8	1.0	0.5	0.3	0.4	0.6	0.5	0.6	0.9	0.8	0.9	1.3	1.0	1.1	1.6	1.6	1.6	1.7	1.7	1.7	3	
<b>Nicosia</b>	1.9	0.4	0.9	2.1	0.7	1.3	1.0	0.3	0.6	1.2	0.5	0.8	1.3	0.6	0.8	1.5	0.6	1.0	2.7	1.1	2.0	2.5	1.2	1.8	25	
<b>Kalavastos</b>	1.4	1.1	1.3	1.1	0.6	0.9	0.8	0.7	0.7	0.7	0.3	0.5	0.8	0.6	0.7	0.8	0.7	0.8	2.6	2.5	2.5	2.3	2.2	2.2	5	
<b>Pachna</b>	2.2	0.6	1.3	2.4	1.0	1.6	1.1	0.4	0.7	1.1	0.6	0.8	1.5	0.5	0.8	1.7	0.7	1.0	2.7	1.0	2.4	2.5	1.0	2.1	28	
<b>Pachna (Koronia Member)</b>	1.5	0.9	1.2	1.9	1.2	1.6	0.9	0.5	0.8	0.9	0.6	0.9	0.7	0.5	0.6	1.0	0.7	0.8	2.8	2.3	2.6	2.5	2.0	2.3	7	
<b>Pachna (Terra Member)</b>	2.6	1.3	1.9	2.6	2.0	2.2	1.5	0.8	1.2	1.3	0.9	1.1	0.7	0.6	0.7	1.0	0.6	0.8	2.7	2.5	2.6	2.6	2.2	2.5	6	
<b>Lefkara</b>	2.1	0.6	1.4	2.2	1.2	1.7	1.2	0.3	0.8	1.1	0.6	0.9	0.8	0.7	0.7	1.0	0.8	0.9	2.7	2.3	2.5	2.4	1.8	2.2	14	
<b>Kannaviou</b>	0.6		1.1		0.6		0.6		0.6		0.9		2.6		2.0		1									

Table 5 - 2 (continue from Table 5-1): Laboratory measured values of thermal conductivity ( $\lambda$ ), thermal diffusivity ( $\alpha$ ), specific heat capacity ( $c_p$ ) and density ( $\rho$ ) grouped by geological formation.

Geological formation	Thermal Conductivity $\lambda$ (W m <sup>-1</sup> K <sup>-1</sup> )						Thermal Diffusivity $\alpha$ $\times 10^{-6}$ (m <sup>2</sup> s <sup>-1</sup> )						Specific Heat Capacity $c_p$ $\times 10^{-3}$ (J K <sup>-1</sup> kg <sup>-1</sup> )						Density $\rho$ $\times 10^{-3}$ (kg m <sup>-3</sup> )						No. of samples	
	DRY			WATER SATURATED			DRY			WATER SATURATED			DRY			WATER SATURATED			DRY			WATER SATURATED				
	max	min	average	max	min	average	max	min	average	max	min	average	max	min	average	max	min	average	max	min	average	max	min	average		max
<b>Troodos Sedimentary Ophiolite</b>																										
<b>Upper Pillow Lavas</b>	1.1	1.1	1.1	1.4	1.2	1.3	0.7	0.6	0.6	0.7	0.6	0.6	0.7	0.7	0.7	0.9	0.8	0.9	2.6	2.5	2.5	2.3	2.3	2.3	2	
<b>Lower Pillow Lavas</b>	2.1	0.9	1.3	2.1	1.1	1.4	1.2	0.5	0.7	1.0	0.6	0.8	0.7	0.6	0.7	0.9	0.6	0.8	2.7	2.5	2.6	2.6	2.2	2.4	7	
<b>Basal Group</b>	2.8	1.4	2.1	3.0	1.6	2.2	1.3	0.8	1.1	1.3	0.8	1.1	0.8	0.7	0.7	0.8	0.7	0.8	2.7	2.6	2.7	2.7	2.5	2.6	4	
<b>Sheeted Dykes (Diabase)</b>	2.2	1.7	2.0	2.4	1.8	2.0	1.2	0.9	1.0	1.1	0.9	1.0	0.8	0.6	0.7	0.8	0.7	0.8	3.0	2.7	2.8	3.0	2.6	2.8	7	
<b>Plagiogre</b>			3.4			3.6			1.6			1.5			0.8			0.9			2.8			0.7	1	
<b>Gabbro</b>	2.8	1.8	2.2	3.7	2.2	2.8	1.9	1.1	1.4	1.6	1.0	1.3	0.7	0.5	0.6	0.9	0.7	0.8	2.9	2.8	2.8	2.8	2.6	2.7	3	
<b>Pyroxenite</b>			4.2			4.5			1.8			1.9			0.7			0.8			3.2			3.1	1	
<b>Wehrlite</b>	3.0	2.9	2.9	3.0	2.8	2.9	1.3	1.3	1.3	1.4	1.2	1.3	0.8	0.8	0.8	0.8	0.8	0.8	2.8	2.7	2.8	2.8	2.7	2.7	2	
<b>Dunite</b>			2.4			2.3			1.1			1.2			0.8			0.8			2.7			2.6	1	
<b>Harzburgite</b>	2.0	1.3	1.7	1.9	1.5	1.8	1.0	0.8	0.9	0.9	0.7	0.8	0.8	0.7	0.8	0.9	0.8	0.8	2.7	2.6	2.6	2.7	2.4	2.5	3	
<b>Serpentinite</b>	2.3	1.7	2.0	2.5	2.2	2.3	1.1	0.8	1.0	1.2	1.0	1.1	0.8	0.8	0.8	0.9	0.8	0.9	2.7	2.6	2.6	2.5	2.4	2.4	2	
<b>Keryneia Terrane</b>																										
<b>Kythrea</b>	0.4	0.9	0.7	Not calculated			0.4	0.6	0.5	Not calculated			0.7	0.7	0.7	Not calculated			1.9	2.2	2.1	Not calculated			3	

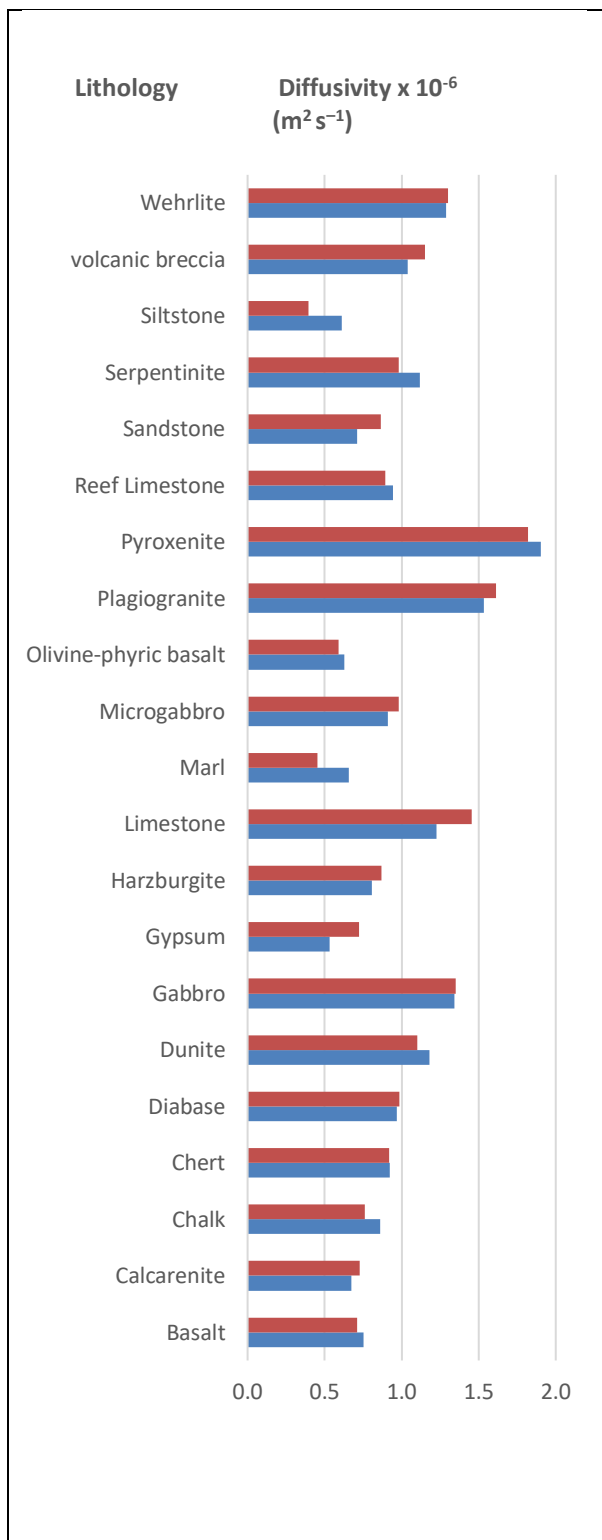


Figure 5 - 9: Mean values of thermal diffusivity  $\alpha$  per lithology: dry samples (red color) and water saturated samples (blue color)

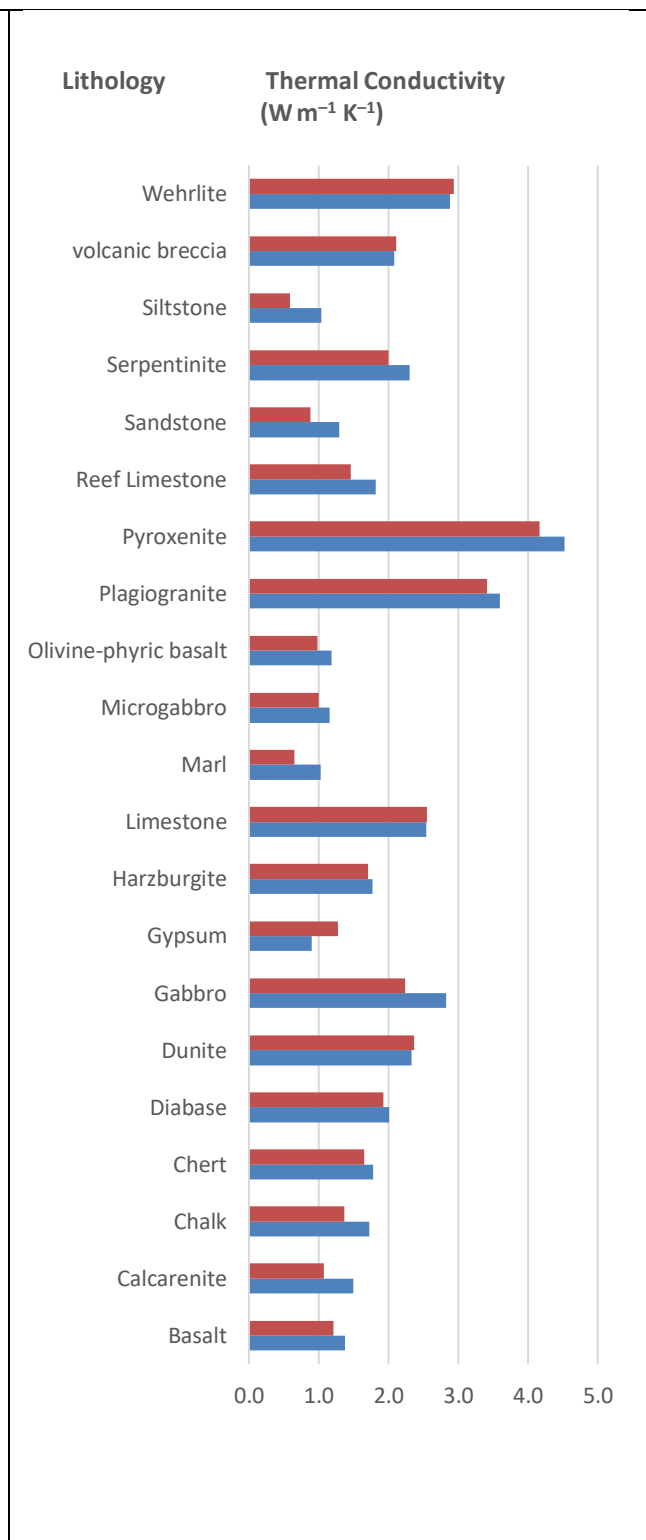


Figure 5 - 10: Mean values of thermal conductivity  $\lambda$  per lithology: dry samples (red color) and water saturated samples (blue color)

Table 5 - 3: Laboratory measured values of thermal conductivity ( $\lambda$ ), thermal diffusivity ( $\alpha$ ) and specific heat capacity ( $c_p$ ) per lithology

LITHOLOGY	Thermal Conductivity $\lambda$ ( $\text{W m}^{-1} \text{K}^{-1}$ )						Thermal Diffusivity $\alpha \times 10^{-6}$ ( $\text{m}^2 \text{s}^{-1}$ )						Specific Heat Capacity $c_p \times 10^{-3}$ ( $\text{J K}^{-1} \text{kg}^{-1}$ )						No. of samples
	DRY			WATER SATURATED			DRY			WATER SATURATED			DRY			WATER SATURATED			
	max	min	average	max	min	average	max	min	average	max	min	average	max	min	average	max	min	average	
Basalt	1.5	1.1	1.2	1.5	1.3	1.4	0.9	0.6	0.7	0.9	0.7	0.8	0.7	0.6	0.7	0.9	0.6	0.8	4
Calcarenite	2.0	0.4	1.1	2.1	0.9	1.5	1.2	0.3	0.7	0.8	0.5	0.7	0.9	0.5	0.7	1.0	0.6	0.8	23
Chalk	2.2	0.6	1.4	2.4	1.2	1.7	1.2	0.3	0.8	1.1	0.6	0.9	0.9	0.6	0.7	1.2	0.7	0.9	28
Chert	2.1	1.4	1.7	2.0	1.6	1.8	1.2	0.8	0.9	1.1	0.8	0.9	0.8	0.7	0.7	0.9	0.8	0.9	6
Diabase	2.8	1.0	1.9	3.0	1.1	2.0	1.3	0.6	1.0	1.3	0.6	1.0	0.8	0.6	0.7	0.8	0.7	0.8	9
Dunite	2.4	2.4	2.4	2.3	2.3	2.3	1.1	1.1	1.1	1.2	1.2	1.2	0.8	0.8	0.8	0.7	0.7	0.7	1
Gabbro	2.8	1.8	2.2	3.7	2.2	2.8	1.9	1.1	1.4	1.6	1.0	1.3	0.7	0.5	0.6	0.9	0.7	0.8	3
Gypsum	1.4	1.1	1.3	1.1	0.6	0.9	0.8	0.7	0.7	0.7	0.3	0.5	0.8	0.6	0.7	0.8	0.7	0.8	5
Harzburgite	2.0	1.3	1.7	1.9	1.5	1.8	1.0	0.8	0.9	0.9	0.7	0.8	0.8	0.7	0.8	0.9	0.8	0.8	3
Limestone	2.6	2.6	2.6	2.5	2.5	2.5	1.5	1.5	1.5	1.2	1.2	1.2	0.7	0.7	0.7	0.8	0.8	0.8	1
Marl	0.9	0.5	0.7	1.3	0.7	1.0	0.6	0.3	0.5	0.8	0.5	0.7	1.3	0.8	1.0	1.5	0.9	1.1	9
Microgabbro	1.0	1.0	1.0	1.2	1.2	1.2	1.2	0.6	1.0	1.1	0.6	0.9	0.7	0.6	0.7	0.8	0.7	0.7	4
Olivine-phyric basalt	1.1	0.9	1.0	1.2	1.2	1.2	0.7	0.5	0.6	0.7	0.6	0.6	0.7	0.7	0.7	0.9	0.8	0.8	2
Plagiogranite	3.4	3.4	3.4	3.6	3.6	3.6	1.6	1.6	1.6	1.5	1.5	1.5	0.8	0.8	0.8	0.9	0.9	0.9	1
Pyroxenite	4.2	4.2	4.2	4.5	4.5	4.5	1.8	1.8	1.8	1.9	1.9	1.9	0.7	0.7	0.7	0.8	0.8	0.8	1
Reef Limestone	2.2	0.8	1.5	2.5	1.2	1.8	1.4	0.5	0.9	1.3	0.6	0.9	0.8	0.5	0.6	1.0	0.6	0.8	14
Sandstone	1.9	0.4	0.9	1.9	0.8	1.3	1.0	0.3	0.9	1.2	0.5	0.7	1.0	0.6	0.8	1.4	0.6	0.8	10
Serpentinite	2.3	1.7	2.0	2.5	2.2	2.3	1.1	0.8	1.0	1.2	1.0	1.1	0.8	0.8	0.8	0.9	0.8	0.8	2
Siltstone	0.6	0.6	0.6	1.0	1.0	1.0	0.4	0.4	0.4	0.6	0.6	0.6	1.5	0.9	1.2	1.7	1.1	1.4	2
Volcanic Breccia	2.1	2.1	2.1	2.1	2.1	2.1	1.2	1.2	1.2	1.0	1.0	1.0	0.7	0.7	0.7	0.8	0.8	0.8	1
Wehrlite	2.9	2.9	2.9	1.9	2.7	2.9	1.3	1.3	1.3	1.4	1.2	1.3	0.8	0.8	0.8	0.8	0.8	0.8	2

### 5.4.3 Comparison with thermal conductivity values of lithologies for other countries

Thermal properties of the ground concerning different lithotypes is a common issue in all countries as the same lithology may have different properties according to the place of origin. To examine this, a series of data were collected for samples having the same lithology but different origin. Such cases are the thermal conductivity values of limestone from Gaziantep, Turkey (Canakci et al., 2007), from the Tarim Basin, Northwest China and from North China (Liu et al., 2011; Miao et al., 2014), from Southern Israel (Schutz et al., 2012), from the Altensalzwedel area, Germany (Norden et al., 2012), USA (Woodside and Messmer, 1961; Birch and Clark, 1940) as well as from various countries (Gegenhuber and Schoen, 2012). All these values measured on dry samples together with the corresponding measured values obtained from Cyprus are illustrated in Table 5 - 4.

Table 5 - 4: Thermal conductivity mean values ( $W m^{-1} K^{-1}$ ) measured on dry samples in various countries

Country	Sandstone	Limestone	Basalt	Gabbro	Country	Sandstone	Limestone	Gabbro
Austria (Deutschgoritz)	2.8				Germany (Pirna)	3.5		
Austria (Nondorf)				2.4	Israel South	4.9	2.7	
Austria (Puliberg, Kobersdorf)			2.6		Paraguay	5.2		
Austria (Seckau)	2.8				Turkey (Gaziantep)		1.7	
Austria (Weitendorf, Wildon)			1.7		U.S.A (California, Berkeley)	6.49		
China (Tarim Basin)	2.1	2.5	1.3		U.S.A (Missouri, St. Peters)	3.56		
China North				2.4	U.S.A (Ohio, Berea)	2.39		
Cyprus	0.9	2.6	1.2	2.2	U.S.A (West Virginia, French Creek)			2.29
Germany (Altensalzwedel)	2.8				U.S.A (Wisconsin, Meller)			1.99
Germany (Oberfranken)	2.6				U.S.A (Wyoming, Tensleep)	3.04		

Values vary greatly and as no more data for comparison were available (porosity, density, mineralogical composition, etc.) in the cases under consideration, one cannot reach a definite conclusion about the thermal behavior of lithotypes in various areas of the world. The only safe statement to make is that for each country/area and each lithology thermal properties must be measured.

#### 5.4.4 Relation of the thermal conductivity and the geological age of rock samples

In order to investigate the effect of the geological age of rocks on measured thermal conductivities, samples of the same lithotype but of different age were considered. For this investigation reef limestone and calcarenite lithologies were further analyzed.

In Figure 5 - 11, the average value of measured thermal conductivity of 12 reef limestone samples were plotted (measurements were repeated twice for each sample). All samples belong to the same lithology (reef limestone) but they have different geological ages. 7 of the tested samples were identified as Pachna Formation/Koronia Member (KM) and they belong to the Upper Miocene (Neogene) based on the Geological Map of Cyprus (1995). 5 samples belong to Pachna Formation/Terra Member (TM) of the Lower Miocene (Neogene). Samples of KM (average value presented with orange color in Figure 5 - 11) in their majority present lower thermal conductivity values than samples of TM (green color in Figure 5 - 11), which are much oldest (Figure 5 - 11). Any exception may be due to the purity of the sample and the relatively not homogeneous composition. In addition, calculated standard deviation of all samples equals to 0.4 W/mK and average value 1.5 W/mK.

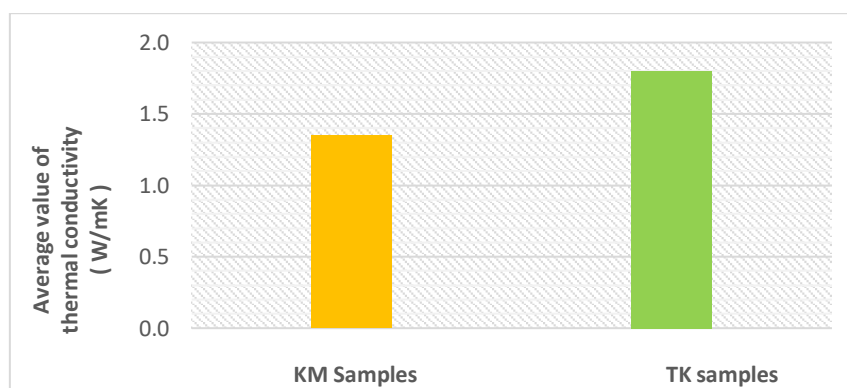


Figure 5 - 11: Thermal conductivity values measured on samples with different geological age (Orange color: Koronia Member samples / Upper Miocene, Green color: Terra Member samples / Lower Miocene)

As a second case the calcarenite samples taken from three quarries in Cyprus, one from Gerolakkos area and two from Kivides area were studied. All quarries extract calcarenite stones to be used as building material.

Geological samples from Gerolakkos area, which were used for hundreds of years as a building stone in Nicosia, belong to Pliocene age (Pliocene/Neogene) and are much younger than samples from Kivides (Middle Miocene/Neogene) (Geological Map of Cyprus, 1995). Samples from Gerolakkos quarry have high porosity and a mean value of thermal conductivity of only  $0.42 \text{ W m}^{-1} \text{ K}^{-1}$ . On the other hand, samples from the two quarries in the Kivides area have much lower porosity and their average thermal conductivities are 1.18 and  $1.43 \text{ W m}^{-1} \text{ K}^{-1}$ .

## 5.5 Geothermal Maps

The Thermal Conductivity and the Thermal Diffusivity Maps of Cyprus were compiled in order to help engineers design geothermal heat exchangers and ground-source heat pump systems based on scientific information and analysis. Geothermal heat exchangers and ground-source heat pump systems require detailed design in order to be cost effective and energy efficient. For this reason, only the physical ground properties are presented here to be used as an input to design software. Heat flux maps cannot be drawn since every system has its own characteristics that must be considered. For the applications under consideration not only the ground physical properties, thermal conductivity  $\lambda$ , thermal diffusivity  $\alpha$ , ground temperature, etc, need to be accurately known but also the ground heat exchanger characteristics and properties, the BH thermal resistance, the heating and cooling load of the building and the characteristics of the ground coupled heat pump (thermal power, coefficient of performance, inlet and outlet temperatures, flow rate, etc.).

A Geographic Information System (GIS), also known as a Geographical Information System or Geospatial Information System, is any system that captures, stores, analyzes, manages, and presents data that are linked to a geographic location. GIS is a platform for designing and managing solutions through the application of geographic knowledge. Users range from information storage, spatial pattern identification, visual presentation of spatial relationships, remote sensing - all sometimes made available through internet web interfaces, involving large numbers of users, data collectors, specialists and/or community participants.

In this research, the ArcGIS software (ESRI) was used. It was chosen because it is used worldwide by many large organizations and also most of the government services in Cyprus.

### **5.5.1 Map Compilation**

Geological boundaries presented on the Geothermal Maps of Cyprus were based on the Geological Map of Cyprus 1:250,000 (1995), which was supplied by the Cyprus Geological Survey Department in GIS format. Geological maps are used by engineers as a primary source of information for various aspects of land-use planning, as they give information concerning the distribution of different rock types lying in surficial and bedrock layers, as well as locations of geological structure features, such as faults and folds.

With the use of ArcGIS, mean values calculated for each geological formation were assigned to each area, according to the area's geological formation. In more detail, each geological polygon has been assigned a value for thermal conductivity ( $\lambda$ ) and thermal diffusivity ( $\alpha$ ). Finally, the 4 different Geothermal Maps of Cyprus were compiled, one for each thermal property, separately for dry and water saturated conditions (Figure 5 - 12, Figure 5 - 13, Figure 5 - 14, Figure 5 - 15). Areas with missing data are shown with grey colour.

Additionally, the Bedrock Density Map of the island was compiled in the same way as the rest of the maps, as density ( $\rho$ ) is a property required in almost all engineering applications (Figure 5 - 16). More specifically, with regards to Ground Heat Exchangers (GHE), the density influences construction costs.

GIS data of the compiled maps are available online in a web application at <https://amc-cy.maps.arcgis.com/apps/ImageryViewer/index.html?appid=d81a63acc03c4c35a80c65e8c1689c77>.

### **5.5.2 Map Results**

The data presented on the maps are the outcome of the laboratory experiments. From maps it can be distinguished between the two terranes that have been the main object of the present



study, the Circum Troodos Sedimentary Succession and the Troodos Mountain, which both had a very important and unique role in the development of the island through the years.

From the geothermal point of view, the Troodos Ophiolite offers the highest GHE performance, even though installation costs in the area will be higher than other areas due to the higher density of the ground.

The effect of water in underground layers has also been studied and results can be seen on the Thermal Conductivity Map (Figure 5 - 13) and Thermal Diffusivity Map at 100% moisture conditions (Figure 5 - 15). These maps present equal or higher values than the corresponding values measured under dry conditions (Figure 5 - 12, and wet conditions, Figure 5 - 13).

The only exception is Gypsum and geological formations containing Gypsum, i.e. Kalavassos Formation, which have better thermal properties under dry conditions. This is due to the influence of water on the molecular structure of Gypsum.

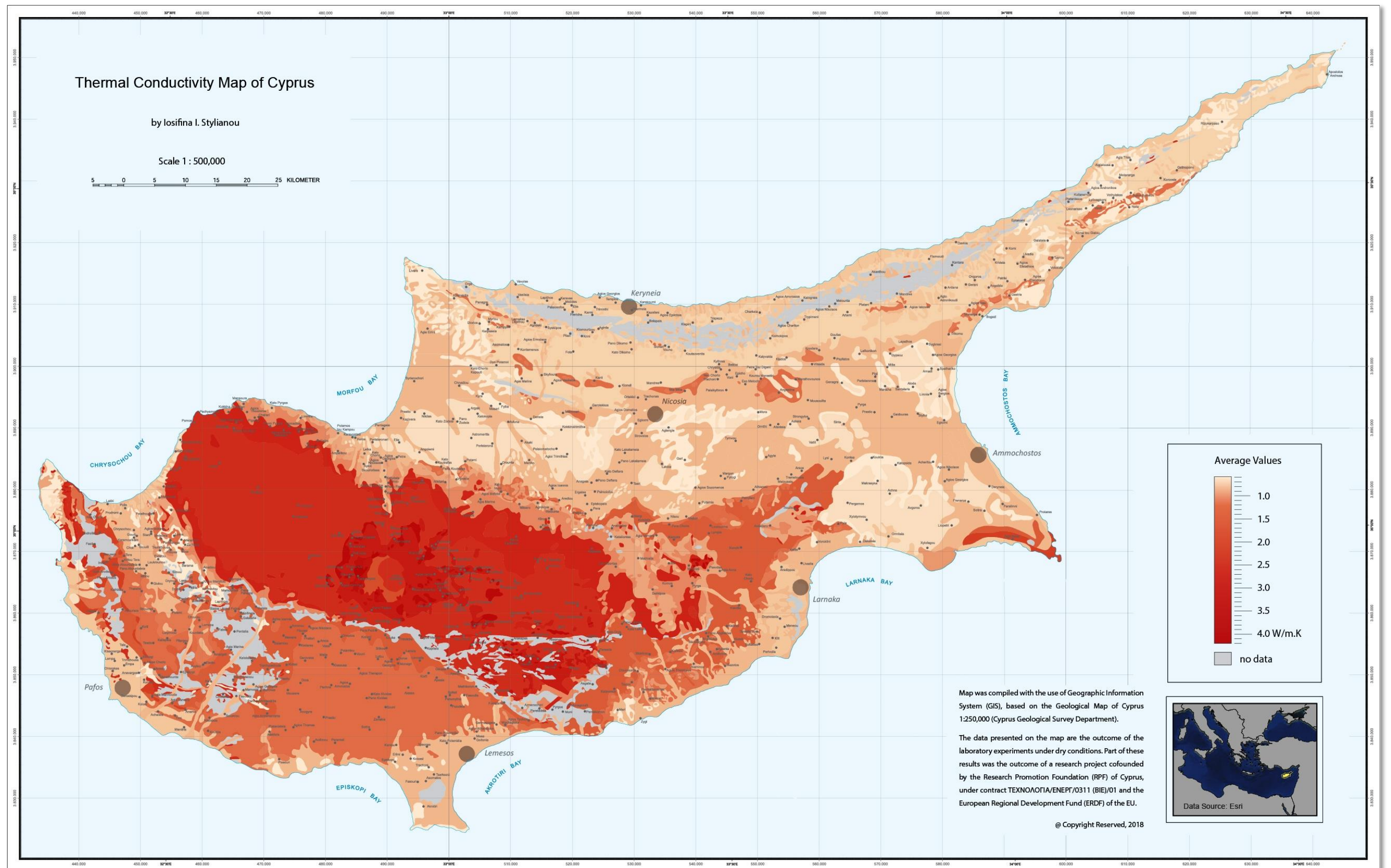


Figure 5 - 12: Thermal Conductivity Map of Cyprus (Dry)

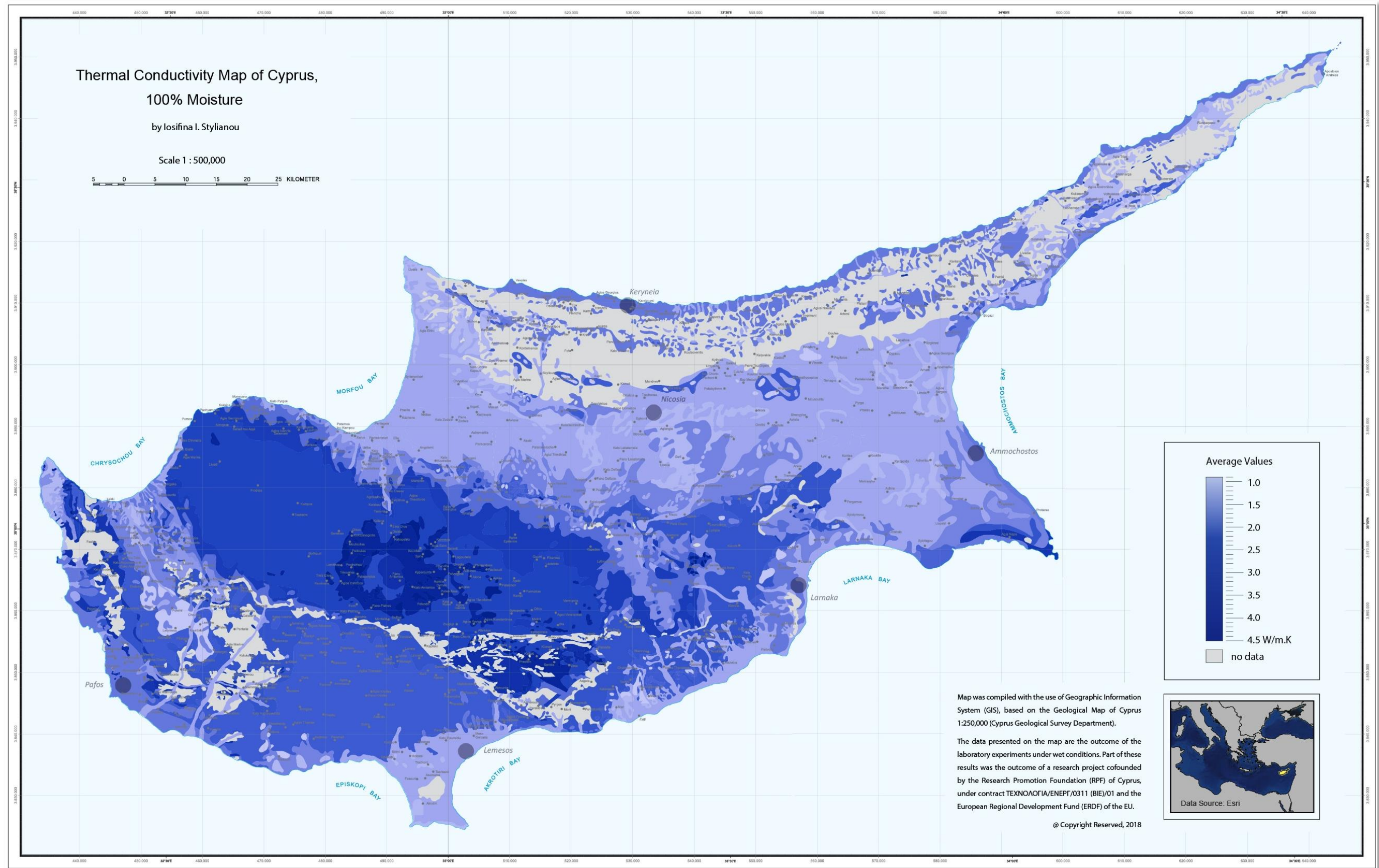


Figure 5 - 13: Thermal Conductivity Map of Cyprus (Water Saturated)

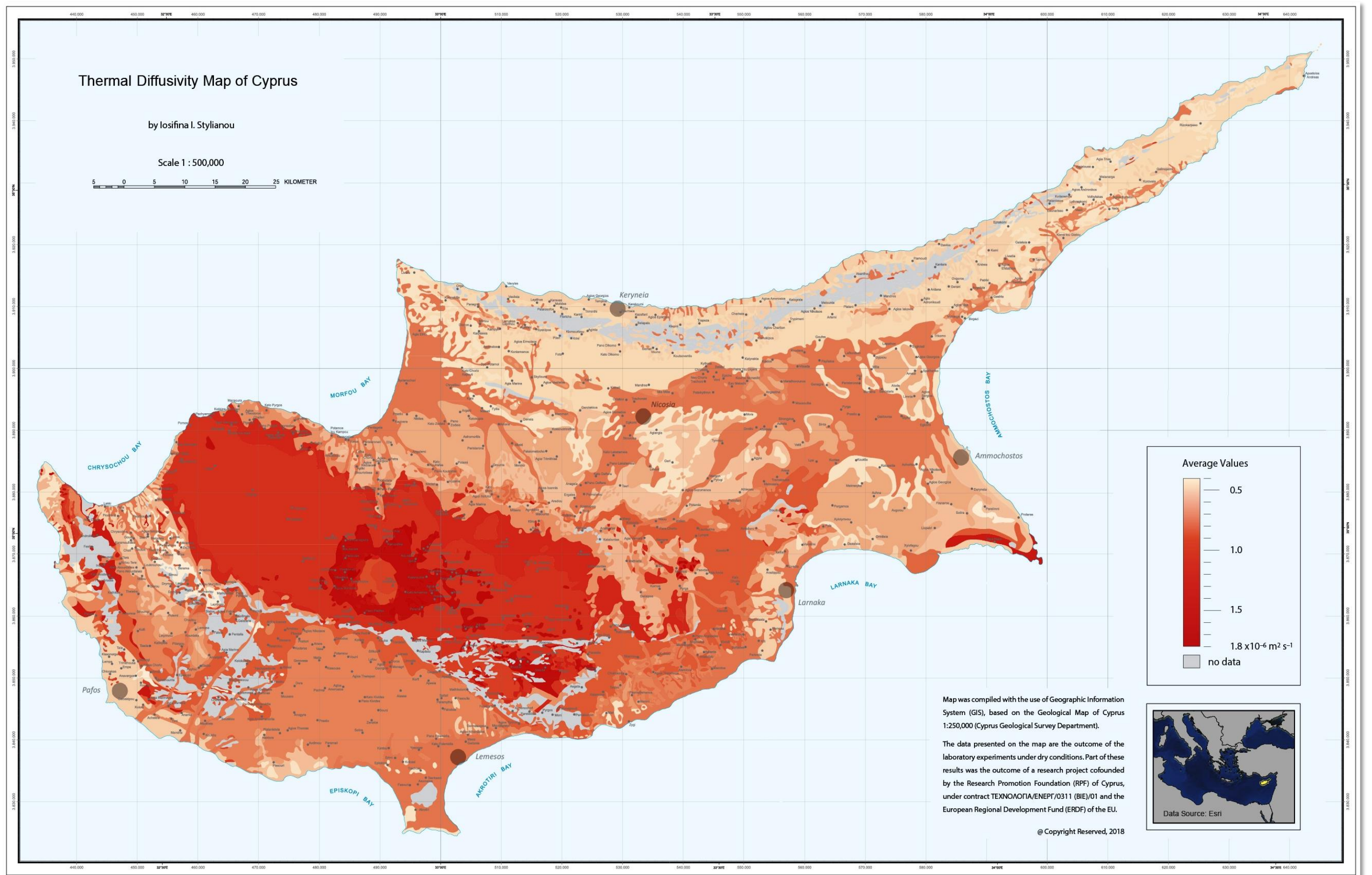


Figure 5 - 14: Thermal Diffusivity Map of Cyprus (Dry)

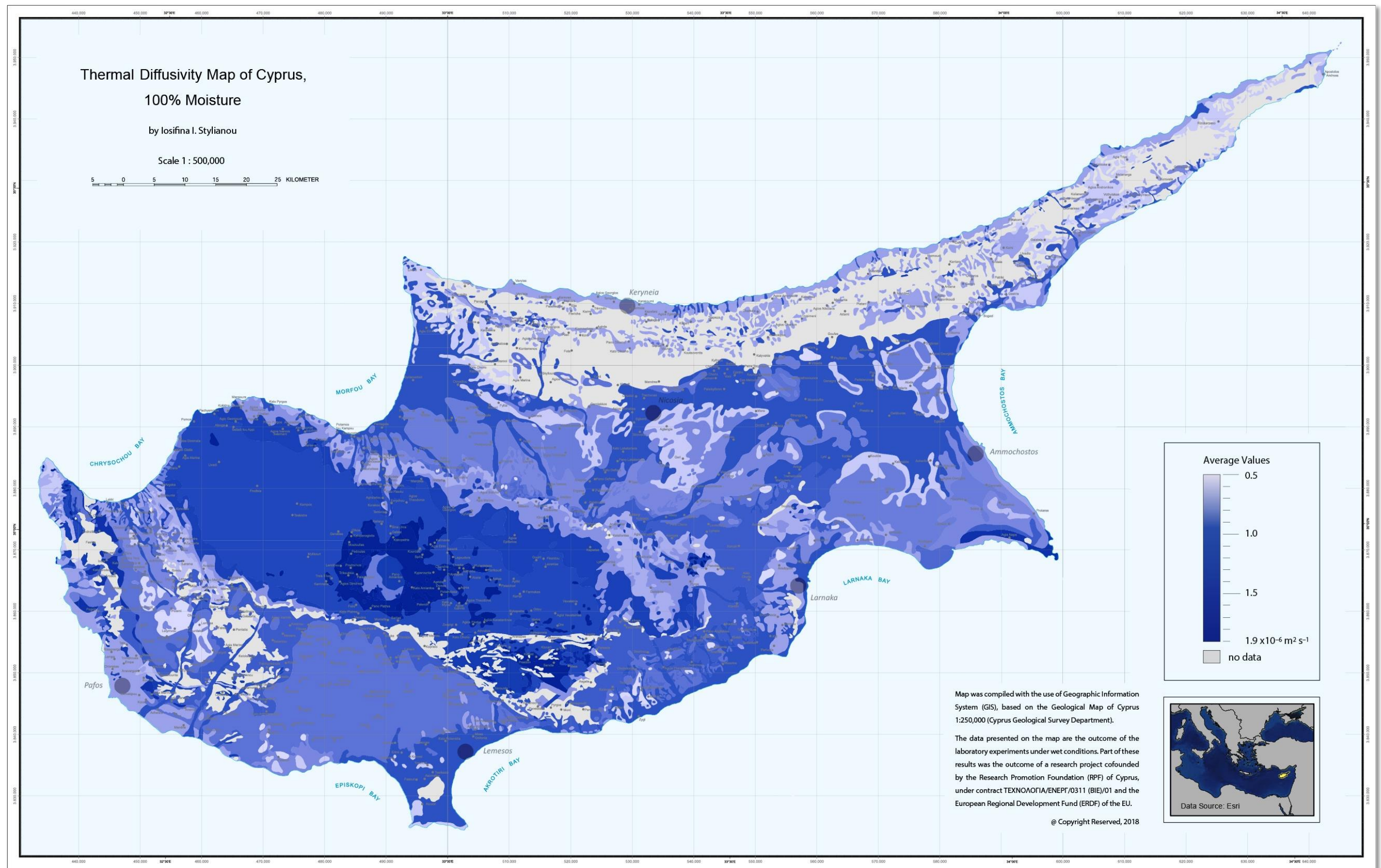


Figure 5 - 15: Thermal Diffusivity Map of Cyprus (Water Saturated)

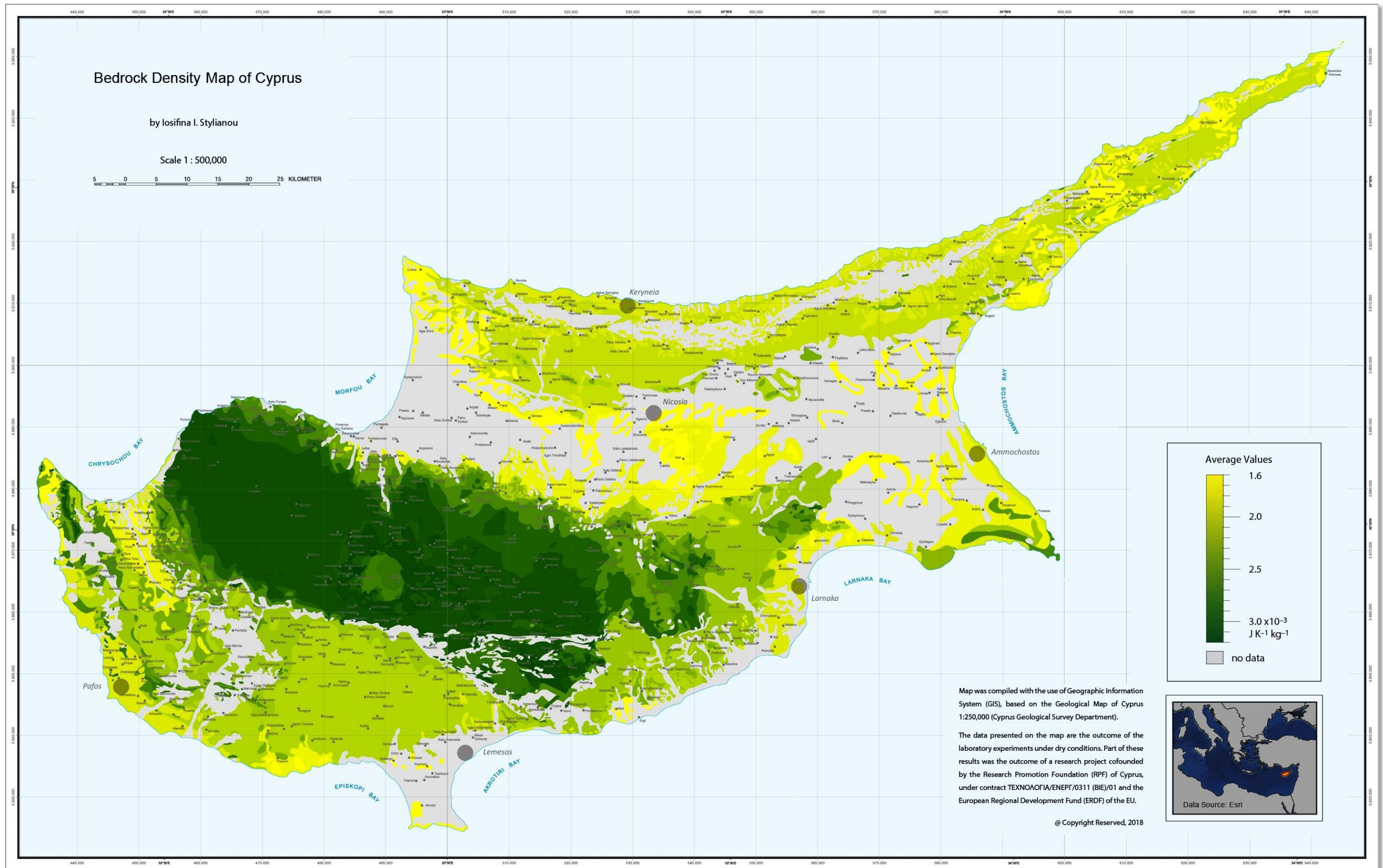


Figure 5 - 16: Density Maps of Cyprus (Bulk Density)

## 5.6 Summary

Measurements of thermo-physical properties of the same or similar rock types in Cyprus show considerable differences, suggesting that properties on their own cannot be used to distinguish between rock types. On the other hand, if the geological type is known, a range of values of thermal properties can be assigned to the geological formation or lithology.

Laboratory results of each geological type fall within a range of values for each thermophysical property; measured values of thermal properties differ considerably between and within rock types. This variation is due to the fact that samples of the same type may contain different proportions of minerals, may have different geological ages or simply include impurities. Furthermore rock samples as found in nature are not homogeneous and not isotropic. The smaller the range of values measured for a lithotype the higher the homogeneous composition of the lithotype.

Laboratory results also show a difference between formations of the Circum Troodos Sedimentary Succession and formations of the Troodos Ophiolite. Mean values of thermal diffusivity and thermal conductivity are definitely higher for the geological formations of the Troodos Ophiolite than the Circum Troodos Sedimentary Succession.

The effect of water in samples has also been presented. Measured values of thermal conductivity and thermal diffusivity of samples in 100% moist conditions have been found to be higher or equal to the corresponding values measured under dry conditions. The increasing effect of moisture content is due to the thermal conductivity of water, which is considerably higher than the thermal conductivity of air that fills the pores of rocks in dry conditions. The main exception is Gypsum and geological formations containing gypsum, i.e. Kalavassos Formation, which have better thermal properties under dry conditions. This is due to the molecular structure of Gypsum in the presence of water.

The outcome of the laboratory experiments were used to construct the Thermal Conductivity and Thermal Diffusivity Maps of Cyprus, which are very useful tools for engineers involved in geothermal energy projects. The Troodos Ophiolite from a geothermal point of view can be considered as a separate region as it has the highest thermal conductivity and diffusivity values.

Regarding the thermal properties of the Terrain of Circum Troodos Sedimentary Succession, it is highly affected by rainfall and the presence of underground aquifers.

The thermal properties of each rock type may differ according to the place of origin. Comparison of data of similar lithologies but from different regions or countries, it was identified that properties can vary and therefore data cannot be generalized. Measurements must be made specifically for each region.

The impact of geological age on thermal conductivity was another parameter investigated in this study. Analysis on reef limestone and calcarenite samples of different geological ages showed that the thermal conductivity of lithologies increases with geological age.



## **Chapter 6: Estimation of ground heat absorption rate of a GHE at a particular location**

### **6.1 Introduction**

This Chapter focuses on the measurement and analysis of the thermal properties of lithologies encountered in an area, in order to be used in conjunction with the FlexPDE (PDE Solutions Inc) software for the calculation of heat injection of GHEs to the ground. The main objective is to predict the thermal response of the system and the appropriate capacity of ground source heat pumps for specific heating and cooling applications.

The focus of the study is the greater Nicosia area of Cyprus. The result is a series of thermal maps which can be employed by engineers in the sizing of vertical GHEs for heating and cooling applications. GIS data of the compiled maps are available online in a web application at <https://amc-cy.maps.arcgis.com/apps/ImageryViewer/index.html?appid=d81a63acc03c4c35a80c65e8c1689c77>.

### **6.2 3D Geological Modeling of the Study Area**

Nicosia (Lefkosia) is the capital city of Cyprus, located in the center of the island in the Mesaoria Plain, which is a rather flat area between the Troodos mountain range to the south-east and the Pentadaktylos mountain range to the north. The climate is Mediterranean, with long, warm, dry summers from June to October and mild winters with occasional rain, from December to April. The following temperatures were recorded by the Meteorological Service of the Republic of Cyprus, in 2017, at Athalassa Meteorological Station, near Nicosia city: during winter from  $-1.7^{\circ}\text{C}$  (nighttime) to  $20.9^{\circ}\text{C}$  (daytime) and during summer from  $20.7^{\circ}\text{C}$  (nighttime) to  $44.6^{\circ}\text{C}$  (daytime). Under these climatic conditions, GHEs have the potential to be used together with ground source heat pumps for heating and especially for cooling. For these reason the area was chosen for a detailed study of the potential for use of GHEs in Cyprus.

The area covered by the study is shown in Figure 6 - 1 (area within the red rectangle). From the geological point of view, the area was analysed by Harrison et. al. (2008) "Bedrock

Geologic Map of the Greater Nicosia Area”, which was a part of the “Seismic Hazard and Risk Assessment of the Greater Nicosia Area” project.

For the needs of this study, a 3D geological model was created (Figure 6 - 2) in order to visualize the study area, examine its thermal response and the potential of vertical GHE usage in the area. The 3D model was designed with the use of the ArcGIS and Adobe Illustrator software.

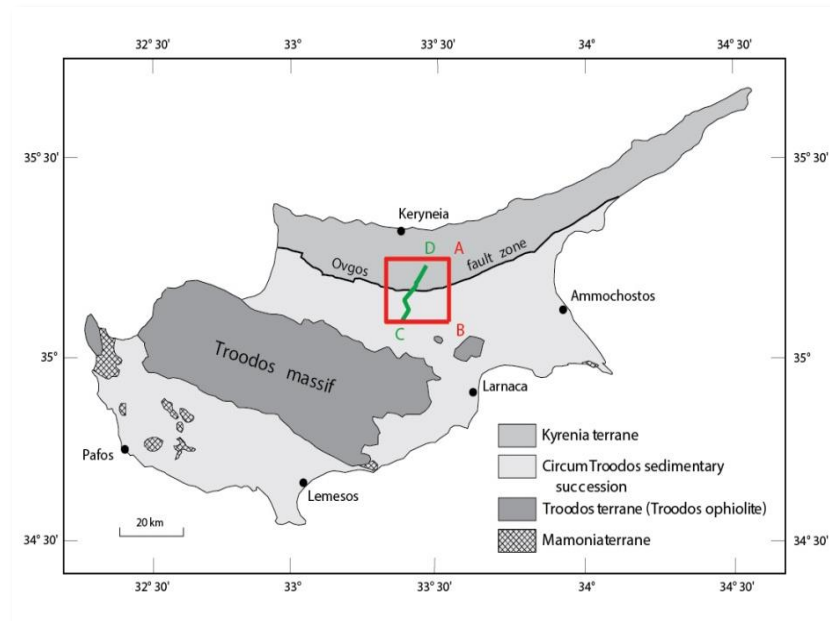


Figure 6 - 1: Map of the four major tectonic-stratigraphic terranes of Cyprus (Harrison et al., 2008 and the Geological Map of Cyprus, 1995). The red box shows the boundary of the Nicosia geologic map. The green line (C-D) is the cross section line shown in Figure 6-2.

For the design of the 3D model, geological data derived from the project “Seismic Hazard and Risk Assessment of the Greater Nicosia Area” were used. The program was launched in 1998 with funds provided by the United States Agency for International Development (USAID) and by the United Nations Development Program (UNDP) and finished in 2004. The geological mapping was based on fieldwork mapping, geological age dates, and data from a number of boreholes in the area. All geological units presented in the study area can be found in the legend of Figure 6 - 2. The lithology of all geological units is explained in Chapter 2, Geology of Cyprus.

In addition, the Nicosia Formation, is divided into seven geological members (Figure 6 - 2):

1. The Marine Littoral Member - Gravel, sand and silt deposited in an intertidal zone.
2. The Aspropamboulos Oolite Member - Fine-grained oolite. Unidirectional, planar cross beds directed to the south.

3. The Lithic Sand Member - Dominantly lithic sand, but also includes lesser marl, silty marl and calcarenite.
4. The Athalassa Member - Calcarenite and bioclastic calcarenite.
5. The Kephales Member - Marine gravel, cobbles, pebbles, and sand. Clasts are dominantly derived from the Troodos Ophiolite and lesser from Tertiary carbonate deposits.
6. The Marl Member - Marl, silty marl, and lesser sandy marl. Fossiliferous and typically khaki-green in color; weathered surfaces are yellow-brown in color.
7. The Basal Conglomerate Member - Gravel, cobbles, coarse sand. Clasts are dominantly derived from the Troodos Ophiolite Complex.

### **6.3 Thermal Properties of Nicosia Lithologies**

#### **6.3.1 Geological sampling**

Due to the difficulty of measuring thermal properties in situ, a geological sampling was performed in the study area and measurements of properties were performed in the laboratory. The Basal Conglomerate Member and the Marine Littoral Member of the Nicosia Formation are very small areas on the map and were not included in this study. In addition, Marine Member layers do not exceed thicknesses of more than 10 m in any area and Basal Conglomerate can be found only in very small areas having, hence they were also excluded as they have very little significance in GHE applications in the area.

#### **6.3.2 Thermal properties of the ground**

The thermal properties of the geological samples were determined in the laboratory using the methodology described in Chapter 5: Measurement and Analysis of the Thermal Properties of Rocks for the Compilation of Geothermal Maps.

#### **6.3.3 Test Results**

Totally 16 samples were collected from the Nicosia Formation: 3 from the Lapatza Formation, 3 from the Kythrea Formation, 3 from the Apalos Formation and 1 from the Kalavassos Formation (Figure 6 - 2).

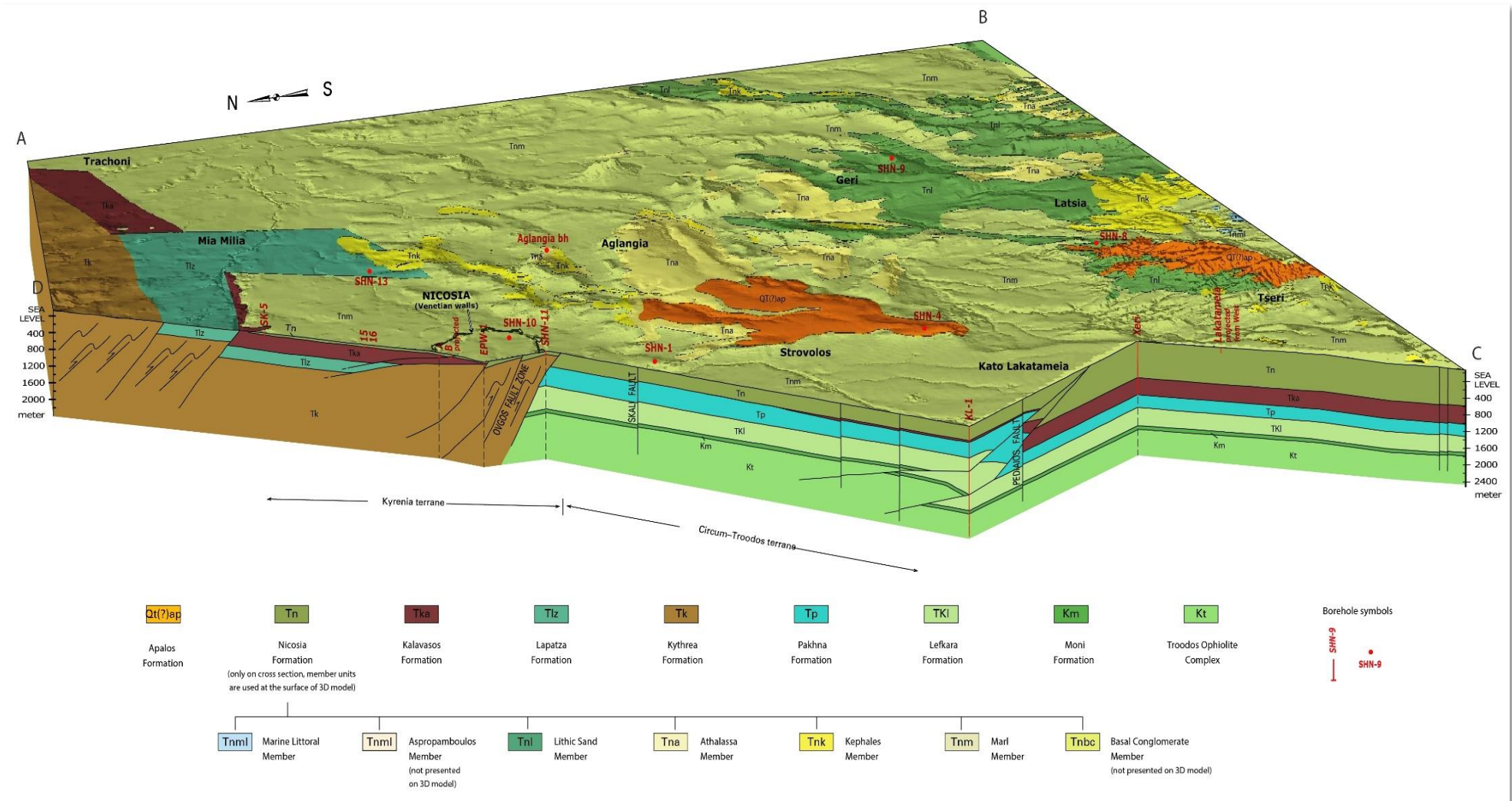


Figure 6 - 2: 3D Geological Model based on data of the “Bedrock Geologic Map of the Greater Nicosia Area” (Harrison et al., 2008)

The range of data obtained from the analysis for thermal conductivity and specific heat capacity are shown in Figure 6 - 3 and Figure 6 - 4 respectively. The data are also summarised in Table 6 - 1. It can be seen that the mean values of thermal conductivity  $\lambda$  of the samples are between 0.6 and 1.5  $\text{W m}^{-1} \text{K}^{-1}$ .

Calculated values for specific heat capacity are also in the range 0.6 to  $1.0 \times 10^{-3} \text{ J K}^{-1} \text{ kg}^{-1}$ . It should be noted that the specific heat capacity  $c_p$  was calculated using the measurement of volumetric heat capacity VCH divided by the density  $\rho$  (methodology described in Chapter 5, Section 5.3 Laboratory Tests).

From the results presented in Figure 6 - 3 and Figure 6 - 4, it can be seen that each geological formation can have a range of values for each thermal property. This is due to the variety of lithologies present in each geological formation (see Section 6.2) and many other factors such as grain size, amount and type of impurities, geological compression when the sample was formed amongst others.

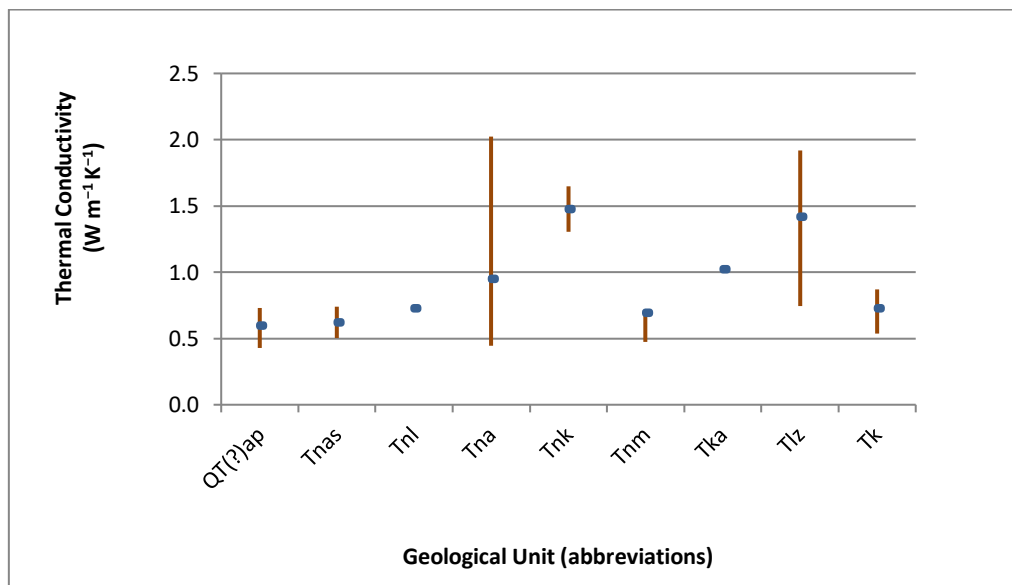


Figure 6 - 3: Range of values measured in the laboratory for thermal conductivity  $\lambda$  grouped by the geological formation/member of sample (the mean value is presented with a dot in blue color)

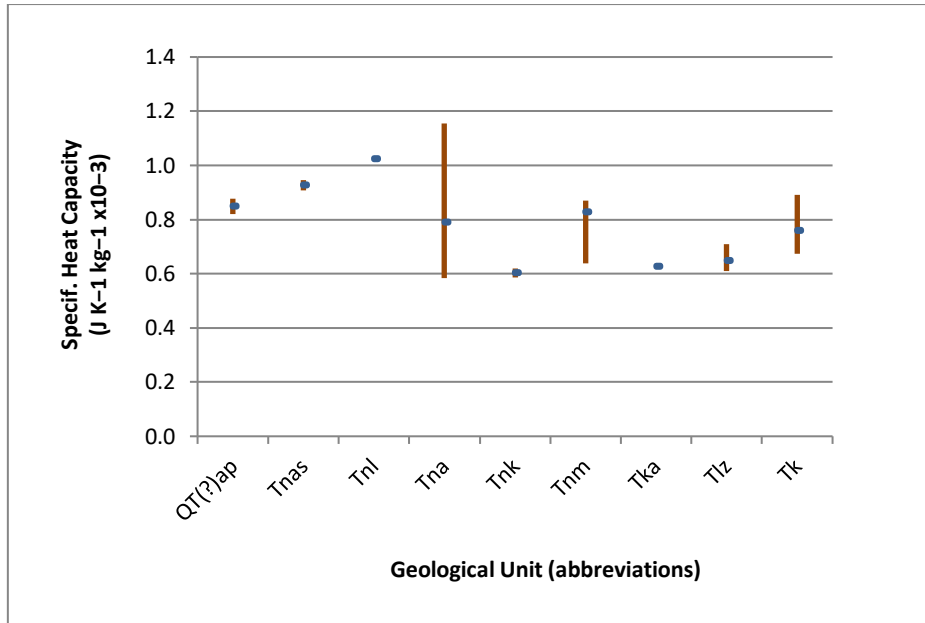


Figure 6 - 4: Range of values for specific heat capacity  $c_p$  grouped by the geological formation/member of sample (the mean value is presented with a dot in blue color)

Table 6 - 1: Mean values of measured thermal conductivity  $\lambda$ , thermal diffusivity  $\alpha$ , density  $\rho$  and calculated specific heat capacity  $c_p$  per geological unit.

Geological Unit (abbreviation)		Thermal Diffusivity $\times 10^{-6}$ ( $m^2s^{-1}$ )	Thermal Conductivity ( $Wm^{-1}K^{-1}$ )	CALCULATED Specific Heat Capacity $\times 10^{-3}$ ( $JK^{-1}kg^{-1}$ )	no of samples tested
Apalos Formation (QT(?)ap)		0.4	0.6	0.9	3
Nicosia Formation (Tn)	Aspropamboulos Oolite Member (Tnas)	0.4	0.6	0.9	2
	Lithic Sand Member (Tnl)	0.5	0.7	1.0	1
	Athalassa Member (Tna)	0.6	0.9	0.8	9
	Kephales Member (Tnk)	0.9	1.5	0.6	2
	Marl Member (Tnm)	0.4	0.6	0.8	2
Kalavassos Formation (Tka)		0.7	1.0	0.6	1
Lapatza Formation (Tlz)		1.0	1.4	0.7	3
Kythrea Formation (Tk)		0.5	0.7	0.8	3

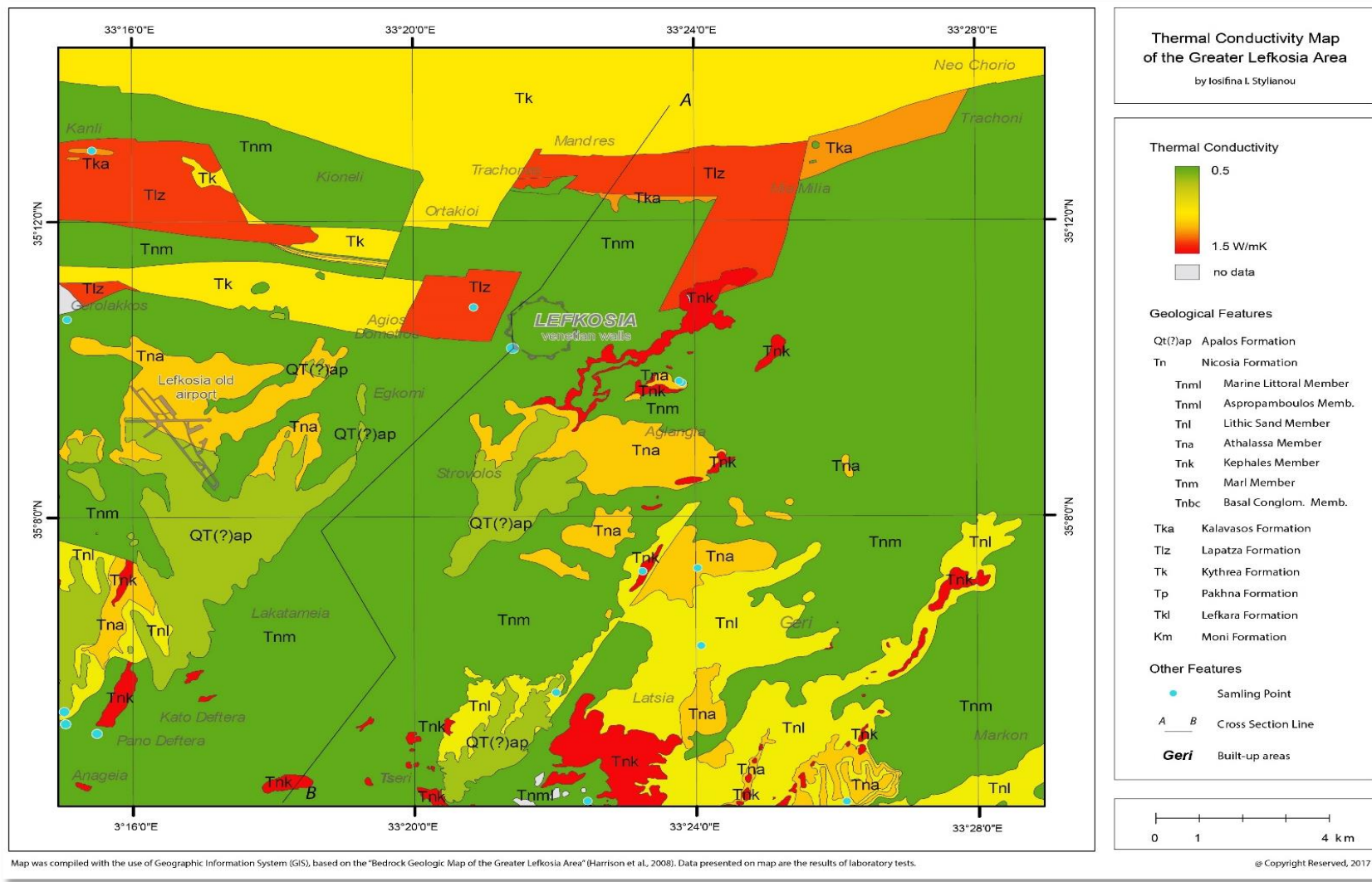


Figure 6 - 5: Thermal Conductivity Map of the Greater Nicosia Area  
(Boundaries as presented on the "Bedrock Geologic Map of the Greater Nicosia Area" (Harrison et al., 2008))

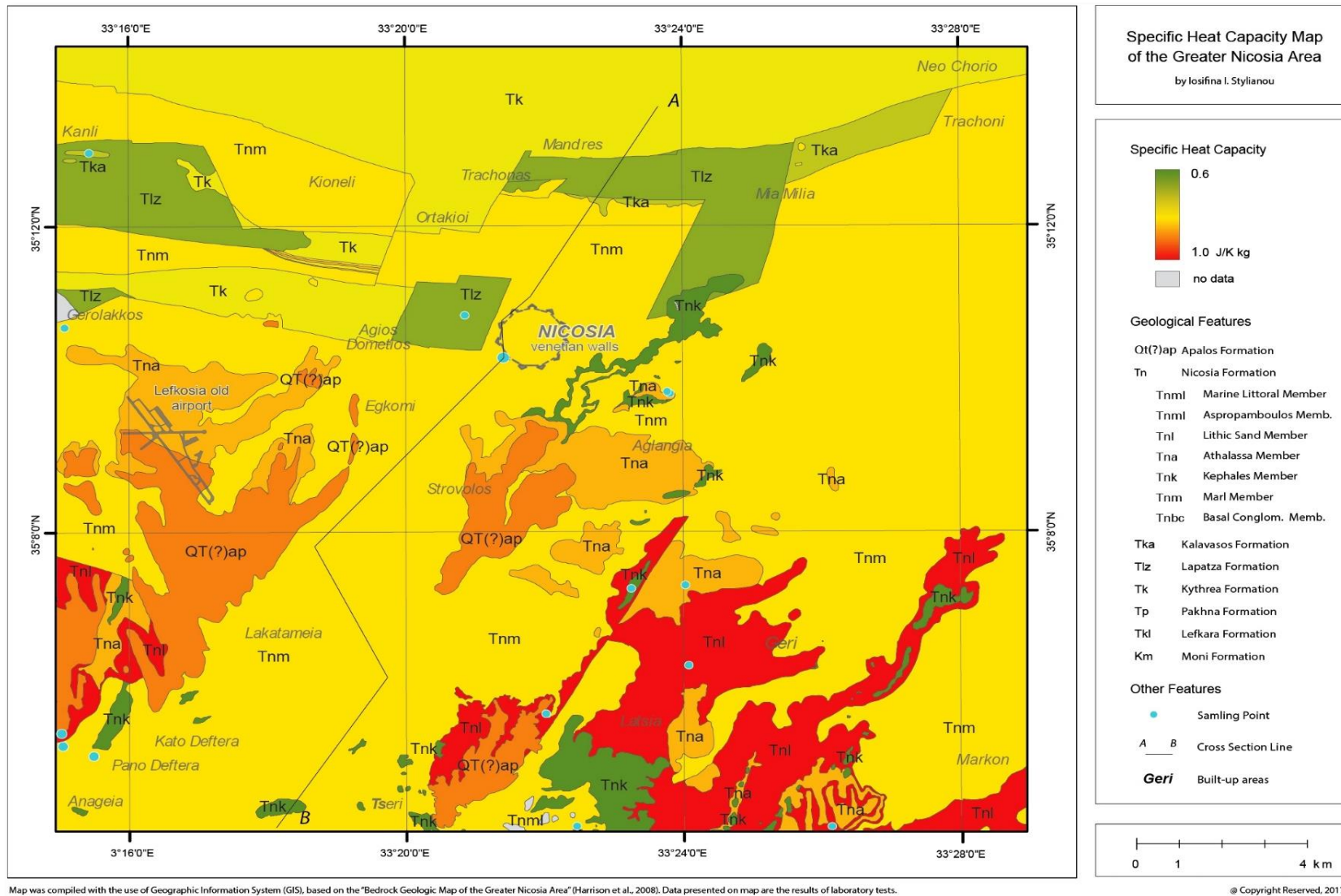


Figure 6 - 6: Specific Heat Capacity Map of the Greater Nicosia Area  
(Boundaries as presented on the "Bedrock Geologic Map of the Greater Nicosia Area" (Harrison et al., 2008))



### 6.3.4 Thermal Conductivity and Specific Heat Capacity Maps of the Greater Nicosia Area

Thermal Conductivity and Specific Heat Capacity Maps (Figure 6 - 5 and Figure 6 - 6) were created using the ArcGIS software. In the software, each bedrock geological unit in the greater Nicosia area was assigned the mean value of the properties of the corresponding tested samples in Table 6 - 1.

From the Thermal Conductivity Map in Figure 6 - 5, it can be seen that the larger area on the map has relatively low thermal conductivity in the region of  $0.6-0.7 \text{ W m}^{-1} \text{ K}^{-1}$  with only few smaller areas having values close to the maximum of  $1.4-1.5 \text{ W m}^{-1} \text{ K}^{-1}$ . The Specific Heat Capacity Map (Figure 6 - 6) shows that specific heat capacity varies over a narrower range with most area having a value of around  $0.6 \times 10^{-3} \text{ JK}^{-1} \text{ Kg}^{-1}$ .

## 6.4 Application of Ground Heat Exchangers in the Greater Nicosia Area

As mentioned earlier, the main objective of this Chapter is to provide engineers with a methodology and data for the sizing of vertical GHEs for a study area. For the Nicosia area, 22 different locations were chosen, where boreholes exist, as shown in Figure 6-7 for the analysis. For each location, the influence of the ground properties was considered to determine the thermal energy per meter depth that can be transferred to the ground in each borehole.

### 6.4.1 Mathematical model

The performance of the GHEs for each location was predicted using the validated FlexPDE model discussed in Chapter 3: Modeling Vertical Ground Heat Exchangers.

A vertical GHE of length 100 m was assumed in each borehole consisting of a descending and an ascending leg of polyethylene pipe connected at their ends with a U-joint. Boreholes were assumed to have a diameter of 0.2 m and filled with thermally enhanced bentonitic clay. Bentonitic clay has the ability to expand and completely fill the borehole and hold firmly the GHE in place (Delaleux et al., 2011). Water was assumed as the heat carrier fluid, circulating in the tubes. In the analysis the area considered was equal to 0.5 m around the borehole and a

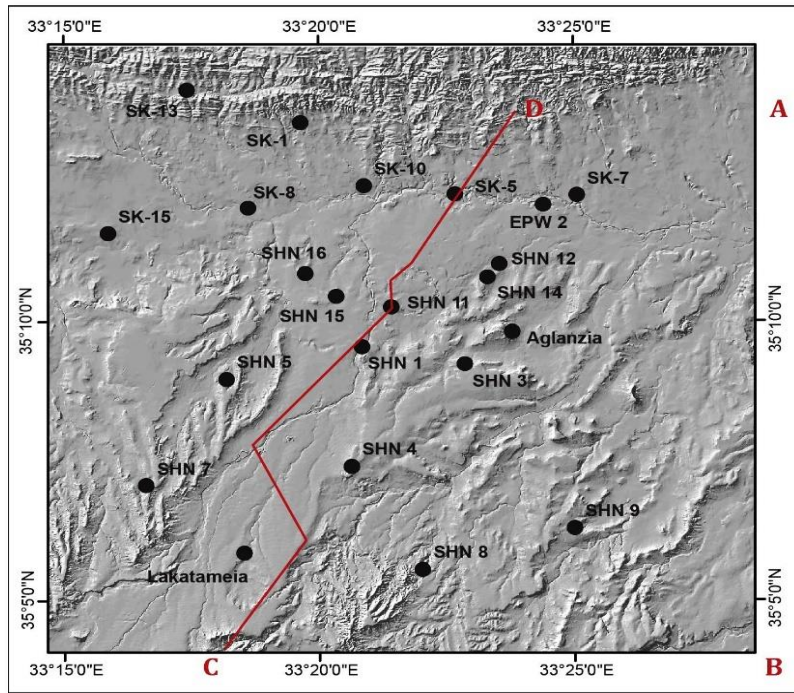


Figure 6 - 7: Location map of boreholes used as study cases and cross section shown in Figure 6-2 (the background was provided by the Cyprus Geological Survey Department).

depth of 100 m. The tubes were assumed to have 0.0285 m inner diameter and 3.5 mm wall thickness. The distance between the center of the tube and the center of the borehole was 0.048 m. The initial temperature of the ground was set to 22° C for the entire study area based on temperatures measured in Lakatameia BH (see Chapter 4, Section 4.2.2) and the temperature of water entering the borehole 40° C in order to satisfy the requirements of the heat pump. The heat pump characteristics were chosen in accordance to the results of the Technical Requirements Checklist (TRC) test that took place again at Lakatameia BH (Pouloupatis, 2014). The borehole basic parameters used in the simulations are summarized in Table 6 - 2.

The geological formation at each borehole is shown in Figure 6 - 8. Geological changes for the surface layer (up to 7-8 m depth) were not taken into consideration in the analysis, as their influence is very small for vertical GHEs.

Flow of underground water may have an important influence on the cooling effect of vertical heat exchangers. Data on groundwater water velocity were obtained from the Geological Survey Department of Cyprus and ranged from 20 up to  $30 \times 10^{-7} \text{m s}^{-1}$ . The only exception

was for the Marl lithology where the underground water velocity used in the calculations was only  $0.1 \times 10^{-7} \text{ m s}^{-1}$ .

Table 6 - 2: GHE parameters used in the simulation

<b>Property</b>	<b>Value</b>	<b>Unit</b>
Fluid velocity in tubes	0.32	$\text{m s}^{-1}$
Fluid initial temperature in tubes	40.0	$^{\circ} \text{C}$
Wall thickness of heat exchanger tube	0.0035	m
Distance between center of borehole to center of each heat exchanger tube	0.048	m
Temperature of ground	22	$^{\circ} \text{C}$
Borehole radius	0.1	m
Length of heat exchanger	100	m

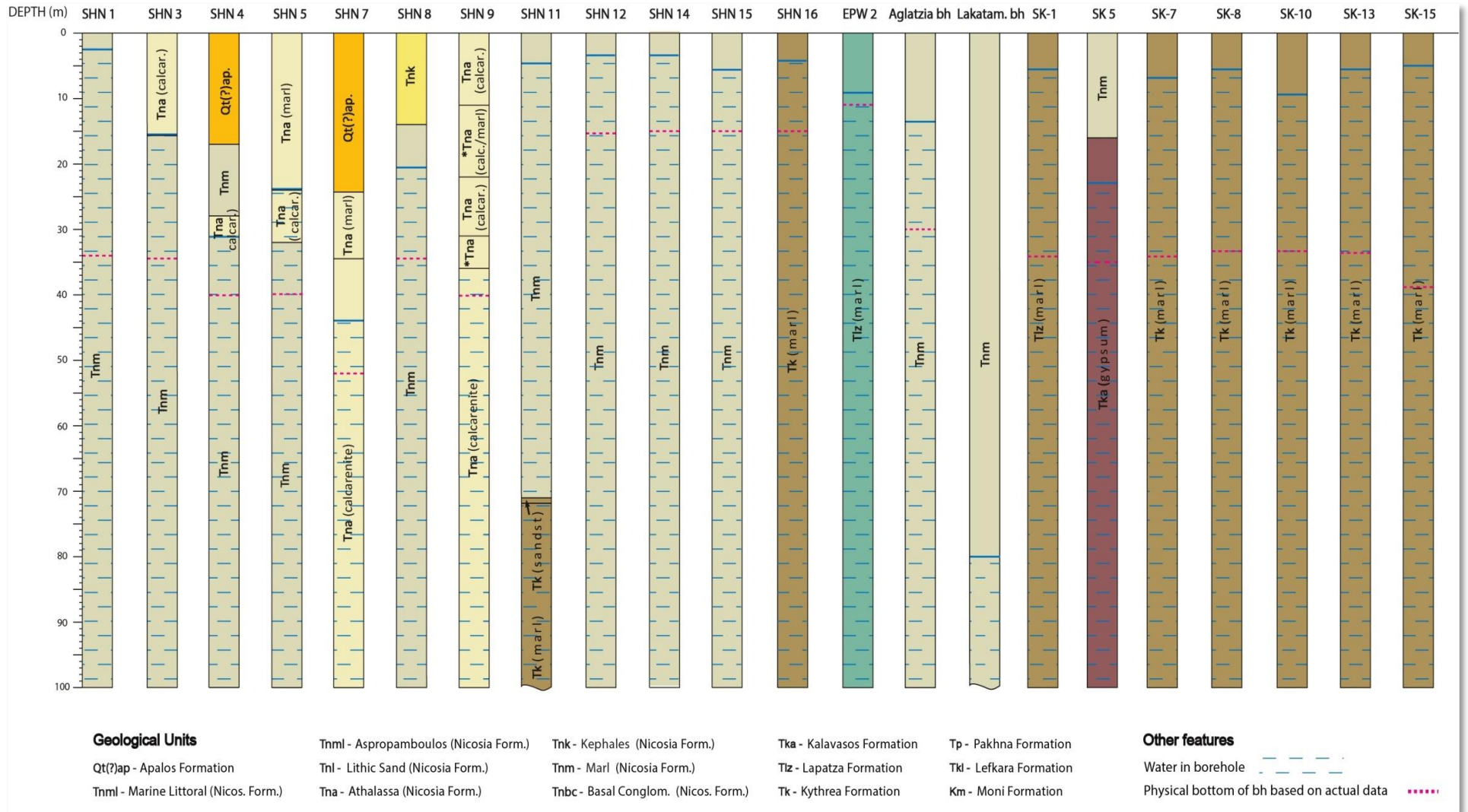


Figure 6 - 8: Geological borehole logs of the twenty-two study cases as used in FlexPDE software.

### 6.4.2 Results

Figure 6 - 9 shows the results for the heat load transferred to the earth through the GHE. A summary of results is also presented in Table 6 - 3 for 12, 18 and 24 hours of continuous operation. It can be seen that heat rejection decreases with time, as the temperature difference between the circulating water and the ground decreases but the decrease flattens out after approximately 12 hours of operation. It can be seen that the highest load is for borehole SHN7 and the lowest for borehole SHN4.

Table 6 - 3: GHE heat loss per meter ( $\text{W m}^{-1}$ ) after 12, 18 and 24 working hours

Borehole	Heat load per meter ( $\text{W m}^{-1}$ )		
	after 12h	after 18h	after 24h
SHN 7	46	44	42
SHN 15	42	39	38
SHN 1, SHN 5, SHN 11, SHN 12, SHN 14, SK-1, SK-7, SK-8, SK-10, SK-13, SK-15, EPW 2, Aglanzia BH	40	37	36
SHN 3, Lakatameia BH	38	36	34
SK-5, SHN 9	37	35	34
SHN 8	33	31	30
SHN 16	40	33	29
SHN 4	30	28	26

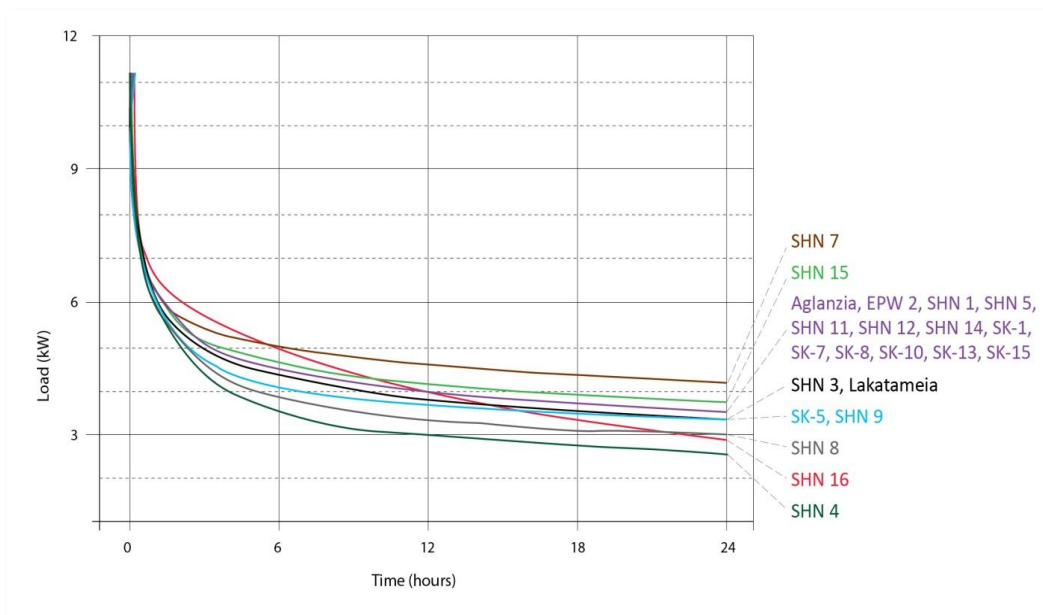
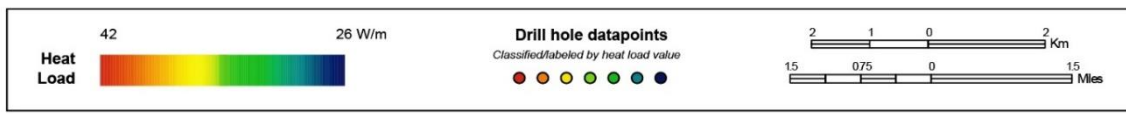
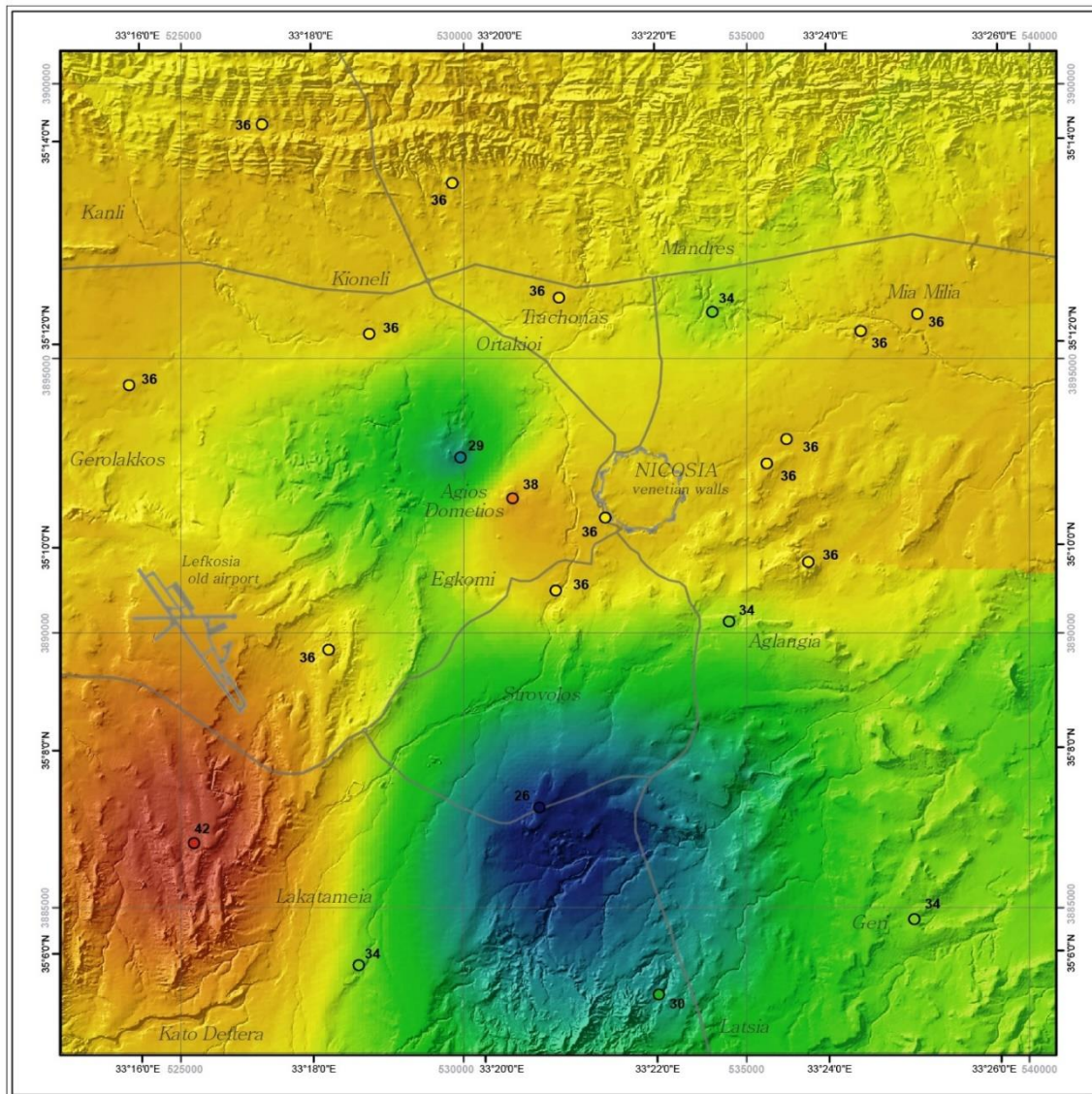


Figure 6 - 9: GHE heat loss (kW) for each study case as calculated by FlexPDE software.

## DESIGN LOAD MAP OF GROUND HEAT EXCHANGERS FOR THE GREATER NICOSIA AREA, CYPRUS

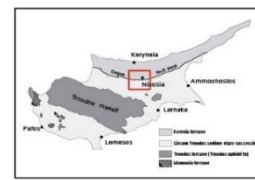
by Iosifina I. Stylianou



Map presents the performance of Vertical Ground Heat Exchangers up to 100 m depth, after 24 hours of operation in cooling mode. Calculated data present the heat load per meter depth that can be transferred to the ground in each borehole of the greater Nicosia area.

Map was compiled with the use of Geographic Information System (GIS). Small areas with dense data surrounded by wide areas containing sparse data are characteristic of the heat load map. As such, the user should keep in mind that the heat loss map is well constrained in areas of dense data and more interpretive in areas of sparse data.

The digital elevation model presented on the background of the map was supplied by the Cyprus Geological Survey Department.



© Copyright Reserved, 2017

Figure 6 - 10: GHE Suitability Map for the Greater Nicosia Area  
(for GHEs up to 100 m depth, after 24 hours of operation in the cooling mode)

### 6.4.3 GHE Suitability Map for the Greater Nicosia Area

Figure 6 - 10 shows a “Design Load Map of Ground Heat Exchangers for the Greater Nicosia Area” constructed from the results presented above and for operation of the GHE for 24 hours in the cooling mode.

Values vary between 26 and 42 W m<sup>-1</sup>. The wide range demonstrates the importance of the data and the map in determining the size and number of boreholes necessary for a specific load.

## 6.5 Summary

The chapter described a methodology for measuring and analyzing the thermal properties of the lithologies encountered in an area, and the use of the data for the compilation of a thermal map that can be employed for the estimation of the potential for use of ground heat exchangers for heating and cooling. The study focused on the Greater Nicosia Area and the “Design Load Map of Ground Heat Exchangers for the Greater Nicosia Area” was compiled alongside maps of the variation of important ground properties such as specific heat and thermal conductivity.

The results show that depending on the ground formation, thermal conductivity,  $\lambda$ , can vary between 0.5 and 1.5 W m<sup>-1</sup>K<sup>-1</sup>, while specific heat capacity  $c_p$  from 0.6 to 1.0 J K<sup>-1</sup> kg<sup>-1</sup>. Values of thermal load (heat transfer to the ground) for GHEs up to 100 m depth were found to vary between 26 and 42 W m<sup>-1</sup> in the cooling mode.

## **Chapter 7: Conclusions and recommendations for future work**

### **7.1 Introduction**

The main objective of this research was to provide a methodology, useful guides and tools for the sizing of vertical Ground Heat Exchangers (GHEs) to facilitate technical and economic optimisation of GHE systems.

The research involved the measurement and analysis of the thermal properties of lithologies encountered in an area, and the use of these in a mathematical model in the FlexPDE modelling environment, to predict the thermal response of a GHE of specific design characteristics in that location. Outputs from the model were used to compile geothermal maps for Cyprus that can be used by engineers for the Design of GHEs and associated heat pump systems for heating and cooling applications.

This chapter presents a summary of the outputs and conclusions from the work followed by suggestions for future work in the area.

### **7.2 Main Conclusions**

1. In this research, equations that govern the heat transfer between vertical GHEs in water saturated and unsaturated conditions with or without groundwater flow, and the ground have been presented. Based on these equations, a model was developed within the FlexPDE software environment to investigate the influence of key design parameters on the performance of Ground Heat Exchangers. For accurate results, the model requires as input the thermal gradient of the ground at the particular location. This information was available from two boreholes, one in Prodromi and the other in Lakadameia. The model was then validated against data from Thermal Response Tests (TRTs) for these two locations. In order to obtain more realistic results when calculating the efficiency of a GHE, a temperature gradient must be imposed on the numerical model for the depth profile, so as to match the actual temperature of the ground. The



actual borehole characteristics must be also used, as any inaccuracy may change the whole design of the GHE system.

2. Due to very little existing information on the thermal properties of the ground in Cyprus, geological sampling and analysis of the samples needed to be carried out. The sampling sites were selected according to the geological formation, the lithology and their geographical location in order to provide as much information as possible for the ground in Cyprus. In total, 148 geological samples were collected and analysed in the laboratory.

3. Measurements of thermo-physical properties of the same or similar rock types in Cyprus, have shown significant differences. This is in agreement with the findings of investigators in other countries, suggesting that properties cannot be used to distinguish between rock types. Based on this, it is therefore necessary to establish the properties of the ground at the particular area where the installation of the GHE is considered and the properties cannot be assumed based on the lithology alone.

The variation of the properties of lithologies based on location, is a function of many factors which include the presence of minerals or other impurities and the geological age of the rocks. The results showed that the thermal conductivity of each lithotype increases with the geological age.

Measured values of thermal conductivity and thermal diffusivity of samples in 100% moist conditions have been found to usually be higher than or equal to the corresponding values measured under dry conditions. The increasing effect of moisture content is due to the thermal conductivity of water, which is considerably higher than the thermal conductivity of air that fills the pores of rocks in dry conditions.

4. The outcome of the laboratory experiments, with the use of the Geographic Information System (GIS), was used to compile a series of GeoThermal Maps for Cyprus. In more detail, the compiled maps, which can constitute a great tool in the hands of engineers are:

- The Thermal Conductivity Map of Cyprus (wet conditions)
- The Thermal Conductivity Map of Cyprus (dry conditions)
- The Thermal Diffusivity Map of Cyprus (wet conditions)
- The Thermal Diffusivity Map of Cyprus (dry conditions)

- The Density Map of Cyprus Dry (dry conditions)
- The Specific Heat Capacity Map of The Greater Nicosia Area
- The Thermal Conductivity Map of The Greater Nicosia Area

From the maps and geothermal point of view, the Troodos Ophiolite can be visualized as a separate part from the rest of the island by having the highest thermal conductivity, diffusivity and density values. The thermal properties in this region improve further in the presence of water.

5. The heat transfer in GHE is very complex and depends on many factors including the properties of the ground and their variation with depth, the presence of water, the properties of the grouting material, the properties of the tube material and the distance between the two legs of the GHE and the velocity and temperature of the heat transfer fluid circulating in the heat exchanger. The consideration of the influence of individual parameters and the interactions between the parameters, requires the use of computer programmes and in this thesis the FlexPDE software environment was employed for this purpose. FlexPDE is a Multi-Physics Finite Element Solution Environment for Partial Differential Equations that can be employed for the solution of variety of problems, including heat flow problems as is the case in this thesis.

6. In order to identify areas favourable for the installation of GHEs and Ground Source Pumps and to provide engineers with a useful guide for sizing vertical GHEs for a location, a methodology has been developed and applied to demonstrate this. The application area chosen was the Greater Nicosia Area of Cyprus where 22 boreholes exist. Information from the geology and lithologies of the area and data from the boreholes were used with the FlexPDE model to determine the geothermal performance of GHEs in the boreholes. Based on the simulation results and GIS software the “Design Load Map for Ground Heat Exchangers for the Greater Nicosia Area” was compiled for boreholes up to 100 m length.

- a) The load map shows that the thermal load transferred to the ground after 24 hours of operation of the GHE in the cooling mode in the summer can be in the range between 26 and 42 W m<sup>-1</sup>.
- b) Ground water level and flow can have a positive effect on the thermal load transfer due

to the cooling effect of the water flow and the increase in the thermal conductivity of the ground in the presence of water.

7. The proposed methodology can be applied in any vertical GHE system as it describes: (a) the full procedure of sampling and thermal testing, (b) the compilation of thermal conductivity, thermal diffusivity and density maps with the use of GIS, (c) the basic formulas used for calculating the geothermal response of a vertical BH with respect to the water level, porosity and the thermal properties of each lithology present in the borehole, which lead to (d) the compilation of a GHE suitability map in an area on interest.

### **7.3 Recommendations for Future Work**

This thesis has investigated the design and performance of heat exchangers for application in different locations in Cyprus. The performance of heat pumps that will utilize the ground for heat rejection in the summer and heat addition in the winter has not been considered in detail in this investigation. This is an important area of work that can be addressed in the future. It may involve both monitoring of a real GHE and heat pump installation in a domestic or commercial application and transient simulation of the integrated system to understand the influence of key system parameters design and control parameters on the seasonal efficiency of the system.

Another important area of future work is the comparison of the seasonal performance and economics of GHE and ground source heat pumps with air source heat pumps to identify the size of dwellings and loads as well as locations where ground source systems may offer economic advantage over air source heat pumps.

## Reference

Abdulagatova, Z., Abdulagatov, I. M., & Emirov, V. N. (2009). Effect of temperature and pressure on the thermal conductivity of sandstone. *International Journal of Rock Mechanics & Mining Sciences*, 46 (2009) 1055–1071.

Abesser, C. & Lewis, M. 2013, “The open loop ground source heat pump screening tool for England and Wales”. *European Geothermal Congress 2013*.

Abesser, C. (2012). User Guide - Web tool for the initial assessment of subsurface conditions for open-loop ground source heat pump installations (West Midlands), *British Geological Survey*, Energy Science Programme, Open Report OR/12/069.

Abesser, C., Lewis, M. A., Marchant, A. P. & Hulbert, A. G. (2014). Technical Note: Mapping suitability for open-loop ground source heat pump systems: A screening tool for England and Wales, UK. *Quarterly Journal of Engineering Geology and Hydrogeology*, 47, 373–380.

Alfè, D. (2009). Temperature of the inner-core boundary of the Earth-Melting of iron at high pressure from first-principles coexistence simulations. *Phys. Rev. B*, 79, 060101(R) (2009)

Al-Khoury, R., Kolbel, T. & Schramedei, R. (2010). Efficient numerical modeling of borehole heat exchangers. *Computers & Geosciences*, 36, 1301–1315.

Bernier, M.A. (2001). Ground-coupled heat pump system simulation in *ASHRAE Trans*, 106(1):605–16.

Bezelgues, S., Martin, J., Schomburgk, S., Monnot, P., Nguyen-The, D., Nguyen, D., Brun, M. and Desplan, A. 2010, “Geothermal Potential of Shallow Aquifers: Decision-Aid Tool for Heat-Pump Installation”. *Proceedings World Geothermal Congress 2010*.

Bidarmaghz, A., Narsilio, G. & Johnston, I. 2013 “Numerical Modeling of Ground Heat Exchangers with Different Ground Loop Configurations for Direct Geothermal Applications”. *Proceedings of the 18th International Conference of Soil Mechanics and*

*Geotechnical*, Department of Infrastructure Engineering, The University of Melbourne, Australia.

Birch, F. & Clark, H. (1940). The thermal conductivity of rocks and its dependence upon temperature and composition. *American Journal of Science*, 238(8): 529–558.

Blum, P., Campillo, G. & Kölbl, T. (2011). Techno-economic and spatial analysis of vertical ground source heat pump systems in Germany. *Energy*, 36 (2011), 3002-3011.

Buckley, C., Pasquali, R., Lee, M., Dooley J. & Williams H.T. (2015). Ground Source Heat & Shallow Geothermal Energy in Homeowner Manual Version 1.0. *Geological Survey of Ireland*,

Busby, J. (2015). UK shallow ground temperatures for ground coupled heat Exchangers. *Quarterly Journal of Engineering Geology and Hydrogeology*, doi:10.1144/qjegh2015-077. Available at <http://qjegh.lyellcollection.org> [Accessed December 1, 2015].

Busby, J. (2009). Initial geological considerations before installing ground source heat pump systems. *University of St Andrews*. Available at <http://qjegh.lyellcollection.org> [Accessed December 7, 2014].

Canakci, H., Demirboga, R., Karakoc, M. B. & Sirin, O. (2007). Thermal conductivity of limestone from Gaziantep (Turkey). *Building and Environment*, 42 (2007), 1777–1782.

Carslaw, H.S. & Jaeger, J.C. 1993, *Conduction of Heat in Solids*, 2nd ed., Clarendon Press, Oxford.

Cataldi, R., Hodgson, S.F. & Lund, J.W (1999). Stories from a Heated Earth—Our Geothermal Heritage in Davis, C. A., *Geothermal Resources Council and International Geothermal Association*, USA, 1999; p. 569.

Casasso, A., Della, V.S., Filippo, A., Capodaglio, P., Cavorsin, R., Guglielminotti, R. & Sethi R. (2018). Ground Source Heat Pumps in Aosta Valley (NW Italy): assessment of existing systems and planning tools for future installations. *Rendiconti Online Societa Geologica Italiana*. Available at <https://doi.org/10.3301/ROL.2018.53>, pp 59-66. [Accessed January 18, 2019].

Christodoulides, P., Florides, G., Pouloupatis, P., Messaritis, V. & Lazari, L. (2012). Ground Heat Exchanger Modeling Developed for Energy Flows of an Incompressible Fluid. *World Academic of Science, Engineering and Technology*, 63, 2012.

Christodoulides, P., Florides, G. & Pouloupatis, P. (2016). A practical method for computing the thermal properties of a Ground Heat Exchanger. *Renewable Energy*, 94, pp.81-89.

Cohen, D., Rutherford, N., Morisseau, E., Zissimos, A. 2011, *Geochemical Atlas of Cyprus*, UNSW Press, Sydney, 144pp, ISBN 978 174223 306 2.

Correia, A., Vieira, G. & Ramos M. (2012). Thermal conductivity and thermal diffusivity of cores from a 26 meter deep borehole drilled in Livingston Island, Maritime Antarctic. *Geomorphology*, 155-156 (2012), 7–11.

Delaleux, F., Py, X., Olives, R. & Dominguez A. (2011). Enhancement of geothermal borehole heat exchangers performances by improvement of bentonite grouts conductivity. *Applied Thermal Engineering*, Volumes 33–34, pp 92–99.

D.R.Kohlman,inc. Available at : [https:// www.drkohlman.com](https://www.drkohlman.com) [Accessed: 22 October 2015].

DTE Energy. Available at: [www.dteenergy.com](http://www.dteenergy.com) [Accessed:20 November 2015].

FlexPDE. (1995). PDE Solutions Inc.

*FlexPDE 6 Manual*, 2010, PDE Solutions Inc. Available at: <http://www.pdesolutions.com> [Accessed 15 June 2013].

Florides, G., Pouloupatis, P., Kalogirou, S., Messaritis, V., Panayides, I., Zomeni, Z., Partasides, G., Lizides, A., Sophocleous, E. & Koutsoumpas, K. (2011). The geothermal characteristics of the ground and the potential of using ground coupled heat pumps in Cyprus. *Energy*, Vol. 36, Issue 8, 5027-5036.

Florides, G. & Kalogirou, S. (2008). First in situ determination of the thermal performance of a U-pipe borehole heat exchanger in Cyprus. *Applied Thermal Eng*, 28(2–3), 157–63.

Florides, G., Christodoulides, P. & Pouloupatis, P. (2011). An analysis of heat flow through a borehole heat exchanger validated model. *Applied Energy*, 92, 523–33.

Florides, G., Pouloupatis, P., Kalogirou, S., Messaritis, V., Panayides, I., Zomeni, Z., Partasides, G., Lizides, A., Sophocleous, E. & Koutsoumpas, K. 2010, “Geothermal properties of the ground in Cyprus and their effect on the efficiency of ground coupled heat pumps”. *World Renewable Energy Congress XI 25-30 September 2010, Abu Dhabi, UAE*.

Florides, G., Pouloupatis, P., Kalogirou, S., Messaritis, V., Panayides, I., Zomeni, Z., Partasides, G., Lizides, A., Sophocleous, E. & Koutsoumpas, K. (ed.) 2011, *Map of Ground Temperature and Thermal Conductivity of Cyprus*, Cyprus Geological Survey, Cyprus.

Florides, G., Theofanous, E., Stylianou, I. I., Tassou, S., Christodoulides, P., Zomeni, Z., Tsiolakis, E., Kalogirou, S., Messaritis, V., Pouloupatis, P. & Panayiotou, G. (2013). Modeling and assessment of the efficiency of horizontal and vertical ground heat exchangers. *Energy*, 58, 655-663.

Fujii, H., Inatomi, T., Itoi, R. & Uchida, Y. (2007). Development of suitability maps for ground-coupled heat pump systems using groundwater and heat transport models. *Geothermics*, 36, 459–472.

Fujii, H., Komaniwa, Y., Onishi, K. & Chou, N. (2013). Improvement of the Capacity of Ground Heat Exchangers by Water Injection. *GRC Transactions*, Vol. 37.

Gass, I. G. 1989, “Magmatic processes at and near constructive plate margins as deduced from the Troodos (Cyprus) & Semail Nappe (N. Oman) ophiolites”, in Saunders, A.D. & Norry, M.J. (eds), *Magmatism in the ocean basins*, Geol. Soc. Lond. Spec. Publ., 42, pp. 1-15.

Gass, I.G. 1990, “Ophiolites and Ocean Lithosphere” in Malpas J., Moores E., Panayiotou A. & Xenophontos C., *Ophiolites, Ocean Crustal Analogues*, Proceedings of the Symposium “Troodos 1987”, pp 1-10.

Gegenhuber, N. & Schoen, J. (2012). New approaches for the relationship between compressional wave velocity and thermal conductivity. *Journal of Applied Geophysics*, 76, 50–55.

*Geological Map of Cyprus*, revised 1995, Geological Survey Department of Cyprus, Cyprus. Cyprus Geological Survey Department, Available at : <https://www.moa.gov.cy/gsd>. [Accessed: 22 October 2015].

Geothermal Heat Pump Consortium. Available at: <http://www.geoexchangers.org>. [Accessed: 22 October 2015].

Gibson, I. L., Malpas, J., Robinson, P. T. & Xenophontos, C. 1989, *Cyprus Crustal Study Project: Initial Report, Hole CY-4*. Ottawa: Geological Society of Canada. ISBN 0 660 13279 6. Paper 88-9. vii + 393 pp. Available at: <https://doi.org/10.1017/S0016756800015363> Published online: 01 May 2009 [Accessed 11 Nov. 2018].

Gorgulu, K., Duruturk, S. Y., Demirci, A. & Poyraz, B. (2008). Influences of uniaxial stress and moisture content on the thermal conductivity of rocks. *International Journal of Rock Mechanics and Mining Sciences*, 45 (8), 1439-1445.

Gustav, B. (1840). Internal Heat of the Globe. *Chemistry and Technology, University of Bonn*, Vol. I.

Harrison, R., Newell, W., Panayides, I., Stone, B., Tsiolakis, E., Necdet, M., Batihanli, H., Ozgur, A., Lord, A., Berksoy, O., Zomeni, Z., & Schindler, J.S. (ed.) 2008, *Bedrock geologic map of the greater Nicosia (Lefkosia) area, Cyprus*, U.S. Geological Survey Scientific Investigations Map 3046, ISBN 978-1-4113-2323-0, Pamphlet to accompany Scientific Investigations Map 3046, ISBN 978-1-4113-2323-0, U.S.

Heath, R. (1983). Basic ground-water hydrogeology in Water-Supply, *U.S. Geological Survey*, Paper 2220, 86 p.

Hepbasli, A., Akdemir, O. & Hancioglou, E. (2003). Experimental study of a closed loop vertical ground source heat pump systems. *Energy Conversions and Management*, 44, 527-448.

Holmberg, H., Acuña, J., Næss, E. & Sønju O. 2015, “Deep Borehole Heat Exchangers, Application to Ground Source Heat Pump Systems” in *Proceedings World Geothermal Congress 2015*, Melbourne, Australia.



Jorand, R., Fehr, A., Koch, A. & Clauser, C. (2011). Study of the variation of thermal conductivity with water saturation using nuclear magnetic resonance. *Journal of Geophysical Research*, vol. 116, B08208, doi:10.1029/2010JB007734.

Kalogirou, S. & Florides, G. (2007). Ground heat exchangers—A review of systems, models and applications. *Renewable Energy*, 32, 2461–2478.

Kalogirou, S., Florides, G, Pouloupatis, P., Panayides, I, Joseph-Stylianou J. & Zomeni, Z. (2012). Artificial neural networks for the generation of geothermal maps of ground temperature at various depths by considering land configuration. *Energy*, 48, 233-240.

Kavanaugh, S. (1995). A design method for commercial ground-coupled heat pumps. *ASHRAE Trans*, 101(2), 1088–94.

Kious, W. & Tilling, R. 1996, *This Dynamic Earth: The Story of Plate Tectonics*, U.S. Government Printing Office, ISBN 0-16-048220-8.

Laidler, K. 1993, *The World of Physical Chemistry*, Oxford University Press, Melbourne, ISBN 0-19-855919-4.

Lee, C. K. (2001). Classification of Geothermal Resources. *Exergy Geothermics*, 30(4), 431–442.

Lee C. K. (2011). Effects of multiple ground layers on thermal response test analysis and ground-source heat pump simulation. *Applied Energy*, 88(12), 4405–10.

Liu, S., Feng, C., Wang, L. & Li, C. (2011). Measurements and Analysis of Thermal Conductivity of Rocks in the Tarim Basin, Northwest China. *Acta Geological Sinica*, Vol.85 (English Edition), No 3, pp. 598-609.

Lund, J. & Boyd, T. (2016). Direct utilization of geothermal energy 2015 worldwide review. *Geothermics*, 60, 66–93.

Malpas, J., Moores, E., Panayiotou, A. & Xenophontos, C. 1990, *Ophiolites, Ocean Crustal Analogues, Proceedings of the Symposium “Troodos 1987”*, Cyprus Geological Survey Department, Cyprus.

Mands, E. & Sanner, B. (2005), Shallow geothermal energy. Available at: <http://www.ubeg.de/Downloads/ShallowGeothEngl.pdfS;2005> [Accessed 11 April 2015].

Meteorological Service Cyprus, Available at : <https://www.moa.gov.cy/ms>. [Accessed: 22 October 2015].

Miao, S.Q., Li, H.P. & Chen, G. (2014). Temperature dependence of thermal diffusivity, specific heat capacity, and thermal conductivity for several types of rocks. *Journal of Thermal Analysis and Calorimetry*, 115, 1057–1063.

Mogensen, P. 1983, “Fluid to Duct Wall Heat Transfer in Duct System Heat Storages”, *International Conference on Subsurface Heat Storage in Theory and Practice*, ss. Appendix, Part II, p.652-657, Stockholm.

Momose, T. & Kasubuchi, T. (2002). Effect of reduced air pressure on soil thermal conductivity over a wide range of water content and temperature. *European Journal of Soil Science*, vol 53, pp599-606.

Montgomery, R.B. (1947). Viscosity and thermal conductivity of air and Diffusivity of water vapor in air. *Woods Hole Oceanographic Institute*, Contribution no. 388.

Morgan, P. (1975). Porosity Determinations and the thermal conductivity of rock fragments with application to heat flow on Cyprus. *Earth and Planetary Science Letters*, 26, 253-262.

Morgan, P. 1973, *Terrestrial Heat Flow Studies in Cyprus and Kenya*, PhD Thesis, Imperial Collage London, U.K.

Nam, Y. & Ooka, R. (2011). Development of potential map for ground and groundwater heat pump systems and the application to Tokyo. *Energy and Buildings*, 43, 677–685.

Neuendorf, K., Mehl, J. & Jackson J. (Revised) 2011, *Glossary of Geology*, 5th Edition, American Geosciences Institute Alexandria, Virginia, ISBN 978-0-922152-89-6.

Norden, B., Forster, A., Behrends, K., Krause, K., Stecken, L. & Meyer, R. (2012). Geological 3-D model of the larger Altensalzwedel area, Germany, for temperature prognosis and reservoir simulation. *Environmental Earth Science*, 67, 511–526, DOI 10.1007/s12665-012-1709-9.

Pahud, D. & Matthey, B. (2001). Comparison of the thermal performance of double U-pipe borehole heat exchangers measured in situ. *Energy and Building*, vol 33, pp 503-507. Available at: [https://doi.org/10.1016/S0378-7788\(00\)00106-7](https://doi.org/10.1016/S0378-7788(00)00106-7).

Panayides, I. (2009). Cyprus in Gillespie, R. & Glague, D. (Eds.), *Encyclopedia of Islands*. University of California Press, pp. 212-216, ISBN 978-0-520-25649-1.

Pollack, H.N., Hurter, J. S. & Johnson R. J. (1993). Heat flow from the Earth's interior: analysis of the global data set (Rev.). *Geophysics.*, 31, 267-280.

Popiel, O., Wojtkowiak, J. & Biernacka, B. (2001). Measurements of temperature distribution in ground. *Journal of Experimental Thermal and Fluid Science*, 25, 301-9.

Porwal, C. (2015). High Specific Speed in Circulating Water Pump Can Cause Cavitation, Noise and Vibration. *World Academy of Science, Engineering and Technology International Journal of Mechanical and Mechatronics Engineering*, Vol 9, 12.

Pouloupatis, P., Florides, G. & Tassou S. (2010). Measurements of ground temperatures in Cyprus for ground thermal applications. *Renewable Energy*, Volume 36, 804-814. Available at: <https://doi.org/10.1016/j.renene.2010.07.029>.

Pouloupatis, P. 2014, *Determination of the thermal characteristic of the ground in Cyprus and their effect on ground heat exchangers*, PhD Thesis, Brunel University, UK.

Raymond, J., Mercier, S. & Nguyen, L. (2015). Designing coaxial ground heat exchangers with a thermally enhanced outer pipe, *Geothermal Energy* volume 3, Article number: 7. Available at: <https://geothermal-energy-journal.springeropen.com/articles/10.1186/s40517-015-0027-3>. [Accessed 15 November 2019].

ReGeoCities Project: Developing Geothermal Heat Pumps in Smart Cities and Communities, Authors: European Geothermal Energy Council (EGEC), Belgium Universidad Politécnica de Valencia (UPVLC), Spain Romanian Geoexchange Society (RGS), Romania Bureau Recherches Géologiques Minières (BRGM), France UBeG GbR of Wetzlar (UBEG), Germany Centre for Renewable Energy Sources and Saving (CRES), Greece SP Technical Research Institute of Sweden (SP), Sweden Nationale Geologiske Undersøgelser for Danmark og Grønland (GEUS), Denmark SLR Consulting (SLR), Ireland IF Technology

(IF), The Netherlands Scuola Superiore di Studi Universitari e di Perfezionamento Sant'Anna (SSSA), Italy Service Public de Wallonie (SPW), Belgium, 2015.

Robertson, F. 2000, "Tectonic evolution of Cyprus in its Easternmost Mediterranean setting" in Panayides, I., Xenophontos, C. & Malpas, J. (eds.), *Proceedings Third International Conference of the Geology of The Eastern Mediterranean*, pp 11-44, ISBN 9963-1-7506-06.

Robinson, P.T. & Malpas, J. 1990, "The Troodos ophiolite of Cyprus: New perspectives on its origin and emplacement" in Malpas, J., Moores, E., Panayiotou, A. & Xenophontos, C., *Ophiolites, Ocean Crustal Analogues, Proceedings of the Symposium "Troodos 1987"*, pp 13-26.

Rybach, L. & Sanner, B. (2000). Ground-Source Heat Pump Systems – The European Experience. *GHC Bulletin*, pp 16-26.

Sanner, B., Karytsas, C., Mendrinou, D., Rybach, L. (2003). Current status of ground source heat pumps and underground thermal energy storage in Europe. *Geothermics*, 32, 579-588.

Schütz, F., Norden, B., Förster, A. and DESIRE Group (2012). Thermal properties of sediments in southern Israel: a comprehensive data set for heat flow and geothermal energy studies. *Basin Research*, 24, 357-376.

Sliwa, T. & Rosen, M. (2015). Natural and Artificial Methods for Regeneration of Heat Resources for Borehole Heat Exchangers to Enhance the Sustainability of Underground Thermal Storages: A Review. *Sustainability*, 7, 13104-13125. Available at: doi:10.3390/su71013104, ISSN 2071-1050.

Stylianou, I.I., Tassou, S., Christodoulides, P., Panayides, I. & Florides, G. (2016). Measurement and analysis of thermal properties of rocks for the compilation of geothermal maps of Cyprus. *Renewable Energy*, 88, 418-429.

Stylianou, I.I., Tassou, S., Florides, G., Christodoulides, P. and Aresti, L. (2019). Modeling of Vertical Ground Heat Exchangers in the Presence of Groundwater Flow and Underground Temperature Gradient. *Energy & Buildings*, 192 (2019) 15–30, <https://doi.org/10.1016/j.enbuild.2019.03.020>.

Svec, J. O., Goodrish, E. L. & Palmer, H. L. (1983). Heat transferred Characteristics of in-ground heat exchangers. *Energy Research*, vol 7, 265-278.

Sweet, .J 1979, “Pressure Effects on Thermal Conductivity and Expansion of Geologic Materials”, Master Thesis, SAND78-1991.

Tong, F., Jing, L. and Zimmerman, W. R. (2009). An effective thermal conductivity mode of geological porous media for coupled thermo-hydro-mechanical systems with multiphase flow. *International Journal of Rock Mechanics & Mining Sciences*, 46, 1358–1369.

Vasseur, G., Brigaud, F. & Demongodin, L. (1995). Thermal conductivity estimation in sedimentary basins. *Tectonophysics*, 244, 167-174.

Venart, S. & Prasad, C. (1980). Thermal Conductivity of Water and Oleum. *Journal of Chemical and Engineering Data*, 25, 196-198.

Vijdea, A., Weindl, C., Cosac, A., Asimopolos, N. & Bertermann, D. (2014). Estimating the thermal properties of soils and soft rocks for the ground source heat pumps installation in Constanta country, Romania. *Journal of Thermal Analysis and Calorimetry*, 118, 1135-1144, DOI 10.1007/s10973-014-3951-8.

Woodside, W. & Messmer, H. J. (1961). Thermal Conductivity of Porous Media, II, Consolidated Rocks. *Journal of Applied Physics*, Vol. 32, No 9.

Yang, H., Cui, P. & Fang, Z. (2010). Vertical-borehole ground-coupled heat pumps: a review of models and systems. *Applied Energy*, 87(1), 16–27.

Zeng, Y., Diao, R. & Fang, H. (2002). A finite line-source model for boreholes in geothermal heat exchangers. *Heat Transfer Asian Research*, 31(7), 558–67.

Zhang, Y. & Li, J. 2010, “Design of Offshore Wind Turbine Foundation Monitoring System Based on Excel”. *Asia-Pacific Power and Energy Engineering Conference*, ISBN 97814244448128, pp. 1 – 4.

## **APPENDIX I**

## Script used in FlexPDE software

Explanation notes are written in { }

**TITLE** 'Analysis of Multilayer Geothermal Borehole crossing an Aquifer'

**COORDINATES** { coordinate system is specified }

cartesian3 { three -Dimensional Domain XYZ }

**SELECT NGRID** =10 { maximum cell size used }

**SELECT ERRLIM**=1e-2 { accepted estimation of the relative error in the dependent variables }

**SELECT NODELIMIT**=1600 { suggested Node Limit }

**SELECT upfactor**=4 { Multiplier on upwind diffusion terms. Larger values can sometimes stabilize a marginal hyperbolic system }

**prefer\_stability** { This selector chooses parameters for nonlinear time-dependent problems that result in greatest solution stability in ill-behaved problems }

**VARIABLES** { variables to be analyzed }

temp(0.01) { Temperature variable }

**GLOBAL VARIABLES** { define auxiliary values }

Tfluidin(0.01) { temperature of heat carrier fluid IN  $\pm 0.01$  so to satisfy ERRLIM=1e-2 }

Tcac(0.01) { temperature at the center axis 0,0 of the borehole  $\pm 0.01$  so to satisfy ERRLIM=1e-2 }

**DEFINITIONS** { parameters are given names and default values }

D\_a=100 { length of pipes carrying the fluid in the borehole }

D\_b = 2 { additional depth below pipes caring the fluid }

D\_total=D\_a+D\_b { equation used for calculating total depth of study area }

dtopo1=10 { bottom depth of first lithology layer }

dtopo2=60 { bottom depth of second lithology layer }

dtopo3=70 { bottom depth of third lithology layer }

zscale=0.01 { scaling factor for resizing z axis so to deduce the size of final mesh. In this way we reduce calculation time }

D\_bscl=D\_b\*zscale { equation used for scaling the size of pipes carrying the fluid in the borehole }

D\_ascl = D\_a\*zscale { equation used for scaling additional depth below pipes carrying the fluid }

D\_totalscl=D\_total\*zscale { equation used for scaling the total depth of the borehole }

$d_{top1sc1} = d_{topo1} * z_{scale}$  { equation used for scaling the length between top and the bottom of first lithology layer }  
 $d_{top2sc1} = d_{topo2} * z_{scale}$  { equation used for scaling the length between top and the bottom of second lithology layer }  
 $d_{top3sc1} = d_{topo3} * z_{scale}$  { equation used for scaling the length between top and the bottom of third lithology layer }  
 $D_{Rb} = 0.1$  { radius of borehole and grout }  
 $D_{cpc} = 0.0048$  { distance between the center of the each pipe and the center of total simulated area 0.0 }  
 $D_{poutside} = 0.032$  { external diameter of pipes carrying the fluid }  
 $D_{pthick} = 0.0035$  { thickness of pipes carrying the fluid }  
 $d_{in} = D_{poutside} - 2 * D_{pthick}$  { equation used to calculate the diameter of the fluid contained in the pipes }  
 $T_{pipe1} = EVAL(temp, D_{cpc}, 0, z)$  { Temperature at the center of the right pipe }  
 $T_{pipe2} = EVAL(temp, -D_{cpc}, 0, z)$  { Temperature at the center of the left pipe }  
 $ca = D_{ascl}$   
 $T_{cac0} = Sintegral(temp, "5", "fluid in") / Sintegral(1, "5", "fluid in")$  { Temperature at the center of the bottom of the borehole }  
 $z_{top} = D_{totalscl}$   
 $T_{fluidout} = Sintegral(temp, "top", "fluid out") / Sintegral(1, "top", "fluid out")$  { Temperature of the fluid in the pipes at the "top" surface }  
 $T_{aver} = (T_{fluidin} + T_{fluidout}) / 2$  { equation used for calculating the average temperature of fluid getting in the pipes and getting out from the pipes }  
 $K$  { values of thermal conductivity will be given in each region separately }  
 $n = 0.2$  { porosity of materials }  
 $k_{dry} = 0.9$  { values of thermal conductivity for dry soil/rock }  
 $k_{satur} = 1.1$  { values of thermal conductivity for saturated soil/rock }  
 $K_{ground} = (1 - n) * k_{dry} + n * k_{satur}$  { thermal conductivity of porous matrix }  
 $u$  { fluid velocity in z direction }  
 $ro$  { density will be given for each material separately }  
 $cp$  { specific heat will be given for each material separately }  
 $v$  { fluid velocity in y direction }  
 $u_{pipe} = 0.5$  { velocity of the fluid moving in the pipes in z direction }  
 $V_{grwater} = 0.05$  { Hydraulic conductivity of aquifer moving in x direction }  
 $t_{relax} = 10$  { no of steps used by software for calculations }  
 $L = 0.5$  { the half length in x direction of the bottom area }



ho=2145 { convection heat transfer coefficient }  
 rsw=2234 { density of porous matrix }  
 cs=718 { volume heat capacity for dry soil/rock }  
 cw=4180 { volume heat capacity for saturated soil/rock }  
 csw=(1-n)\*cs+n\*cw { volume heat capacity of porous matrix }

**initial values** { Initial values for the variables }

Temp=23.2 { Temperature }  
 Tfluidin=23.2 { temperature of heat carrier fluid getting in the borehole }  
 Tcac = 23.2 { temperature at the axis at the Center of study Area 0.0}

**EQUATIONS** { main equations used for the solution of the problem }

Tfluidin:  $dt(Tfluidin) = (Tfluidout+2.7-Tfluidin)/trelax$  { difference of input and output fluid temperature to maintain a constant heat flux }

Tcac:  $dt(Tcac) = (Tcac0-Tcac)/ trelax$  { temperature at the center of the borehole at z=0 }

Temp:  $dx(-k*dx(temp))/zscale+dy(-k*dy(temp))/zscale + dz(-k*zscale*dz(temp)) + ro*cp*u*dz(temp) + ro*cp*v*dy(temp)/zscale+ro*cp*dt(temp)/zscale=0$

**EXTRUSION** { describe the geometry of our models by specifying the dividing SURFACES and the intervening LAYERS, starting with the one having the smallest z }

**SURFACE "bottom" Z=0**

LAYER "bottom"

SURFACE "5" Z=D\_bscl

LAYER "LITHOLOGY4"

SURFACE "4" Z=D\_totalscl-dtop3scl

LAYER "LITHOLOGY3\_AQUIF"

SURFACE "3" Z= D\_totalscl-dtop2scl

LAYER "LITHOLOGY2"

**SURFACE "2" Z= D\_totalscl-dtop1scl**

LAYER "LITHOLOGY1"

SURFACE "top" Z= D\_totalscl

**BOUNDARIES** { 3D shapes of each REGION is described by walking their perimeter, stepping from one join point to another, with LINE or ARC segments }

REGION 1 { REGION 1 simulated area }

```

! parameters K, ro, cp, u and v are given regional values
K=1.5
ro = 1800
cp=780
u=0
v=0
! Walking REGION 1 boundary
SURFACE "bottom"      { bottom surface of REGION 1 }
START(-L,-L)         { start from this x,y point }
LAYER "bottom"       { cross this layer }
ARC(CENTER=0,0) ANGLE=360 TO CLOSE { creates an arc with center 0,0 and angle 360
i.e. create a circle}

```

```

REGION 2              { REGION 2 simulated area }
! parameters K, ro, cp, u and v are given regional values
K=1.7
ro = 1290
cp=780
u=0
v=0
! Walking REGION 2 boundary
SURFACE "5"          { bottom surface of REGION 2 }
START(-L,-L)        { start from this x,y point }
LAYER "LITHOLOGY4"   { cross this layer }
ARC(CENTER=0,0) ANGLE=360 TO CLOSE { creates an arc with center 0,0 and angle 360 i.e.
create a circle}

```

```

REGION 3              { LITHOLOGY3_AQUIF simulated area }
! parameters K, ro, cp, u and v are given regional values
K=Kground
ro = rsw
cp=csw
u=0
v=Vgrwater
! Walking REGION 3 boundary
SURFACE "4"          { bottom surface of REGION 3 }

```

```
START(-L,-L)      { start from this x,y point }
LAYER "LITHOLOGY3_AQUIF"      { cross this layer }
ARC(CENTER=0,0) ANGLE=360 TO CLOSE { creates an arc with center 0,0 and angle 360 i.e.
create a circle}
```

```
REGION 4          { REGION 4 simulated area }
! parameters K, ro, cp, u and v are given regional values
```

```
K=1.7
```

```
ro = 2000
```

```
cp=880
```

```
u=0
```

```
v=0
```

```
! Walking REGION 4 boundary
```

```
SURFACE "3"      { bottom surface of REGION 1 }
```

```
START(-L,-L)    { start from this x,y point }
```

```
LAYER "LITHOLOGY2"      { cross this layer }
```

```
ARC(CENTER=0,0) ANGLE=360 TO CLOSE { creates an arc with center 0,0 and angle 360 i.e.
create a circle}
```

```
REGION 5          { REGION 5 simulated area }
```

```
! parameters K, ro, cp, u and v are given regional values
```

```
K=0.8
```

```
ro = 1000
```

```
cp=780
```

```
u=0
```

```
v=0
```

```
! Walking REGION 5 boundary
```

```
SURFACE "2"      { bottom surface of REGION 5 }
```

```
START(-L,-L)    { start from this x,y point }
```

```
LAYER "LITHOLOGY1"      { cross this layer }
```

```
ARC(CENTER=0,0) ANGLE=360 TO CLOSE { creates an arc with center 0,0 and angle 360 i.e.
create a circle}
```

```
limited REGION 6 " borehole area -betonite- L4"
```

```
! parameters K, ro, cp, u and v are given regional values
```

```
K=0.8
```

```

ro = 1000
cp=780
u=0
v=0
! Walking REGION 6 boundary
surface "5"      { bottom surface of LIMITED REGION 6 }
START(D_Rb,0)   { Start from this x,y point }
LAYER "LITHOLOGY4"  { cross this layer }
mesh_spacing = 1 { the desired spacing between mesh nodes }
ARC(CENTER=0,0) ANGLE=360 TO CLOSE { creates an arc with center 0,0 and angle 360 i.e.
create a circle}

```

limited REGION 7 " borehole area -betonite -L3-aq"

! parameters K, ro, cp, u and v are given regional values

K=0.8

ro = 1000

cp=2000

u=0

v=0

! Walking LIMITED REGION 7 boundary

```

surface "4"  { bottom surface of LIMITED REGION 7 }

```

```

START(D_Rb,0)  { Start from this x,y point }

```

```

LAYER "LITHOLOGY3_AQUIF"  { cross LAYER «LITHOLOGY3_AQUIF» }

```

```

mesh_spacing = 1  { the desired spacing between mesh nodes }

```

```

ARC(CENTER=0,0) ANGLE=360 TO CLOSE { creates an arc with center 0,0 and angle 360 i.e.
create a circle}

```

limited REGION 8 " borehole area -betonite- L2"

! parameters K, ro, cp, u and v are given regional values

K=0.8

ro = 1000

cp=780

u=0

v=0

! Walking LIMITED REGION 8 boundary

```

surface "3"  { bottom surface of LIMITED REGION 8 }

```

```

START(D_Rb,0)      { Start from this x,y point }
LAYER "LITHOLOGY2"  { cross LAYER «LITHOLOGY2» }
mesh_spacing = 1   { the desired spacing between mesh nodes }
ARC(CENTER=0,0) ANGLE=360 TO CLOSE      { create an arc with center 0,0 and angle 360
i.e. creates a circle}

```

limited REGION 9 " borehole area -betonite- L1"

! parameters K, ro, cp, u and v are given regional values

K=0.8

ro = 1000

cp=780

u=0

v=0

! Walking LIMITED REGION 9 boundary

surface "2" { bottom surface of LIMITED REGION 9 }

```
START(D_Rb,0)      { Start from this x,y point }
```

```
LAYER "LITHOLOGY1"  { cross LAYER «LITHOLOGY1» }
```

```
mesh_spacing = 1   { cross this layer }
```

```
ARC(CENTER=0,0) ANGLE=360 TO CLOSE      { creates an arc with center 0,0 and angle 360
```

```
i.e. create a circle}
```

limited REGION 10 { fluid in pipe / right pipe }

! parameters K, ro, cp, u and v are given regional values

K =0.51

ro = 950

cp =1800

u=0

v=0

! Walking LIMITED REGION 10 boundary

```
mesh_spacing =10   { the desired spacing between mesh nodes }
```

```
SURFACE "5"      { bottom surface of fluid in pipe }
```

```
START(D_cpc+D_poutside/2, 0)      { Start from this x,y point }
```

```
LAYER "LITHOLOGY4"  { cross LAYER «LITHOLOGY4» }
```

```
LAYER "LITHOLOGY3_AQUIF"  { cross LAYER «LITHOLOGY3_AQUIF» }
```

```

LAYER "LITHOLOGY2"          { cross LAYER «LITHOLOGY2» }
LAYER "LITHOLOGY1"          { cross LAYER «LITHOLOGY1» }
ARC(CENTER=D_cpc,0) ANGLE=360 TO          { creates an arc with center D_cpc,0 and
angle 360 i.e. create a circle}

```

```

limited REGION 11 "fluid in"

```

```

! parameters K, ro, cp, u and v are given regional values

```

```

u= -upipe

```

```

K =0.58

```

```

ro =1000

```

```

cp =4182

```

```

v=0

```

```

mesh_spacing = 10

```

```

! Walking LIMITED REGION 11 boundary and setting boundary conditions

```

```

SURFACE "5"          { bottom surface of REGION «fluid in» }

```

```

SURFACE "top" value(temp) =Tfluidin          { value of temp at SURFACE "top" }

```

```

START(D_cpc+din/2, 0)          { Start from this x,y point of bottom surface }

```

```

natural(temp)=ho*(Tpipe1-temp)

```

```

LAYER "LITHOLOGY4"          { cross LAYER «LITHOLOGY4» }

```

```

natural(temp)=ho*(Tpipe1-temp)

```

```

LAYER "LITHOLOGY3_AQUIF"          { cross LAYER «LITHOLOGY3_AQUIF» }

```

```

natural(temp)=ho*(Tpipe1-temp)

```

```

LAYER "LITHOLOGY2"          { cross LAYER «LITHOLOGY2» }

```

```

natural(temp)=ho*(Tpipe1-temp)

```

```

LAYER "LITHOLOGY1"          { cross LAYER «LITHOLOGY1» }

```

```

ARC(CENTER=D_cpc,0) ANGLE=360 TO CLOSE          { creates an arc with center
D_cpc,0 and angle 360 i.e. create a circle}

```

```

limited REGION 12          { left pipe }

```

```

! parameters K, ro, cp, u and v are given regional values

```

```

K =0.51

```

```

ro = 950

```

```

cp =1800

```

```

u=0

```

```

v=0

```

```

! Walking LIMITED REGION 12 boundary

```

```

SURFACE "5"      { bottom surface of left pipe }
mesh_spacing = 10      { the desired spacing between mesh nodes }
START(-D_cpc-D_poutside/2, 0)      { Start from this x,y point }
LAYER "LITHOLOGY4"      { cross LAYER «LITHOLOGY4» }
LAYER "LITHOLOGY3_AQUIF"      { cross LAYER «LITHOLOGY3_AQUIF» }
LAYER "LITHOLOGY2"      { cross LAYER «LITHOLOGY2» }
LAYER "LITHOLOGY1"      { cross LAYER «LITHOLOGY1» }
ARC(CENTER=-D_cpc,0) ANGLE=360 TO      { creates an arc with center 0,0 and angle
360 i.e. create a circle}

```

limited REGION 13 "fluid out"

! parameters K, ro, cp, u and v are given regional values

u= upipe

K =0.58

ro =1000

cp =4182

v=0

```

mesh_spacing =10      { the desired spacing between mesh nodes }

```

! Walking LIMITED REGION 13 boundary and setting boundary conditions

```

SURFACE "5" value(temp) =Tcac { bottom surface of REGION «fluid out» with boundary contition
}

```

```

START(-D_cpc-din/2, 0)      { Start from this x,y point of bottom surface }

```

```

natural(temp)=ho*(Tpipe2-temp)

```

```

LAYER "LITHOLOGY4"      { cross this layer }

```

```

natural(temp)=ho*(Tpipe2-temp)

```

```

LAYER "LITHOLOGY3_AQUIF"      { cross LAYER «LITHOLOGY3_AQUIF» }

```

```

natural(temp)=ho*(Tpipe2-temp)

```

```

LAYER "LITHOLOGY2"      { cross LAYER «LITHOLOGY2» }

```

```

natural(temp)=ho*(Tpipe2-temp)

```

```

LAYER "LITHOLOGY1"      { cross LAYER «LITHOLOGY1» }

```

```

ARC(CENTER=-D_cpc,0) ANGLE=360 TO CLOSE { create an arc with center -D_cpc,0 and angle
360 degrees 360 i.e. create a circle}

```

```

time 0 to 180000 by 0.5      { time range is 180000 seconds with 0.5 second step }

```

```

PLOTS      { OUTPUT RESULTS : CONTOUR, SURFACE, VECTOR, GRID output format
display data values on the computation plane }

```

```

for t=0 by 10 to 1000 by 100 to 10000 by 200 to 180000

```

```

history (Tfluidin, Tfluidout, Tcac) { specifies values for which a time history is desired }
contour(temp) on Z= D_totalscl as " Z= D_totalscl Temp" { Creates contour lines for temperature
on Z=D_totalscl and label " Z= D_totalscl Temp" }
contour(temp) on Z= 0.35 as " Z=0.35-flow" { Creates contour lines for temperature on Z=0.35
ie in the aquifer and label " Z=0.35-flow " }
contour(temp) on Z= D_ascl as " Z= D_ascl Temp" { Creates contour lines for temperature on Z=
D_ascl and label " Z= D_ascl Temp" }
contour(temp) on x=D_cpc as "x =D_cpc Temp" { Creates contour lines for temperature on x=
D_cpc and label " x= D_cpc Temp" }
contour(temp) on y=-D_cpc as "y =-D_cpc Temp" { Creates contour lines for temperature on y=-
D_cpc and label " y=- D_cpc Temp" }
contour(temp) on y=0 as "ZX Temp" { Creates contour lines for temperature on y=0 and label " ZX
Temp" }

END { FINISH }

```



## **APPENDIX II**

**I. Sample List and Sampling Locations (coordinate system WGS 84, Zone 36 N)**

No	Lithology	Formation	X Coordinate	Y Coordinate
1	Calcarenite	Nicosia	535311	3886534
2	Chert	Lefkara	543601	3872324
3	Calcarenite	Athalassa Member	536106	3891273
4	Chert	Lefkara	543601	3872324
5	Calcarenite	Nicosia	535311	3886534
6	Sandy Marl	Nicosia	536106	3891273
7	Calcarenite	Nicosia	536106	3891273
8	Basalt	Lower Pillow Lavas	536148	3858276
9	Chalk	Pachna	544662	3873078
10	Volcanic Breccia	Lower Pillow Lavas	526716	3855826
11	Chert	Lefkara	528391	3856546
12	Marly Chalk	Pachna	549813	3871124
13	Sandy Marl	Nicosia	559431	3871182
14	Calcarenite	Terrace Deposits (Marine Terrace)	562609	3870508
15	Reddish brown sandy clay with gravel	Terrace Deposits (Fluvial Deposits)	572549	3872883
16	Reef Limestone	Pachna - Koronia Member	590648	3879271
17	Brownish clayey Sand	Terrace Deposits (Marine Terrace)	595327	3876709
18	Calcarenite	Terrace Deposits (Marine Terrace)	596569	3871418
19	Reef Limestone	Pachna - Koronia Member	593558	3871279
20	Microgabbro, Dykes	Lower Pillow Lavas	551461	3874105
21	Fossiliferous sandy Marl	Marl Member	536155	3891223
22	Gray sandy silt	Terrace Deposits (Fluvial Deposits)	548971	3878990
23	Chalk	Pachna	544662	3873078
24	Chalk	Pachna	549813	3871124
25	Olivine-Phyric Basalt	Lower Pillow Lavas	551461	3874105
26	Diabase	Lower Pillow Lavas	551461	3874105
27	Microgabbro	Sheeted Dykes (Diabase)	526716	3855826
28	Chert	Lefkara	528391	3856546
29	Silicified chalk	Lefkara	528391	3856546
30	Calcarenite	Terrace Deposits (Marine Terrace)	596569	3871414
31	Reef Limestone	Pachna - Terra Member	593558	3871279
32	Marl	Nicosia	559431	3871182
33	Brownish Clay with gravels	Terrace Deposits (Fluvial Deposits)	443955	3855696

No	Lithology	Formation	X Coordinate	Y Coordinate
34	Grey Marl	Nicosia Marl Member	532251	3878242
35	Reef Limestone	Pachna - Terra Member	442981	3860785
36	Marly Chalk	Pachna	444872	3862635
37	Gabbro (weathered)	Gabbro	438696	3875841
38	Serpentinited Harzburgite	Harzburgite	438523	3877311
39	Fossiliferous Marl	Nicosia	450429	3869236
40	Calcarenite	Aeolian Deposits	448194	3845358
41	Fossiliferous Sandy Marl	Nicosia	448194	3845358
42	Marly Chalk	Pachna	449296	3846014
43	Marly Chalk	Pachna	478607	3855963
44	Chalk	Pachna	517671	3842147
45	Reef Limestone	Pachna - Terra Member	442981	3860785
46	Gabbro	Gabbro	438696	3875841
47	Reef Limestone Breccia		449296	3846014
48	Chalk	Pachna	557183	3872301
49	Olive phyric Basalt	Upper Pillow Lavas	557015	3873920
50	Siltstone	Pachna	457222	3862016
51	Serpentinite	Serpentinite	460967	3863423
52	Chalk	Lefkara	455791	3866215
53	Reef Limestone	Pachna - Terra Member	593350	3871736
54	White chalk	Lefkara	547986	3870736
55	Offwhite chalk	Pachna	545538	3872081
56	Marble, Laminated Gypsum	Kalavastos	523414	3897019
57	Diabase	Basal Group	540564	3867831
58	Chert	Lefkara	544243	3867617
59	basalt	Lower Pillow Lavas	537855	3869513
60	Harzburgite	Harzburgite	489460	3869420
61	White chalk	Lefkara	593895	3874682
62	Diabase	Sheeted Dykes (Diabase)	516685	3860115
63	Diabase	Sheeted Dykes (Diabase)	519780	3861850
64	Sandy Marl	Nicosia (Athalassa Member)	539719	3880504
65	Sandstone	Nicosia (Aspropamboulos Oolite Member)	534149	3880579
66	Sandstone	Nicosia (Kephales Member)	533456	3883450
67	Brown Silty Sand	Apalos - Athalassa - Kakkaristra (Apalos Formation)	522751	3882970
68	Sandstone	Nicosia (Lithic Sand Member with corals)	523541	3882467

No	Lithology	Formation	X Coordinate	Y Coordinate
69	Sandstone	Nicosia (Kephales Member)	533456	3883450
70	Lithic sand	Nicosia (Aspropamboulos Oolite Member)	534149	3880579
71	Marly Sandstone	Nicosia (Athalassa Member)	539719	3880504
72	Calcarenite	Nicosia (Athalassa Member)	539719	3880504
73	Yellowish silty sand	Apalos - Athalassa - Kakkaristra (Apalos Formation)	522751	3882970
74	Reddish silty sand	Apalos - Athalassa - Kakkaristra (Apalos Formation)	522751	3882970
75	Calcarenite	Pachna	486562	3846226
76	Marly Chalk	Pachna	481536	3849670
77	Marly Chalk	Pachna	479415	3848305
78	Chalk	Pachna	479930	3852974
79	Marly Chalk	Pachna	479222	3853108
80	Chalk	Pachna	478329	3855558
81	Limestone	Pachna - Terra Member	477055	3853559
82	Chalk	Pachna	481147	3854973
83	Chalk	Lefkara	482639	3857634
84	Reef Limestone	Pachna - Terra Member	483471	3850621
85	Gypsum	Kalavastos	456654	3861931
86	Volcanioclastic Sandstone	Kannaviou	461640	3863319
87	Gabbro	Gabbro	493459	3866325
88	Serpentinite	Serpentinite	492216	3865365
89	Plagiogranite	Plagiogranite	482906	3867964
90	Chert	Lefkara	488105	3856390
91	Chalk	Lefkara	488105	3856390
92	Massive Chalk	Lefkara	487977	3856159
93	Diabase	Sheeted Dykes (Diabase)	491238	3872411
94	Diabase	Basal Group	491316	3877491
95	Microgabbro	Sheeted Dykes (Diabase)	502197	3861611
96	Diabase	Sheeted Dykes (Diabase)	508422	3863780
97	Diabase	Sheeted Dykes (Diabase)	510478	3865043
98	Basalt	Lower Pillow Lavas	495332	3881993
99	Reef Limestone	Pachna - Koronia Member	496000	3883056
100	Calcarenite	Nicosia	518306	3892433
101	Reef Limestone	Pachna - Koronia Member	509836	3878656

No	Lithology	Formation	X Coordinate	Y Coordinate
102	Chalk	Lefkara	511365	3878629
103	Basalt	Upper Pillow Lavas	513241	3878031
104	Chalk	Pachna	513975	3878331
105	Dunite	Dunite	486998	3866750
106	Wehrlite	Wehrlite	485250	3865459
107	Pyroxenite	Pyroxenite	485936	3867028
108	Harzburgite	Harzburgite	487350	3863197
109	Poikilitic wehrlite	Wehrlite	487131	3862512
110	Microgabbro	Basal Group	536950	3856315
111	Gypsum	Kalavastos	532634	3846250
112	Chalky Marl	Pachna	532634	3846250
113	Calcarenite	Pachna	532634	3846250
114	Chalk	Pachna	532634	3846250
115	Breccia Reef Limestone	Terrace Deposits (Fluvial Deposits)	509964	3841510
116	Gypsum	Kalavastos	509964	3841510
117	Reef Limestone	Pachna - Koronia Member	532647	3847010
118	Reef Limestone	Pachna - Koronia Member	532647	3847010
119	Chalk	Pachna	532647	3847010
120	Calcarenite	Pachna	532647	3847010
121	Gypsum	Kalavastos	542233	3854311
122	Gypsum	Kalavastos	542233	3854311
123	Calcarenite	Nicosia	536570	3884653
124	Calcarenite	Nicosia	475204	3834194
125	Calcarenite	Nicosia	536570	3884653
126	Sandy Marl	Nicosia	475204	3834194
127	Calcarenite	Pachna	478132	3846942
128	Calcarenite	Pachna	535575	3847389
129	Calcarenite	Pachna	475198	3844976
130	Chalk	Pachna	544644	3871724
131	Calcarenite	Nicosia (Athalassa Member)	522908	3892791
132	Reef limestone	Pachna - Koronia Member	511188	3879130
133	Diabase	Basal Group	512801	3866623
134	Calcarenite	Terrace Deposits (Marine Terrace)	445664	3851742
135	Calcarenite	Nicosia	448121	3847072
136	Calcarenite	Aeolian Deposits	446735	3846683
137	Calcarenite	Aeolian Deposits	446735	3846683
138	Limestone	Lapatsa	531669	3892991
139	Chalks	Lapatsa	531669	3892991
140	Chalky Marls	Lapatsa	531669	3892991

No	Lithology	Formation	X Coordinate	Y Coordinate
141	Sandstone	Kythrea Formation	517687	3872926
142	Marls	Kythrea Formation	517687	3872926
143	Marls	Kythrea Formation	517687	3872926
144	soil and small gravel	Colluvium (Apalos Formation)	522846	3882699
145	soil and small gravel	Alluvium	511234	3887885
	large gravel	Alluvium		
146	soil	Fanglomerate	500800	3886285
	large gravel	Fanglomerate		
147	soil and small gravel	Fanglomerate	498242	3884897
	large gravel	Fanglomerate		
148	soil and small gravel	Alluvium	497599	3884874
	large gravel	Alluvium		

## II. Analytical laboratory results for dry samples

Samples - Dry Conditions															
No	Lithology	Formation	1st Measurement			2nd Measurement			3rd Measurement			MEAN VALUES			
			Diffusivity x 10 <sup>-6</sup> (m <sup>2</sup> /s)	Volumetric heat capacity x 10 <sup>6</sup> (J/m <sup>3</sup> K)	Thermal conductivity (W/mK)	Diffusivity x 10 <sup>-6</sup> (m <sup>2</sup> /s)	Volumetric heat capacity x 10 <sup>6</sup> (J/m <sup>3</sup> K)	Thermal conductivity (W/mK)	Diffusivity x 10 <sup>-6</sup> (m <sup>2</sup> /s)	Volumetric heat capacity x 10 <sup>6</sup> (J/m <sup>3</sup> K)	Thermal conductivity (W/mK)	Diffusivity x 10 <sup>-6</sup> (m <sup>2</sup> /s)	Volumetric heat capacity x 10 <sup>6</sup> (J/m <sup>3</sup> K)	Thermal conductivity (W/mK)	CALCULATED Specific heat capacity x 10 <sup>-3</sup> (J/K kg)
1	Calcarenite	Nicosia	0.75	1.64	1.23	0.66	1.35	0.89	---	---	---	0.70	1.50	1.06	0.58
2	Chert	Lefkara	0.81	1.74	1.42	0.84	1.71	1.44	---	---	---	0.83	1.73	1.43	0.74
3	Calcarenite	Athalassa Member	1.10	1.52	1.67	1.43	1.54	2.20	1.14	1.75	2.20	1.22	1.60	2.02	0.65
4	Chert	Lefkara	0.83	1.96	1.62	0.85	1.67	1.42	---	---	---	0.84	1.82	1.52	0.78
5	Calcarenite	Nicosia	0.37	1.38	0.52	0.35	1.37	0.48	---	---	---	0.36	1.38	0.50	0.90
6	Sandy Marl	Nicosia	0.37	1.41	0.51	0.31	1.50	0.47	---	---	---	0.34	1.46	0.49	1.15
7	Calcarenite	Nicosia	---	---	0.41	---	---	0.48	---	---	---	---	---	0.45	---
8	Basalt	Lower Pillow Lavas	0.78	1.53	1.19	0.66	1.80	1.19	---	---	---	0.72	1.67	1.19	0.61
9	Chalk	Pachna	0.74	1.86	1.38	0.87	1.60	1.40	---	---	---	0.81	1.73	1.39	0.74
10	Volcanic Breccia	Lower Pillow Lavas	1.23	1.85	2.28	0.99	1.94	1.92	1.23	1.72	2.12	1.15	1.84	2.11	0.69
11	Chert	Lefkara	1.22	1.56	1.91	1.25	1.87	2.34	1.12	1.83	2.06	1.20	1.75	2.10	0.72
12	Marly Chalk	Pachna	0.68	1.80	1.21	0.67	1.75	1.18	---	---	---	0.67	1.78	1.20	0.68
13	Sandy Marl	Nicosia	0.60	1.36	0.82	0.63	1.36	0.85	0.63	1.39	0.87	0.62	1.37	0.85	0.82
14	Calcarenite	Terrace Deposits (Marine Terrace)	0.59	1.91	1.02	0.58	1.42	0.81	0.56	1.43	0.82	0.57	1.59	0.88	0.67

No	Lithology	Formation	Diffusivity x 10 <sup>-6</sup> ( m <sup>2</sup> /s)	Volumetric heat capacity x 10 <sup>6</sup> (J/m <sup>3</sup> K)	Thermal conductivity ( W/mK )	Diffusivity x 10 <sup>-6</sup> ( m <sup>2</sup> /s)	Volumetric heat capacity x 10 <sup>6</sup> (J/m <sup>3</sup> K)	Thermal conductivity ( W/mK )	Diffusivity x 10 <sup>-6</sup> ( m <sup>2</sup> /s)	Volumetric heat capacity x 10 <sup>6</sup> (J/m <sup>3</sup> K)	Thermal conductivity ( W/mK )	Diffusivity x 10 <sup>-6</sup> ( m <sup>2</sup> /s)	Volumetric heat capacity x 10 <sup>6</sup> (J/m <sup>3</sup> K)	Thermal conductivity ( W/mK )	CALCULATE D Specific heat capacity x 10 <sup>-3</sup> (J/K.kg)
15	Reddish brown sandy clay with gravel	Terrace Deposits (Fluvial Deposits)	0.59	1.40	0.75	---	---	---	---	---	---	0.59	1.40	0.75	0.98
16	Reef Limestone	Pachna - Koronia Member	0.73	1.49	1.08	0.79	1.63	1.29	---	---	---	0.76	1.56	1.19	0.68
17	Brownish clayey Sand	Terrace Deposits (Marine Terrace)	0.40	1.41	0.57	0.40	1.40	0.57	---	---	---	0.40	1.41	0.57	0.82
18	Calcarenite	Terrace Deposits (Marine Terrace)	0.96	1.50	1.45	0.87	1.63	1.41	---	---	---	0.92	1.57	1.43	0.62
19	Reef Limestone	Pachna - Koronia Member	0.99	1.42	1.40	0.79	1.41	1.12	0.86	1.36	1.17	0.88	1.40	1.23	0.53
20	Microgabbro, Dykes	Lower Pillow Lavas	0.72	1.42	1.03	0.58	1.68	0.97	---	---	---	0.65	1.55	1.00	0.61
21	Fossiliferous sandy Marl	Marl Member	0.35	1.46	0.51	0.36	1.35	0.49	0.31	1.40	0.43	0.34	1.40	0.48	0.87
22	Gray sandy silt	Terrace Deposits (Fluvial Deposits)	0.41	1.47	0.61	0.39	1.38	0.53	0.37	1.41	0.52	0.39	1.42	0.55	0.95
23	Chalk	Pachna	0.65	1.75	1.14	0.72	1.45	1.05	---	---	---	0.69	1.60	1.10	0.70
24	Chalk	Pachna	0.67	1.69	1.14	0.69	1.47	1.02	---	---	---	0.68	1.58	1.08	0.60
25	Olivine-Phyric Basalt	Lower Pillow Lavas	0.50	1.63	0.82	0.56	1.68	0.95	---	---	---	0.53	1.66	0.88	0.65
26	Diabase	Lower Pillow Lavas	0.67	1.57	1.05	0.60	1.66	0.99	---	---	---	0.63	1.62	1.02	0.64
27	Microgabbro	Sheeted Dykes (Diabase)	1.21	1.68	2.03	1.13	1.94	2.18	---	---	---	1.17	1.81	2.11	0.68
28	Chert	Lefkara	0.82	1.75	1.43	0.86	1.66	1.42	---	---	---	0.84	1.71	1.43	0.68
29	Silicified chalk	Lefkara	1.10	1.83	2.02	1.03	1.80	1.85	---	---	---	1.07	1.82	1.94	0.68
30	Calcarenite	Terrace Deposits (Marine Terrace)	0.43	1.85	0.79	0.82	1.55	1.26	0.99	1.59	1.58	0.75	1.66	1.21	0.64
31	Reef Limestone	Pachna - Terra Member	0.81	1.62	1.32	0.83	1.56	1.29	---	---	---	0.82	1.59	1.31	0.62



No	Lithology	Formation	Diffusivity x 10 <sup>-6</sup> ( m <sup>2</sup> /s)	Volumetric heat capacity x 10 <sup>6</sup> (J/m <sup>3</sup> K)	Thermal conductivity ( W/mK )	Diffusivity x 10 <sup>-6</sup> ( m <sup>2</sup> /s)	Volumetric heat capacity x 10 <sup>6</sup> (J/m <sup>3</sup> K)	Thermal conductivity ( W/mK )	Diffusivity x 10 <sup>-6</sup> ( m <sup>2</sup> /s)	Volumetric heat capacity x 10 <sup>6</sup> (J/m <sup>3</sup> K)	Thermal conductivity ( W/mK )	Diffusivity x 10 <sup>-6</sup> ( m <sup>2</sup> /s)	Volumetric heat capacity x 10 <sup>6</sup> (J/m <sup>3</sup> K)	Thermal conductivity ( W/mK )	CALCULATE D Specific heat capacity x 10 <sup>-3</sup> (J/K.kg)
32	Marl	Nicosia	0.53	1.35	0.70	---	---	---	---	---	---	0.53	1.35	0.70	1.01
33	Brownish Clay with gravels	Terrace Deposits (Fluvial Deposits)	0.35	1.35	0.47	0.35	1.35	0.46	0.41	1.39	0.57	0.37	1.36	0.50	0.95
34	Grey Marl	Nicosia Marl Member	0.47	1.44	0.68	0.48	1.40	0.68	0.39	1.56	0.61	0.45	1.47	0.65	0.65
35	Reef Limestone	Pachna - Terra Member	1.34	1.72	2.31	1.02	1.76	1.80	---	---	---	1.18	1.74	2.06	0.68
36	Marly Chalk	Pachna	0.69	1.87	1.30	0.71	1.89	1.33	---	---	---	0.70	1.88	1.32	0.76
37	Gabbro (weathered)	Gabbro	1.19	1.72	2.04	0.87	1.62	1.41	1.18	1.54	1.81	1.08	1.63	1.75	0.59
38	Serpentinited Harzburgite	Harzburgite	0.69	1.86	1.28	0.88	1.46	1.29	---	---	---	0.78	1.66	1.29	0.65
39	Fossiliferous Marl	Nicosia	0.43	1.47	0.64	---	---	---	---	---	---	0.43	1.47	0.64	1.26
40	Calcarenite	Aeolian Deposits	0.30	1.37	0.41	---	---	---	---	---	---	0.30	1.37	0.41	0.63
41	Fossiliferous Sandy Marl	Nicosia	0.46	1.44	0.66	0.48	1.36	0.65	0.45	1.36	0.62	0.46	1.39	0.64	0.83
42	Marly Chalk	Pachna	0.67	1.74	1.16	0.72	1.66	1.19	---	---	---	0.69	1.70	1.18	0.67
43	Marly Chalk	Pachna	0.98	1.95	1.91	0.98	1.89	1.85	---	---	---	0.98	1.92	1.88	0.72
44	Chalk	Pachna	0.80	1.72	1.38	0.81	1.49	1.20	---	---	---	0.81	1.61	1.29	0.64
45	Reef Limestone	Pachna - Terra Member	0.86	1.89	1.63	1.04	1.51	1.57	---	---	---	0.95	1.70	1.60	0.69
46	Gabbro	Gabbro	1.85	1.53	2.84	2.00	1.42	2.82	---	---	---	1.93	1.48	2.83	0.52
47	Reef Limestone Breccia		0.70	1.75	1.22	0.68	1.80	1.22	0.70	1.79	1.25	0.69	1.78	1.23	0.71
48	Chalk	Pachna	0.63	1.71	1.08	0.59	1.58	0.94	---	---	---	0.61	1.65	1.01	0.74
49	Olive phyric Basalt	Upper Pillow Lavas	0.60	1.76	1.05	0.70	1.57	1.10	0.66	1.67	1.09	0.65	1.67	1.08	0.68

No	Lithology	Formation	Diffusivity x 10 <sup>-6</sup> ( m <sup>2</sup> /s)	Volumetric heat capacity x 10 <sup>6</sup> (J/m <sup>3</sup> K)	Thermal conductivity ( W/mK )	Diffusivity x 10 <sup>-6</sup> ( m <sup>2</sup> /s)	Volumetric heat capacity x 10 <sup>6</sup> (J/m <sup>3</sup> K)	Thermal conductivity ( W/mK )	Diffusivity x 10 <sup>-6</sup> ( m <sup>2</sup> /s)	Volumetric heat capacity x 10 <sup>6</sup> (J/m <sup>3</sup> K)	Thermal conductivity ( W/mK )	Diffusivity x 10 <sup>-6</sup> ( m <sup>2</sup> /s)	Volumetric heat capacity x 10 <sup>6</sup> (J/m <sup>3</sup> K)	Thermal conductivity ( W/mK )	CALCULATE D Specific heat capacity x 10 <sup>-3</sup> (J/K.kg)
50	Siltstone	Pachna	0.39	1.84	0.71	0.41	1.45	0.59	0.40	1.45	0.58	0.40	1.58	0.63	1.53
51	Serpentinite	Serpentinite	1.12	2.07	2.32	1.13	1.99	2.25	---	---	---	1.13	2.03	2.29	0.79
52	Chalk	Lefkara	0.64	1.76	1.13	0.65	1.76	1.14	---	---	---	0.64	1.76	1.14	0.73
53	Reef Limestone	Pachna - Terra Member	1.33	1.62	2.16	1.48	1.48	2.19	---	---	---	1.41	1.55	2.18	0.58
54	White chalk	Lefkara	0.34	1.64	0.56	0.34	1.64	0.56	---	---	---	0.34	1.64	0.56	0.72
55	Offwhite chalk	Pachna	0.60	1.81	1.08	0.60	1.83	1.11	---	---	---	0.60	1.82	1.10	0.83
56	Marble, Laminated Gypsum	Kalavastos	0.71	1.69	1.19	0.63	1.48	0.93	0.60	1.56	0.95	0.65	1.58	1.02	0.63
57	Diabase	Basal Group	1.31	2.19	2.87	1.24	2.12	2.63	---	---	---	1.28	2.16	2.75	0.79
58	Chert	Lefkara	0.79	1.96	1.55	0.78	1.98	1.54	---	---	---	0.78	1.97	1.55	0.83
59	basalt	Lower Pillow Lavas	0.59	1.81	1.07	0.62	1.84	1.14	---	---	---	0.61	1.83	1.11	0.67
60	Harzburgite	Harzburgite	0.83	2.14	1.77	0.87	2.12	1.86	---	---	---	0.85	2.13	1.82	0.82
61	White chalk	Lefkara	0.63	1.76	1.10	0.72	1.51	1.08	---	---	---	0.67	1.64	1.09	0.70
62	Diabase	Sheeted Dykes (Diabase)	1.04	2.10	2.19	1.08	2.03	2.19	---	---	---	1.06	2.07	2.19	0.75
63	Diabase	Sheeted Dykes (Diabase)	0.96	2.17	2.07	0.96	2.14	2.05	---	---	---	0.96	2.16	2.06	0.78
64	Sandy Marl	Nicosia (Athalassa Member)	0.53	1.59	0.85	0.54	1.59	0.85	---	---	---	0.54	1.59	0.85	1.07
65	Sandstone	Nicosia (Aspropamboulos Oolite Member)	0.47	1.56	0.73	0.55	1.37	0.75	---	---	---	0.51	1.47	0.74	0.95
66	Sandstone	Nicosia (Kephales Member)	0.92	1.55	1.43	0.80	1.49	1.18	---	---	---	0.86	1.52	1.31	0.59

No	Lithology	Formation	Diffusivity x 10 <sup>-6</sup> ( m <sup>2</sup> /s)	Volumetric heat capacity x 10 <sup>6</sup> (J/m <sup>3</sup> K)	Thermal conductivity ( W/mK )	Diffusivity x 10 <sup>-6</sup> ( m <sup>2</sup> /s)	Volumetric heat capacity x 10 <sup>6</sup> (J/m <sup>3</sup> K)	Thermal conductivity ( W/mK )	Diffusivity x 10 <sup>-6</sup> ( m <sup>2</sup> /s)	Volumetric heat capacity x 10 <sup>6</sup> (J/m <sup>3</sup> K)	Thermal conductivity ( W/mK )	Diffusivity x 10 <sup>-6</sup> ( m <sup>2</sup> /s)	Volumetric heat capacity x 10 <sup>6</sup> (J/m <sup>3</sup> K)	Thermal conductivity ( W/mK )	CALCULATE D Specific heat capacity x 10 <sup>-3</sup> (J/K.kg)
67	Brown Silty Sand	Apalos - Athalassa - Kakkaristra (Apalos Formation)	0.29	1.44	0.41	0.31	1.43	0.45	---	---	---	0.30	1.44	0.43	---
68	Sandstone	Nicosia (Lithic Sand Member with corals)	0.49	1.49	0.73	0.48	1.50	0.72	---	---	---	0.49	1.50	0.73	1.02
69	Sandstone	Nicosia (Kephales Member)	0.99	1.80	1.77	1.12	1.36	1.51	0.91	1.82	1.66	1.01	1.66	1.65	0.62
70	Lithic sand	Nicosia (Aspropamboulos Oolite Member)	---	---	0.59	0.31	1.49	0.47	0.30	1.49	0.45	0.31	1.49	0.50	0.91
71	Marly Sandstone	Nicosia (Athalassa Member)	1.05	1.78	1.86	1.01	1.81	1.84	---	---	---	1.03	1.80	1.85	0.67
72	Calcarenite	Nicosia (Athalassa Member)	0.55	1.43	0.79	0.59	1.44	0.84	---	---	---	0.57	1.44	0.82	0.61
73	Yellowish silty sand	Apalos - Athalassa - Kakkaristra (Apalos Formation)	0.49	1.40	0.68	0.43	1.36	0.58	---	---	0.43	0.46	1.38	0.63	0.82
74	Reddish silty sand	Apalos - Athalassa - Kakkaristra (Apalos Formation)	0.44	1.37	0.61	0.53	1.50	0.80	0.52	1.50	0.79	0.50	1.46	0.73	0.88
75	Calcarenite	Pachna	0.69	1.58	1.09	0.69	1.44	0.99	---	---	---	0.69	1.51	1.04	0.60
76	Marly Chalk	Pachna	0.82	1.94	1.59	0.84	1.87	1.58	---	---	---	0.83	1.91	1.59	0.73
77	Marly Chalk	Pachna	0.87	1.97	1.71	0.84	2.02	1.69	---	---	---	0.85	2.00	1.70	0.75
78	Chalk	Pachna	0.81	1.72	1.39	0.77	1.77	1.36	---	---	---	0.79	1.75	1.38	0.66
79	Marly Chalk	Pachna	0.64	1.62	1.04	0.59	1.86	1.09	---	---	---	0.61	1.74	1.07	0.66
80	Chalk	Pachna	1.15	1.89	2.19	1.12	1.96	2.20	---	---	---	1.14	1.93	2.20	0.74

No	Lithology	Formation	Diffusivity x 10 <sup>-6</sup> ( m <sup>2</sup> /s)	Volumetric heat capacity x 10 <sup>6</sup> (J/m <sup>3</sup> K)	Thermal conductivity ( W/mK )	Diffusivity x 10 <sup>-6</sup> ( m <sup>2</sup> /s)	Volumetric heat capacity x 10 <sup>6</sup> (J/m <sup>3</sup> K)	Thermal conductivity ( W/mK )	Diffusivity x 10 <sup>-6</sup> ( m <sup>2</sup> /s)	Volumetric heat capacity x 10 <sup>6</sup> (J/m <sup>3</sup> K)	Thermal conductivity ( W/mK )	Diffusivity x 10 <sup>-6</sup> ( m <sup>2</sup> /s)	Volumetric heat capacity x 10 <sup>6</sup> (J/m <sup>3</sup> K)	Thermal conductivity ( W/mK )	CALCULATE D Specific heat capacity x 10 <sup>-3</sup> (J/K.kg)
81	Limestone	Pachna - Terra Member	1.43	1.71	2.43	1.48	1.81	2.68	---	---	---	1.46	1.76	2.56	0.67
82	Chalk	Pachna	0.87	2.06	1.80	0.89	2.03	1.80	---	---	---	0.88	2.05	1.80	0.77
83	Chalk	Lefkara	0.84	1.97	1.65	0.92	1.82	1.68	---	---	---	0.88	1.90	1.67	0.72
84	Reef Limestone	Pachna - Terra Member	1.13	1.68	1.89	1.05	1.76	1.84	---	---	---	1.09	1.72	1.87	0.64
85	Gypsum	Kalavastos	0.66	1.96	1.29	0.66	1.97	1.30	---	---	---	0.66	1.97	1.30	0.76
86	Volcanioclastic Sandstone	Kannaviou	0.41	1.47	0.60	0.42	1.46	0.61	---	---	---	0.41	1.47	0.60	0.57
87	Gabbro	Gabbro	1.09	2.02	2.20	1.01	2.04	2.06	---	---	---	1.05	2.03	2.13	0.71
88	Serpentinite	Serpentinite	0.84	2.06	1.73	0.84	2.03	1.71	---	---	---	0.84	2.05	1.72	0.77
89	Plagiogranite	Plagiogranite	1.56	2.13	3.32	1.78	2.09	3.72	1.50	2.13	3.21	1.61	2.12	3.42	0.77
90	Chert	Lefkara	1.03	1.86	1.92	1.04	1.83	1.89	---	---	---	1.04	1.85	1.91	0.74
91	Chalk	Lefkara	0.92	1.97	1.82	0.91	1.88	1.72	---	---	---	0.92	1.93	1.77	0.73
92	Massive Chalk	Lefkara	0.63	2.00	1.26	0.68	1.91	1.29	---	---	---	0.65	1.96	1.28	0.77
93	Diabase	Sheeted Dykes (Diabase)	0.89	2.05	1.80	1.20	1.41	1.69	1.02	1.84	1.89	1.04	1.77	1.79	0.63
94	Diabase	Basal Group	0.84	1.62	1.35	0.80	1.82	1.44	---	---	---	0.82	1.72	1.40	0.67
95	Microgabbro	Sheeted Dykes (Diabase)	1.10	1.89	2.06	1.10	1.89	2.07	---	---	---	1.10	1.89	2.07	0.63
96	Diabase	Sheeted Dykes (Diabase)	1.03	2.17	2.23	0.96	2.11	2.03	---	---	---	1.00	2.14	2.13	0.75
97	Diabase	Sheeted Dykes (Diabase)	0.89	1.86	1.65	0.97	1.80	1.76	0.91	1.78	1.61	0.92	1.81	1.67	0.68
98	Basalt	Lower Pillow Lavas	0.99	1.41	1.39	0.82	1.87	1.53	---	---	---	0.90	1.64	1.46	0.64
99	Reef Limestone	Pachna - Koronia Member	0.83	1.59	1.32	0.82	1.39	1.14	---	---	---	0.83	1.49	1.23	0.58

No	Lithology	Formation	Diffusivity x 10 <sup>-6</sup> ( m <sup>2</sup> /s)	Volumetric heat capacity x 10 <sup>6</sup> (J/m <sup>3</sup> K)	Thermal conductivity ( W/mK )	Diffusivity x 10 <sup>-6</sup> ( m <sup>2</sup> /s)	Volumetric heat capacity x 10 <sup>6</sup> (J/m <sup>3</sup> K)	Thermal conductivity ( W/mK )	Diffusivity x 10 <sup>-6</sup> ( m <sup>2</sup> /s)	Volumetric heat capacity x 10 <sup>6</sup> (J/m <sup>3</sup> K)	Thermal conductivity ( W/mK )	Diffusivity x 10 <sup>-6</sup> ( m <sup>2</sup> /s)	Volumetric heat capacity x 10 <sup>6</sup> (J/m <sup>3</sup> K)	Thermal conductivity ( W/mK )	CALCULATE D Specific heat capacity x 10 <sup>-3</sup> (J/K.kg)
100	Calcarenite	Nicosia	0.60	1.39	0.84	0.59	1.38	0.81	0.79	1.47	1.17	0.66	1.41	0.94	0.63
101	Reef Limestone	Pachna - Koronia Member	0.87	1.72	1.49	0.90	1.73	1.54	---	---	---	0.88	1.73	1.52	0.69
102	Chalk	Lefkara	0.50	1.80	0.90	0.48	1.55	0.74	0.48	1.57	0.76	0.49	1.64	0.80	0.65
103	Basalt	Upper Pillow Lavas	0.63	1.81	1.15	0.59	1.82	1.07	---	---	---	0.61	1.82	1.11	0.69
104	Chalk	Pachna	0.64	1.74	1.12	0.63	1.81	1.14	---	---	---	0.64	1.78	1.13	0.73
105	Dunite	Dunite	1.15	2.14	2.52	1.05	2.11	2.21	---	---	---	1.10	2.13	2.37	0.80
106	Wehrlite	Wehrlite	1.29	2.26	2.91	1.26	2.34	2.95	---	---	---	1.28	2.30	2.93	0.84
107	Pyroxenite	Pyroxenite	1.87	2.27	4.25	1.77	2.31	4.09	---	---	---	1.82	2.29	4.17	0.72
108	Harzburgite	Harzburgite	0.94	2.19	2.07	0.95	2.16	2.05	1.01	1.96	1.98	0.97	2.10	2.03	0.78
109	Poikilitic wehrlite	Wehrlite	1.27	2.19	2.79	1.36	2.26	3.07	1.34	2.23	2.98	1.32	2.23	2.95	0.80
110	Microgabbro	Basal Group	1.00	1.99	1.99	1.02	1.95	1.99	---	---	---	1.01	1.97	1.99	0.73
111	Gypsum	Kalavastos	0.67	1.74	1.17	0.78	1.41	1.09	---	---	---	0.72	1.58	1.13	0.63
112	Chalky Marl	Pachna	0.45	1.50	0.68	0.46	1.53	0.70	---	---	---	0.45	1.52	0.69	0.88
113	Calcarenite	Pachna	0.84	1.52	1.28	0.66	1.53	1.00	0.53	1.41	0.75	0.68	1.49	1.01	0.64
114	Chalk	Pachna	1.15	1.84	2.11	1.16	1.78	2.07	---	---	---	1.16	1.81	2.09	0.70
115	Breccia Reef Limestone	Terrace Deposits (Fluvial Deposits)	0.56	1.46	0.82	0.53	1.39	0.74	---	---	---	0.55	1.43	0.78	0.55
116	Gypsum	Kalavastos	0.75	1.84	1.39	0.88	1.48	1.30	---	---	---	0.81	1.66	1.35	0.64
117	Reef Limestone	Pachna - Koronia Member	0.55	1.65	0.90	0.54	1.66	0.89	---	---	---	0.54	1.66	0.90	0.58
118	Reef Limestone	Pachna - Koronia Member	0.93	1.43	1.34	0.81	1.48	1.21	---	---	---	0.87	1.46	1.28	0.56
119	Chalk	Pachna	1.05	2.02	2.12	1.10	1.67	1.85	1.25	1.50	1.87	1.13	1.73	1.95	0.65
120	Calcarenite	Pachna	1.01	1.36	1.37	0.96	1.36	1.29	---	---	---	0.98	1.36	1.33	0.54

No	Lithology	Formation	Diffusivity x 10 <sup>-6</sup> ( m <sup>2</sup> /s)	Volumetric heat capacity x 10 <sup>6</sup> (J/m <sup>3</sup> K)	Thermal conductivity ( W/mK )	Diffusivity x 10 <sup>-6</sup> ( m <sup>2</sup> /s)	Volumetric heat capacity x 10 <sup>6</sup> (J/m <sup>3</sup> K)	Thermal conductivity ( W/mK )	Diffusivity x 10 <sup>-6</sup> ( m <sup>2</sup> /s)	Volumetric heat capacity x 10 <sup>6</sup> (J/m <sup>3</sup> K)	Thermal conductivity ( W/mK )	Diffusivity x 10 <sup>-6</sup> ( m <sup>2</sup> /s)	Volumetric heat capacity x 10 <sup>6</sup> (J/m <sup>3</sup> K)	Thermal conductivity ( W/mK )	CALCULATE D Specific heat capacity x 10 <sup>-3</sup> (J/K.kg)
121	Gypsum	Kalavastos	0.59	1.96	1.15	0.76	1.71	1.31	---	---	---	0.68	1.84	1.23	0.72
122	Gypsum	Kalavastos	0.72	1.87	1.35	0.75	1.88	1.41	---	---	---	0.74	1.88	1.38	0.76
123	Calcarenite	Nicosia	1.04	1.64	1.71	0.98	1.78	1.73	---	---	---	1.01	1.71	1.72	0.70
124	Calcarenite	Nicosia	1.06	1.69	1.79	0.98	1.68	1.64	---	---	---	1.02	1.69	1.72	0.66
125	Calcarenite	Nicosia	0.68	1.55	1.06	0.75	1.45	1.09	---	---	---	0.72	1.50	1.08	0.65
126	Sandy Marl	Nicosia	0.36	1.48	0.54	0.37	1.49	0.55	0.39	1.49	0.58	0.37	1.49	0.56	0.89
127	Calcarenite	Pachna	0.66	1.72	1.14	0.69	1.74	1.21	---	---	---	0.68	1.73	1.18	0.78
128	Calcarenite	Pachna	0.60	1.75	1.04	0.60	1.70	1.02	---	---	---	0.60	1.73	1.03	0.74
129	Calcarenite	Pachna	0.98	1.66	1.62	0.75	1.85	1.38	0.88	1.45	1.29	0.87	1.65	1.43	0.75
130	Chalk	Pachna	0.43	1.61	0.69	0.43	1.61	0.70	---	---	---	0.43	1.61	0.69	0.89
131	Calcarenite	Nicosia (Athalassa Member)	---	---	0.45	---	---	0.38	---	---	0.45	---	---	0.42	---
132	Reef limestone	Pachna - Koronia Member	1.11	1.88	2.08	1.07	2.00	2.13	---	---	---	1.09	1.94	2.11	0.77
133	Diabase	Basal Group	1.18	1.98	2.35	1.17	1.94	2.28	---	---	---	1.18	1.96	2.32	0.72
134	Calcarenite	Terrace Deposits (Marine Terrace)	0.65	1.68	1.09	0.68	1.55	1.05	---	---	---	0.66	1.62	1.07	0.68
135	Calcarenite	Nicosia	0.79	1.38	1.09	0.77	1.37	1.06	---	---	---	0.78	1.38	1.08	0.55
136	Calcarenite	Aeolian Deposits	0.81	1.69	1.36	0.77	1.56	1.21	---	---	---	0.79	1.63	1.29	0.68
137	Calcarenite	Aeolian Deposits	0.57	1.46	0.83	0.43	1.42	0.61	0.42	1.40	0.60	0.47	1.43	0.68	0.60
138	Limestone	Lapatsa	0.99	1.61	1.59	---	---	---	---	---	---	0.99	1.61	1.59	0.58
139	Chalks	Lapatsa	1.42	1.37	1.95	1.25	1.52	1.89	---	---	---	1.34	1.45	1.92	0.69
140	Chalky Marls	Lapatsa	0.57	1.36	0.78	0.52	1.38	0.71	---	---	---	0.54	1.37	0.75	0.71
141	Sandstone	Kythrea Formation	0.38	1.38	0.53	0.40	1.38	0.55	---	---	---	0.39	1.38	0.54	0.77

No	Lithology	Formation	Diffusivity x 10 <sup>-6</sup> ( m <sup>2</sup> /s)	Volumetric heat capacity x 10 <sup>6</sup> (J/m <sup>3</sup> K)	Thermal conductivity ( W/mK )	Diffusivity x 10 <sup>-6</sup> ( m <sup>2</sup> /s)	Volumetric heat capacity x 10 <sup>6</sup> (J/m <sup>3</sup> K)	Thermal conductivity ( W/mK )	Diffusivity x 10 <sup>-6</sup> ( m <sup>2</sup> /s)	Volumetric heat capacity x 10 <sup>6</sup> (J/m <sup>3</sup> K)	Thermal conductivity ( W/mK )	Diffusivity x 10 <sup>-6</sup> ( m <sup>2</sup> /s)	Volumetric heat capacity x 10 <sup>6</sup> (J/m <sup>3</sup> K)	Thermal conductivity ( W/mK )	CALCULATE D Specific heat capacity x 10 <sup>-3</sup> (J/K kg)
142	Marls	Kythrea Formation	0.63	1.42	0.89	0.60	1.42	0.85	---	---	---	0.61	1.42	0.87	0.67
143	Marls	Kythrea Formation	0.53	1.51	0.79	0.51	1.51	0.77	---	---	---	0.52	1.51	0.78	0.69
144	soil and small gravel	Colluvium (Apalos Formation)	---	---	0.25	---	---	0.44	---	---	0.26	---	---	0.32	--
145	soil and small gravel	Alluvium	0.31	1.47	0.45	0.33	1.44	0.47	0.22	1.47	0.17	0.28	1.46	0.36	0.53
	large gravel	Alluvium	1.51	1.49	2.25	1.60	1.48	2.37	1.43	1.39	1.99	1.51	1.45	2.20	0.53
146	soil	Fanglomerate			0.14	---	---	0.09	---	---	---	---	---	0.11	
	large gravel	Fanglomerate	1.02	1.41	1.44	0.95	1.42	1.34			0.59	0.98	1.42	1.12	1.02
147	soil and small gravel	Fanglomerate			0.33	---	---	0.23	0.22	1.36	0.30	0.22	1.36	0.29	
	large gravel	Fanglomerate	0.87	1.38	1.20	---	---	0.99	---	---	---	0.87	1.38	1.10	
148	soil and small gravel	Alluvium	0.22	1.47	0.33	0.31	1.51	0.47	0.24	1.49	0.36	0.26	1.49	0.38	0.54
	large gravel	Alluvium	1.02	1.37	1.40	---	---	1.09				1.02	1.37	1.25	---

### III. Analytical laboratory results of water saturated samples

			Samples - Water Saturated Conditions									
			1st Measurement			2nd Measurement			MEAN VALUES			
No	Lithology	Formation	Diffusivity x 10 <sup>-6</sup> (m <sup>2</sup> /s)	Volumetric heat capacity x 10 <sup>6</sup> (J/m <sup>3</sup> K)	Thermal conductivity (W/mK)	Diffusivity x 10 <sup>-6</sup> (m <sup>2</sup> /s)	Volumetric heat capacity x 10 <sup>6</sup> (J/m <sup>3</sup> K)	Thermal conductivity (W/mK)	Diffusivity x 10 <sup>-6</sup> (m <sup>2</sup> /s)	Volumetric heat capacity x 10 <sup>6</sup> (J/m <sup>3</sup> K)	Thermal conductivity (W/mK)	CALCULATED Specific heat capacity x 10 <sup>-3</sup> (J/K kg)
1	Calcarenite	Nicosia	0.97	2.20	2.14	1.05	2.01	2.12	1.01	2.11	2.13	0.86
2	Chert	Lefkara	0.85	2.03	1.73	0.88	1.84	1.63	0.87	1.94	1.68	0.88
3	Calcarenite	Athalassa Member	0.98	1.37	1.34	1.13	1.41	1.59	1.05	1.39	1.47	0.62
4	Chert	Lefkara	0.79	2.06	1.63	0.78	1.97	1.55	0.79	2.02	1.59	0.92
5	Calcarenite	Nicosia	0.81	1.46	1.18	0.82	1.39	1.14	0.82	1.43	1.16	0.93
6	Sandy Marl	Nicosia	0.82	1.79	1.46	0.54	1.96	1.05	0.68	1.88	1.26	1.49
7	Calcarenite	Nicosia	---	---	0.86	---	---	0.89	---	---	0.88	---
8	Basalt	Lower Pillow Lavas	0.84	1.54	1.29	0.87	1.59	1.38	0.85	1.57	1.34	0.61
9	Chalk	Pachna	0.92	1.61	1.48	0.86	1.82	1.56	0.89	1.72	1.52	0.83
10	Volcanic Breccia	Lower Pillow Lavas	1.02	2.15	2.19	1.06	1.88	1.98	1.04	2.02	2.09	0.78



No	Lithology	Formation	Diffusivity x 10 <sup>-6</sup> (m <sup>2</sup> /s)	Volumetric heat capacity x 10 <sup>6</sup> (J/m <sup>3</sup> K)	Thermal conductivity (W/mK)	Diffusivity x 10 <sup>-6</sup> (m <sup>2</sup> /s)	Volumetric heat capacity x 10 <sup>6</sup> (J/m <sup>3</sup> K)	Thermal conductivity (W/mK)	Diffusivity x 10 <sup>-6</sup> (m <sup>2</sup> /s)	Volumetric heat capacity x 10 <sup>6</sup> (J/m <sup>3</sup> K)	Thermal conductivity (W/mK)	CALCULATED Specific heat capacity x 10 <sup>-3</sup> (J/K kg)
11	Chert	Lefkara	0.95	2.14	2.03	1.32	1.43	1.88	1.13	1.79	1.96	0.76
12	Marly Chalk	Pachna	0.83	2.03	1.68	0.82	2.00	1.65	0.83	2.02	1.67	0.93
13	Sandy Marl	Nicosia	0.80	1.59	1.27	---	---	---	0.80	1.59	1.27	0.98
14	Calcarenite	Terrace Deposits (Marine Terrace)	0.73	1.64	1.19	0.82	1.53	1.25	0.77	1.59	1.22	0.77
15	Reddish brown sandy clay with gravel	Terrace Deposits (Fluvial Deposits)	0.76	1.52	1.16	---	---	---	0.76	1.52	1.16	1.08
16	Reef Limestone	Pachna - Koronia Member	0.78	1.97	1.54	0.85	2.01	1.71	0.81	1.99	1.63	1.00
17	Brownish clayey Sand	Terrace Deposits (Marine Terrace)	0.71	2.09	1.49	0.72	2.10	1.49	0.71	2.10	1.49	1.23
18	Calcarenite	Terrace Deposits (Marine Terrace)	0.98	1.83	1.79	0.92	1.81	1.67	0.95	1.82	1.73	0.79
19	Reef Limestone	Pachna - Koronia Member	1.01	1.60	1.62	0.81	1.67	1.35	0.91	1.64	1.49	0.71
20	Microgabbro, Dykes	Lower Pillow Lavas	0.65	1.64	1.06	0.64	1.98	1.26	0.64	1.81	1.16	0.76
21	Fossiliferous sandy Marl	Marl Member	0.47	1.42	0.66	---	---	---	0.47	1.42	0.66	0.90
22	Gray sandy silt	Terrace Deposits (Fluvial Deposits)	0.63	1.65	1.04	---	---	---	0.63	1.65	1.04	1.11
23	Chalk	Pachna	0.74	2.05	1.51	0.72	2.07	1.49	0.73	2.06	1.50	1.04
24	Chalk	Pachna	0.78	2.14	1.67	0.82	1.96	1.60	0.80	2.05	1.64	0.95
25	Olivine-Phyric Basalt	Lower Pillow Lavas	0.69	1.87	1.30	0.63	1.81	1.13	0.66	1.84	1.22	0.85
26	Diabase	Lower Pillow Lavas	0.58	1.96	1.13	0.59	1.93	1.13	0.58	1.95	1.13	0.85
27	Microgabbro	Sheeted Dykes (Diabase)	1.21	1.94	2.35	0.92	1.93	1.77	1.06	1.94	2.06	0.73
28	Chert	Lefkara	0.87	2.11	1.84	0.93	1.96	1.83	0.90	2.04	1.84	0.89

No	Lithology	Formation	Diffusivity x 10 <sup>-6</sup> ( m <sup>2</sup> /s)	Volumetric heat capacity x 10 <sup>6</sup> (J/m <sup>3</sup> ·K)	Thermal conductivity ( W/m·K )	Diffusivity x 10 <sup>-6</sup> ( m <sup>2</sup> /s)	Volumetric heat capacity x 10 <sup>6</sup> (J/m <sup>3</sup> ·K)	Thermal conductivity ( W/m·K )	Diffusivity x 10 <sup>-6</sup> ( m <sup>2</sup> /s)	Volumetric heat capacity x 10 <sup>6</sup> (J/m <sup>3</sup> ·K)	Thermal conductivity ( W/m·K )	CALCULATED Specific heat capacity x 10 <sup>-3</sup> (J/K kg)
29	Silicified chalk	Lefkara	1.01	2.13	2.15	1.05	2.10	2.19	1.03	2.12	2.17	0.88
30	Calcarenite	Terrace Deposits (Marine Terrace)	0.84	2.11	1.78	0.94	1.98	1.86	0.89	2.05	1.82	0.86
31	Reef Limestone	Pachna - Terra Member	1.62	1.66	2.68	0.86	2.10	1.80	1.24	1.88	2.24	0.80
32	Marl	Nicosia	0.70	1.36	0.95	---	---	---	0.70	1.36	0.95	1.05
33	Brownish Clay with gravels	Terrace Deposits (Fluvial Deposits)	0.53	2.01	1.06	---	---	---	0.53	2.01	1.06	1.46
34	Grey Marl	Nicosia Marl Member										
35	Reef Limestone	Pachna - Terra Member	0.93	2.13	1.99	1.03	1.92	1.98	0.98	2.03	1.99	0.84
36	Marly Chalk	Pachna	0.80	2.10	1.68	0.84	2.01	1.69	0.82	2.06	1.69	0.92
37	Gabbro (weathered)	Gabbro	1.34	1.97	2.64	1.43	1.71	2.44	1.39	1.84	2.54	0.71
38	Serpentinited Harzburgite	Harzburgite	0.69	2.13	1.47	0.75	1.97	1.47	0.72	2.05	1.47	0.87
39	Fossiliferous Marl	Nicosia	0.78	1.52	1.18	---	---	---	0.78	1.52	1.18	1.32
40	Calcarenite	Aeolian Deposits	0.63	1.38	0.87	---	---	---	0.63	1.38	0.87	0.64
41	Fossiliferous Sandy Marl	Nicosia	0.77	1.52	1.16	---	---	---	0.77	1.52	1.16	0.93
42	Marly Chalk	Pachna	0.90	1.94	1.74	0.79	2.08	1.63	0.84	2.01	1.69	0.91
43	Marly Chalk	Pachna	1.06	2.18	2.31	1.02	2.07	2.11	1.04	2.13	2.21	0.87
44	Chalk	Pachna	0.89	1.95	1.74	0.82	2.03	1.67	0.86	1.99	1.71	0.93
45	Reef Limestone	Pachna - Terra Member	0.93	2.14	1.98	0.90	2.17	1.95	0.91	2.16	1.97	0.96
46	Gabbro	Gabbro	1.65	2.31	3.82	1.61	2.28	3.66	1.63	2.30	3.74	0.85

No	Lithology	Formation	Diffusivity x 10 <sup>-6</sup> (m <sup>2</sup> /s)	Volumetric heat capacity x 10 <sup>6</sup> (J/m <sup>3</sup> K)	Thermal conductivity (W/mK)	Diffusivity x 10 <sup>-6</sup> (m <sup>2</sup> /s)	Volumetric heat capacity x 10 <sup>6</sup> (J/m <sup>3</sup> K)	Thermal conductivity (W/mK)	Diffusivity x 10 <sup>-6</sup> (m <sup>2</sup> /s)	Volumetric heat capacity x 10 <sup>6</sup> (J/m <sup>3</sup> K)	Thermal conductivity (W/mK)	CALCULATED Specific heat capacity x 10 <sup>-3</sup> (J/K kg)
47	Reef Limestone Breccia		0.78	2.02	1.57	0.78	2.04	1.60	0.78	2.03	1.59	0.94
48	Chalk	Pachna	0.77	1.88	1.44	0.75	1.93	1.44	0.76	1.91	1.44	0.97
49	Olive phyric Basalt	Upper Pillow Lavas	0.58	1.91	1.10	0.61	1.98	1.22	0.59	1.95	1.16	0.83
50	Siltstone	Pachna	0.56	1.74	0.98	0.63	1.75	1.10	0.60	1.75	1.04	1.69
51	Serpentinite	Serpentinite	1.19	2.08	2.46	1.25	1.96	2.46	1.22	2.02	2.46	0.80
52	Chalk	Lefkara	0.61	1.90	1.16	0.67	1.72	1.15	0.64	1.81	1.16	0.95
53	Reef Limestone	Pachna - Terra Member	1.19	2.19	2.61	1.20	2.01	2.41	1.20	2.10	2.51	0.80
54	White chalk	Lefkara	0.65	1.86	1.21	0.64	1.83	1.18	0.65	1.85	1.20	1.03
55	Offwhite chalk	Pachna	0.69	2.08	1.44	0.70	1.95	1.38	0.70	2.02	1.41	1.04
56	Marble, Laminated Gypsum	Kalavastos	0.45	1.88	0.85	0.58	1.90	1.11	0.52	1.89	0.98	0.84
57	Diabase	Basal Group	1.36	2.18	2.96	1.28	2.37	3.03	1.32	2.28	3.00	0.84
58	Chert	Lefkara	0.91	1.78	1.61	0.87	1.98	1.72	0.89	1.88	1.67	0.86
59	basalt	Lower Pillow Lavas	0.67	1.92	1.29	0.68	1.91	1.30	0.68	1.92	1.30	0.79
60	Harzburgite	Harzburgite	0.94	2.08	1.96	0.91	2.02	1.83	0.93	2.05	1.90	0.80
61	White chalk	Lefkara	0.65	2.07	1.34	0.78	2.00	1.55	0.71	2.04	1.45	1.01
62	Diabase	Sheeted Dykes (Diabase)	0.97	2.23	2.16	0.97	2.22	2.17	0.97	2.23	2.17	0.81
63	Diabase	Sheeted Dykes (Diabase)	1.03	1.93	1.99	1.04	1.94	2.01	1.04	1.94	2.00	0.71
64	Sandy Marl	Nicosia (Athalassa Member)	0.57	1.58	0.90	0.61	1.51	0.93	0.59	1.55	0.91	1.06
65	Sandstone	Nicosia (Aspropamboulos Oolite Member)	0.63	1.78	1.13	0.72	1.81	1.31	0.68	1.80	1.22	1.17

No	Lithology	Formation	Diffusivity x 10 <sup>-6</sup> (m <sup>2</sup> /s)	Volumetric heat capacity x 10 <sup>6</sup> (J/m <sup>3</sup> K)	Thermal conductivity (W/mK)	Diffusivity x 10 <sup>-6</sup> (m <sup>2</sup> /s)	Volumetric heat capacity x 10 <sup>6</sup> (J/m <sup>3</sup> K)	Thermal conductivity (W/mK)	Diffusivity x 10 <sup>-6</sup> (m <sup>2</sup> /s)	Volumetric heat capacity x 10 <sup>6</sup> (J/m <sup>3</sup> K)	Thermal conductivity (W/mK)	CALCULATED Specific heat capacity x 10 <sup>-3</sup> (J/K kg)
66	Sandstone	Nicosia (Kephales Member)	0.82	2.15	1.77	1.28	1.65	2.11	1.05	1.90	1.94	0.81
67	Brown Silty Sand	Apalos - Athalassa - Kakkaristra (Apalos Formation)	0.67	1.61	1.08	0.60	1.77	1.06	0.64	1.69	1.07	
68	Sandstone	Nicosia (Lithic Sand Member with corals)	0.56	2.06	1.15	0.54	2.07	1.12	0.55	2.07	1.14	1.44
69	Sandstone	Nicosia (Kephales Member)	1.13	1.46	1.65	1.21	1.38	1.68	1.17	1.42	1.67	0.57
70	Lithic sand	Nicosia (Aspropamboulos Oolite Member)	0.59	1.68	0.99	0.50	1.98	1.00	0.55	1.83	0.99	1.16
71	Marly Sandstone	Nicosia (Athalassa Member)	0.88	2.11	1.87	0.86	2.07	1.79	0.87	2.09	1.83	0.84
72	Calcarenite	Nicosia (Athalassa Member)	0.84	1.57	1.31	0.89	1.43	1.27	0.86	1.50	1.29	0.75
73	Yellowish silty sand	Apalos - Athalassa - Kakkaristra (Apalos Formation)	0.43	1.45	0.62	0.53	1.78	0.95	0.48	1.62	0.78	1.00
74	Reddish silty sand	Apalos - Athalassa - Kakkaristra (Apalos Formation)	0.53	1.99	1.05	---	---	---	0.53	1.99	1.05	1.25
75	Calcarenite	Pachna	0.89	1.86	1.66	0.82	1.84	1.51	0.86	1.85	1.59	0.83
76	Marly Chalk	Pachna	0.93	2.01	1.86	0.90	2.04	1.84	0.91	2.03	1.85	0.86
77	Marly Chalk	Pachna	0.98	2.01	1.96	0.92	2.14	1.96	0.95	2.08	1.96	0.85
78	Chalk	Pachna	1.03	1.36	1.41	0.95	1.83	1.73	0.99	1.60	1.57	0.69
79	Marly Chalk	Pachna	0.79	2.11	1.66	0.77	2.11	1.63	0.78	2.11	1.65	0.94
80	Chalk	Pachna	1.12	2.23	2.49	1.06	2.14	2.27	1.09	2.19	2.38	0.88
81	Limestone	Pachna - Terra Member	1.35	2.01	2.71	1.10	2.15	2.38	1.23	2.08	2.55	0.81
82	Chalk	Pachna	0.92	2.20	2.01	0.95	2.20	2.09	0.93	2.20	2.05	0.91

No	Lithology	Formation	Diffusivity x 10 <sup>-6</sup> (m <sup>2</sup> /s)	Volumetric heat capacity x 10 <sup>6</sup> (J/m <sup>3</sup> K)	Thermal conductivity (W/mK)	Diffusivity x 10 <sup>-6</sup> (m <sup>2</sup> /s)	Volumetric heat capacity x 10 <sup>6</sup> (J/m <sup>3</sup> K)	Thermal conductivity (W/mK)	Diffusivity x 10 <sup>-6</sup> (m <sup>2</sup> /s)	Volumetric heat capacity x 10 <sup>6</sup> (J/m <sup>3</sup> K)	Thermal conductivity (W/mK)	CALCULATED Specific heat capacity x 10 <sup>-3</sup> (J/K kg)
83	Chalk	Lefkara	0.98	2.00	1.96	1.00	1.84	1.84	0.99	1.92	1.90	0.84
84	Reef Limestone	Pachna - Terra Member	1.37	1.54	2.11	1.20	1.64	1.97	1.29	1.59	2.04	0.64
85	Gypsum	Kalavastos	0.46	1.84	0.84	0.49	1.66	0.82	0.47	1.75	0.83	0.77
86	Volcanioclastic Sandstone	Kannaviou	0.63	1.73	1.09	0.59	1.85	1.09	0.61	1.79	1.09	0.91
87	Gabbro	Gabbro	0.96	2.18	2.10	1.06	2.15	2.29	1.01	2.17	2.20	0.76
88	Serpentinite	Serpentinite	0.98	2.13	2.08	1.06	2.09	2.22	1.02	2.11	2.15	0.89
89	Plagiogranite	Plagiogranite	1.58	2.33	3.69	1.49	2.36	3.51	1.54	2.35	3.60	0.86
90	Chert	Lefkara	0.98	1.98	1.94	0.94	2.07	1.94	0.96	2.03	1.94	0.87
91	Chalk	Lefkara	0.99	1.99	1.97	0.95	2.13	2.02	0.97	2.06	2.00	0.86
92	Massive Chalk	Lefkara	1.01	1.68	1.69	0.97	1.76	1.70	0.99	1.72	1.70	0.77
93	Diabase	Sheeted Dykes (Diabase)	0.85	2.12	1.81	0.86	2.04	1.75	0.86	2.08	1.78	0.76
94	Diabase	Basal Group	0.78	1.98	1.55	0.78	2.00	1.56	0.78	1.99	1.56	0.79
95	Microgabbro	Sheeted Dykes (Diabase)	0.95	2.08	1.97	0.97	2.10	2.03	0.96	2.09	2.00	0.70
96	Diabase	Sheeted Dykes (Diabase)	1.05	2.22	2.33	1.14	2.08	2.37	1.10	2.15	2.35	0.76
97	Diabase	Sheeted Dykes (Diabase)	1.04	1.97	2.06	0.81	2.14	1.74	0.93	2.06	1.90	0.78
98	Basalt	Lower Pillow Lavas	0.77	1.91	1.47	0.82	1.80	1.48	0.80	1.86	1.48	0.77
99	Reef Limestone	Pachna - Koronia Member	0.92	1.69	1.56	0.96	1.75	1.67	0.94	1.72	1.62	0.76
100	Calcarenite	Nicosia	1.01	1.42	1.43	0.97	1.71	1.67	0.99	1.57	1.55	0.78
101	Reef Limestone	Pachna - Koronia Member	0.95	2.03	1.93	0.94	2.03	1.90	0.94	2.03	1.92	0.87
102	Chalk	Lefkara	0.74	2.01	1.48	0.72	2.07	1.48	0.73	2.04	1.48	1.00
103	Basalt	Upper Pillow Lavas	0.68	2.02	1.38	0.69	2.02	1.40	0.69	2.02	1.39	0.87

No	Lithology	Formation	Diffusivity x 10 <sup>-6</sup> ( m <sup>2</sup> /s)	Volumetric heat capacity x 10 <sup>6</sup> ( J/m <sup>3</sup> ·K)	Thermal conductivity ( W/m·K )	Diffusivity x 10 <sup>-6</sup> ( m <sup>2</sup> /s)	Volumetric heat capacity x 10 <sup>6</sup> ( J/m <sup>3</sup> ·K)	Thermal conductivity ( W/m·K )	Diffusivity x 10 <sup>-6</sup> ( m <sup>2</sup> /s)	Volumetric heat capacity x 10 <sup>6</sup> ( J/m <sup>3</sup> ·K)	Thermal conductivity ( W/m·K )	CALCULATED Specific heat capacity x 10 <sup>-3</sup> ( J/K kg)
104	Chalk	Pachna	0.80	2.00	1.61	0.77	2.08	1.60	0.79	2.04	1.61	0.96
105	Dunite	Dunite	1.24	1.98	2.46	1.12	1.96	2.20	1.18	1.97	2.33	0.75
106	Wehrlite	Wehrlite	1.23	2.28	2.80	1.21	2.23	2.69	1.22	2.26	2.75	0.83
107	Pyroxenite	Pyroxenite	1.74	2.51	4.36	2.07	2.27	4.69	1.91	2.39	4.53	0.76
108	Harzburgite	Harzburgite	0.78	1.98	1.97	0.78	2.00	1.91	0.78	1.99	1.94	0.75
109	Poikilitic wehrlite	Wehrlite	1.27	2.30	2.91	1.44	2.17	3.11	1.36	2.24	3.01	0.81
110	Microgabbro	Basal Group	0.94	2.13	2.00	1.01	1.85	1.87	0.97	1.99	1.94	0.75
111	Gypsum	Kalavastos	0.66	1.62	1.08	0.68	1.73	1.17	0.67	1.68	1.13	0.76
112	Chalky Marl	Pachna	0.46	1.89	0.87	0.71	1.45	1.03	0.59	1.67	0.95	1.01
113	Calcarenite	Pachna	0.97	2.02	1.96	0.76	2.07	1.57	0.87	2.05	1.77	0.96
114	Chalk	Pachna	1.12	2.19	2.45	1.13	2.01	2.29	1.13	2.10	2.37	0.84
115	Breccia Reef Limestone	Terrace Deposits (Fluvial Deposits)	0.74	2.13	1.57	0.70	2.11	1.48	0.72	2.12	1.53	1.01
116	Gypsum	Kalavastos	0.63	1.69	1.07	0.67	1.58	1.06	0.65	1.64	1.07	0.72
117	Reef Limestone	Pachna - Koronia Member	0.58	2.04	1.18	0.69	1.67	1.16	0.64	1.86	1.17	0.74
118	Reef Limestone	Pachna - Koronia Member	0.93	1.80	1.67	0.77	1.96	1.51	0.85	1.88	1.59	0.76
119	Chalk	Pachna	0.92	2.22	2.05	1.00	2.16	2.17	0.96	2.19	2.11	0.89
120	Calcarenite	Pachna	0.92	2.04	1.88	1.01	2.00	2.03	0.97	2.02	1.96	0.85
121	Gypsum	Kalavastos	0.55	1.56	0.86	0.52	1.57	0.82	0.54	1.57	0.84	0.70
122	Gypsum	Kalavastos	0.33	1.90	0.63	0.34	1.90	0.64	0.33	1.90	0.63	0.83
123	Calcarenite	Nicosia	0.97	1.88	1.82	1.00	1.83	1.83	0.98	1.86	1.83	0.80
124	Calcarenite	Nicosia	1.06	1.92	2.03	1.09	1.91	2.08	1.08	1.92	2.06	0.80

No	Lithology	Formation	Diffusivity x 10 <sup>-6</sup> (m <sup>2</sup> /s)	Volumetric heat capacity x 10 <sup>6</sup> (J/m <sup>3</sup> K)	Thermal conductivity (W/mK)	Diffusivity x 10 <sup>-6</sup> (m <sup>2</sup> /s)	Volumetric heat capacity x 10 <sup>6</sup> (J/m <sup>3</sup> K)	Thermal conductivity (W/mK)	Diffusivity x 10 <sup>-6</sup> (m <sup>2</sup> /s)	Volumetric heat capacity x 10 <sup>6</sup> (J/m <sup>3</sup> K)	Thermal conductivity (W/mK)	CALCULATED Specific heat capacity x 10 <sup>-3</sup> (J/K kg)
125	Calcarenite	Nicosia	0.72	1.89	1.36	0.72	1.98	1.42	0.72	1.94	1.39	0.94
126	Sandy Marl	Nicosia	0.55	1.55	0.85	0.57	1.60	0.91	0.56	1.58	0.88	0.95
127	Calcarenite	Pachna	0.71	1.99	1.42	0.73	2.01	1.48	0.72	2.00	1.45	0.96
128	Calcarenite	Pachna	0.67	2.00	1.34	0.71	1.85	1.32	0.69	1.93	1.33	0.92
129	Calcarenite	Pachna	0.77	1.88	1.45	0.76	2.01	1.53	0.77	1.95	1.49	0.92
130	Chalk	Pachna	0.67	1.95	1.30	0.51	2.03	1.04	0.59	1.99	1.17	1.23
131	Calcarenite	Nicosia (Athalassa Member)	0.70	1.46	1.02	0.63	1.65	1.04	0.67	1.56	1.03	0.91
132	Reef limestone	Pachna - Koronia Member	1.04	2.12	2.21	1.00	2.14	2.15	1.02	2.13	2.18	0.86
133	Diabase	Basal Group	1.22	1.62	1.97	1.09	2.26	2.45	1.16	1.94	2.21	0.72
134	Calcarenite	Terrace Deposits (Marine Terrace)	0.77	1.95	1.50	0.70	1.86	1.29	0.73	1.91	1.40	0.92
135	Calcarenite	Nicosia	1.04	1.58	1.64	0.98	1.47	1.45	1.01	1.53	1.55	0.66
136	Calcarenite	Aeolian Deposits	0.88	1.84	1.62	0.85	1.81	1.54	0.86	1.83	1.58	0.86
137	Calcarenite	Aeolian Deposits	0.72	1.70	1.23	0.75	1.84	1.37	0.73	1.77	1.30	0.92
138	Limestone	Lapatsa	---	---	---	---	---	---	---	---	---	---
139	Chalks	Lapatsa	---	---	---	---	---	---	---	---	---	---
140	Chalky Marls	Lapatsa	---	---	---	---	---	---	---	---	---	---
141	Sandstone	Kythrea Formation	---	---	---	---	---	---	---	---	---	---
142	Marls	Kythrea Formation	---	---	---	---	---	---	---	---	---	---
143	Marls	Kythrea Formation	---	---	---	---	---	---	---	---	---	---
144	soil and small gravel	Colluvium (Apalos Formation)	0.53	1.77	0.93	0.59	1.45	0.85	0.57	1.63	0.93	0.56
145	soil and small gravel	Alluvium	0.62	1.99	1.24	0.70	2.13	1.49	0.66	2.01	1.33	0.66

No	Lithology	Formation	Diffusivity x 10 <sup>-6</sup> ( m <sup>2</sup> /s)	Volumetric heat capacity x 10 <sup>6</sup> (J/m <sup>3</sup> K)	Thermal conductivity ( W/mK )	Diffusivity x 10 <sup>-6</sup> ( m <sup>2</sup> /s)	Volumetric heat capacity x 10 <sup>6</sup> (J/m <sup>3</sup> K)	Thermal conductivity ( W/mK )	Diffusivity x 10 <sup>-6</sup> ( m <sup>2</sup> /s)	Volumetric heat capacity x 10 <sup>6</sup> (J/m <sup>3</sup> K)	Thermal conductivity ( W/mK )	CALCULATED Specific heat capacity x 10 <sup>-3</sup> (J/K kg)
145	large gravel	Alluvium	1.29	1.55	2.00	1.28	1.41	1.82	1.37	1.54	2.11	1.31
146	soil	Fanglomerate	---	---	0.66	---	---	0.53	---	---	---	---
146	large gravel	Fanglomerate	---	---	0.94	0.93	1.63	1.52	---	---	---	0.93
147	soil and small gravel	Fanglomerate	0.66	1.87	1.24	0.58	2.03	1.18	---	---	0.96	0.62
147	large gravel	Fanglomerate	0.87	1.44	1.25	---	---	---	---	---	---	0.87
148	soil and small gravel	Alluvium	0.60	2.03	1.22	0.59	1.95	1.15	0.43	2.01	0.86	0.54
148	large gravel	Alluvium	1.64	1.40	2.29	1.53	1.42	2.16	1.59	1.41	2.23	1.59



**IV. Analytical laboratory results of density on dry and water saturated samples**

			Density							
			1st Method (CYS EN 13383 - 2:2011)				2rd Method ( Displacement Method )			
No	Lithology	Formation	Dry Density ( Mg/m <sup>3</sup> )	Water Saturated Density ( Mg/m <sup>3</sup> )	Bulk Density ( Mg/m <sup>3</sup> )	Absorption ( % )	Dry Density ( Mg/m <sup>3</sup> )	Bulk Density ( Mg/m <sup>3</sup> )	Water Saturated Density ( Mg/m <sup>3</sup> )	Moisture ( % )
1	Calcarenite	Nicosia	2.4	2.46	2.56	2.57	---	---	---	---
2	Chert	Lefkara	2.09	2.2	2.34	5.26	---	---	---	---
3	Calcarenite	Athalassa Member	2.13	2.26	2.45	6.25	---	---	---	---
4	Chert	Lefkara	2.08	2.18	2.32	5.08	---	---	---	---
5	Calcarenite	Nicosia	---	---	---	---	1.52	1.53	1.54	0.91
6	Sandy Marl	Nicosia	---	---	---	---	1.23	1.26	1.26	2.22
7	Calcarenite	Nicosia	1.44	1.74	2.05	20.58	---	---	---	---
8	Basalt	Lower Pillow Lavas	2.46	2.55	2.71	3.70	---	---	---	---
9	Chalk	Pachna	1.86	2.06	2.34	11.17	---	---	---	---
10	Volcanic Breccia	Lower Pillow Lavas	2.56	2.60	2.66	1.52	---	---	---	---
11	Chert	Lefkara	2.27	2.34	2.45	3.16	---	---	---	---
12	Marly Chalk	Pachna	1.89	2.17	2.61	14.46	---	---	---	---
13	Sandy Marl	Nicosia	---	---	---	---	1.57	1.67	1.63	3.83
14	Calcarenite	Terrace Deposits (Marine Terrace)	1.82	2.05	2.36	12.47	---	---	---	---

No	Lithology	Formation	Dry Density ( Mg/m <sup>3</sup> )	Water Saturated Density ( Mg/m <sup>3</sup> )	Bulk Density ( Mg/m <sup>3</sup> )	Absorption ( % )	Dry Density ( Mg/m <sup>3</sup> )	Bulk Density ( Mg/m <sup>3</sup> )	Water Saturated Density ( Mg/m <sup>3</sup> )	Moisture ( % )
15	Reddish brown sandy clay with gravel	Terrace Deposits (Fluvial Deposits)	---	---	---	---	1.36	1.43	1.41	3.61
16	Reef Limestone	Pachna - Koronia Member	1.77	1.99	2.28	12.66	---	---	---	---
17	Brownish clayey Sand	Terrace Deposits (Marine Terrace)	---	---	---	---	1.71	1.71	1.71	0.19
18	Calcarenite	Terrace Deposits (Marine Terrace)	2.13	2.29	2.53	7.49	---	---	---	---
19	Reef Limestone	Pachna - Koronia Member	2.09	2.30	2.63	9.70	---	---	---	---
20	Microgabbro, Dykes	Lower Pillow Lavas	2.28	2.38	2.53	4.46	---	---	---	---
21	Fossiliferous sandy Marl	Marl Member	---	---	---	---	1.51	1.61	1.57	4.00
22	Gray sandy silt	Terrace Deposits (Fluvial Deposits)	---	---	---	---	1.47	1.50	1.49	1.10
23	Chalk	Pachna	1.77	1.99	2.28	12.66	---	---	---	---
24	Chalk	Pachna	1.86	2.15	2.63	15.69	---	---	---	---
25	Olivine-Phyric Basalt	Lower Pillow Lavas	1.91	2.16	2.53	12.76	---	---	---	---
26	Diabase	Lower Pillow Lavas	2.15	2.30	2.53	6.88	---	---	---	---
27	Microgabbro	Sheeted Dykes (Diabase)	2.62	2.64	2.68	0.89	---	---	---	---
28	Chert	Lefkara	2.15	2.29	2.51	6.82	---	---	---	---
29	Silicified chalk	Lefkara	2.25	2.41	2.66	6.76	---	---	---	---
30	Calcarenite	Terrace Deposits (Marine Terrace)	2.27	2.39	2.59	5.40	---	---	---	---
31	Reef Limestone	Pachna - Terra Member	2.23	2.36	2.58	6.17	---	---	---	---
32	Marl	Nicosia	---	---	---	---	1.15	1.34	1.29	12.54
33	Brownish Clay with gravels	Terrace Deposits (Fluvial Deposits)	---	---	---	---	1.27	1.43	1.38	8.89

No	Lithology	Formation	Dry Density (Mg/m <sup>3</sup> )	Water Saturated Density (Mg/m <sup>3</sup> )	Bulk Density (Mg/m <sup>3</sup> )	Absorption (%)	Dry Density (Mg/m <sup>3</sup> )	Bulk Density (Mg/m <sup>3</sup> )	Water Saturated Density (Mg/m <sup>3</sup> )	Moisture (%)
34	Grey Marl	Nicosia Marl Member	---	---	---	---	---	---	---	2.27
35	Reef Limestone	Pachna - Terra Member	2.35	2.42	2.55	3.35	---	---	---	---
36	Marly Chalk	Pachna	2.06	2.23	2.49	8.48	---	---	---	---
37	Gabbro (weathered)	Gabbro	2.49	2.59	2.77	3.99	---	---	---	---
38	Serpentinited Harzburgite	Harzburgite	2.23	2.36	2.55	5.60	---	---	---	---
39	Fossiliferous Marl	Nicosia	---	---	---	---	1.03	1.17	1.15	11.60
40	Calcarenite	Aeolian Deposits	---	---	---	---	2.15	2.17	2.16	0.48
41	Fossiliferous Sandy Marl	Nicosia	---	---	---	---	1.58	1.67	1.63	3.43
42	Marly Chalk	Pachna	2.01	2.21	2.52	9.94	---	---	---	---
43	Marly Chalk	Pachna	2.33	2.45	2.65	5.15	---	---	---	---
44	Chalk	Pachna	1.89	2.13	2.50	12.84	---	---	---	---
45	Reef Limestone	Pachna - Terra Member	2.08	2.24	2.48	7.78	---	---	---	---
46	Gabbro	Gabbro	2.63	2.69	2.81	2.41	---	---	---	---
47	Reef Limestone Breccia		1.90	2.15	2.52	12.92	---	---	---	---
48	Chalk	Pachna	1.73	1.96	2.23	13.07	---	---	---	---
49	Olive phyric Basalt	Upper Pillow Lavas	2.27	2.35	2.46	3.44	---	---	---	---
50	Siltstone	Pachna	---	---	---	---	0.89	1.03	1.03	14.92
51	Serpentinite	Serpentinite	2.46	2.51	2.58	1.87	---	---	---	---
52	Chalk	Lefkara	1.53	1.90	2.41	23.76	---	---	---	---
53	Reef Limestone	Pachna - Terra Member	2.59	2.63	2.69	1.44	---	---	---	---
54	White chalk	Lefkara	1.44	1.80	2.27	25.50	---	---	---	---
55	Offwhite chalk	Pachna	1.73	1.94	2.19	12.14	---	---	---	---

No	Lithology	Formation	Dry Density ( Mg/m <sup>3</sup> )	Water Saturated Density ( Mg/m <sup>3</sup> )	Bulk Density ( Mg/m <sup>3</sup> )	Absorption ( % )	Dry Density ( Mg/m <sup>3</sup> )	Bulk Density ( Mg/m <sup>3</sup> )	Water Saturated Density ( Mg/m <sup>3</sup> )	Moisture ( % )
56	Marble, Laminated Gypsum	Kalavastos	2.08	2.25	2.51	8.32	---	---	---	---
57	Diabase	Basal Group	2.69	2.71	2.74	0.64	---	---	---	---
58	Chert	Lefkara	2.07	2.19	2.36	6.09	---	---	---	---
59	basalt	Lower Pillow Lavas	2.23	2.41	2.71	7.95	---	---	---	---
60	Harzburgite	Harzburgite	2.51	2.55	2.61	1.45	---	---	---	---
61	White chalk	Lefkara	1.77	2.01	2.32	13.28	---	---	---	---
62	Diabase	Sheeted Dykes (Diabase)	2.72	2.74	2.76	0.58	---	---	---	---
63	Diabase	Sheeted Dykes (Diabase)	2.71	2.73	2.76	0.57	---	---	---	---
64	Sandy Marl	Nicosia (Athalassa Member)	---	---	---	---	1.41	1.48	1.46	3.61
65	Sandstone	Nicosia (Aspropamboulos Oolite Member)	---	---	---	---	1.48	1.55	1.53	3.01
66	Sandstone	Nicosia (Kephales Member)	2.19	2.34	2.59	6.99	---	---	---	---
67	Brown Silty Sand	Apalos - Athalassa - Kakkaristra (Apalos Formation)	---	---	---	---	---	---	---	---
68	Sandstone	Nicosia (Lithic Sand Member with corals)	---	---	---	---	1.37	1.46	1.43	4.36
69	Sandstone	Nicosia (Kephales Member)	2.36	2.48	2.68	5.12	---	---	---	---
70	Lithic sand	Nicosia (Aspropamboulos Oolite Member)	---	---	---	---	1.49	1.64	1.58	6.30
71	Marly Sandstone	Nicosia (Athalassa Member)	2.38	2.49	2.67	4.50	---	---	---	---
72	Calcarenite	Nicosia (Athalassa Member)	1.75	2.01	2.35	14.52	---	---	---	---

No	Lithology	Formation	Dry Density (Mg/m <sup>3</sup> )	Water Saturated Density (Mg/m <sup>3</sup> )	Bulk Density (Mg/m <sup>3</sup> )	Absorption (%)	Dry Density (Mg/m <sup>3</sup> )	Bulk Density (Mg/m <sup>3</sup> )	Water Saturated Density (Mg/m <sup>3</sup> )	Moisture (%)
73	Yellowish silty sand	Apalos - Athalassa - Kakkaristra (Apalos Formation)	---	---	---	---	1.52	1.68	1.62	6.31
74	Reddish silty sand	Apalos - Athalassa - Kakkaristra (Apalos Formation)	---	---	---	---	1.48	1.66	1.59	7.38
75	Calcarenite	Pachna	2.04	2.23	2.52	9.43	---	---	---	---
76	Marly Chalk	Pachna	2.19	2.35	2.62	7.53	---	---	---	---
77	Marly Chalk	Pachna	2.32	2.45	2.67	5.71	---	---	---	---
78	Chalk	Pachna	2.09	2.30	2.63	9.74	---	---	---	---
79	Marly Chalk	Pachna	2.00	2.24	2.64	12.13	---	---	---	---
80	Chalk	Pachna	2.38	2.47	2.60	3.45	---	---	---	---
81	Limestone	Pachna - Terra Member	2.53	2.57	2.63	1.47	---	---	---	---
82	Chalk	Pachna	2.26	2.41	2.67	6.80	---	---	---	---
83	Chalk	Lefkara	2.06	2.28	2.64	10.61	---	---	---	---
84	Reef Limestone	Pachna - Terra Member	2.37	2.49	2.67	4.67	---	---	---	---
85	Gypsum	Kalavastos	2.06	2.26	2.57	9.69	---	---	---	---
86	Volcanioclastic Sandstone	Kannaviou	1.58	1.96	2.55	24.05	---	---	---	---
87	Gabbro	Gabbro	2.82	2.84	2.87	0.70	---	---	---	---
88	Serpentinite	Serpentinite	2.19	2.36	2.65	7.92	---	---	---	---
89	Plagiogranite	Plagiogranite	2.71	2.73	2.76	0.74	---	---	---	---
90	Chert	Lefkara	2.23	2.33	2.48	4.61	---	---	---	---
91	Chalk	Lefkara	2.25	2.40	2.64	6.66	---	---	---	---
92	Massive Chalk	Lefkara	2.01	2.22	2.55	10.50	---	---	---	---
93	Diabase	Sheeted Dykes (Diabase)	2.73	2.75	2.80	0.95	---	---	---	---
94	Diabase	Basal Group	2.48	2.52	2.57	1.41	---	---	---	---

No	Lithology	Formation	Dry Density (Mg/m <sup>3</sup> )	Water Saturated Density (Mg/m <sup>3</sup> )	Bulk Density (Mg/m <sup>3</sup> )	Absorption (%)	Dry Density (Mg/m <sup>3</sup> )	Bulk Density (Mg/m <sup>3</sup> )	Water Saturated Density (Mg/m <sup>3</sup> )	Moisture (%)
95	Microgabbro	Sheeted Dykes (Diabase)	2.96	2.97	2.99	0.28	---	---	---	---
96	Diabase	Sheeted Dykes (Diabase)	2.82	2.83	2.85	0.41	---	---	---	---
97	Diabase	Sheeted Dykes (Diabase)	2.60	2.63	2.68	1.15	---	---	---	---
98	Basalt	Lower Pillow Lavas	2.33	2.42	2.55	3.69	---	---	---	---
99	Reef Limestone	Pachna - Koronia Member	2.08	2.26	2.55	8.85	---	---	---	---
100	Calcarenite	Nicosia	1.82	2.01	2.24	10.18	---	---	---	---
101	Reef Limestone	Pachna - Koronia Member	2.24	2.34	2.49	4.54	---	---	---	---
102	Chalk	Lefkara	1.69	2.03	2.54	19.80	---	---	---	---
103	Basalt	Upper Pillow Lavas	2.13	2.31	2.62	8.79	---	---	---	---
104	Chalk	Pachna	1.91	2.12	2.42	11.00	---	---	---	---
105	Dunite	Dunite	2.62	2.63	2.66	0.54	---	---	---	---
106	Wehrlite	Wehrlite	2.70	2.72	2.74	0.47	---	---	---	---
107	Pyroxenite	Pyroxenite	3.11	3.13	3.19	0.79	---	---	---	---
108	Harzburgite	Harzburgite	2.63	2.65	2.68	0.59	---	---	---	---
109	Poikilitic wehrlite	Wehrlite	2.75	2.76	2.77	0.33	---	---	---	---
110	Microgabbro	Basal Group	2.60	2.64	2.71	1.51	---	---	---	---
111	Gypsum	Kalavastos	2.03	2.21	2.49	9.18	---	---	---	---
112	Chalky Marl	Pachna	---	---	---	---	1.55	1.72	1.65	6.35
113	Calcarenite	Pachna	1.99	2.13	2.33	7.44	---	---	---	---
114	Chalk	Pachna	2.42	2.49	2.59	2.60	---	---	---	---
115	Breccia Reef Limestone	Terrace Deposits (Fluvial Deposits)	1.79	2.09	2.57	17.03	---	---	---	---
116	Gypsum	Kalavastos	2.06	2.27	2.61	10.20	---	---	---	---
117	Reef Limestone	Pachna - Koronia Member	2.35	2.52	2.83	7.28	---	---	---	---

No	Lithology	Formation	Dry Density (Mg/m <sup>3</sup> )	Water Saturated Density (Mg/m <sup>3</sup> )	Bulk Density (Mg/m <sup>3</sup> )	Absorption (%)	Dry Density (Mg/m <sup>3</sup> )	Bulk Density (Mg/m <sup>3</sup> )	Water Saturated Density (Mg/m <sup>3</sup> )	Moisture (%)
118	Reef Limestone	Pachna - Koronia Member	2.37	2.46	2.62	4.09	---	---	---	---
119	Chalk	Pachna	2.33	2.45	2.66	5.41	---	---	---	---
120	Calcarenite	Pachna	2.27	2.38	2.54	4.69	---	---	---	---
121	Gypsum	Kalavastos	2.04	2.24	2.54	9.74	---	---	---	---
122	Gypsum	Kalavastos	2.17	2.29	2.46	5.51	---	---	---	---
123	Calcarenite	Nicosia	2.24	2.32	2.44	3.62	---	---	---	---
124	Calcarenite	Nicosia	2.27	2.39	2.57	5.12	---	---	---	---
125	Calcarenite	Nicosia	1.87	2.06	2.32	10.44	---	---	---	---
126	Sandy Marl	Nicosia	---	---	---	---	1.61	1.67	1.65	2.51
127	Calcarenite	Pachna	1.97	2.09	2.23	5.98	---	---	---	---
128	Calcarenite	Pachna	1.93	2.10	2.33	9.05	---	---	---	---
129	Calcarenite	Pachna	2.05	2.12	2.21	3.51	---	---	---	---
130	Chalk	Pachna	1.39	1.62	1.80	16.59	---	---	---	---
131	Calcarenite	Nicosia (Athalassa Member)	1.40	1.70	2.01	21.56	---	---	---	---
132	Reef limestone	Pachna - Koronia Member	2.46	2.48	2.52	1.00	---	---	---	---
133	Diabase	Basal Group	2.66	2.68	2.71	0.67	---	---	---	---
134	Calcarenite	Terrace Deposits (Marine Terrace)	1.86	2.07	2.37	11.63	---	---	---	---
135	Calcarenite	Nicosia	2.20	2.32	2.50	5.48	---	---	---	---
136	Calcarenite	Aeolian Deposits	1.93	2.13	2.40	10.08	---	---	---	---
137	Calcarenite	Aeolian Deposits	1.60	1.93	2.37	20.20	---	---	---	---
138	Limestone	Lapatsa	---	---	---	---	---	---	---	2.75
139	Chalks	Lapatsa	---	---	---	---	---	---	---	2.01
140	Chalky Marls	Lapatsa	---	---	---	---	---	---	---	1.93

No	Lithology	Formation	Dry Density ( Mg/m <sup>3</sup> )	Water Saturated Density ( Mg/m <sup>3</sup> )	Bulk Density ( Mg/m <sup>3</sup> )	Absorption ( % )	Dry Density ( Mg/m <sup>3</sup> )	Bulk Density ( Mg/m <sup>3</sup> )	Water Saturated Density ( Mg/m <sup>3</sup> )	Moisture ( % )
141	Sandstone	Kythrea Formation	---	---	---	---	---	---	---	1.79
142	Marls	Kythrea Formation	---	---	---	---	---	---	---	2.12
143	Marls	Kythrea Formation	---	---	---	---	---	---	---	2.18
144	soil and small gravel	Colluvium (Apalos Formation)	Density is not possible to be calculated as the samples are not homogeneous but are compose of different materials in different stages and lithologies (soil and gravels)							
145	soil and small gravel	Alluvium								
145	large gravel	Alluvium								
146	soil	Fanglomerate								
146	large gravel	Fanglomerate								
147	soil and small gravel	Fanglomerate								
147	large gravel	Fanglomerate								
148	soil and small gravel	Alluvium								
148	large gravel	Alluvium								



## **APPENDIX III**

## Sample Catalog Gallery



A sample catalog was created in order to help engineers to identify their geological samples. Here it should be highlighted that this is not an effort to overtake geologists, or their important role at geothermal projects.

Sample catalog includes samples photo collection and matches (a) the geological formation/stratigraphic unit of each sample with (b) the lithology, (c) its image and (d) its thermal properties. In more detail, for each sample, next to the main photo are located two smaller photos showing in more detail the sample's grains and structure. The first one illustrates the surface of the sample as it was found in nature and the second one the surface created after cutting and lapping process. Photos, in some cases, present lines which have nothing to do with the structure of the sample and were created at cutting process. Finally, a table shows the mean value for each thermophysical property of all actual measurements taken on the sample, under dry and 100% saturated conditions. On the background we can see a scale bar and a color code wheel, so as to match the colors presented on the sample.

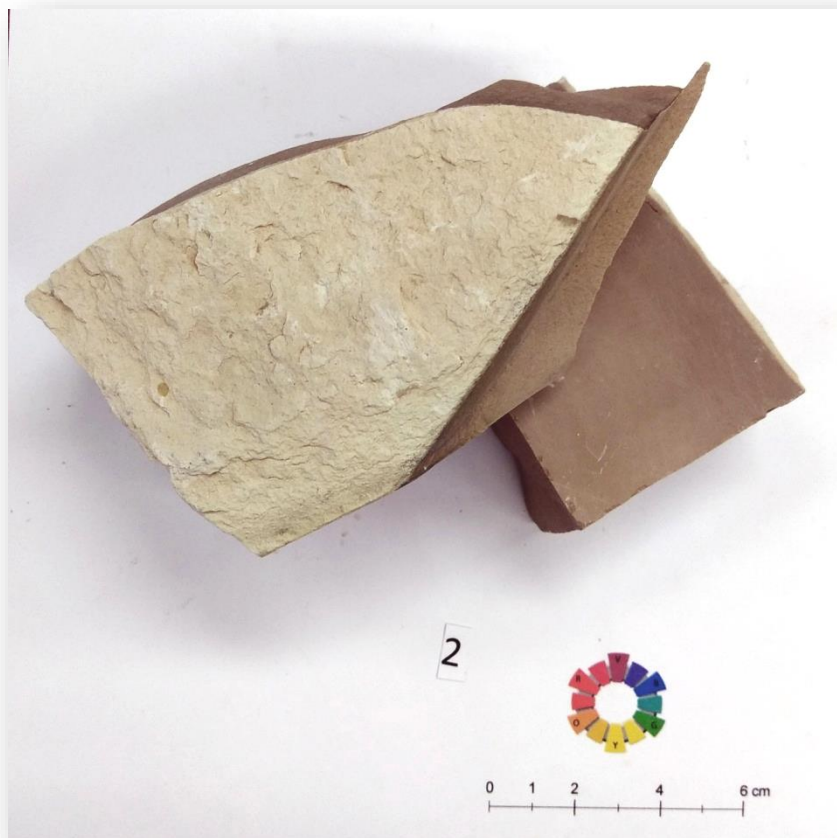
Totally 148 samples are presented. A part of these samples was collected in the framework of a research project cofounded by the Research Promotion Foundation (RPF) of Cyprus under contract TEXNOΛΟΓΙΑ/ΕΝΕΠΓ/0311 (BIE)/01 and the European Regional Development Fund (ERDF) of the EU. The complete list of the samples, numbered with the same order as below, is found in Appendix II. In Appendix II, we can also find the coordinates of the collection point of each sample.



**Sample 001** – Calcarenite, Nicosia Formation



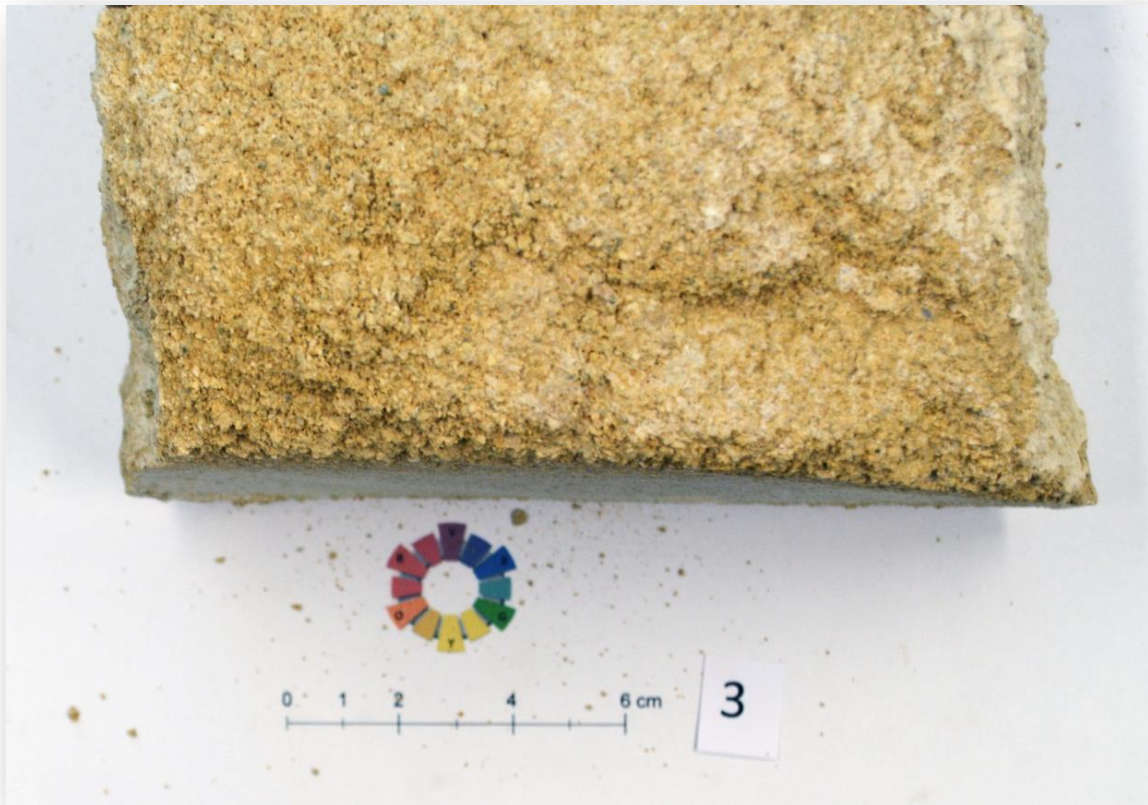
 <p><b>smooth</b></p>		<b>Dry</b>	<b>Water Saturated</b>	<b>units</b>
	<b>Diffusivity x 10<sup>-6</sup></b>	0.70	1.01	m <sup>2</sup> /s
	<b>Thermal Conductivity</b>	1.06	2.13	W/mK
	<b>Specific Heat Capacity x 10<sup>-3</sup></b>	0.584	0.86	J/K kg
	<b>Density x 10<sup>-6</sup></b>	2.56	2.46	kg/m <sup>3</sup>
	<b>Absorption/ Moisture</b>	2.57		%
	<b>Formation/Stratigraphic Unit</b>	Nicosia		
	<b>Lithology</b>	Calcarenite		



**Sample 002** – Chert, Lefkara Formation



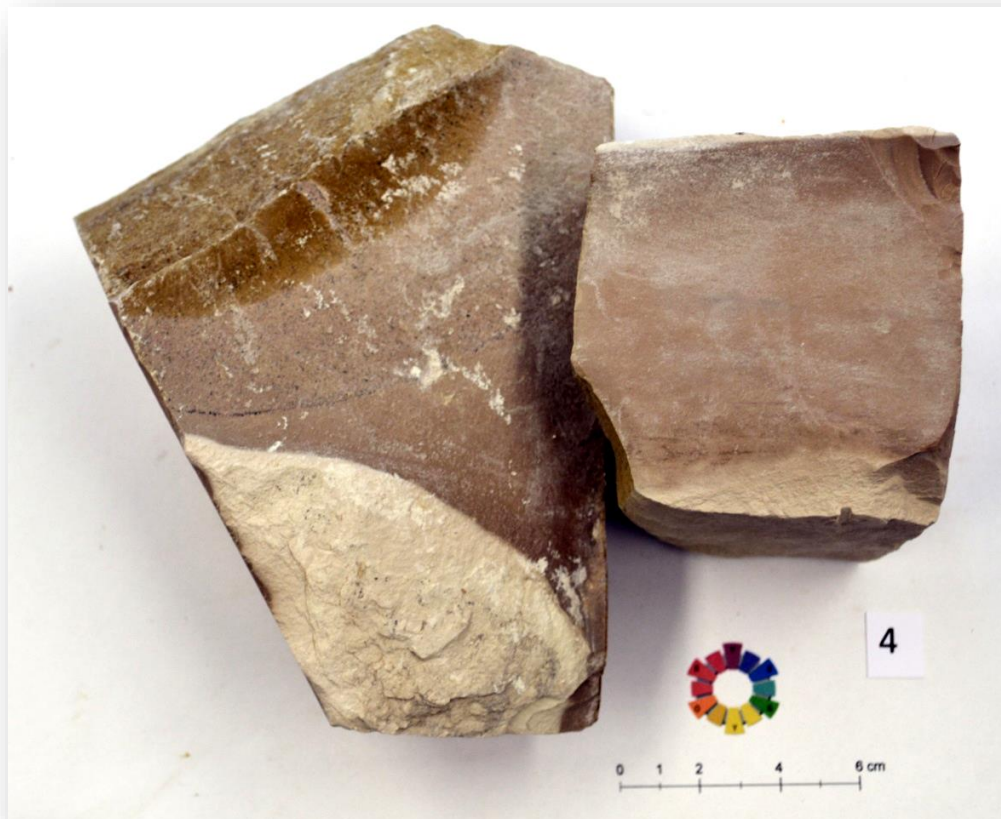
 <p><b>smooth</b></p>		<b>Dry</b>	<b>Water Saturated</b>	<b>units</b>
	<b>Diffusivity x 10<sup>-6</sup></b>	0.83	0.87	m <sup>2</sup> /s
	<b>Thermal Conductivity</b>	1.43	1.68	W/mK
	<b>Specific Heat Capacity x 10<sup>-3</sup></b>	0.74	0.88	J/K kg
	<b>Density x 10<sup>-6</sup></b>	2.34	2.20	kg/m <sup>3</sup>
	<b>Absorption/ Moisture</b>	5.26		%
	<b>Formation/Stratigraphic Unit</b>	Lefkara		
	<b>Lithology</b>	Chert		



**Sample 003 - Calcarenite**



 <p><b>smooth</b></p>		<b>Dry</b>	<b>Water Saturated</b>	<b>units</b>
	<b>Diffusivity x 10<sup>-6</sup></b>	1.22	1.05	m <sup>2</sup> /s
	<b>Thermal Conductivity</b>	2.02	1.47	W/mK
	<b>Specific Heat Capacity x 10<sup>-3</sup></b>	0.65	0.62	J/K kg
	<b>Density x 10<sup>-6</sup></b>	2.45	2.26	kg/m <sup>3</sup>
	<b>Absorption/ Moisture</b>	6.25		%
	<b>Formation/Stratigraphic Unit</b>	Not defined		
	<b>Lithology</b>	Calcarenite		



**Sample 004** – Chert, Lefkara Formation



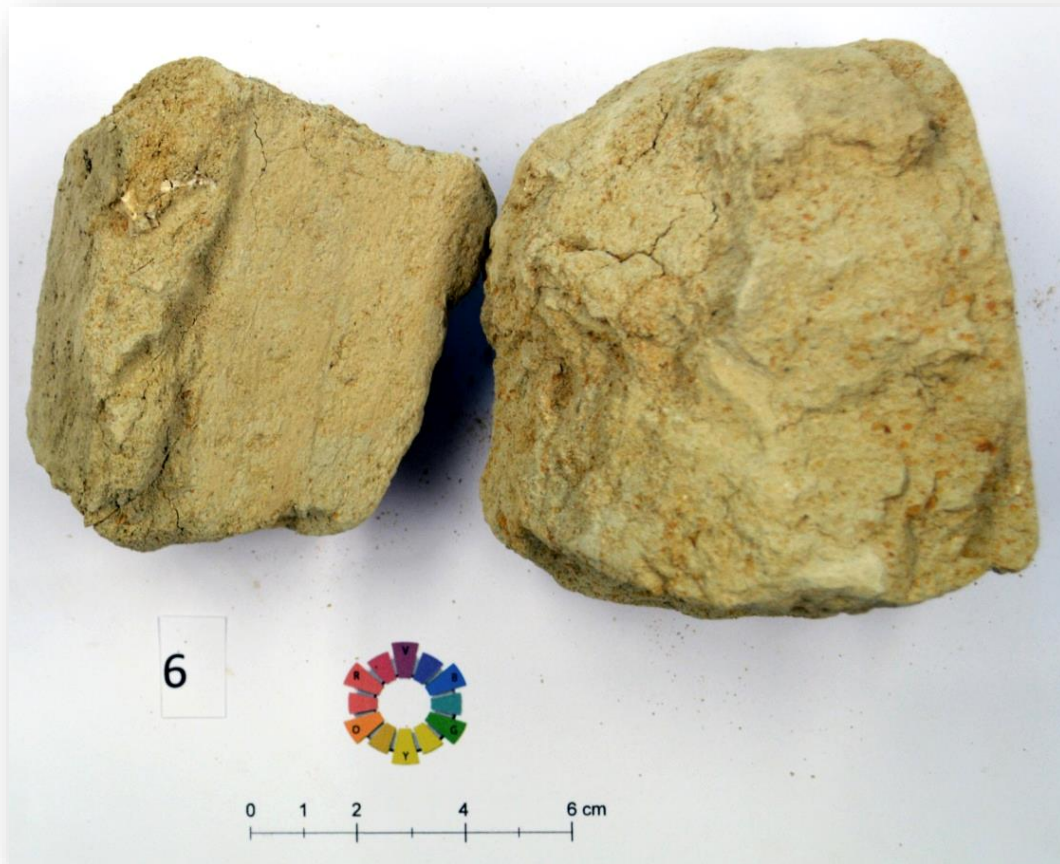
 <b>smooth</b>		<b>Dry</b>	<b>Water Saturated</b>	<b>units</b>
	<b>Diffusivity x 10<sup>-6</sup></b>	0.84	0.79	m <sup>2</sup> /s
	<b>Thermal Conductivity</b>	1.52	1.59	W/mK
	<b>Specific Heat Capacity x 10<sup>-3</sup></b>	0.78	0.92	J/K kg
	<b>Density x 10<sup>-6</sup></b>	2.32	2.18	kg/m <sup>3</sup>
	<b>Absorption/ Moisture</b>	5.08		%
	<b>Formation/Stratigraphic Unit</b>	Lefkara		
	<b>Lithology</b>	Chert		

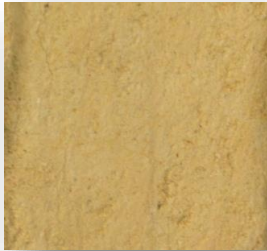

**Sample 005** – Calcarenite, Nicosia Formation



 <p><b>smooth</b></p>		<b>Dry</b>	<b>Water Saturated</b>	<b>units</b>
	<b>Diffusivity x 10<sup>-6</sup></b>	0.36	0.82	m <sup>2</sup> /s
	<b>Thermal Conductivity</b>	0.50	1.16	W/mK
	<b>Heat Capacity x 10<sup>-3</sup></b>	0.90	0.93	J/K kg
	<b>Density x 10<sup>-6</sup></b>	1.54	1.53	kg/m <sup>3</sup>
	<b>Absorption/ Moisture</b>	0.91		%
	<b>Formation/Stratigraphic Unit</b>	Nicosia		
	<b>Lithology</b>	Calcarenite		

**Sample 006 - Sandy Marl, Nicosia Formation**





 <b>smooth</b>		<b>Dry</b>	<b>Water Saturated</b>	<b>units</b>
	<b>Diffusivity x 10<sup>-6</sup></b>	0.34	0.68	m <sup>2</sup> /s
	<b>Thermal Conductivity</b>	0.49	1.26	W/mK
	<b>Specific Heat Capacity x 10<sup>-3</sup></b>	1.16	1.49	J/K kg
	<b>Density x 10<sup>-6</sup></b>	1.26	1.26	kg/m <sup>3</sup>
	<b>Absorption/ Moisture</b>	2.22		%
	<b>Formation/Stratigraphic Unit</b>	Nicosia		
	<b>Lithology</b>	Sandy Marl		





**Sample 007 – Calcarenite, Nicosia Formation**



 <b>smooth</b>		<b>Dry</b>	<b>Water Saturated</b>	<b>units</b>
	<b>Diffusivity x 10<sup>-6</sup></b>	-----	-----	m <sup>2</sup> /s
	<b>Thermal Conductivity</b>	0.45	0.88	W/mK
	<b>Heat Capacity x 10<sup>-3</sup></b>	-----	-----	J/K kg
	<b>Density x 10<sup>-6</sup></b>	2.05	1.74	kg/m <sup>3</sup>
	<b>Absorption/ Moisture</b>	20.58		%
	<b>Formation/Stratigraphic Unit</b>	Nicosia		
	<b>Lithology</b>	Calcarenite		



**Sample 008 – Basalt, Volcanic Sequence (Lower Pillow Lavas)**



 <p><b>smooth</b></p>		<b>Dry</b>	<b>Water Saturated</b>	<b>units</b>
	<b>Diffusivity x 10<sup>-6</sup></b>	0.72	0.85	m <sup>2</sup> /s
	<b>Thermal Conductivity</b>	1.19	1.34	W/mK
	<b>Specific Heat Capacity x 10<sup>-3</sup></b>	0.61	0.61	J/K kg
	<b>Density x 10<sup>-6</sup></b>	2.71	2.55	kg/m <sup>3</sup>
	<b>Absorption/ Moisture</b>	3.70		
	<b>Formation/Stratigraphic Unit</b>	Volcanic Sequence (Lower Pillow Lavas)		
	<b>Lithology</b>	Basalt		



**Sample 009** – Chalk, Pachna Formation



 <p><b>smooth</b></p>		<b>Dry</b>	<b>Water Saturated</b>	<b>units</b>
	<b>Diffusivity x 10<sup>-6</sup></b>	0.81	0.89	m <sup>2</sup> /s
	<b>Thermal Conductivity</b>	1.39	1.52	W/mK
	<b>Heat Capacity x 10<sup>-3</sup></b>	0.74	0.83	J/K kg
	<b>Density x 10<sup>-6</sup></b>	2.34	2.06	kg/m <sup>3</sup>
	<b>Absorption/ Moisture</b>	11.17		%
	<b>Formation/Stratigraphic Unit</b>	Pachna		
	<b>Lithology</b>	Chalk		



**Sample 010 - Volcanic breccias, Volcanic Sequence (Lower Pillow Lavas)**



		<b>Dry</b>	<b>Water Saturated</b>	<b>units</b>
	<b>Diffusivity x 10<sup>-6</sup></b>	1.15	1.04	m <sup>2</sup> /s
	<b>Thermal Conductivity</b>	2.11	2.09	W/mK
<b>Specific Heat Capacity x 10<sup>-3</sup></b>		0.69	0.78	J/K kg
<b>smooth</b>				
	<b>Density x 10<sup>-6</sup></b>	2.66	2.60	kg/m <sup>3</sup>
	<b>Absorption/ Moisture</b>	1.52		%
	<b>Formation/Stratigraphic Unit</b>	Volcanic Sequence (Lower Pillow Lavas)		
	<b>Lithology</b>	Volcanic breccia		



**Sample 011** – Chert, Lefkara Formation



 <p><b>smooth</b></p>		<b>Dry</b>	<b>Water Saturated</b>	<b>units</b>
	<b>Diffusivity x 10<sup>-6</sup></b>	1.20	1.13	m <sup>2</sup> /s
	<b>Thermal Conductivity</b>	2.10	1.96	W/mK
	<b>Specific Heat Capacity x 10<sup>-3</sup></b>	0.72	0.76	J/K kg
	<b>Density x 10<sup>-6</sup></b>	2.45	2.34	kg/m <sup>3</sup>
	<b>Absorption/ Moisture</b>	3.16		%
	<b>Formation/Stratigraphic Unit</b>	Lefkara		
	<b>Lithology</b>	Chert		



**Sample 012** - Marly Chalk, Pachna Formation



 <b>smooth</b>		<b>Dry</b>	<b>Water Saturated</b>	<b>units</b>
	<b>Diffusivity x 10<sup>-6</sup></b>	0.68	0.83	m <sup>2</sup> /s
	<b>Thermal Conductivity</b>	1.20	1.67	W/mK
	<b>Specific Heat Capacity x 10<sup>-3</sup></b>	0.68	0.93	J/K kg
	<b>Density x 10<sup>-6</sup></b>	2.61	2.17	kg/m <sup>3</sup>
	<b>Absorption/ Moisture</b>	14.46		%
	<b>Formation/Stratigraphic Unit</b>	Pachna		
	<b>Lithology</b>	Marly Chalk		



**Sample 013** - Sandy Marl, Nicosia Formation



 <b>smooth</b>		<b>Dry</b>	<b>Water Saturated</b>	<b>units</b>
	<b>Diffusivity x 10<sup>-6</sup></b>	0.62	0.80	m <sup>2</sup> /s
	<b>Thermal Conductivity</b>	0.85	1.27	W/mK
	<b>Specific Heat Capacity x 10<sup>-3</sup></b>	0.82	0.98	J/K kg
	<b>Density x 10<sup>-6</sup></b>	1.63	1.67	kg/m <sup>3</sup>
	<b>Absorption/ Moisture</b>	3.83		%
	<b>Formation/Stratigraphic Unit</b>	Nicosia		
	<b>Lithology</b>	Sandy Marl		

**Sample 014** – Calcarenite, Marine Terrace





 <p><b>smooth</b></p>		<b>Dry</b>	<b>Water Saturated</b>	<b>units</b>
	<b>Diffusivity x 10<sup>-6</sup></b>	0.57	0.77	m <sup>2</sup> /s
	<b>Thermal Conductivity</b>	0.89	1.22	W/mK
	<b>Specific Heat Capacity x 10<sup>-3</sup></b>	0.67	0.77	J/K kg
	<b>Density x 10<sup>-6</sup></b>	2.36	2.05	kg/m <sup>3</sup>
	<b>Absorption/ Moisture</b>	12.47		%
	<b>Formation/Stratigraphic Unit</b>	Marine Terrace		
	<b>Lithology</b>	Calcarenite		





**Sample 015** - Reddish brown sandy clay with gravel, Fluvial deposits



 <b>smooth</b>		<b>Dry</b>	<b>Water Saturated</b>	<b>units</b>
	<b>Diffusivity x 10<sup>-6</sup></b>	0.59	0.76	m <sup>2</sup> /s
	<b>Thermal Conductivity</b>	0.75	1.160	W/mK
	<b>Specific Heat Capacity x 10<sup>-3</sup></b>	0.98	1.08	J/K kg
	<b>Density x 10<sup>-6</sup></b>	1.41	1.43	kg/m <sup>3</sup>
	<b>Absorption/ Moisture</b>	3.61		%
	<b>Formation/Stratigraphic Unit</b>	Fluvial deposits		
	<b>Lithology</b>	Reddish brown sandy clay with gravel		


**Sample 016** - Reef limestone, Pachna Formation (Koronia Member)



		<b>Dry</b>	<b>Water Saturated</b>	<b>units</b>
	<b>Diffusivity x 10<sup>-6</sup></b>	0.76	0.82	m <sup>2</sup> /s
	<b>Thermal Conductivity</b>	1.19	1.63	W/mK
	<b>Specific Heat Capacity x 10<sup>-3</sup></b>	0.68	1.00	J/K kg
<b>smooth</b>				
	<b>Density x 10<sup>-6</sup></b>	2.28	1.99	kg/m <sup>3</sup>
	<b>Absorption/ Moisture</b>	12.66		%
	<b>Formation/Stratigraphic Uni</b>	Pachna (Koronia Member)		
	<b>Lithology</b>	Reef limestone		



**Sample 017 - Brownish clayey Sand, Marine Terrace**



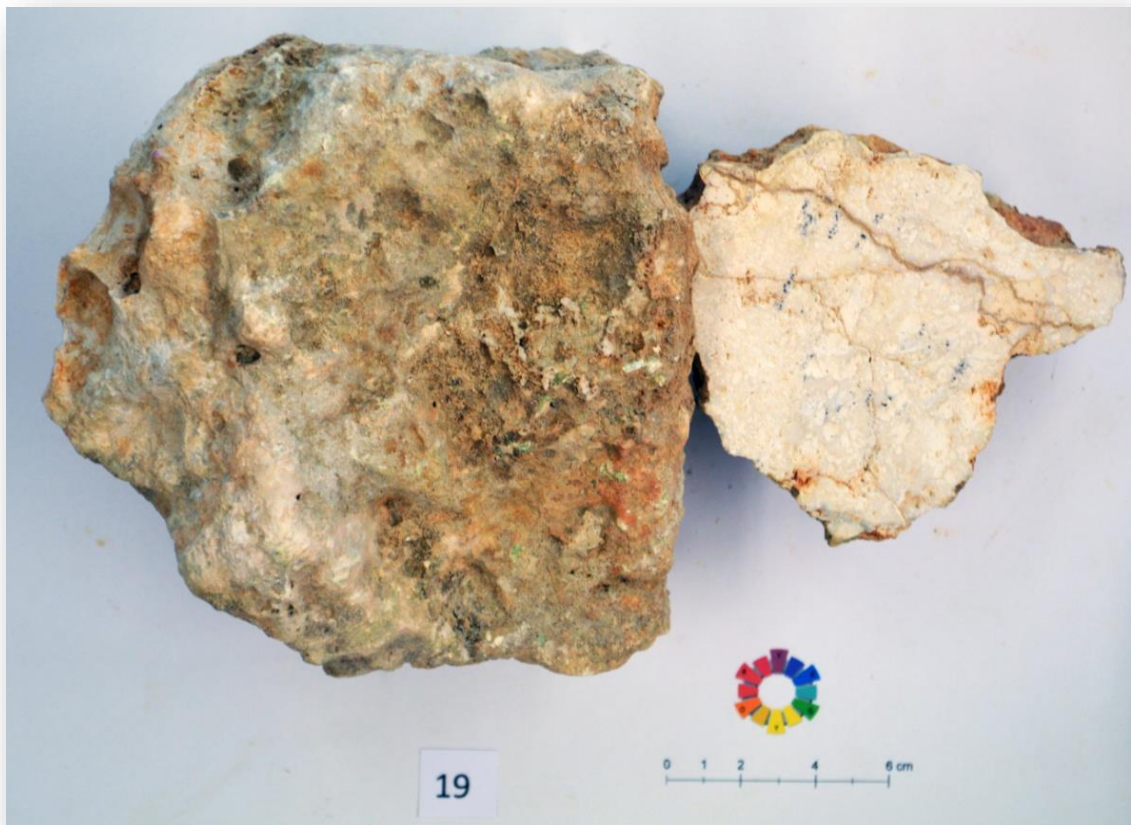
 <b>smooth</b>		<b>Dry</b>	<b>Water Saturated</b>	<b>units</b>
	<b>Diffusivity x 10<sup>-6</sup></b>	0.40	0.71	m <sup>2</sup> /s
	<b>Thermal Conductivity</b>	0.57	1.49	W/mK
	<b>Specific Heat Capacity x 10<sup>-3</sup></b>	0.82	1.23	J/K kg
	<b>Density x 10<sup>-6</sup></b>	1.71	1.71	kg/m <sup>3</sup>
	<b>Absorption/ Moisture</b>	0.19		%
	<b>Formation/Stratigraphic Unit</b>	Marine Terrace		
	<b>Lithology</b>	Brownish clayey Sand		

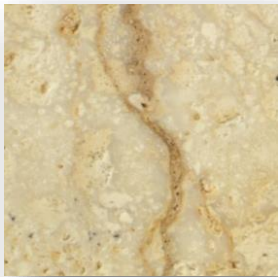

**Sample 018** – Calcareenite, Marine Terrace



 <p><b>smooth</b></p>		<b>Dry</b>	<b>Water Saturated</b>	<b>units</b>
	<b>Diffusivity x 10<sup>-6</sup></b>	0.92	0.95	m <sup>2</sup> /s
	<b>Thermal Conductivity</b>	1.43	1.73	W/mK
	<b>Specific Heat Capacity x 10<sup>-3</sup></b>	0.62	0.80	J/K kg
	<b>Density x 10<sup>-6</sup></b>	2.53	2.29	kg/m <sup>3</sup>
	<b>Absorption/ Moisture</b>	7.49		%
	<b>Formation/Stratigraphic Unit</b>	Marine Terrace		
	<b>Lithology</b>	Calcareenite		



**Sample 019 - Reef Limestone, Pachna Formation (Koronia Member)**



 <b>smooth</b>		<b>Dry</b>	<b>Water Saturated</b>	<b>units</b>
	<b>Diffusivity x 10<sup>-6</sup></b>	0.88	0.91	m <sup>2</sup> /s
	<b>Thermal Conductivity</b>	1.23	1.49	W/mK
	<b>Specific Heat Capacity x 10<sup>-3</sup></b>	0.53	0.71	J/K kg
	<b>Density x 10<sup>-6</sup></b>	2.63	2.30	kg/m <sup>3</sup>
	<b>Absorption/ Moisture</b>	9.70		%
	<b>Formation/Stratigraphic Unit</b>	Pachna (Koronia Member)		
	<b>Lithology</b>	Reef Limestone		


**Sample 020** – Microgabbro, Volcanic Sequence (Lower Pillow Lavas)



 <p><b>smooth</b></p>		<b>Dry</b>	<b>Water Saturated</b>	<b>units</b>
	<b>Diffusivity x 10<sup>-6</sup></b>	0.65	0.64	m <sup>2</sup> /s
	<b>Thermal Conductivity</b>	1.00	1.16	W/mK
	<b>Specific Heat Capacity x 10<sup>-3</sup></b>	0.61	0.76	J/K kg
	<b>Density x 10<sup>-6</sup></b>	2.53	2.38	kg/m <sup>3</sup>
	<b>Absorption/ Moisture</b>	4.46		%
	<b>Formation/Stratigraphic Unit</b>	Volcanic Sequence (Lower Pillow Lavas)		
	<b>Lithology</b>	Microgabbro		



**Sample 021 - Fossiliferous sandy Marl, Nicosia Formation**



 <b>smooth</b>		<b>Dry</b>	<b>Water Saturated</b>	<b>units</b>
	<b>Diffusivity x 10<sup>-6</sup></b>	0.34	0.47	m <sup>2</sup> /s
	<b>Thermal Conductivity</b>	0.48	0.66	W/mK
	<b>Specific Heat Capacity x 10<sup>-3</sup></b>	0.87	0.90	J/K kg
	<b>Density x 10<sup>-6</sup></b>	1.57	1.61	kg/m <sup>3</sup>
	<b>Absorption/ Moisture</b>	4.00		%
	<b>Formation/Stratigraphic Unit</b>	Nicosia		
	<b>Lithology</b>	Fossiliferous sandy Marl		

**Sample 022 - Gray sandy Silt, Fluvial deposits**





 <p><b>smooth</b></p>		<b>Dry</b>	<b>Water Saturated</b>	<b>units</b>
	<b>Diffusivity x 10<sup>-6</sup></b>	0.39	0.63	m <sup>2</sup> /s
	<b>Thermal Conductivity</b>	0.55	1.04	W/mK
	<b>Specific Heat Capacity x 10<sup>-3</sup></b>	0.95	1.11	J/K kg
	<b>Density x 10<sup>-6</sup></b>	1.49	1.50	kg/m <sup>3</sup>
	<b>Absorption/ Moisture</b>	1.10		%
	<b>Formation/Stratigraphic Unit</b>	Fluvial deposits		
	<b>Lithology</b>	Gray sandy Silt		




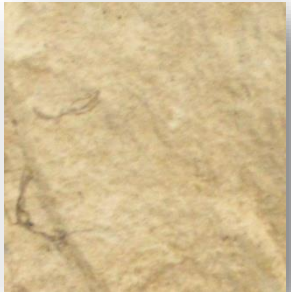
**Sample 023** – Chalk, Pachna Formation



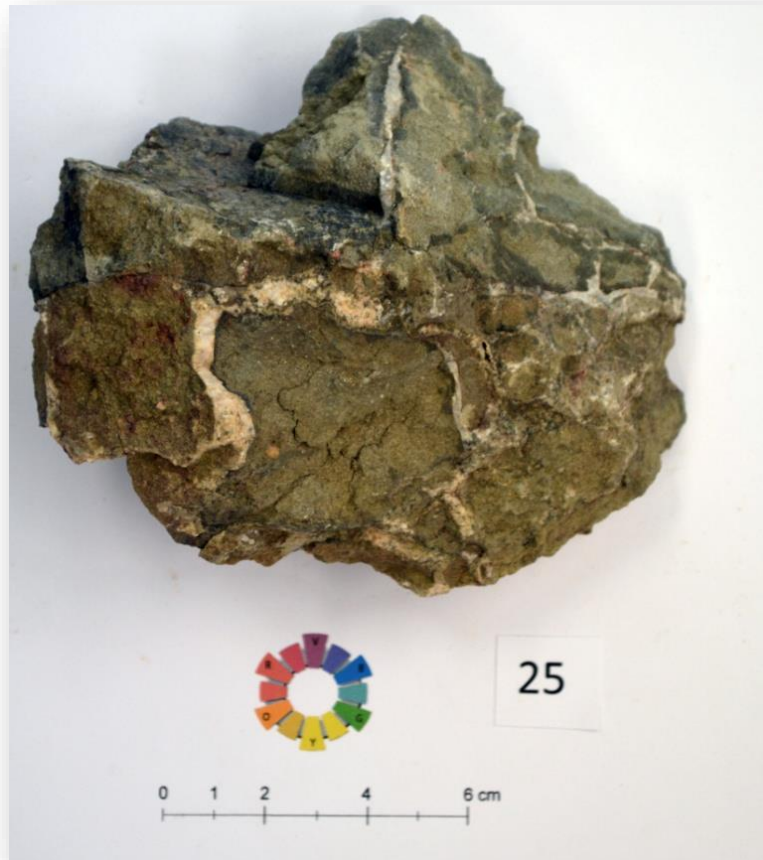
 <b>smooth</b>		<b>Dry</b>	<b>Water Saturated</b>	<b>units</b>
	<b>Diffusivity x 10<sup>-6</sup></b>	0.69	0.73	m <sup>2</sup> /s
	<b>Thermal Conductivity</b>	1.10	1.50	W/mK
	<b>Specific Heat Capacity x 10<sup>-3</sup></b>	0.70	1.04	J/K kg
	<b>Density x 10<sup>-6</sup></b>	2.28	1.99	kg/m <sup>3</sup>
	<b>Absorption/ Moisture</b>	12.66		%
	<b>Formation/Stratigraphic Unit</b>	Pachna		
	<b>Lithology</b>	Chalk		



**Sample 024** – Chalk, Pachna Formation



 <b>smooth</b>		<b>Dry</b>	<b>Water Saturated</b>	<b>units</b>
	<b>Diffusivity x 10<sup>-6</sup></b>	0.68	0.80	m <sup>2</sup> /s
	<b>Thermal Conductivity</b>	1.08	1.64	W/mK
	<b>Specific Heat Capacity x 10<sup>-3</sup></b>	0.60	0.95	J/K kg
	<b>Density x 10<sup>-6</sup></b>	2.63	2.15	kg/m <sup>3</sup>
	<b>Absorption/ Moisture</b>	15.69		%
	<b>Formation/Stratigraphic Unit</b>	Pachna		
	<b>Lithology</b>	Chalk		



**Sample 025** - Olivine-phyric Basalt, Volcanic Sequence (Lower Pillow Lavas)



 <p><b>smooth</b></p>		<b>Dry</b>	<b>Water Saturated</b>	<b>units</b>
	<b>Diffusivity x 10<sup>-6</sup></b>	0.53	0.66	m <sup>2</sup> /s
	<b>Thermal Conductivity</b>	0.88	1.22	W/mK
	<b>Specific Heat Capacity x 10<sup>-3</sup></b>	0.65	0.85	J/K kg
	<b>Density x 10<sup>-6</sup></b>	2.53	2.16	kg/m <sup>3</sup>
	<b>Absorption/ Moisture</b>	12.76		%
	<b>Formation/Stratigraphic Unit</b>	Volcanic Sequence (Lower Pillow Lavas)		
	<b>Lithology</b>	Olivine-phyric Basalt		



**Sample 026 - Vocanic Sequence (Lower Pillow Lavas)**



		<b>Dry</b>	<b>Water Saturated</b>	<b>units</b>
	<b>Diffusivity x 10<sup>-6</sup></b>	0.63	0.58	m <sup>2</sup> /s
	<b>Thermal Conductivity</b>	1.02	1.13	W/mK
<b>smooth</b> 		0.64	0.85	J/K kg
	<b>Density x 10<sup>-6</sup></b>	2.53	2.30	kg/m <sup>3</sup>
	<b>Absorption/ Moisture</b>	6.88		%
	<b>Formation/Stratigraphic Unit</b>	Vocanic Sequence (Lower Pillow Lavas)		
<b>Lithology</b>	Not defined			

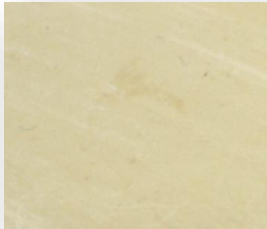

**Sample 027 – Microgabbro, Sheeted Dykes**



 <p><b>smooth</b></p>		<b>Dry</b>	<b>Water Saturated</b>	<b>units</b>
	<b>Diffusivity x 10<sup>-6</sup></b>	1.17	1.06	m <sup>2</sup> /s
	<b>Thermal Conductivity</b>	2.11	2.06	W/mK
	<b>Specific Heat Capacity x 10<sup>-3</sup></b>	0.68	0.73	J/K kg
	<b>Density x 10<sup>-6</sup></b>	2.68	2.64	kg/m <sup>3</sup>
	<b>Absorption/ Moisture</b>	0.89		%
	<b>Formation/Stratigraphic Unit</b>	Sheeted Dykes		
	<b>Lithology</b>	Microgabbro		



**Sample 028 – Chert, Lefkara Formation**



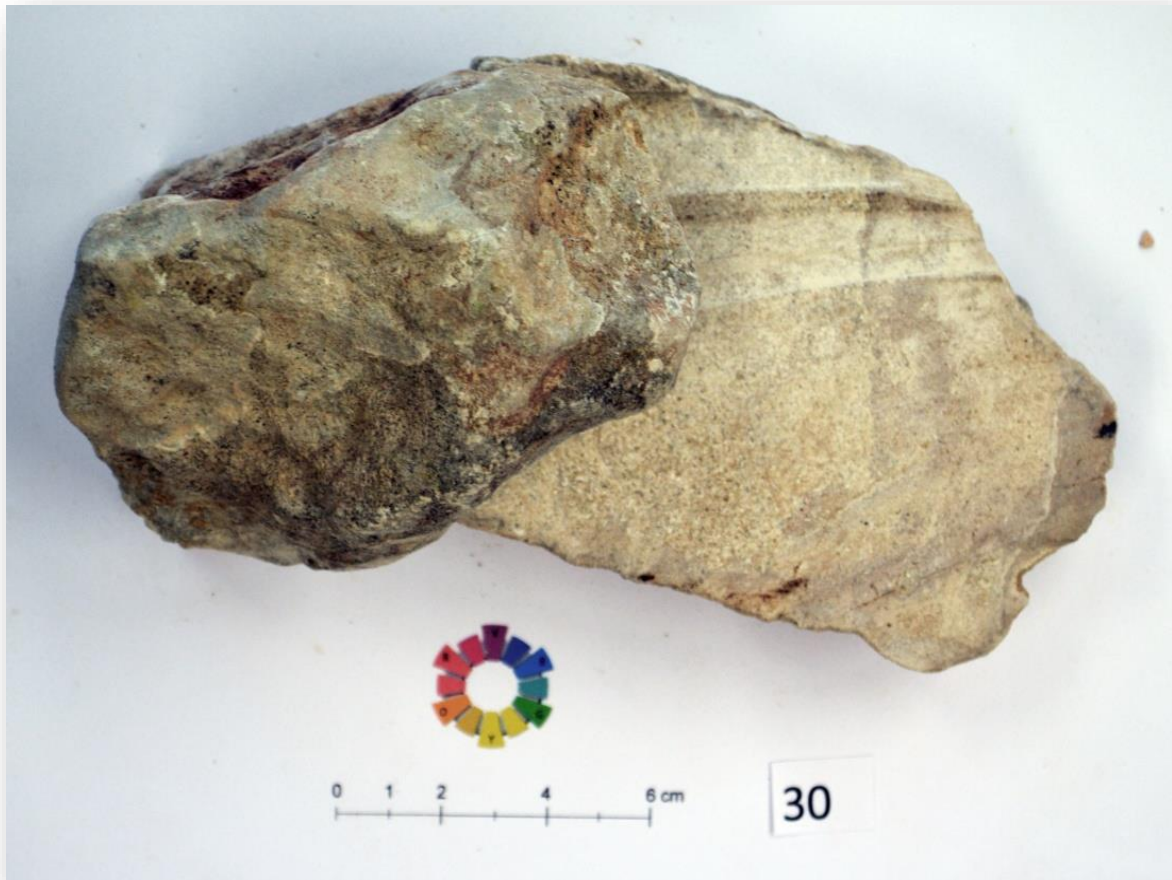
 <b>smooth</b>		<b>Dry</b>	<b>Water Saturated</b>	<b>units</b>
	<b>Diffusivity x 10<sup>-6</sup></b>	0.84	0.90	m <sup>2</sup> /s
	<b>Thermal Conductivity</b>	1.43	1.84	W/mK
	<b>Specific Heat Capacity x 10<sup>-3</sup></b>	0.68	0.89	J/K kg
	<b>Density x 10<sup>-6</sup></b>	2.51	2.29	kg/m <sup>3</sup>
	<b>Absorption/ Moisture</b>	6.82		%
	<b>Formation/Stratigraphic Unit</b>	Lefkara		
	<b>Lithology</b>	Chert		



**Sample 029 - Silicified Chalk, Lefkara**



 <p><b>smooth</b></p>		<b>Dry</b>	<b>Water Saturated</b>	<b>units</b>
	<b>Diffusivity x 10<sup>-6</sup></b>	1.07	1.03	m <sup>2</sup> /s
	<b>Thermal Conductivity</b>	1.94	2.17	W/mK
	<b>Specific Heat Capacity x 10<sup>-3</sup></b>	0.68	0.88	J/K kg
	<b>Density x 10<sup>-6</sup></b>	2.66	2.41	kg/m <sup>3</sup>
	<b>Absorption/ Moisture</b>	6.76		%
	<b>Formation/Stratigraphic Unit</b>	Lefkara		
	<b>Lithology</b>	Silicified Chalk		

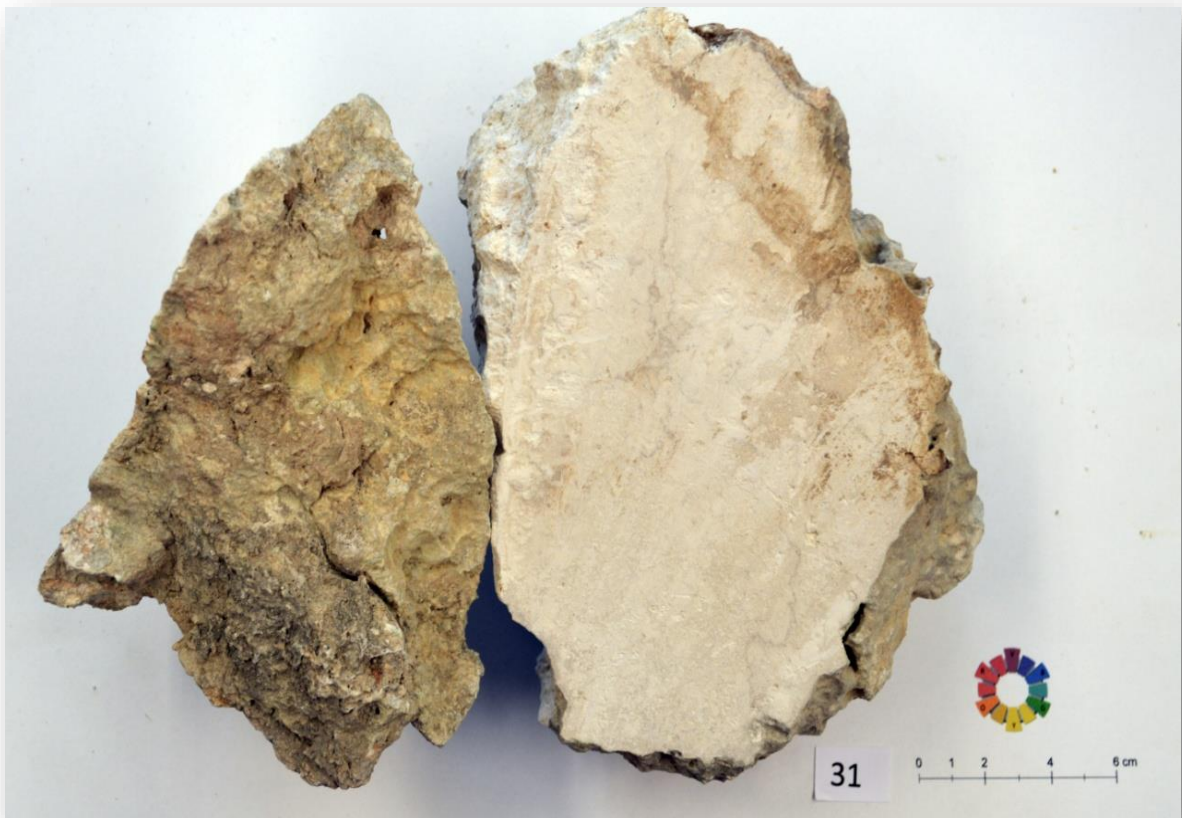
**Sample 030** – Calcareenite, Marine Terrace





 <p><b>smooth</b></p>		<b>Dry</b>	<b>Water Saturated</b>	<b>units</b>
	<b>Diffusivity x 10<sup>-6</sup></b>	0.75	0.89	m <sup>2</sup> /s
	<b>Thermal Conductivity</b>	1.21	1.82	W/mK
	<b>Specific Heat Capacity x 10<sup>-3</sup></b>	0.64	0.86	J/K kg
	<b>Density x 10<sup>-6</sup></b>	2.59	2.39	kg/m <sup>3</sup>
	<b>Absorption/ Moisture</b>	5.40		%
	<b>Formation/Stratigraphic Unit</b>	Marine Terrace		
	<b>Lithology</b>	Calcareenite		




**Sample 031 - Reef Limestone, Pachna Formation (Terra Member)**



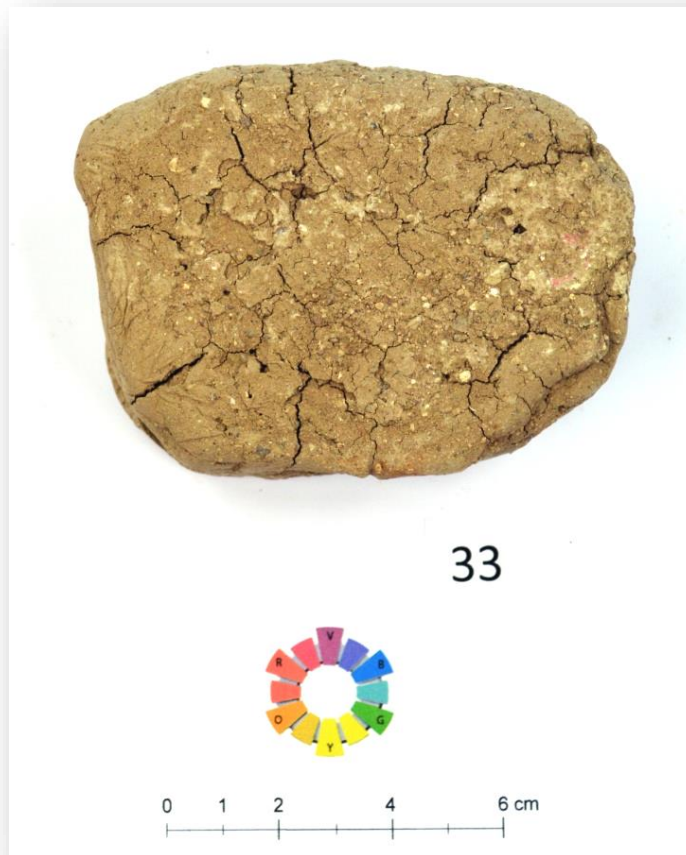
 <p><b>smooth</b></p>		<b>Dry</b>	<b>Water Saturated</b>	<b>units</b>
	<b>Diffusivity x 10<sup>-6</sup></b>	0.82	1.24	m <sup>2</sup> /s
	<b>Thermal Conductivity</b>	1.31	2.24	W/mK
	<b>Specific Heat Capacity x 10<sup>-3</sup></b>	0.62	0.80	J/K kg
	<b>Density x 10<sup>-6</sup></b>	2.58	2.36	kg/m <sup>3</sup>
	<b>Absorption/ Moisture</b>	6.17		%
	<b>Formation/Stratigraphic Unit</b>	Pachna (Terra Member)		
	<b>Lithology</b>	Reef Limestone		


**Sample 032 – Marl, Nicosia Formation**



 <b>smooth</b>		<b>Dry</b>	<b>Water Saturated</b>	<b>units</b>
	<b>Diffusivity x 10<sup>-6</sup></b>	0.53	0.70	m <sup>2</sup> /s
	<b>Thermal Conductivity</b>	0.70	0.95	W/mK
	<b>Specific Heat Capacity x 10<sup>-3</sup></b>	1.01	1.05	J/K kg
	<b>Density x 10<sup>-6</sup></b>	1.29	1.34	kg/m <sup>3</sup>
	<b>Absorption/ Moisture</b>	12.54		%
	<b>Formation/Stratigraphic Unit</b>	Nicosia		
	<b>Lithology</b>	Marl		



**Sample 033** - Brownish Clay with gravels, Fluvial deposits



		<b>Dry</b>	<b>Water Saturated</b>	<b>units</b>
	<b>Diffusivity x 10<sup>-6</sup></b>	0.37	0.525	m <sup>2</sup> /s
	<b>Thermal Conductivity</b>	0.50	1.060	W/mK
<b>smooth</b>	<b>Specific Heat Capacity x 10<sup>-3</sup></b>	0.953	1.457	J/K kg
	<b>Density x 10<sup>-6</sup></b>	1.38	1.43	kg/m <sup>3</sup>
	<b>Absorption/ Moisture</b>	8.89		%
	<b>Formation/Stratigraphic Unit</b>	Fluvial deposits		
	<b>Lithology</b>	Brownish Clay with gravels		



**Sample 034 – Marl, Nicosia Formation**



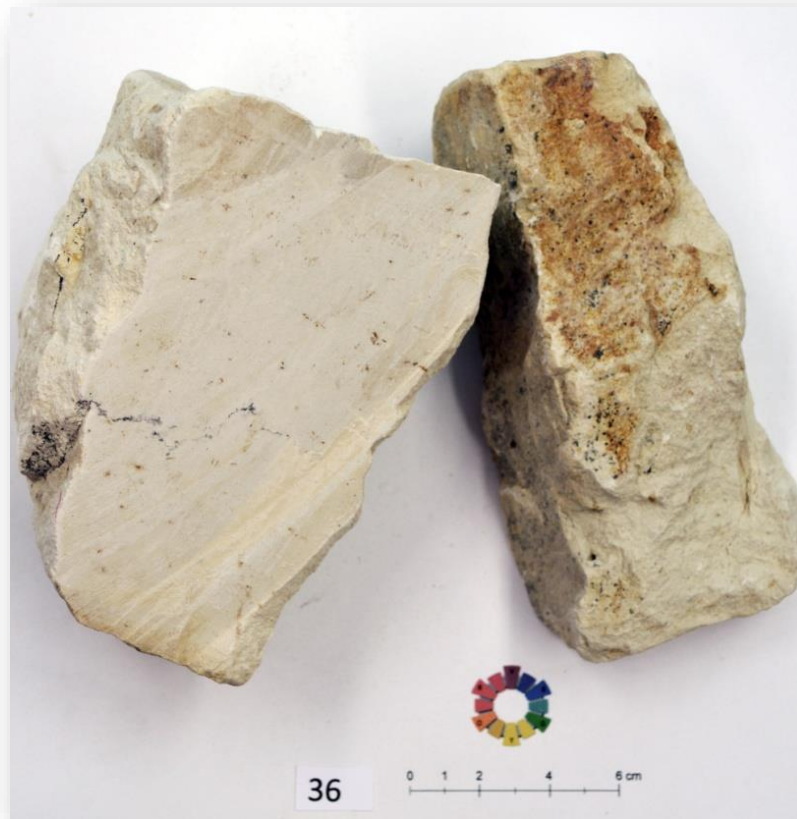
 <p><b>smooth</b></p>		<b>Dry</b>	<b>Water Saturated</b>	<b>units</b>
	<b>Diffusivity x 10<sup>-6</sup></b>	0.37	0.525	m <sup>2</sup> /s
	<b>Thermal Conductivity</b>	0.50	1.060	W/mK
	<b>Specific Heat Capacity x 10<sup>-3</sup></b>	0.953	1.457	J/K kg
	<b>Density x 10<sup>-6</sup></b>	1.38	1.43	kg/m <sup>3</sup>
	<b>Absorption/ Moisture</b>	8.89		%
	<b>Formation/Stratigraphic Unit</b>	Grey Marl		
	<b>Lithology</b>	Nicosia Formation		

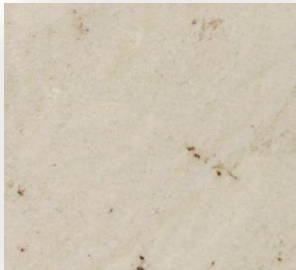

**Sample 035 - Reef Limestone, Pachna (Terra Member)**



 <p><b>smooth</b></p>		<b>Dry</b>	<b>Water Saturated</b>	<b>units</b>
	<b>Diffusivity x 10<sup>-6</sup></b>	1.18	0.98	m <sup>2</sup> /s
	<b>Thermal Conductivity</b>	2.06	1.99	W/mK
	<b>Specific Heat Capacity x 10<sup>-3</sup></b>	0.68	0.84	J/K kg
	<b>Density x 10<sup>-6</sup></b>	2.55	2.42	kg/m <sup>3</sup>
	<b>Absorption/ Moisture</b>	3.35		%
	<b>Formation/Stratigraphic Unit</b>	Pachna (Terra Member)		
	<b>Lithology</b>	Reef Limestone		



**Sample 036 - Marly Chalk, Pachna Formation**



 <b>smooth</b>		<b>Dry</b>	<b>Water Saturated</b>	<b>units</b>
	<b>Diffusivity x 10<sup>-6</sup></b>	0.70	0.82	m <sup>2</sup> /s
	<b>Thermal Conductivity</b>	1.32	1.69	W/mK
	<b>Specific Heat Capacity x 10<sup>-3</sup></b>	0.76	0.92	J/K kg
	<b>Density x 10<sup>-6</sup></b>	2.49	2.23	kg/m <sup>3</sup>
	<b>Absorption/ Moisture</b>	8.48		%
	<b>Formation/Stratigraphic Unit</b>	Pachna		
	<b>Lithology</b>	Marly Chalk		



**Sample 037 - Gabbro (weathered), Plutonic Sequence**



 <p><b>smooth</b></p>		<b>Dry</b>	<b>Water Saturated</b>	<b>units</b>
	<b>Diffusivity x 10<sup>-6</sup></b>	1.08	1.39	m <sup>2</sup> /s
	<b>Thermal Conductivity</b>	1.75	2.54	W/mK
	<b>Specific Heat Capacity x 10<sup>-3</sup></b>	0.59	0.71	J/K kg
	<b>Density x 10<sup>-6</sup></b>	2.77	2.59	kg/m <sup>3</sup>
	<b>Absorption/ Moisture</b>	3.99		%
	<b>Formation/Stratigraphic Unit</b>	Plutonic Sequence		
	<b>Lithology</b>	Gabbro (weathered)		

**Sample 038 - Serpentinized Harzburgite, Mantle Sequence**





		<b>Dry</b>	<b>Water Saturated</b>	<b>units</b>
	<b>Diffusivity x 10<sup>-6</sup></b>	0.79	0.72	m <sup>2</sup> /s
	<b>Thermal Conductivity</b>	1.29	1.47	W/mK
<b>smooth</b> 	<b>Specific Heat Capacity x 10<sup>-3</sup></b>	0.65	0.87	J/K kg
	<b>Density x 10<sup>-6</sup></b>	2.55	2.36	kg/m
	<b>Absorption/ Moisture</b>	5.60		%
	<b>Formation/Stratigraphic Unit</b>	Mantle Sequence		
<b>Lithology</b>	Serpentinized Harzburgite			




**Sample 039 - Fossiliferous Marl, Nicosia Formation**



 <p><b>smooth</b></p>		<b>Dry</b>	<b>Water Saturated</b>	<b>units</b>
	<b>Diffusivity x 10<sup>-6</sup></b>	0.43	0.78	m <sup>2</sup> /s
	<b>Thermal Conductivity</b>	0.64	1.18	W/mK
	<b>Specific Heat Capacity x 10<sup>-3</sup></b>	1.26	1.32	J/K kg
	<b>Density x 10<sup>-6</sup></b>	1.15	1.17	kg/m <sup>3</sup>
	<b>Absorption/ Moisture</b>	11.60		%
	<b>Formation/Stratigraphic Unit</b>	Nicosia		
	<b>Lithology</b>	Fossiliferous Marl		

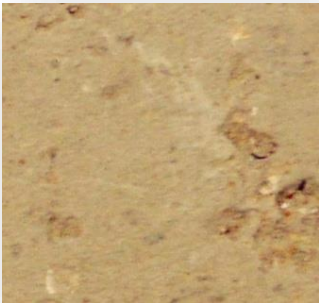
**Sample 040** – Calcarenite, Aeolian deposits



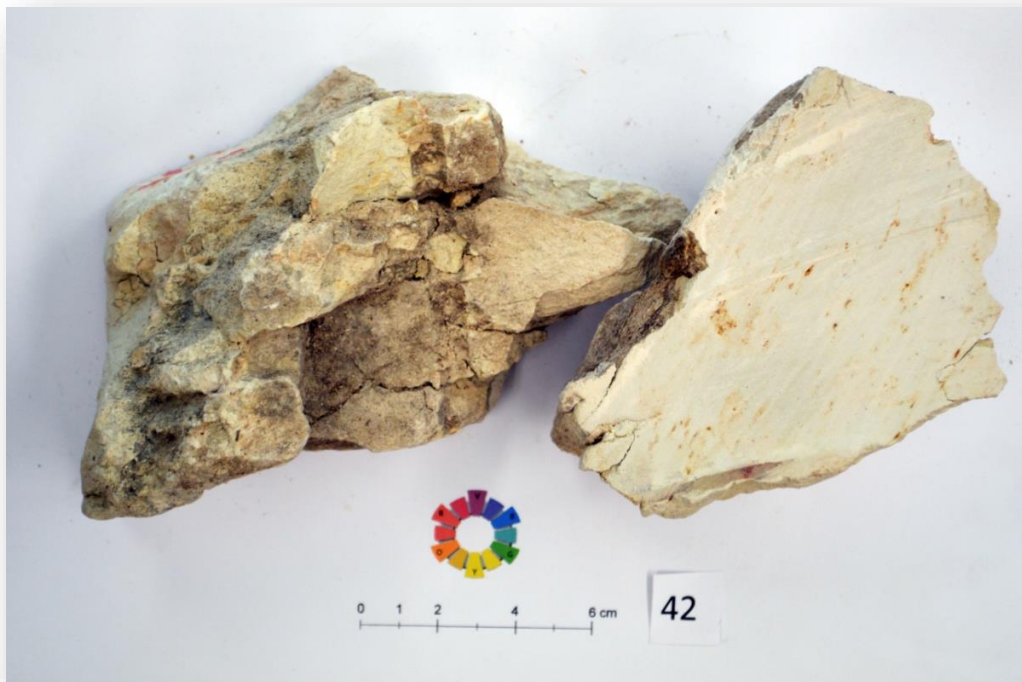
		Dry	Water Saturated	units
	<b>Diffusivity x 10<sup>-6</sup></b>	0.30	0.63	m <sup>2</sup> /s
	<b>Thermal Conductivity</b>	0.41	0.87	W/mK
	<b>Specific Heat Capacity x 10<sup>-3</sup></b>	0.63	0.64	J/K kg
	<b>Density x 10<sup>-6</sup></b>	2.16	2.17	kg/m <sup>3</sup>
	<b>Absorption/ Moisture</b>	0.48		%
	<b>Formation/Stratigraphic Unit</b>	Aeolian deposits		
	<b>Lithology</b>	Calcarenite		


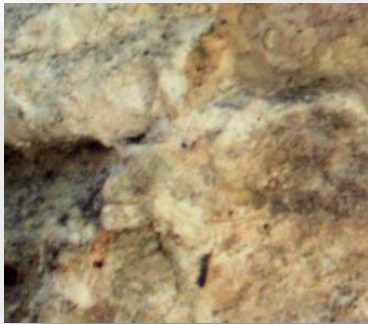
**Sample 041 - Fossiliferous sandy Marl, Nicosia Formation**



 <p><b>smooth</b></p>		<b>Dry</b>	<b>Water Saturated</b>	<b>units</b>
	<b>Diffusivity x 10<sup>-6</sup></b>	0.46	0.77	m <sup>2</sup> /s
	<b>Thermal Conductivity</b>	0.64	1.16	W/mK
	<b>Specific Heat Capacity x 10<sup>-3</sup></b>	0.83	0.93	J/K kg
	<b>Density x 10<sup>-6</sup></b>	1.63	1.67	kg/m <sup>3</sup>
	<b>Absorption/ Moisture</b>	3.43		%
	<b>Formation/Stratigraphic Unit</b>	Nicosia		
	<b>Lithology</b>	Fossiliferous sandy Marl		



**Sample 042 - Marly Chalk, Pachna Formation**



 <p><b>smooth</b></p>		<b>Dry</b>	<b>Water Saturated</b>	<b>units</b>
	<b>Diffusivity x 10<sup>-6</sup></b>	0.69	0.84	m <sup>2</sup> /s
	<b>Thermal Conductivity</b>	1.18	1.69	W/mK
		0.68	0.91	J/K kg
	<b>Specific Heat Capacity x 10<sup>-3</sup></b>			
	<b>Density x 10<sup>-6</sup></b>	2.52	2.21	kg/m <sup>3</sup>
	<b>Absorption/ Moisture</b>	9.94		%
	<b>Formation/Stratigraphic Unit</b>	Pachna		
	<b>Lithology</b>	Marly Chalk		



**Sample 043 - - Marly Chalk, Pachna Formation**



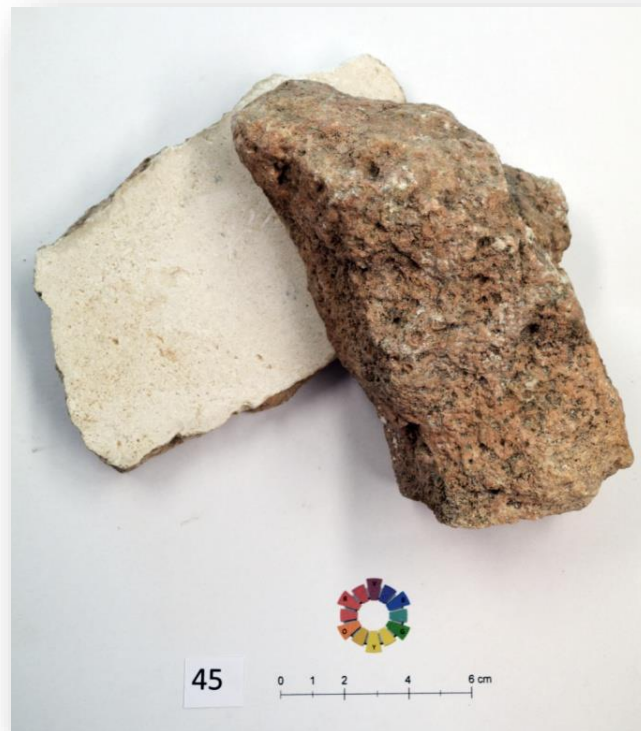
 <p><b>smooth</b></p>		<b>Dry</b>	<b>Water Saturated</b>	<b>units</b>
	<b>Diffusivity x 10<sup>-6</sup></b>	0.98	1.04	m <sup>2</sup> /s
	<b>Thermal Conductivity</b>	1.88	2.21	W/mK
	<b>Specific Heat Capacity x 10<sup>-3</sup></b>	0.73	0.87	J/K kg
	<b>Density x 10<sup>-6</sup></b>	2.65	2.45	kg/m <sup>3</sup>
	<b>Absorption/ Moisture</b>	5.15		%
	<b>Formation/Stratigraphic Unit</b>	Pachna		
	<b>Lithology</b>	Marly Chalk		



**Sample 044** - Chalk, Pachna Formation



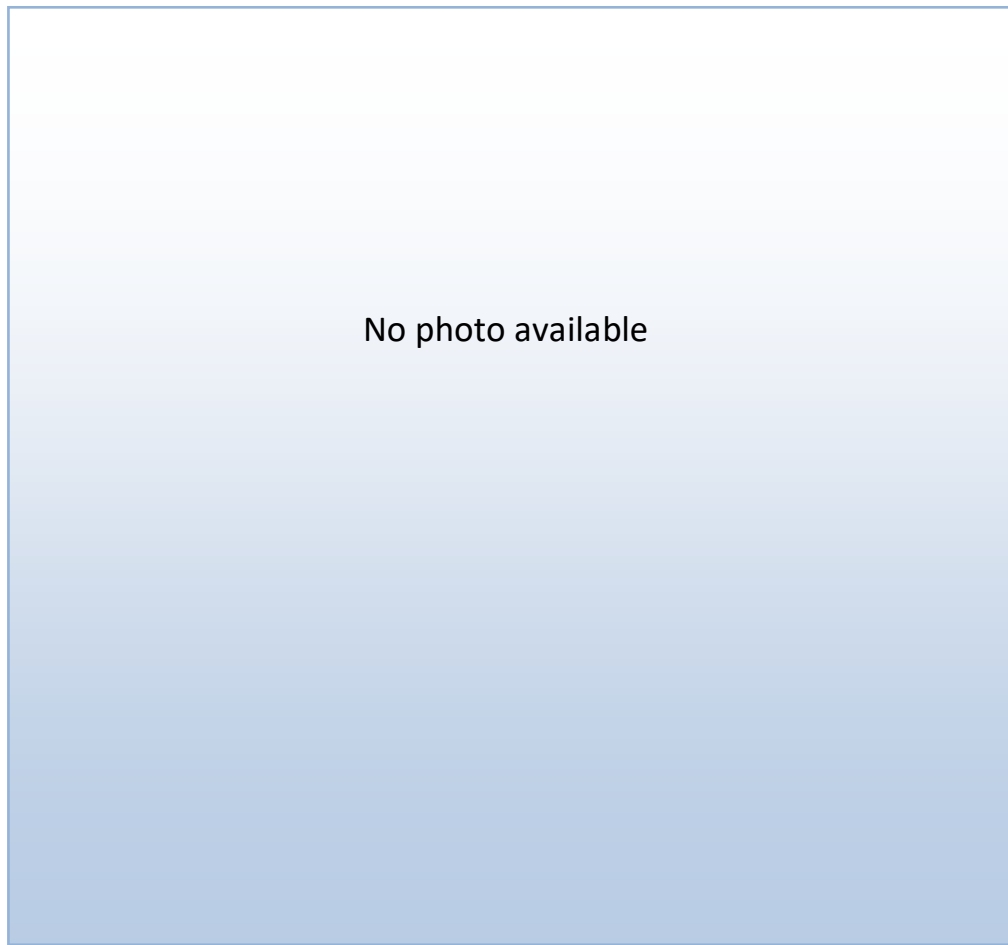
 <p><b>smooth</b></p>		<b>Dry</b>	<b>Water Saturated</b>	<b>units</b>
	<b>Diffusivity x 10<sup>-6</sup></b>	0.81	0.86	m <sup>2</sup> /s
	<b>Thermal Conductivity</b>	1.29	1.71	W/mK
	<b>Specific Heat Capacity x 10<sup>-3</sup></b>	0.64	0.93	J/K kg
	<b>Density x 10<sup>-6</sup></b>	2.50	2.13	kg/m <sup>3</sup>
	<b>Absorption/ Moisture</b>	12.84		%
	<b>Formation/Stratigraphic Unit</b>	Pachna		
	<b>Lithology</b>	Chalk		

**Sample 045 - Reef Limestone, Pachna Formation (Terra Member)**



 <p><b>smooth</b></p>		<b>Dry</b>	<b>Water Saturated</b>	<b>units</b>
	<b>Diffusivity x 10<sup>-6</sup></b>	0.95	0.91	m <sup>2</sup> /s
	<b>Thermal Conductivity</b>	1.60	1.97	W/mK
	<b>Specific Heat Capacity x 10<sup>-3</sup></b>	0.69	0.96	J/K kg
	<b>Density x 10<sup>-6</sup></b>	2.48	2.24	kg/m <sup>3</sup>
	<b>Absorption/ Moisture</b>	7.78		%
	<b>Formation/Stratigraphic Unit</b>	Pachna (Terra Member)		
	<b>Lithology</b>	Reef Limestone		

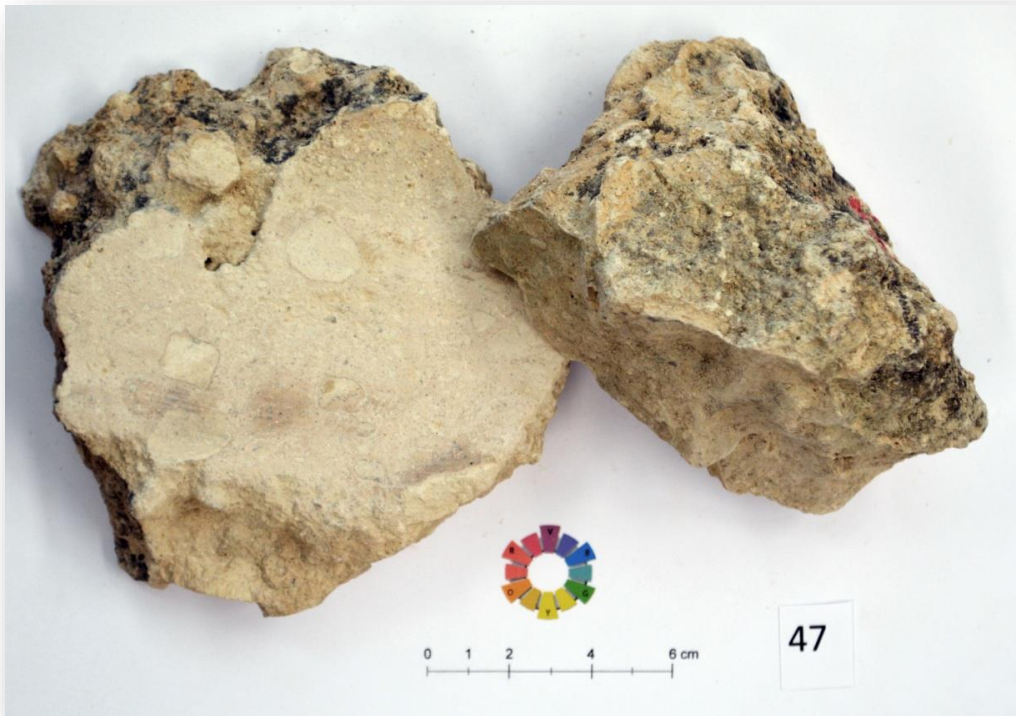
**Sample 046** – Gabbro, Plutonic Sequence





<b>smooth</b>		<b>Dry</b>	<b>Water Saturated</b>	<b>units</b>
	<b>Diffusivity x 10<sup>-6</sup></b>	1.93	1.63	m <sup>2</sup> /s
	<b>Thermal Conductivity</b>	2.83	3.74	W/mK
	<b>Specific Heat Capacity x 10<sup>-3</sup></b>	0.53	0.85	J/K kg
	<b>Density x 10<sup>-6</sup></b>	2.81	2.69	kg/m <sup>3</sup>
	<b>Absorption/ Moisture</b>	2.41		%
	<b>Formation/Stratigraphic Unit</b>	Plutonic Sequence		
	<b>Lithology</b>	Gabbro		





**Sample 047 - Reef Limestone Breccia**



 <b>smooth</b>		<b>Dry</b>	<b>Water Saturated</b>	<b>units</b>
	<b>Diffusivity x 10<sup>-6</sup></b>	0.69	0.78	m <sup>2</sup> /s
	<b>Thermal Conductivity</b>	1.23	1.59	W/m K
	<b>Specific Heat Capacity x 10<sup>-3</sup></b>	0.71	0.94	J/K kg
	<b>Density x 10<sup>-6</sup></b>	2.52	2.15	kg/m <sup>3</sup>
	<b>Absorption/ Moisture</b>	12.92		%
	<b>Formation/Stratigraphic Unit</b>	Not defined		
	<b>Lithology</b>	Reef Limestone Breccia		



**Sample 048** – Chalk, Pachna Formation



 <p><b>smooth</b></p>		<b>Dry</b>	<b>Water Saturated</b>	<b>units</b>
	<b>Diffusivity x 10<sup>-6</sup></b>	0.61	0.76	m <sup>2</sup> /s
	<b>Thermal Conductivity</b>	1.01	1.44	W/mK
	<b>Specific Heat Capacity x 10<sup>-3</sup></b>	0.74	0.97	J/K kg
	<b>Density x 10<sup>-6</sup></b>	2.23	1.96	kg/m <sup>3</sup>
	<b>Absorption/ Moisture</b>	13.07		%
	<b>Formation/Stratigraphic Unit</b>	Pachna		
	<b>Lithology</b>	Chalk		



**Sample 049 - Olive phyric Basalt, Volcanic Sequence (Upper Pillow Lavas)**



 <p><b>smooth</b></p>		<b>Dry</b>	<b>Water Saturated</b>	<b>units</b>
	<b>Diffusivity x 10<sup>-6</sup></b>	0.65	0.60	m <sup>2</sup> /s
	<b>Thermal Conductivity</b>	1.08	1.16	W/mK
	<b>Specific Heat Capacity x 10<sup>-3</sup></b>	0.68	0.83	J/K kg
	<b>Density x 10<sup>-6</sup></b>	2.46	2.35	kg/m <sup>3</sup>
	<b>Absorption/ Moisture</b>	3.44		%
	<b>Formation/Stratigraphic Unit</b>	Volcanic Sequence (Upper Pillow Lavas)		
	<b>Lithology</b>	Olive phyric Basalt		



**Sample 050** – Siltstone, Pachna



 <p><b>smooth</b></p>		<b>Dry</b>	<b>Water Saturated</b>	<b>units</b>
	<b>Diffusivity x 10<sup>-6</sup></b>	0.40	0.60	m <sup>2</sup> /s
	<b>Thermal Conductivity</b>	0.63	1.04	W/mK
	<b>Specific Heat Capacity x 10<sup>-3</sup></b>	1.53	1.69	J/K kg
	<b>Density x 10<sup>-6</sup></b>	1.03	1.03	kg/m <sup>3</sup>
	<b>Absorption/ Moisture</b>	14.92		%
	<b>Formation/Stratigraphic Unit</b>	Pachna		
	<b>Lithology</b>	Siltstone		



**Sample 051** – Serpentinite, Mantle Sequence



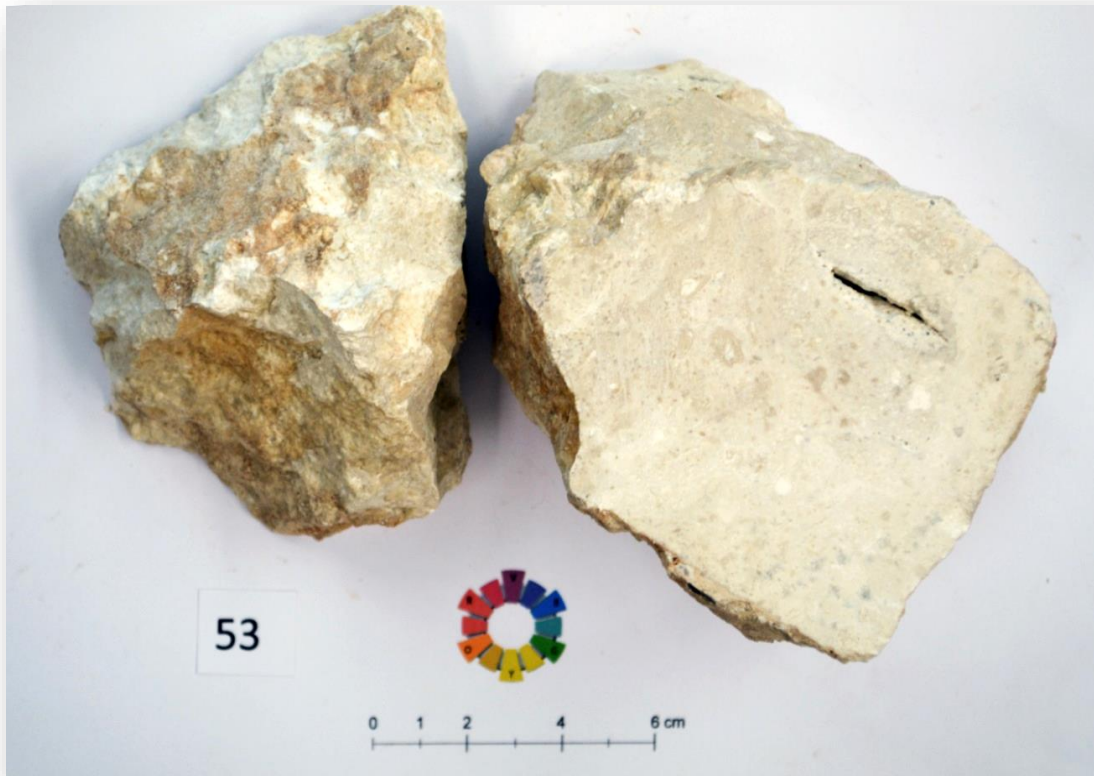
 <p><b>smooth</b></p>		<b>Dry</b>	<b>Water Saturated</b>	<b>units</b>
	<b>Diffusivity x 10<sup>-6</sup></b>	1.13	1.22	m <sup>2</sup> /s
	<b>Thermal Conductivity</b>	2.29	2.46	W/mK
	<b>Specific Heat Capacity x 10<sup>-3</sup></b>	0.79	0.81	J/K kg
	<b>Density x 10<sup>-6</sup></b>	2.58	2.51	kg/m <sup>3</sup>
	<b>Absorption/ Moisture</b>	1.87		%
	<b>Formation/Stratigraphic Unit</b>	Mantle Sequence		
	<b>Lithology</b>	Serpentinite		



**Sample 052 – Chalk, Lefkara**



 <p><b>smooth</b></p>		<b>Dry</b>	<b>Water Saturated</b>	<b>units</b>
	<b>Diffusivity x 10<sup>-6</sup></b>	0.65	0.64	m <sup>2</sup> /s
	<b>Thermal Conductivity</b>	1.14	1.16	W/mK
	<b>Specific Heat Capacity x 10<sup>-3</sup></b>	0.73	0.95	J/K kg
	<b>Density x 10<sup>-6</sup></b>	2.41	1.90	kg/m <sup>3</sup>
	<b>Absorption/ Moisture</b>	23.76		%
	<b>Formation/Stratigraphic Unit</b>	Lefkara		
	<b>Lithology</b>	Chalk		



**Sample 053 - Reef limestone, Pachna Formation (Terra Member)**



 <p><b>smooth</b></p>		<b>Dry</b>	<b>Water Saturated</b>	<b>units</b>
	<b>Diffusivity x 10<sup>-6</sup></b>	1.41	1.20	m <sup>2</sup> /s
	<b>Thermal Conductivity</b>	2.18	2.51	W/mK
	<b>Specific Heat Capacity x 10<sup>-3</sup></b>	0.58	0.80	J/K kg
	<b>Density x 10<sup>-6</sup></b>	2.69	2.63	kg/m <sup>3</sup>
	<b>Absorption/ Moisture</b>	1.44		%
	<b>Formation/Stratigraphic Unit</b>	Pachna (Terra Member)		
	<b>Lithology</b>	Reef limestone		

**Sample 054 - White Chalk, Lefkara Formation**





 <b>smooth</b>		<b>Dry</b>	<b>Water Saturated</b>	<b>units</b>
	<b>Diffusivity x 10<sup>-6</sup></b>	0.34	0.65	m <sup>2</sup> /s
	<b>Thermal Conductivity</b>	0.56	1.20	W/mK
	<b>Specific Heat Capacity x 10<sup>-3</sup></b>	0.72	1.03	J/K kg
	<b>Density x 10<sup>-6</sup></b>	2.27	1.80	kg/m <sup>3</sup>
	<b>Absorption/ Moisture</b>	25.50		%
	<b>Formation/Stratigraphic Unit</b>	Lefkara		
	<b>Lithology</b>	White Chalk		

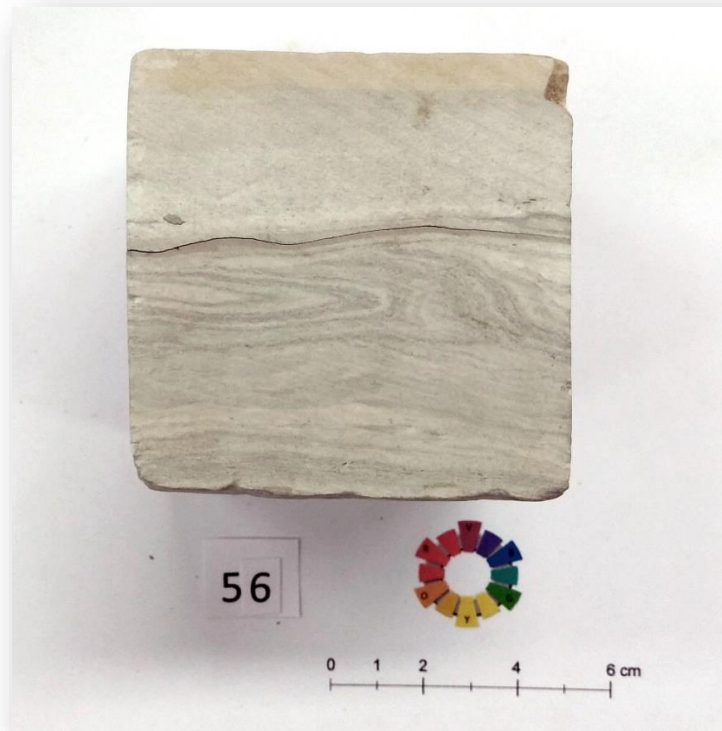



**Sample 055 - Off-white Chalk, Pachna Formation**



 <p><b>smooth</b></p>		<b>Dry</b>	<b>Water Saturated</b>	<b>units</b>
	<b>Diffusivity x 10<sup>-6</sup></b>	0.60	0.70	m <sup>2</sup> /s
	<b>Thermal Conductivity</b>	1.10	1.41	W/mK
	<b>Specific Heat Capacity x 10<sup>-3</sup></b>	0.83	1.04	J/K kg
	<b>Density x 10<sup>-6</sup></b>	2.19	1.94	kg/m <sup>3</sup>
	<b>Absorption/ Moisture</b>	12.14		%
	<b>Formation/Stratigraphic Unit</b>	Pachna		
	<b>Lithology</b>	Off-white Chalk		



**Sample 056 - Marble, Laminated Gypsum, Kalavassos Formation**



 <p><b>smooth</b></p>		<b>Dry</b>	<b>Water Saturated</b>	<b>units</b>
	<b>Diffusivity x 10<sup>-6</sup></b>	0.65	0.52	m <sup>2</sup> /s
	<b>Thermal Conductivity</b>	1.02	0.98	W/mK
	<b>Specific Heat Capacity x 10<sup>-3</sup></b>	0.63	0.84	J/K kg
	<b>Density x 10<sup>-6</sup></b>	2.51	2.25	kg/m <sup>3</sup>
	<b>Absorption/ Moisture</b>	8.32		%
	<b>Formation/Stratigraphic Unit</b>	Kalavassos		
	<b>Lithology</b>	Marble, Laminated Gypsum		



**Sample 057 – Diabase, Volcanic Sequence (Basal Group)**



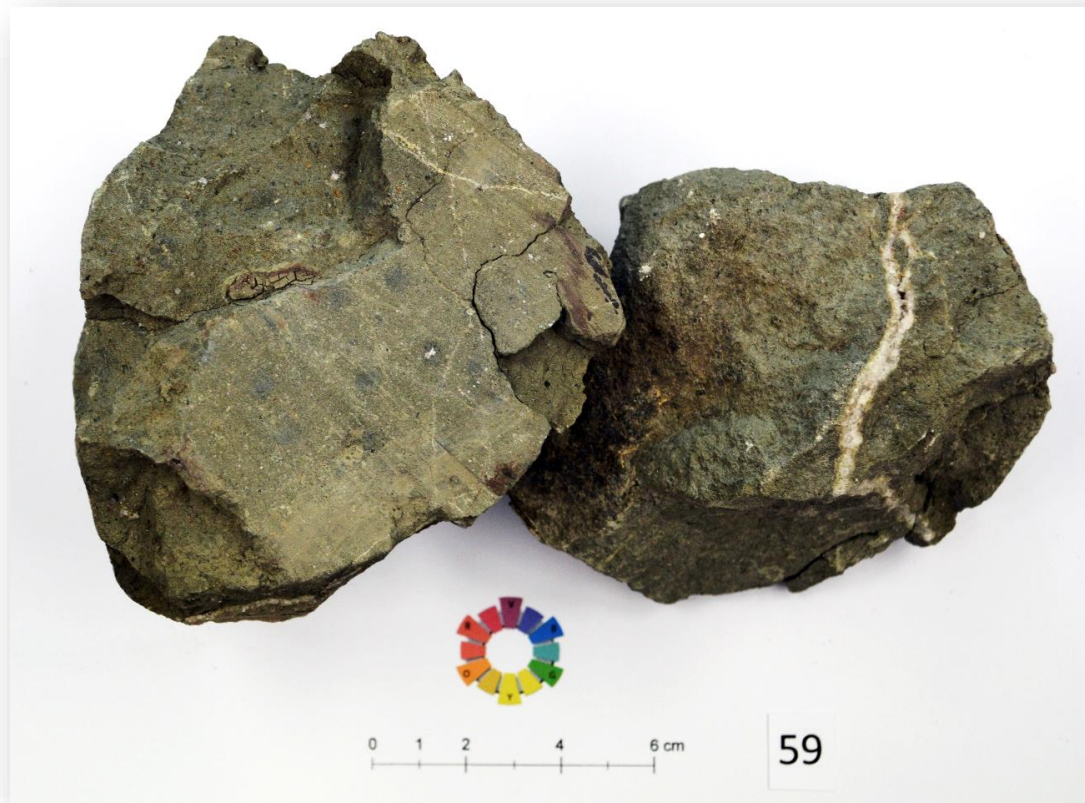
 <p><b>smooth</b></p>		<b>Dry</b>	<b>Water Saturated</b>	<b>units</b>
	<b>Diffusivity x 10<sup>-6</sup></b>	1.28	1.32	m <sup>2</sup> /s
	<b>Thermal Conductivity</b>	2.75	3.00	W/mK
	<b>Specific Heat Capacity x 10<sup>-3</sup></b>	0.79	0.84	J/K kg
	<b>Density x 10<sup>-6</sup></b>	2.74	2.71	kg/m <sup>3</sup>
	<b>Absorption/ Moisture</b>	0.64		%
	<b>Formation/Stratigraphic Unit</b>	Volcanic Sequence (Basal Group)		
	<b>Lithology</b>	Diabase		



**Sample 058** – Chert, Lefkara Formation



 <p><b>smooth</b></p>		<b>Dry</b>	<b>Water Saturated</b>	<b>units</b>
	<b>Diffusivity x 10<sup>-6</sup></b>	0.78	0.89	m <sup>2</sup> /s
	<b>Thermal Conductivity</b>	1.55	1.67	W/mK
		0.84	0.86	J/K kg
	<b>Specific Heat Capacity x 10<sup>-3</sup></b>			
	<b>Density x 10<sup>-6</sup></b>	2.36	2.19	kg/m <sup>3</sup>
	<b>Absorption/ Moisture</b>	6.09		%
	<b>Formation/Stratigraphic Unit</b>	Lefkara		
	<b>Lithology</b>	Chert		



**Sample 059 – Basalt, Volcanic Sequence (Lower Pillow Lavas)**



 <p><b>smooth</b></p>		<b>Dry</b>	<b>Water Saturated</b>	<b>units</b>
	<b>Diffusivity x 10<sup>-6</sup></b>	0.61	0.68	m <sup>2</sup> /s
	<b>Thermal Conductivity</b>	1.11	1.30	W/mK
	<b>Specific Heat Capacity x 10<sup>-3</sup></b>	0.67	0.80	J/K kg
	<b>Density x 10<sup>-6</sup></b>	2.71	2.41	kg/m <sup>3</sup>
	<b>Absorption/ Moisture</b>	7.95		%
	<b>Formation/Stratigraphic Unit</b>	Volcanic Sequence (Lower Pillow Lavas)		
	<b>Lithology</b>	Basalt		



**Sample 060** – Harzburgite, Mantle Sequence



		<b>Dry</b>	<b>Water Saturated</b>	<b>units</b>
	<b>Diffusivity x 10<sup>-6</sup></b>	0.85	0.93	m <sup>2</sup> /s
	<b>Thermal Conductivity</b>	1.82	1.90	W/mK
<b>Specific Heat Capacity x 10<sup>-3</sup></b>		0.82	0.80	J/K kg
<b>smooth</b>				
	<b>Density x 10<sup>-6</sup></b>	2.61	2.55	kg/m <sup>3</sup>
	<b>Absorption/ Moisture</b>	1.45		%
	<b>Formation/Stratigraphic Unit</b>	Mantle Sequence		
	<b>Lithology</b>	Harzburgite		


**Sample 061 - White Chalk, Lefkara Formation**



 <b>smooth</b>		<b>Dry</b>	<b>Water Saturated</b>	<b>units</b>
	<b>Diffusivity x 10<sup>-6</sup></b>	0.67	0.71	m <sup>2</sup> /s
	<b>Thermal Conductivity</b>	1.09	1.45	W/mK
		0.71	1.01	J/K kg
	<b>Density x 10<sup>-6</sup></b>	2.32	2.01	kg/m <sup>3</sup>
	<b>Absorption/ Moisture</b>	13.28		%
	<b>Formation/Stratigraphic Unit</b>	Lefkara		
	<b>Lithology</b>	White Chalk		

**Sample 062 – Diabase, Sheeted Dykes**



		Dry	Water Saturated	units
	<b>Diffusivity x 10<sup>-6</sup></b>	1.06	0.97	m <sup>2</sup> /s
	<b>Thermal Conductivity</b>	2.19	2.17	W/mK
	<b>Specific Heat Capacity x 10<sup>-3</sup></b>	0.75	0.81	J/K kg
	<b>Density x 10<sup>-6</sup></b>	2.76	2.74	kg/m <sup>3</sup>
	<b>Absorption/ Moisture</b>	0.58		%
	<b>Formation/Stratigraphic Unit</b>	Sheeted Dykes		
	<b>Lithology</b>	Diabase		

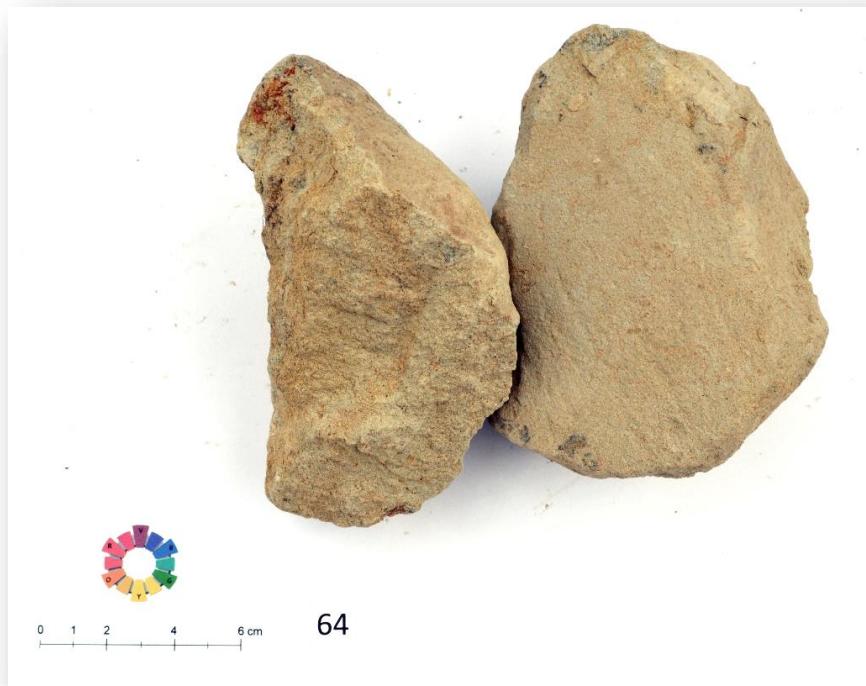




**Sample 063** – Diabase, Sheeted Dykes



 <b>smooth</b>		<b>Dry</b>	<b>Water Saturated</b>	<b>units</b>
	<b>Diffusivity x 10<sup>-6</sup></b>	0.96	1.04	m <sup>2</sup> /s
	<b>Thermal Conductivity</b>	2.06	2.00	W/mK
		0.78	0.71	J/K kg
	<b>Specific Heat Capacity x 10<sup>-3</sup></b>			
	<b>Density x 10<sup>-6</sup></b>	2.76	2.73	kg/m <sup>3</sup>
	<b>Absorption/ Moisture</b>	0.57		%
	<b>Formation/Stratigraphic Unit</b>	Sheeted Dykes		
	<b>Lithology</b>	Diabase		



**Sample 064 - Sandy Marl, Nicosia Formation (Athalassa Member)**



 <p><b>smooth</b></p>		<b>Dry</b>	<b>Water Saturated</b>	<b>units</b>
	<b>Diffusivity x 10<sup>-6</sup></b>	0.54	0.59	m <sup>2</sup> /s
	<b>Thermal Conductivity</b>	0.85	0.91	W/mK
		1.07	1.06	J/K kg
	<b>Specific Heat Capacity x 10<sup>-3</sup></b>			
	<b>Density x 10<sup>-6</sup></b>	1.46	1.06	kg/m <sup>3</sup>
	<b>Absorption/ Moisture</b>	3.61		%
	<b>Formation/Stratigraphic Unit</b>	Nicosia (Athalassa Member)		
	<b>Lithology</b>	Sandy Marl		



**Sample 065** – Sandstone, Nicosia Formation (Aspropamboulos Oolite Member)



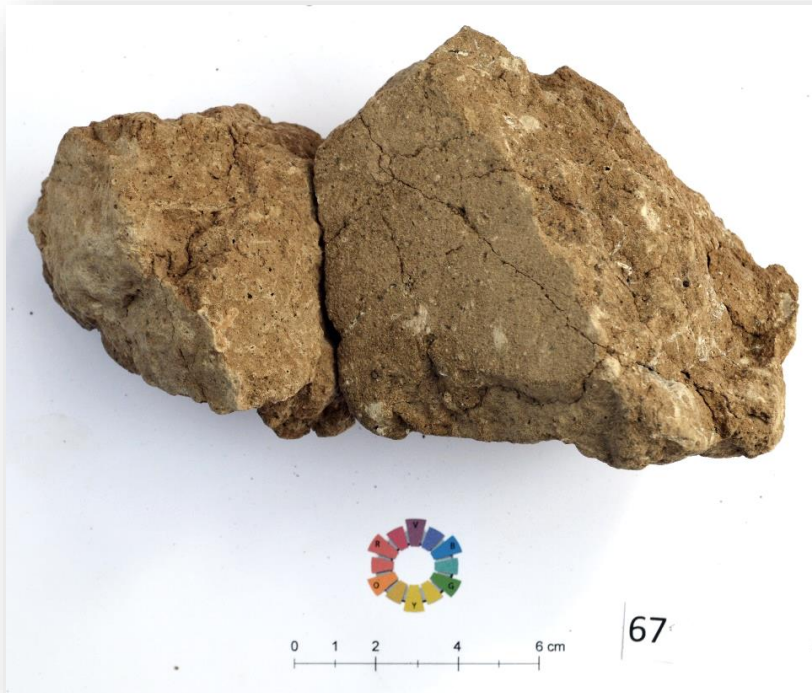
 <b>smooth</b>		<b>Dry</b>	<b>Water Saturated</b>	<b>units</b>
	<b>Diffusivity x 10<sup>-6</sup></b>	0.51	0.68	m <sup>2</sup> /s
	<b>Thermal Conductivity</b>	0.74	1.22	W/mK
	<b>Specific Heat Capacity x 10<sup>-3</sup></b>	0.95	1.17	J/K kg
	<b>Density x 10<sup>-6</sup></b>	1.53	1.55	kg/m <sup>3</sup>
	<b>Absorption/ Moisture</b>	3.01		%
	<b>Formation/Stratigraphic Unit</b>	Nicosia (Aspropamboulos Oolite Member)		
	<b>Lithology</b>	Sandstone		


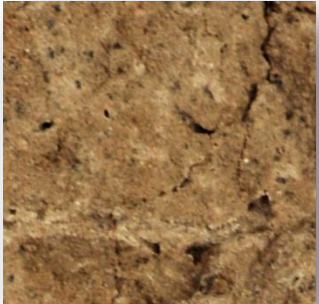
**Sample 066** – Sandstone, Nicosia Formation (Kephales Member)



		<b>Dry</b>	<b>Water Saturated</b>	<b>units</b>
	<b>Diffusivity x 10<sup>-6</sup></b>	0.86	1.05	m <sup>2</sup> /s
	<b>Thermal Conductivity</b>	1.31	1.94	W/mK
<b>smooth</b>	<b>Specific Heat Capacity x 10<sup>-3</sup></b>	0.59	0.81	J/K kg
	<b>Density x 10<sup>-6</sup></b>	2.59	2.34	kg/m <sup>3</sup>
	<b>Absorption/ Moisture</b>	6.99		%
	<b>Formation/Stratigraphic Unit</b>	Nicosia (Kephales Member)		
	<b>Lithology</b>	Sandstone		

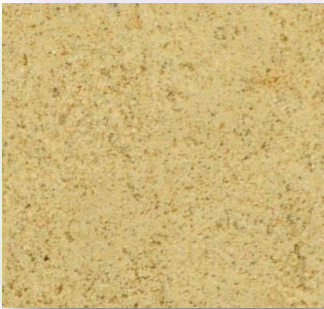

**Sample 067 - Brown silty Sand, Apalos Formation**



 <p><b>smooth</b></p>		<b>Dry</b>	<b>Water Saturated</b>	<b>units</b>
	<b>Diffusivity x 10<sup>-6</sup></b>	0.298	0.636	m <sup>2</sup> /s
	<b>Thermal Conductivity</b>	0.429	1.070	W/mK
	<b>Specific Heat Capacity x 10<sup>-3</sup></b>	-----	-----	J/K kg
	<b>Density x 10<sup>-6</sup></b>	-----	-----	kg/m <sup>3</sup>
	<b>Absorption/ Moisture</b>	-----		%
	<b>Formation/Stratigraphic Unit</b>	Apalos		
	<b>Lithology</b>	Brown silty Sand		



**Sample 068** – Sandstone, Nicosia Formation (Lithic Sand Member)



 <p><b>Smooth</b></p>		<b>Dry</b>	<b>Water Saturated</b>	<b>units</b>
	<b>Diffusivity x 10<sup>-6</sup></b>	0.49	0.55	m <sup>2</sup> /s
	<b>Thermal Conductivity</b>	0.73	1.14	W/mK
	<b>Specific Heat Capacity x 10<sup>-3</sup></b>	1.02	1.44	J/K kg
	<b>Density x 10<sup>-6</sup></b>	1.43	1.46	kg/m <sup>3</sup>
	<b>Absorption/ Moisture</b>	4.36		%
	<b>Formation/Stratigraphic Unit</b>	Nicosia (Lithic Sand Member)		
	<b>Lithology</b>	Sandstone		



**Sample 069** – Sandstone, Nicosia Formation (Kephales Member)



 <p><b>Smooth</b></p>		<b>Dry</b>	<b>Water Saturated</b>	<b>units</b>
	<b>Diffusivity x 10<sup>-6</sup></b>	1.01	1.17	m <sup>2</sup> /s
	<b>Thermal Conductivity</b>	1.65	1.67	W/mK
	<b>Specific Heat Capacity x 10<sup>-3</sup></b>	0.62	0.57	J/K kg
	<b>Density x 10<sup>-6</sup></b>	2.68	2.48	kg/m <sup>3</sup>
	<b>Absorption/ Moisture</b>	5.12		%
	<b>Formation/Stratigraphic Unit</b>	Nicosia (Kephales Member)		
	<b>Lithology</b>	Sandstone		

**Sample 070** - Lithic sand, Nicosia Formation (Aspropamboulos Oolite Member)





 <p><b>Smooth</b></p>		<b>Dry</b>	<b>Water Saturated</b>	<b>units</b>
	<b>Diffusivity x 10<sup>-6</sup></b>	0.31	0.55	m <sup>2</sup> /s
	<b>Thermal Conductivity</b>	0.50	1.00	W/mK
		0.91	1.16	J/K kg
	<b>Specific Heat Capacity x 10<sup>-3</sup></b>			
	<b>Density x 10<sup>-6</sup></b>	1.58	1.64	kg/m <sup>3</sup>
	<b>Absorption/ Moisture</b>	6.30		%
	<b>Formation/Stratigraphic Unit</b>	Nicosia (Aspropamboulos Oolite Member)		
	<b>Lithology</b>	Lithic sand		

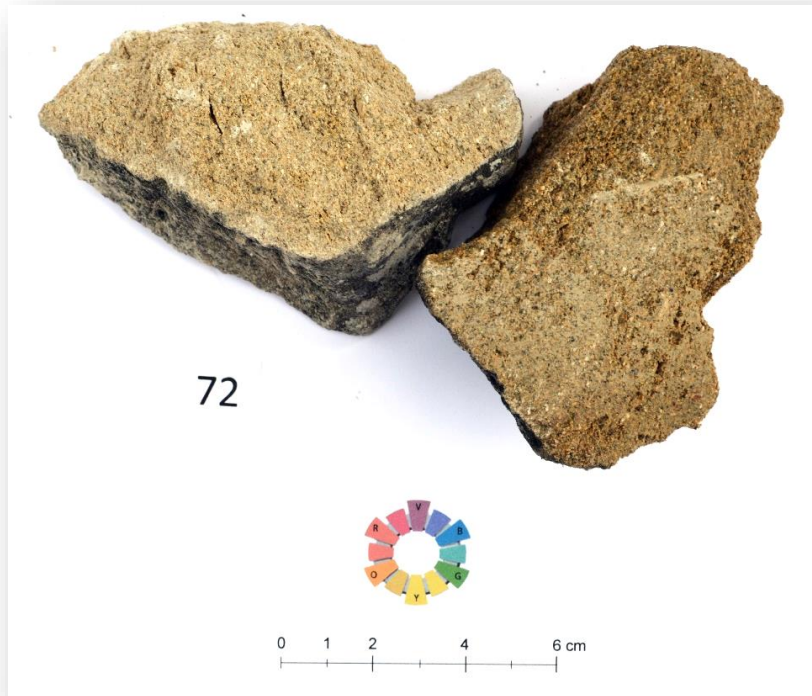


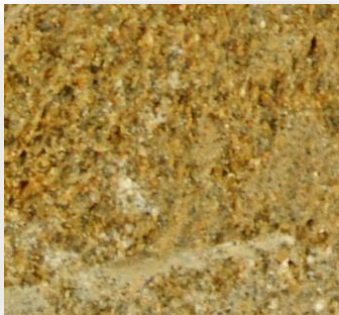

**Sample 071 - Marly Sandstone, Nicosia (Athalassa Member)**



		<b>Dry</b>	<b>Water Saturated</b>	<b>units</b>
	<b>Diffusivity x 10<sup>-6</sup></b>	1.03	0.87	m <sup>2</sup> /s
	<b>Thermal Conductivity</b>	1.85	1.83	W/mK
		0.67	0.84	J/K kg
<b>Smooth</b>				
	<b>Density x 10<sup>-6</sup></b>	2.67	2.49	kg/m <sup>3</sup>
	<b>Absorption/ Moisture</b>	4.50		%
	<b>Formation/Stratigraphic Unit</b>	Nicosia (Athalassa Member)		
	<b>Lithology</b>	Marly Sandstone		


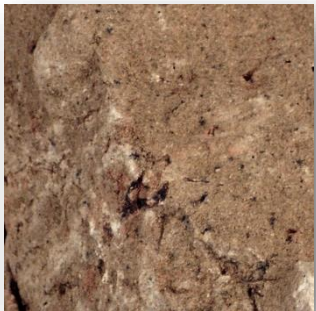
**Sample 072** – Calcarenite, Nicosia Formation (Athalassa Member)



		<b>Dry</b>	<b>Water Saturated</b>	<b>units</b>
	<b>Diffusivity x 10<sup>-6</sup></b>	0.57	0.86	m <sup>2</sup> /s
	<b>Thermal Conductivity</b>	0.82	1.29	W/mK
<b>Smooth</b> 		0.61	0.75	J/K kg
	<b>Specific Heat Capacity x 10<sup>-3</sup></b>			
	<b>Density x 10<sup>-6</sup></b>	2.35	2.01	kg/m <sup>3</sup>
	<b>Absorption/ Moisture</b>	14.52		%
<b>Formation/Stratigraphic Unit</b>	Nicosia (Athalassa Member)			
<b>Lithology</b>	Calcarenite			

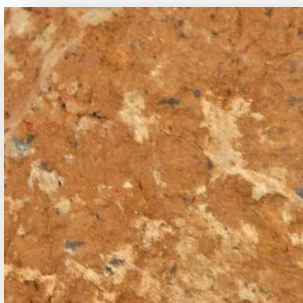

**Sample 073 - Yellowish silty Sand, Apalos Formation**



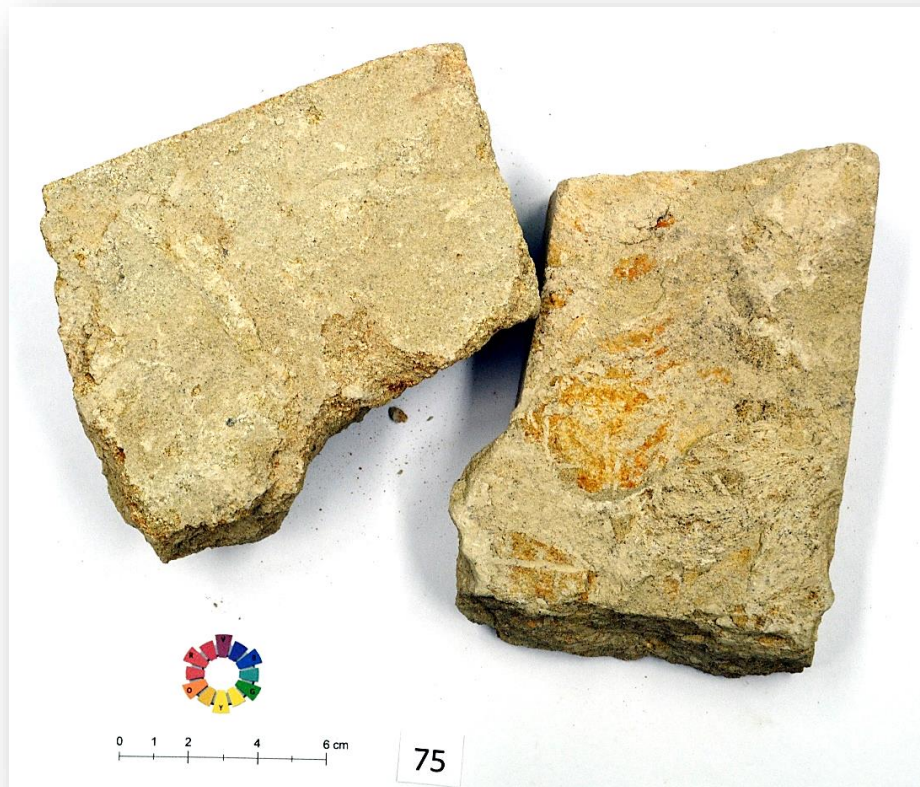
 <p><b>Smooth</b></p>		<b>Dry</b>	<b>Water Saturated</b>	<b>units</b>
	<b>Diffusivity x 10<sup>-6</sup></b>	0.46	0.48	m <sup>2</sup> /s
	<b>Thermal Conductivity</b>	0.63	0.78	W/mK
	<b>Specific Heat Capacity x 10<sup>-3</sup></b>	0.82	1.00	J/K kg
	<b>Density x 10<sup>-6</sup></b>	1.62	1.68	kg/m <sup>3</sup>
	<b>Absorption/ Moisture</b>	6.31		%
	<b>Formation/Stratigraphic Unit</b>	Apalos		
	<b>Lithology</b>	Yellowish silty Sand		



**Sample 074** - Reddish silty Sand, Apalos Formation



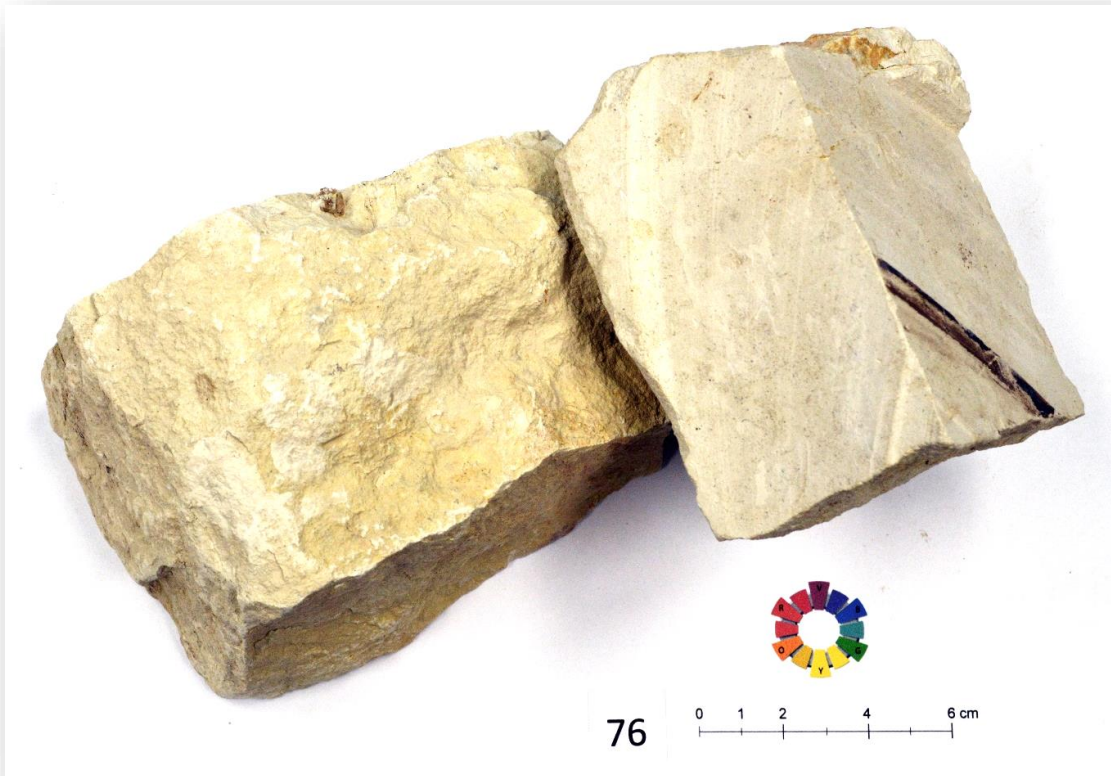
 <p><b>Smooth</b></p>		<b>Dry</b>	<b>Water Saturated</b>	<b>units</b>
	<b>Diffusivity x 10<sup>-6</sup></b>	0.499	0.525	m <sup>2</sup> /s
	<b>Thermal Conductivity</b>	0.729	1.050	W/mK
	<b>Specific Heat Capacity x 10<sup>-3</sup></b>	0.878	1.252	J/K kg
	<b>Density x 10<sup>-6</sup></b>	1.59	1.66	kg/m <sup>3</sup>
	<b>Absorption/ Moisture</b>	7.38		%
	<b>Formation/Stratigraphic Unit</b>	Apalos		
	<b>Lithology</b>	Reddish silty Sand		



**Sample 075 – Calcarenite, Pachna Formation**



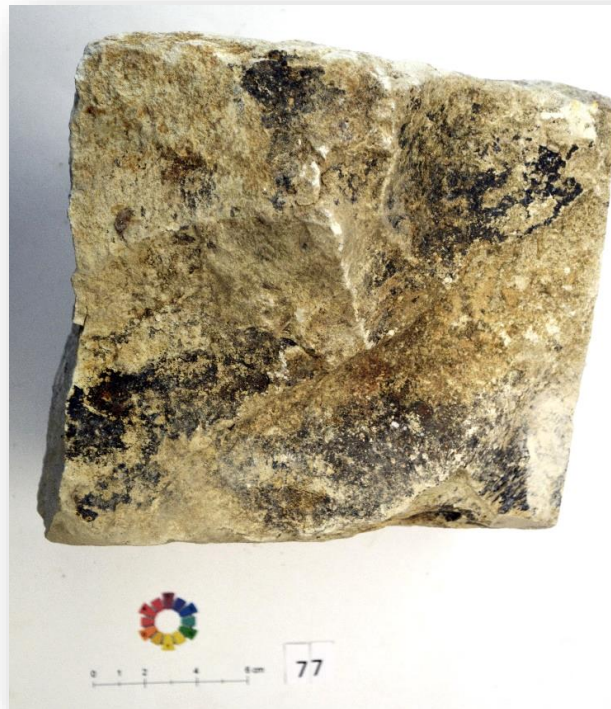
 <p><b>smooth</b></p>		<b>Dry</b>	<b>Water Saturated</b>	<b>units</b>
	<b>Diffusivity x 10<sup>-6</sup></b>	0.69	0.86	m <sup>2</sup> /s
	<b>Thermal Conductivity</b>	1.04	1.59	W/mK
	<b>Specific Heat Capacity x 10<sup>-3</sup></b>	0.60	0.83	J/K kg
	<b>Density x 10<sup>-6</sup></b>	2.52	2.23	kg/m <sup>3</sup>
	<b>Absorption/ Moisture</b>	9.43		%
	<b>Formation/Stratigraphic Unit</b>	Pachna		
	<b>Lithology</b>	Calcarenite		

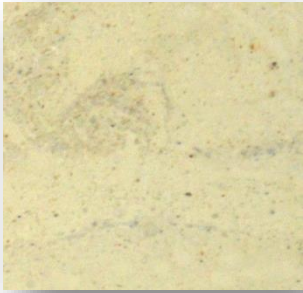

**Sample 076 - Marly Chalk, Pachna Formation**



 <b>smooth</b>		<b>Dry</b>	<b>Water Saturated</b>	<b>units</b>
	<b>Diffusivity x 10<sup>-6</sup></b>	0.83	0.91	m <sup>2</sup> /s
	<b>Thermal Conductivity</b>	1.59	1.85	W/mK
	<b>Specific Heat Capacity x 10<sup>-3</sup></b>	0.73	0.86	J/K kg
	<b>Density x 10<sup>-6</sup></b>	2.62	2.35	kg/m <sup>3</sup>
	<b>Absorption/ Moisture</b>	7.53		%
	<b>Formation/Stratigraphic Unit</b>	Pachna		
	<b>Lithology</b>	Marly Chalk		

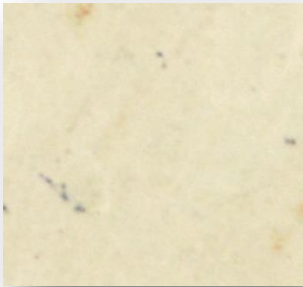

**Sample 077 - Marly Chalk, Pachna Formation**



 <p><b>smooth</b></p>		<b>Dry</b>	<b>Water Saturated</b>	<b>units</b>
	<b>Diffusivity x 10<sup>-6</sup></b>	0.85	0.95	m <sup>2</sup> /s
	<b>Thermal Conductivity</b>	1.70	1.96	W/mK
	<b>Specific Heat Capacity x 10<sup>-3</sup></b>	0.75	0.85	J/K kg
	<b>Density x 10<sup>-6</sup></b>	2.67	2.45	kg/m <sup>3</sup>
	<b>Absorption/ Moisture</b>	5.71		%
	<b>Formation/Stratigraphic Unit</b>	Pachna		
	<b>Lithology</b>	Marly Chalk		

**Sample 078** - Chalk, Pachna Formation





 <p><b>Smooth</b></p>		<b>Dry</b>	<b>Water Saturated</b>	<b>units</b>
	<b>Diffusivity x 10<sup>-6</sup></b>	0.79	0.99	m <sup>2</sup> /s
	<b>Thermal Conductivity</b>	1.38	1.57	W/mK
	<b>Specific Heat Capacity x 10<sup>-3</sup></b>	0.66	0.69	J/K kg
	<b>Density x 10<sup>-6</sup></b>	2.63	2.30	kg/m <sup>3</sup>
	<b>Absorption/ Moisture</b>	9.74		%
	<b>Formation/Stratigraphic Unit</b>	Pachna		
	<b>Lithology</b>	Chalk		

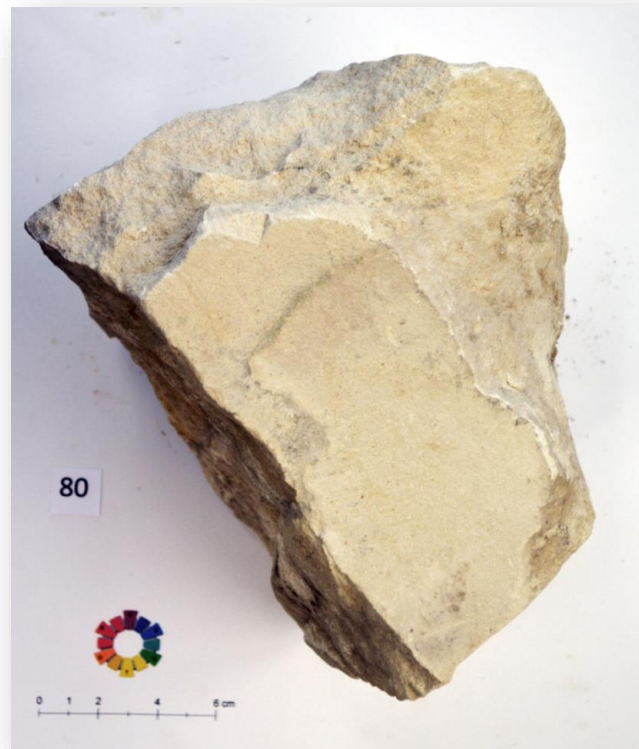




**Sample 079** - Marly Chalk, Pachna Formation



 <p><b>smooth</b></p>		<b>Dry</b>	<b>Water Saturated</b>	<b>units</b>
	<b>Diffusivity x 10<sup>-6</sup></b>	0.61	0.78	m <sup>2</sup> /s
	<b>Thermal Conductivity</b>	1.07	1.65	W/mK
	<b>Specific Heat Capacity x 10<sup>-3</sup></b>	0.66	0.94	J/K kg
	<b>Density x 10<sup>-6</sup></b>	2.64	2.24	kg/m <sup>3</sup>
	<b>Absorption/ Moisture</b>	12.13		%
	<b>Formation/Stratigraphic Unit</b>	Pachna		
	<b>Lithology</b>	Marly Chalk		



**Sample 080** - Chalk, Pachna Formation



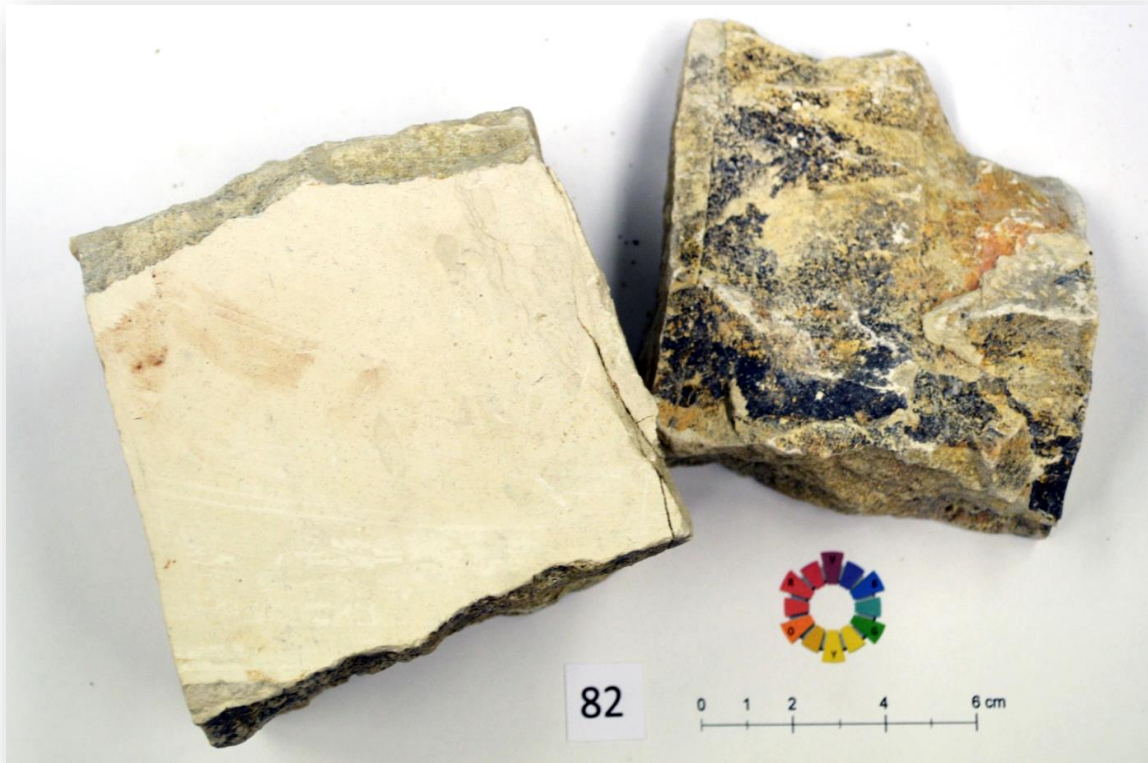
 <p><b>Smooth</b></p>		<b>Dry</b>	<b>Water Saturated</b>	<b>units</b>
	<b>Diffusivity x 10<sup>-6</sup></b>	1.14	1.09	m <sup>2</sup> /s
	<b>Thermal Conductivity</b>	2.20	2.38	W/mK
	<b>Specific Heat Capacity x 10<sup>-3</sup></b>	0.74	0.89	J/K kg
	<b>Density x 10<sup>-6</sup></b>	2.60	2.47	kg/m <sup>3</sup>
	<b>Absorption/ Moisture</b>	3.45		%
	<b>Formation/Stratigraphic Unit</b>	Pachna		
	<b>Lithology</b>	Chalk		

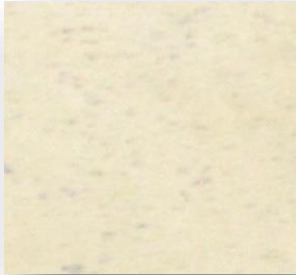

**Sample 081 – Limestone, Pachna Formation (Terra Member)**



 <b>smooth</b>		<b>Dry</b>	<b>Water Saturated</b>	<b>units</b>
	<b>Diffusivity x 10<sup>-6</sup></b>	1.46	1.23	m <sup>2</sup> /s
	<b>Thermal Conductivity</b>	2.56	2.55	W/mK
	<b>Specific Heat Capacity x 10<sup>-3</sup></b>	0.67	0.81	J/K kg
	<b>Density x 10<sup>-6</sup></b>	2.63	2.57	kg/m <sup>3</sup>
	<b>Absorption/ Moisture</b>	1.47		%
	<b>Formation/Stratigraphic Unit</b>	Pachna (Terra Member)		
	<b>Lithology</b>	Limestone		

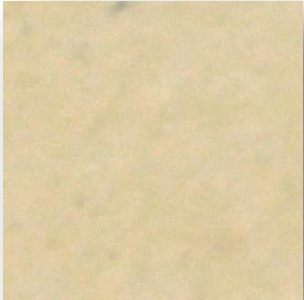

**Sample 082** - Chalk, Pachna Formation



		<b>Dry</b>	<b>Water Saturated</b>	<b>units</b>
	<b>Diffusivity x 10<sup>-6</sup></b>	0.88	0.94	m <sup>2</sup> /s
	<b>Thermal Conductivity</b>	1.80	2.05	W/mK
<b>smooth</b> 	<b>Specific Heat Capacity x 10<sup>-3</sup></b>	0.77	0.91	J/K kg
	<b>Density x 10<sup>-6</sup></b>	2.67	2.41	kg/m <sup>3</sup>
	<b>Absorption/ Moisture</b>	6.80		%
	<b>Formation/Stratigraphic Unit</b>	Pachna		
<b>Lithology</b>	Chalk			

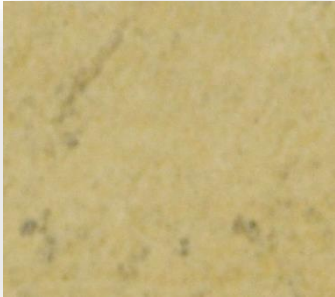

**Sample 083** - Chalk, Lefkara Formation



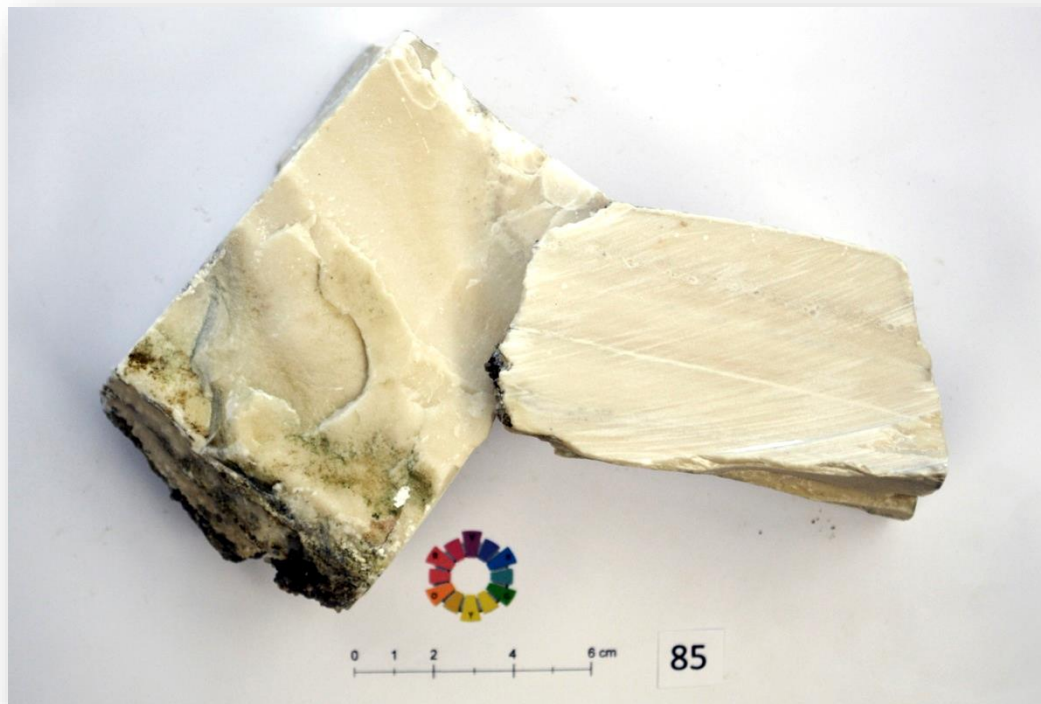
 <b>Smooth</b>		<b>Dry</b>	<b>Water Saturated</b>	<b>units</b>
	<b>Diffusivity x 10<sup>-6</sup></b>	0.88	0.99	m <sup>2</sup> /s
	<b>Thermal Conductivity</b>	1.67	1.90	W/mK
		0.72	0.84	J/K kg
	<b>Density x 10<sup>-6</sup></b>	2.64	2.28	kg/m <sup>3</sup>
	<b>Absorption/ Moisture</b>	10.61		%
	<b>Formation/Stratigraphic Unit</b>	Lefkara		
	<b>Lithology</b>	Chalk		

**Sample 084** - Reef Limestone, Pachna Formation (Terra Member)



 <p><b>Smooth</b></p>		<b>Dry</b>	<b>Water Saturated</b>	<b>units</b>
	<b>Diffusivity x 10<sup>-6</sup></b>	1.09	1.29	m <sup>2</sup> /s
	<b>Thermal Conductivity</b>	1.87	2.04	W/mK
	<b>Specific Heat Capacity x 10<sup>-3</sup></b>	0.64	0.64	J/K kg
	<b>Density x 10<sup>-6</sup></b>	2.67	2.49	kg/m <sup>3</sup>
	<b>Absorption/ Moisture</b>	4.67		%
	<b>Formation/Stratigraphic Unit</b>	Pachna (Terra Member)		
	<b>Lithology</b>	Reef Limestone		



**Sample 085 – Gypsum, Kalavasos Formation**



 <p><b>Smooth</b></p>		<b>Dry</b>	<b>Water Saturated</b>	<b>units</b>
	<b>Diffusivity x 10<sup>-6</sup></b>	0.66	0.47	m <sup>2</sup> /s
	<b>Thermal Conductivity</b>	1.30	0.83	W/mK
	<b>Specific Heat Capacity x 10<sup>-3</sup></b>	0.77	0.77	J/K kg
	<b>Density x 10<sup>-6</sup></b>	2.57	2.26	kg/m <sup>3</sup>
	<b>Absorption/ Moisture</b>	9.69		%
	<b>Formation/Stratigraphic Unit</b>	Kalavasos		
	<b>Lithology</b>	Gypsum		

**Sample 086 - Volcaniclastic Sandstone, Kannaviou Formation**

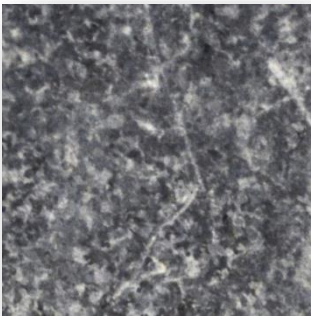



		<b>Dry</b>	<b>Water Saturated</b>	<b>units</b>
	<b>Diffusivity x 10<sup>-6</sup></b>	0.41	0.61	m <sup>2</sup> /s
	<b>Thermal Conductivity</b>	0.60	1.09	W/mK
	<b>Specific Heat Capacity x 10<sup>-3</sup></b>	0.58	0.91	J/K kg
	<b>Density x 10<sup>-6</sup></b>	2.55	1.96	kg/m <sup>3</sup>
	<b>Absorption/ Moisture</b>	24.05		%
	<b>Formation/Stratigraphic Unit</b>	Kannaviou		
	<b>Lithology</b>	Volcaniclastic Sandstone		



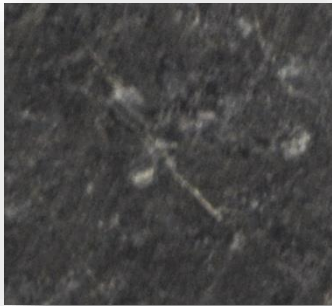

**Sample 087** – Gabbro, Plutonic Sequence



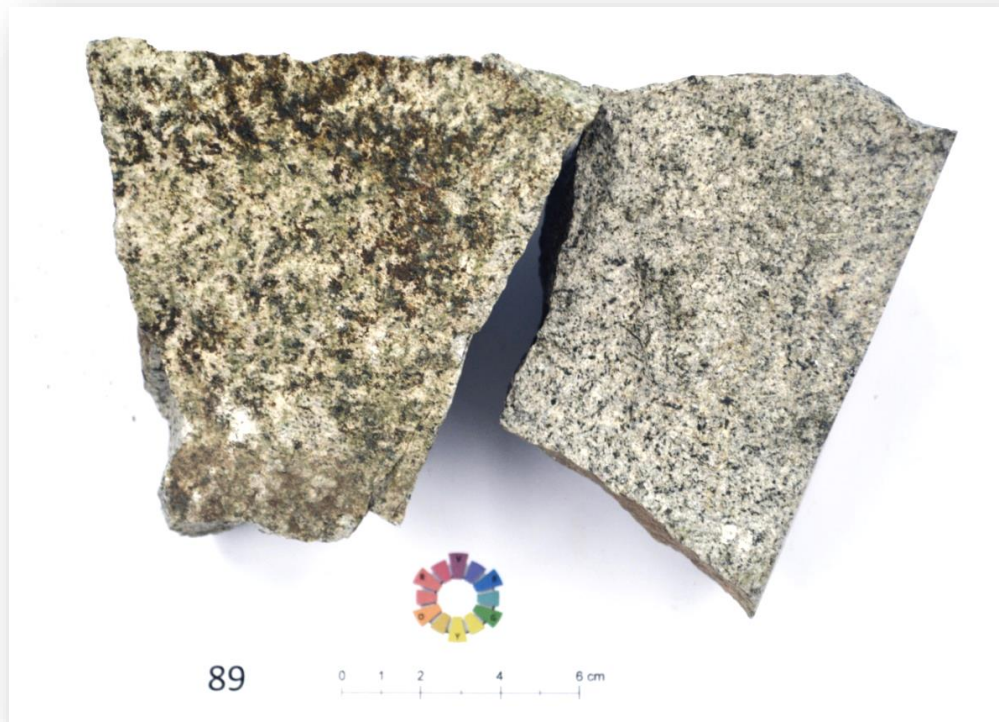
		<b>Dry</b>	<b>Water Saturated</b>	<b>units</b>
	<b>Diffusivity x 10<sup>-6</sup></b>	1.05	1.01	m <sup>2</sup> /s
	<b>Thermal Conductivity</b>	2.13	2.20	W/mK
		0.71	0.76	J/K kg
<b>Specific Heat Capacity x 10<sup>-3</sup></b>				
<b>Smooth</b>				
	<b>Density x 10<sup>-6</sup></b>	2.87	2.84	kg/m <sup>3</sup>
	<b>Absorption/ Moisture</b>	0.70		%
	<b>Formation/Stratigraphic Unit</b>	Plutonic Sequence		
	<b>Lithology</b>	Gabbro		



**Sample 088 – Serpentinite, Mantle Sequence**



 <p><b>Smooth</b></p>		<b>Dry</b>	<b>Water Saturated</b>	<b>units</b>
	<b>Diffusivity x 10<sup>-6</sup></b>	0.84	1.02	m <sup>2</sup> /s
	<b>Thermal Conductivity</b>	1.72	2.15	W/mK
	<b>Specific Heat Capacity x 10<sup>-3</sup></b>	0.77	0.89	J/K kg
	<b>Density x 10<sup>-6</sup></b>	2.65	2.36	kg/m <sup>3</sup>
	<b>Absorption/ Moisture</b>	7.92		%
	<b>Formation/Stratigraphic Unit</b>	Mantle Sequence		
	<b>Lithology</b>	Serpentinite		



**Sample 089** – Plagiogranite, Plutonic Sequence



		<b>Dry</b>	<b>Water Saturated</b>	<b>units</b>
	<b>Diffusivity x 10<sup>-6</sup></b>	1.61	1.54	m <sup>2</sup> /s
	<b>Thermal Conductivity</b>	3.42	3.60	W/mK
		0.77	0.86	J/K kg
	<b>Density x 10<sup>-6</sup></b>	2.76	2.73	kg/m <sup>3</sup>
	<b>Absorption/ Moisture</b>	0.74		%
	<b>Formation/Stratigraphic Unit</b>	Plutonic Sequence		
	<b>Lithology</b>	Plagiogranite		

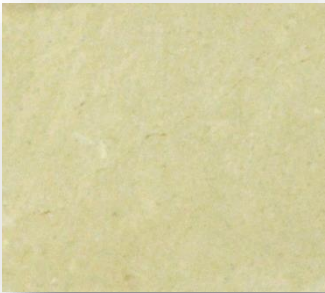

**Sample 090** – Chert, Lefkara Formation



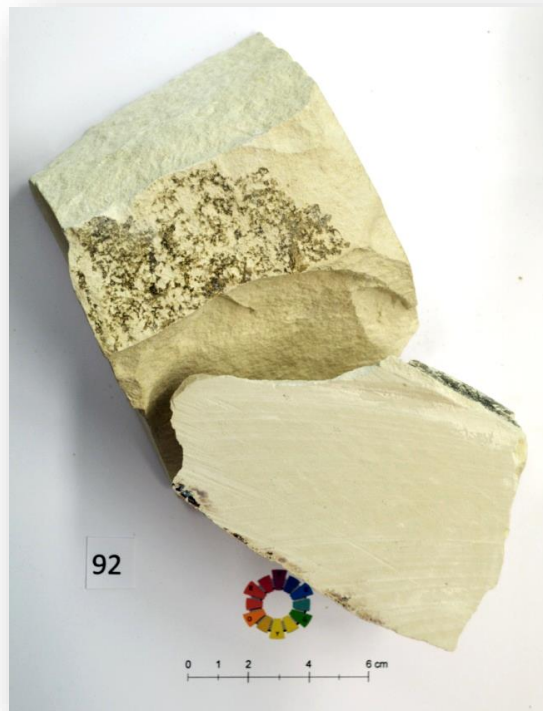
 <p><b>Smooth</b></p>		<b>Dry</b>	<b>Water Saturated</b>	<b>units</b>
	<b>Diffusivity x 10<sup>-6</sup></b>	1.04	0.96	m <sup>2</sup> /s
	<b>Thermal Conductivity</b>	1.91	1.94	W/mK
	<b>Specific Heat Capacity x 10<sup>-3</sup></b>	0.74	0.87	J/K kg
	<b>Density x 10<sup>-6</sup></b>	2.48	2.33	kg/m <sup>3</sup>
	<b>Absorption/ Moisture</b>	4.61		%
	<b>Formation/Stratigraphic Unit</b>	Lefkara		
	<b>Lithology</b>	Chert		


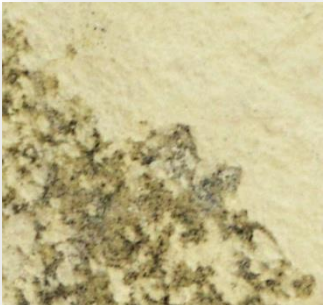
**Sample 091** – Chert, Lefkara Formation



 <b>Smooth</b>		<b>Dry</b>	<b>Water Saturated</b>	<b>units</b>
	<b>Diffusivity x 10<sup>-6</sup></b>	0.92	0.97	m <sup>2</sup> /s
	<b>Thermal Conductivity</b>	1.77	2.00	W/mK
		0.73	0.86	J/K kg
	<b>Density x 10<sup>-6</sup></b>	2.64	2.40	kg/m <sup>3</sup>
	<b>Absorption/ Moisture</b>	6.66		%
	<b>Formation/Stratigraphic Unit</b>	Lefkara		
	<b>Lithology</b>	Chalk		


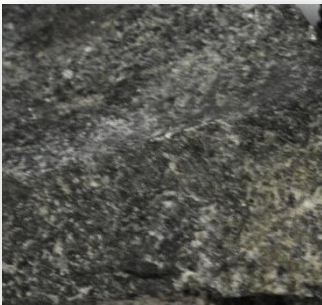
**Sample 092**– Massive Chert, Lefkara Formation



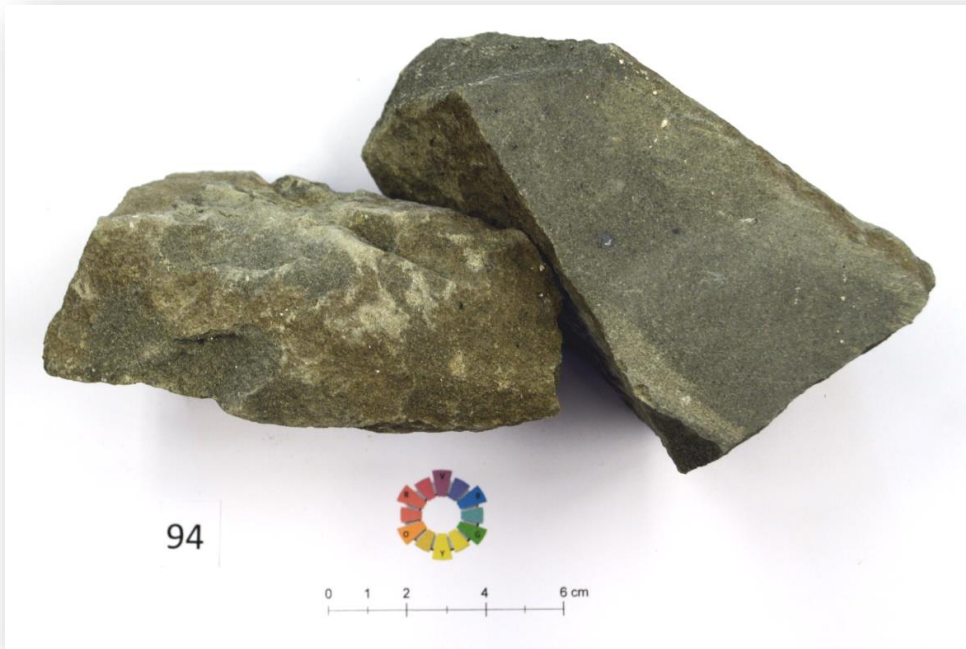
 <p><b>Smooth</b></p>		<b>Dry</b>	<b>Water Saturated</b>	<b>units</b>
	<b>Diffusivity x 10<sup>-6</sup></b>	0.65	0.99	m <sup>2</sup> /s
	<b>Thermal Conductivity</b>	1.28	1.70	W/mK
	<b>Specific Heat Capacity x 10<sup>-3</sup></b>	0.77	0.78	J/K kg
	<b>Density x 10<sup>-6</sup></b>	2.55	2.22	kg/m <sup>3</sup>
	<b>Absorption/ Moisture</b>	10.50		%
	<b>Formation/Stratigraphic Unit</b>	Lefkara		
	<b>Lithology</b>	Massive Chalk		



**Sample 093 – Diabase, Sheeted Dykes**



		<b>Dry</b>	<b>Water Saturated</b>	<b>units</b>
	<b>Diffusivity x 10<sup>-6</sup></b>	1.04	0.86	m <sup>2</sup> /s
	<b>Thermal Conductivity</b>	1.79	1.78	W/mK
<b>Smooth</b> 		0.63	0.76	J/K kg
	<b>Density x 10<sup>-6</sup></b>	2.80	2.75	kg/m <sup>3</sup>
	<b>Absorption/ Moisture</b>	0.95		%
	<b>Formation/Stratigraphic Unit</b>	Sheeted Dykes		
	<b>Lithology</b>	Diabase		

**Sample 094** – Diabase, Volcanic Sequence (Basal Group)



		<b>Dry</b>	<b>Water Saturated</b>	<b>units</b>
	<b>Diffusivity x 10<sup>-6</sup></b>	0.82	0.78	m <sup>2</sup> /s
	<b>Thermal Conductivity</b>	1.40	1.56	W/mK
		0.67	0.79	J/K kg
<b>Specific Heat Capacity x 10<sup>-3</sup></b>				
<b>Smooth</b>				
	<b>Density x 10<sup>-6</sup></b>	2.57	2.52	kg/m <sup>3</sup>
	<b>Absorption/ Moisture</b>	1.41		%
	<b>Formation/Stratigraphic Unit</b>	Volcanic Sequence (Basal Group)		
	<b>Lithology</b>	Diabase		



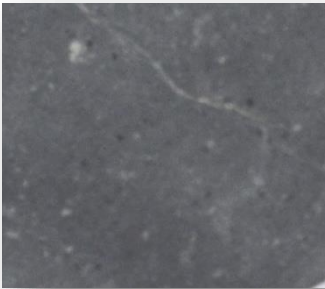

**Sample 095 – Microgabbro, Sheeted Dykes**



 <p><b>Smooth</b></p>		<b>Dry</b>	<b>Water Saturated</b>	<b>units</b>
	<b>Diffusivity x 10<sup>-6</sup></b>	1.10	0.96	m <sup>2</sup> /s
	<b>Thermal Conductivity</b>	2.07	2.00	W/mK
	<b>Specific Heat Capacity x 10<sup>-3</sup></b>	0.63	0.70	J/K kg
	<b>Density x 10<sup>-6</sup></b>	2.99	2.97	kg/m <sup>3</sup>
	<b>Absorption/ Moisture</b>	0.28		%
	<b>Formation/Stratigraphic Unit</b>	Sheeted Dykes		
	<b>Lithology</b>	Microgabbro		

**Sample 096 – Diabase, Sheeted Dykes**



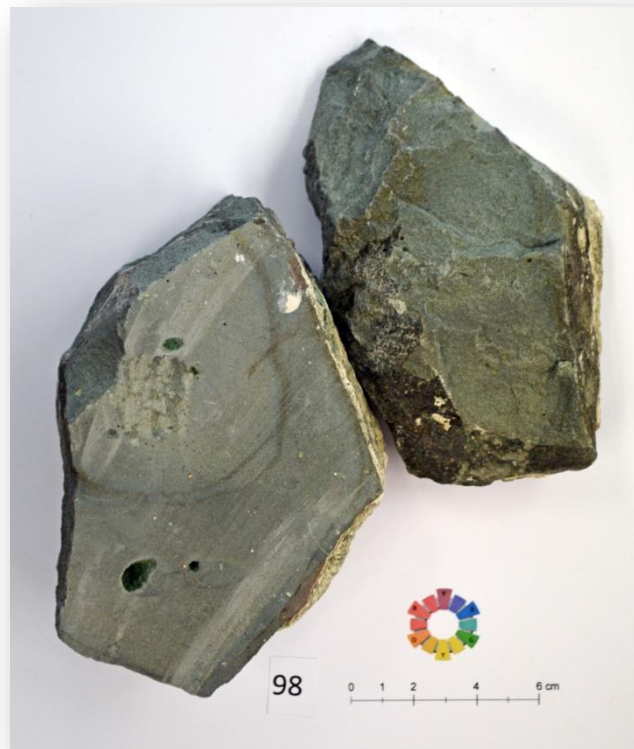
 <p><b>Smooth</b></p>		<b>Dry</b>	<b>Water Saturated</b>	<b>units</b>
	<b>Diffusivity x 10<sup>-6</sup></b>	1.00	1.10	m <sup>2</sup> /s
	<b>Thermal Conductivity</b>	2.13	2.35	W/m K
	<b>Specific Heat Capacity x 10<sup>-3</sup></b>	0.75	0.76	J/K kg
	<b>Density x 10<sup>-6</sup></b>	2.85	2.83	kg/m <sup>3</sup>
	<b>Absorption/ Moisture</b>	0.41		%
	<b>Formation/Stratigraphic Unit</b>	Sheeted Dykes		
	<b>Lithology</b>	Diabase		

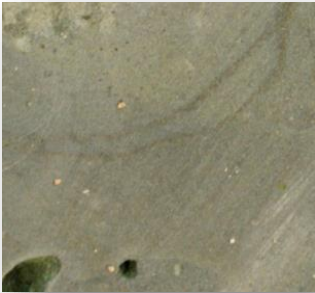

**Sample 097**– Diabase, Sheeted Dykes



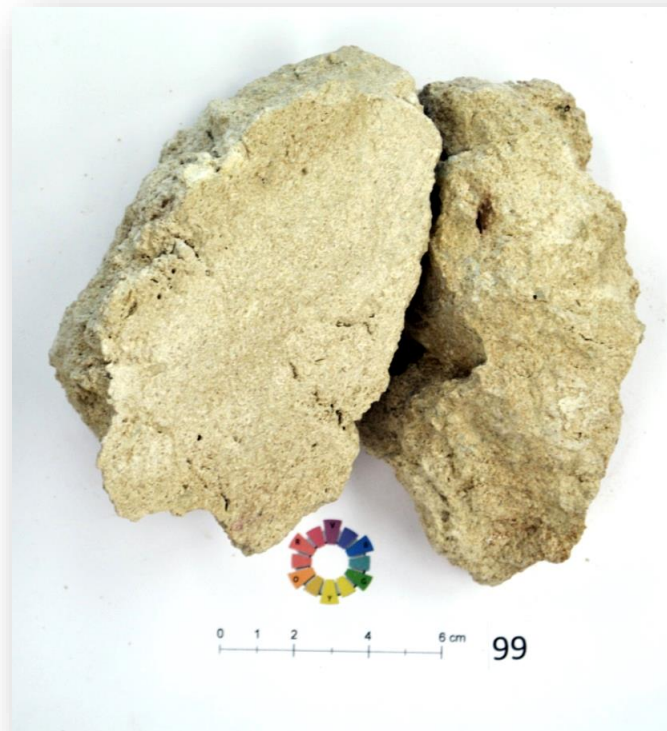
		<b>Dry</b>	<b>Water Saturated</b>	<b>units</b>
	<b>Diffusivity x 10<sup>-6</sup></b>	0.92	0.93	m <sup>2</sup> /s
	<b>Thermal Conductivity</b>	1.67	1.90	W/mK
		0.68	0.78	
	<b>Specific Heat Capacity x 10<sup>-3</sup></b>			J/K kg
<b>Smooth</b>				
	<b>Density x 10<sup>-6</sup></b>	2.68	2.63	kg/m <sup>3</sup>
	<b>Absorption/ Moisture</b>	1.15		%
	<b>Formation/Stratigraphic Unit</b>	Sheeted Dykes		
	<b>Lithology</b>	Diabase		



**Sample 098 – Basalt, Volcanic Sequence (Lower Pillow Lavas)**



 <p><b>Smooth</b></p>		<b>Dry</b>	<b>Water Saturated</b>	<b>units</b>
	<b>Diffusivity x 10<sup>-6</sup></b>	0.90	0.80	m <sup>2</sup> /s
	<b>Thermal Conductivity</b>	1.46	1.48	W/mK
		0.64	0.77	J/K kg
	<b>Density x 10<sup>-6</sup></b>	2.55	2.42	kg/m <sup>3</sup>
	<b>Absorption/ Moisture</b>	3.69		%
	<b>Formation/Stratigraphic Unit</b>	Volcanic Sequence (Lower Pillow Lavas)		
	<b>Lithology</b>	Basalt		


**Sample 099** - Reef Limestone, Pachna Formation (Koronia Member)



 <p><b>Smooth</b></p>		<b>Dry</b>	<b>Water Saturated</b>	<b>units</b>
	<b>Diffusivity x 10<sup>-6</sup></b>	0.83	0.94	m <sup>2</sup> /s
	<b>Thermal Conductivity</b>	1.23	1.62	W/mK
	<b>Specific Heat Capacity x 10<sup>-3</sup></b>	0.58	0.76	J/K kg
	<b>Density x 10<sup>-6</sup></b>	2.55	2.26	kg/m <sup>3</sup>
	<b>Absorption/ Moisture</b>	8.85		%
	<b>Formation/Stratigraphic Unit</b>	Pachna (Koronia Member)		
	<b>Lithology</b>	Reef Limestone		



**Sample 100** – Calcarenite, Nicosia Formation



		<b>Dry</b>	<b>Water Saturated</b>	<b>units</b>
	<b>Diffusivity x 10<sup>-6</sup></b>	0.66	0.99	m <sup>2</sup> /s
	<b>Thermal Conductivity</b>	0.94	1.55	W/mK
	<b>Specific Heat Capacity x 10<sup>-3</sup></b>	0.63	0.78	J/K kg
<b>Smooth</b>				
	<b>Density x 10<sup>-6</sup></b>	2.24	2.01	kg/m <sup>3</sup>
	<b>Absorption/ Moisture</b>	10.18		%
	<b>Formation/Stratigraphic Unit</b>	Nicosia		
	<b>Lithology</b>	Calcarenite		



**Sample 101 - Reef Limestone, Pachna Formation (Koronia Member)**



 <p><b>Smooth</b></p>		<b>Dry</b>	<b>Water Saturated</b>	<b>units</b>
	<b>Diffusivity x 10<sup>-6</sup></b>	0.88	0.94	m <sup>2</sup> /s
	<b>Thermal Conductivity</b>	1.52	1.92	W/mK
	<b>Specific Heat Capacity x 10<sup>-3</sup></b>	0.69	0.87	J/K kg
	<b>Density x 10<sup>-6</sup></b>	2.49	2.34	kg/m <sup>3</sup>
	<b>Absorption/ Moisture</b>	4.54		%
	<b>Formation/Stratigraphic Unit</b>	Pachna (Koronia Member)		
	<b>Lithology</b>	Reef Limestone		

**Sample 102 – Chalk, Lefkara Formation**

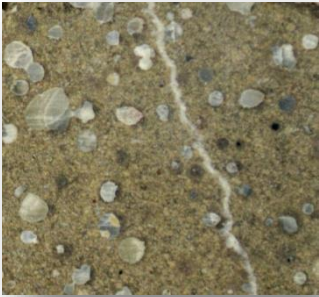
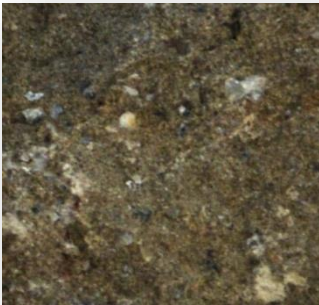


 <b>Smooth</b>		<b>Dry</b>	<b>Water Saturated</b>	<b>units</b>
	<b>Diffusivity x 10<sup>-6</sup></b>	0.49	0.73	m <sup>2</sup> /s
	<b>Thermal Conductivity</b>	0.80	1.48	W/mK
		0.65	1.01	J/K kg
	<b>Density x 10<sup>-6</sup></b>	2.54	2.03	kg/m <sup>3</sup>
	<b>Absorption/ Moisture</b>	19.80		%
	<b>Formation/Stratigraphic Unit</b>	Lefkara		
	<b>Lithology</b>	Chalk		





**Sample 103 – Basalt, Volcanic Sequence (Upper Pillow Lavas)**



 <p><b>smooth</b></p>		<b>Dry</b>	<b>Water Saturated</b>	<b>units</b>
	<b>Diffusivity x 10<sup>-6</sup></b>	0.61	0.69	m <sup>2</sup> /s
	<b>Thermal Conductivity</b>	1.11	1.39	W/mK
	<b>Specific Heat Capacity x 10<sup>-3</sup></b>	0.69	0.87	J/K kg
	<b>Density x 10<sup>-6</sup></b>	2.62	2.31	kg/m <sup>3</sup>
	<b>Absorption/ Moisture</b>	8.79		%
	<b>Formation/Stratigraphic Unit</b>	Volcanic Sequence (Upper Pillow Lavas)		
	<b>Lithology</b>	Basalt		

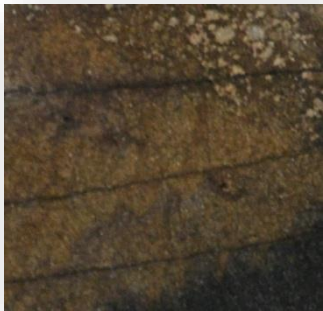

**Sample 104** – Chalk, Pachna Formation



 <b>smooth</b>		<b>Dry</b>	<b>Water Saturated</b>	<b>units</b>
	<b>Diffusivity x 10<sup>-6</sup></b>	0.64	0.79	m <sup>2</sup> /s
	<b>Thermal Conductivity</b>	1.13	1.61	W/mK
		0.73	0.96	J/K kg
	<b>Density x 10<sup>-6</sup></b>	2.42	2.12	kg/m <sup>3</sup>
	<b>Absorption/ Moisture</b>	11.00		%
	<b>Formation/Stratigraphic Unit</b>	Pachna		
	<b>Lithology</b>	Chalk		

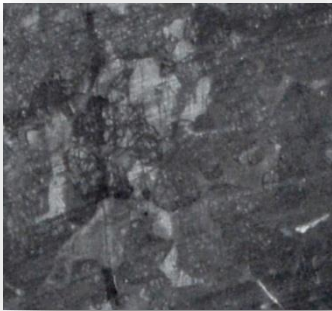

**Sample 105 – Dunite, Plutonic Sequence**



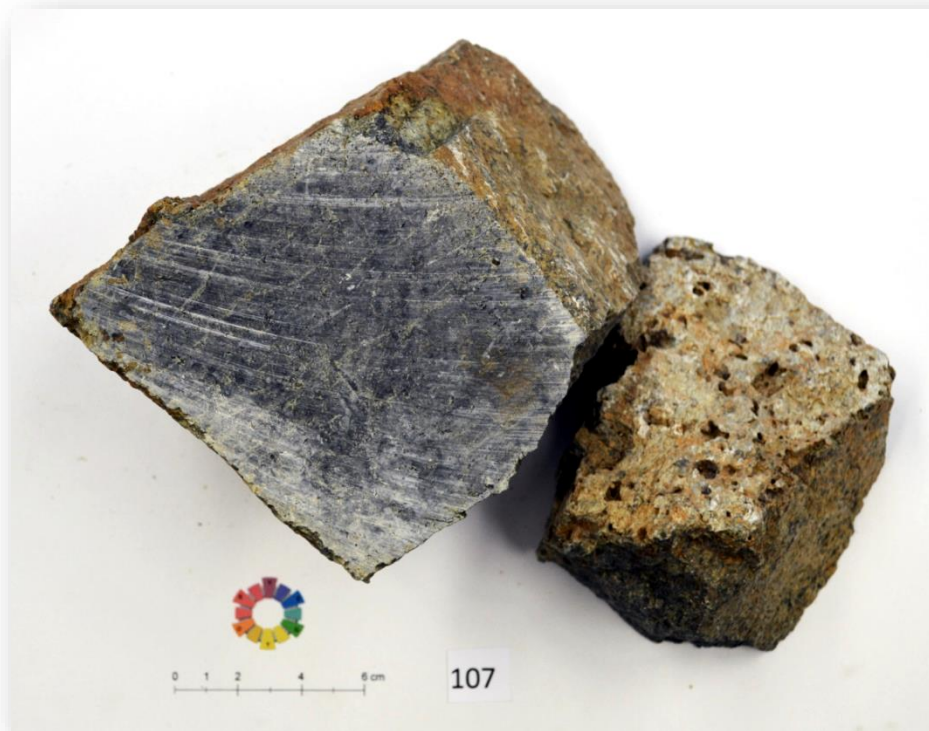
 <p><b>smooth</b></p>		<b>Dry</b>	<b>Water Saturated</b>	<b>units</b>
	<b>Diffusivity x 10<sup>-6</sup></b>	1.10	1.18	m <sup>2</sup> /s
	<b>Thermal Conductivity</b>	2.37	2.33	W/mK
	<b>Specific Heat Capacity x 10<sup>-3</sup></b>	0.80	0.75	J/K kg
	<b>Density x 10<sup>-6</sup></b>	2.66	2.63	kg/m <sup>3</sup>
	<b>Absorption/ Moisture</b>	0.54		%
	<b>Formation/Stratigraphic Unit</b>	Plutonic Sequence		
	<b>Lithology</b>	Dunite		



**Sample 106** – Wehrlite, Plutonic Sequence



		<b>Dry</b>	<b>Water Saturated</b>	<b>units</b>
	<b>Diffusivity x 10<sup>-6</sup></b>	1.28	1.22	m <sup>2</sup> /s
	<b>Thermal Conductivity</b>	2.93	2.75	W/mK
	<b>Specific Heat Capacity x 10<sup>-3</sup></b>	0.84	0.83	J/K kg
<b>smooth</b>				
	<b>Density x 10<sup>-6</sup></b>	2.74	2.72	kg/m <sup>3</sup>
	<b>Absorption/ Moisture</b>	0.47		%
	<b>Formation/Stratigraphic Unit</b>	Plutonic Sequence		
	<b>Lithology</b>	Wehrlite		



**Sample 107 – Pyroxenite, Plutonic Sequence**



 <p><b>smooth</b></p>		<b>Dry</b>	<b>Water Saturated</b>	<b>units</b>
	<b>Diffusivity x 10<sup>-6</sup></b>	1.82	1.91	m <sup>2</sup> /s
	<b>Thermal Conductivity</b>	4.17	4.53	W/m K
	<b>Specific Heat Capacity x 10<sup>-3</sup></b>	0.72	0.76	J/K kg
	<b>Density x 10<sup>-6</sup></b>	3.19	3.13	kg/m <sup>3</sup>
	<b>Absorption/ Moisture</b>	0.79		%
	<b>Formation/Stratigraphic Unit</b>	Plutonic Sequence		
	<b>Lithology</b>	Pyroxenite		



**Sample 108 – Harzburgite, Mantle Sequence**



 <p><b>smooth</b></p>		<b>Dry</b>	<b>Water Saturated</b>	<b>units</b>
	<b>Diffusivity x 10<sup>-6</sup></b>	0.97	0.78	m <sup>2</sup> /s
	<b>Thermal Conductivity</b>	2.03	1.94	W/mK
	<b>Specific Heat Capacity x 10<sup>-3</sup></b>	0.79	0.75	J/K kg
	<b>Density x 10<sup>-6</sup></b>	2.68	2.65	kg/m <sup>3</sup>
	<b>Absorption/ Moisture</b>	0.59		%
	<b>Formation/Stratigraphic Unit</b>	Mantle Sequence		
	<b>Lithology</b>	Harzburgite		

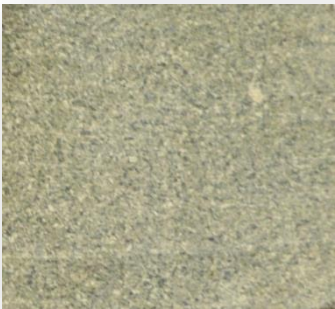
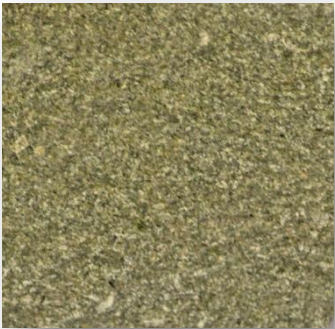
**Sample 109 - Poikilitic Wehrlite, Plutonic Sequence**



 <p>smooth</p>		<b>Dry</b>	<b>Water Saturated</b>	<b>units</b>
	<b>Diffusivity x 10<sup>-6</sup></b>	1.32	1.36	m <sup>2</sup> /s
	<b>Thermal Conductivity</b>	2.95	3.01	W/mK
	<b>Specific Heat Capacity x 10<sup>-3</sup></b>	0.80	0.81	J/K kg
	<b>Density x 10<sup>-6</sup></b>	2.77	2.76	kg/m <sup>3</sup>
	<b>Absorption/ Moisture</b>	0.33		%
	<b>Formation/Stratigraphic Unit</b>	Plutonic Sequence		
	<b>Lithology</b>	Poikilitic Wehrlite		

**Sample 110 – Microgabbro, Volcanic Sequence (Basal Group)**





 <p><b>smooth</b></p>		<b>Dry</b>	<b>Water Saturated</b>	<b>units</b>
	<b>Diffusivity x 10<sup>-6</sup></b>	1.01	0.97	m <sup>2</sup> /s
	<b>Thermal Conductivity</b>	1.99	1.94	W/mK
	<b>Specific Heat Capacity x 10<sup>-3</sup></b>	0.73	0.75	J/K kg
	<b>Density x 10<sup>-6</sup></b>	2.71	2.64	kg/m <sup>3</sup>
	<b>Absorption/ Moisture</b>	1.51		%
	<b>Formation/Stratigraphic Unit</b>	Volcanic Sequence (Basal Group)		
	<b>Lithology</b>	Microgabbro		




**Sample 111 – Gypsum, Kalavasos Formation**



		<b>Dry</b>	<b>Water Saturated</b>	<b>units</b>
	<b>Diffusivity x 10<sup>-6</sup></b>	0.72	0.67	m <sup>2</sup> /s
	<b>Thermal Conductivity</b>	1.13	1.13	W/mK
<b>smooth</b>		0.63	0.76	J/K kg
	<b>Specific Heat Capacity x 10<sup>-3</sup></b>			
	<b>Density x 10<sup>-6</sup></b>	2.49	2.21	kg/m <sup>3</sup>
	<b>Absorption/ Moisture</b>	9.18		%
	<b>Formation/Stratigraphic Unit</b>	Kalavasos		
	<b>Lithology</b>	Gypsum		



**Sample 112 - Chalky Marl, Pachna Formation**



		<b>Dry</b>	<b>Water Saturated</b>	<b>units</b>
	<b>Diffusivity x 10<sup>-6</sup></b>	0.46	0.59	m <sup>2</sup> /s
	<b>Thermal Conductivity</b>	0.69	0.95	W/mK
<b>Specific Heat Capacity x 10<sup>-3</sup></b>	0.88	1.01	J/K kg	
<b>smooth</b>				
	<b>Density x 10<sup>-6</sup></b>	1.65	1.72	kg/m <sup>3</sup>
	<b>Absorption/ Moisture</b>	6.35		%
	<b>Formation/Stratigraphic Unit</b>	Pachna		
	<b>Lithology</b>	Chalky Marl		



**Sample 113 – Calcareenite, Pachna Formation**



 <p><b>smooth</b></p>		<b>Dry</b>	<b>Water Saturated</b>	<b>units</b>
	<b>Diffusivity x 10<sup>-6</sup></b>	0.68	0.87	m <sup>2</sup> /s
	<b>Thermal Conductivity</b>	1.01	1.77	W/mK
	<b>Specific Heat Capacity x 10<sup>-3</sup></b>	0.64	0.96	J/K kg
	<b>Density x 10<sup>-6</sup></b>	2.33	2.13	kg/m <sup>3</sup>
	<b>Absorption/ Moisture</b>	7.44		%
	<b>Formation/Stratigraphic Unit</b>	Pachna		
	<b>Lithology</b>	Calcareenite		



**Sample 114 – Chalk, Pachna Formation**



 <p><b>smooth</b></p>		<b>Dry</b>	<b>Water Saturated</b>	<b>units</b>
	<b>Diffusivity x 10<sup>-6</sup></b>	1.16	1.13	m <sup>2</sup> /s
	<b>Thermal Conductivity</b>	2.09	2.37	W/mK
	<b>Specific Heat Capacity x 10<sup>-3</sup></b>	0.70	0.84	J/K kg
	<b>Density x 10<sup>-6</sup></b>	2.59	2.49	kg/m <sup>3</sup>
	<b>Absorption/ Moisture</b>	2.60		%
	<b>Formation/Stratigraphic Unit</b>	Pachna		
	<b>Lithology</b>	Chalk		

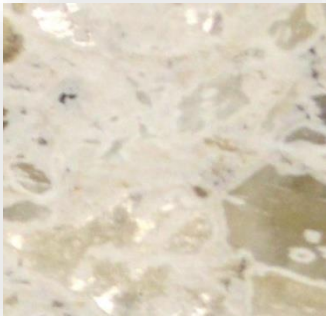

**Sample 115 - Breccia Reef Limestone**



 <p><b>smooth</b></p>		<b>Dry</b>	<b>Water Saturated</b>	<b>units</b>
	<b>Diffusivity x 10<sup>-6</sup></b>	0.55	0.72	m <sup>2</sup> /s
	<b>Thermal Conductivity</b>	0.78	1.53	W/mK
	<b>Specific Heat Capacity x 10<sup>-3</sup></b>	0.55	1.01	J/K kg
	<b>Density x 10<sup>-6</sup></b>	2.57	2.09	kg/m <sup>3</sup>
	<b>Absorption/ Moisture</b>	17.03		%
	<b>Formation/Stratigraphic Unit</b>	Not Defined		
	<b>Lithology</b>	Breccia Reef Limestone		



**Sample 116 – Gypsum, Kalavasos Formation**



 <b>smooth</b>		<b>Dry</b>	<b>Water Saturated</b>	<b>units</b>
	<b>Diffusivity x 10<sup>-6</sup></b>	0.82	0.65	m <sup>2</sup> /s
	<b>Thermal Conductivity</b>	1.35	1.07	W/mK
		0.64	0.72	J/K kg
	<b>Density x 10<sup>-6</sup></b>	2.61	2.27	kg/m <sup>3</sup>
	<b>Absorption/ Moisture</b>	10.20		%
	<b>Formation/Stratigraphic Unit</b>	Kalavasos		
	<b>Lithology</b>	Gypsum		

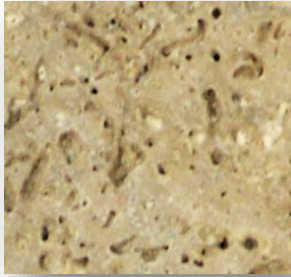

**Sample 117 - Reef Limestone, Pachna Formation (Koronia Member)**



 <p><b>smooth</b></p>		<b>Dry</b>	<b>Water Saturated</b>	<b>units</b>
	<b>Diffusivity x 10<sup>-6</sup></b>	0.54	0.64	m <sup>2</sup> /s
	<b>Thermal Conductivity</b>	0.90	1.17	W/mK
	<b>Specific Heat Capacity x 10<sup>-3</sup></b>	0.59	0.74	J/K kg
	<b>Density x 10<sup>-6</sup></b>	2.83	2.52	kg/m <sup>3</sup>
	<b>Absorption/ Moisture</b>	7.28		%
	<b>Formation/Stratigraphic Unit</b>	Pachna (Koronia Member)		
	<b>Lithology</b>	Reef Limestone		

**Sample 118 - Reef Limestone, Pachna Formation (Koronia Member)**

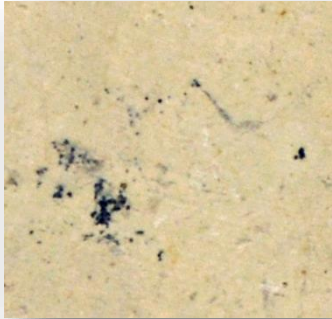


 <p><b>smooth</b></p>		<b>Dry</b>	<b>Water Saturated</b>	<b>units</b>
	<b>Diffusivity x 10<sup>-6</sup></b>	0.87	0.85	m <sup>2</sup> /s
	<b>Thermal Conductivity</b>	1.28	1.59	W/mK
	<b>Specific Heat Capacity x 10<sup>-3</sup></b>	0.56	0.76	J/K kg
	<b>Density x 10<sup>-6</sup></b>	2.62	2.46	kg/m <sup>3</sup>
	<b>Absorption/ Moisture</b>	4.09		%
	<b>Formation/Stratigraphic Unit</b>	Pachna (Koronia Member)		
	<b>Lithology</b>	Reef Limestone		



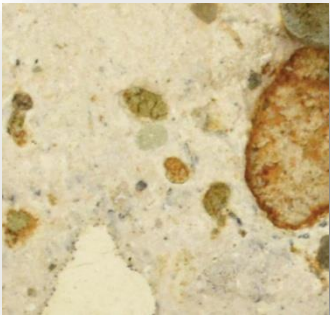
**Sample 119 - Chalk, Pachna Formation**



 <p><b>smooth</b></p>		<b>Dry</b>	<b>Water Saturated</b>	<b>units</b>
	<b>Diffusivity x 10<sup>-6</sup></b>	1.13	0.96	m <sup>2</sup> /s
	<b>Thermal Conductivity</b>	1.95	2.11	W/mK
	<b>Specific Heat Capacity x 10<sup>-3</sup></b>	0.65	0.89	J/K kg
	<b>Density x 10<sup>-6</sup></b>	2.66	2.45	kg/m <sup>3</sup>
	<b>Absorption/ Moisture</b>	5.41		%
	<b>Formation/Stratigraphic Unit</b>	Pachna		
	<b>Lithology</b>	Chalk		



**Sample 120 – Calcareenite, Pachna Formation**



 <b>smooth</b>		<b>Dry</b>	<b>Water Saturated</b>	<b>units</b>
	<b>Diffusivity x 10<sup>-6</sup></b>	0.98	0.97	m <sup>2</sup> /s
	<b>Thermal Conductivity</b>	1.33	1.96	W/mK
	<b>Specific Heat Capacity x 10<sup>-3</sup></b>	0.54	0.85	J/K kg
	<b>Density x 10<sup>-6</sup></b>	2.54	2.38	kg/m <sup>3</sup>
	<b>Absorption/ Moisture</b>	4.69		%
	<b>Formation/Stratigraphic Unit</b>	Pachna		
	<b>Lithology</b>	Calcareenite		

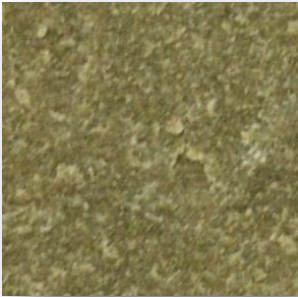
**Sample 121 – Gypsum, Kalavassos Formation**



 <p><b>smooth</b></p>		<b>Dry</b>	<b>Water Saturated</b>	<b>units</b>
	<b>Diffusivity x 10<sup>-6</sup></b>	0.68	0.54	m <sup>2</sup> /s
	<b>Thermal Conductivity</b>	1.23	0.84	W/mK
		0.72	0.70	J/K kg
	<b>Density x 10<sup>-6</sup></b>	2.54	2.24	kg/m <sup>3</sup>
	<b>Absorption/ Moisture</b>	9.74		%
	<b>Formation/Stratigraphic Unit</b>	Kalavassos		
	<b>Lithology</b>	Gypsum		



**Sample 122 – Gypsum, Kalavasos Formation**



		<b>Dry</b>	<b>Water Saturated</b>	<b>units</b>
	<b>Diffusivity x 10<sup>-6</sup></b>	0.74	0.33	m <sup>2</sup> /s
	<b>Thermal Conductivity</b>	1.38	0.63	W/mK
	<b>Specific Heat Capacity x 10<sup>-3</sup></b>	0.76	0.83	J/K kg
	<b>Density x 10<sup>-6</sup></b>	2.46	2.29	kg/m <sup>3</sup>
	<b>Absorption/ Moisture</b>	5.51		%
	<b>Formation/Stratigraphic Unit</b>	Kalavasos		
	<b>Lithology</b>	Gypsum		



**Sample 123 – Calcareenite, Nicosia Formation**



 <p><b>smooth</b></p>		<b>Dry</b>	<b>Water Saturated</b>	<b>units</b>
	<b>Diffusivity x 10<sup>-6</sup></b>	1.01	0.98	m <sup>2</sup> /s
	<b>Thermal Conductivity</b>	1.72	1.83	W/mK
	<b>Specific Heat Capacity x 10<sup>-3</sup></b>	0.70	0.80	J/K kg
	<b>Density x 10<sup>-6</sup></b>	2.44	2.32	kg/m <sup>3</sup>
	<b>Absorption/ Moisture</b>	3.62		%
	<b>Formation/Stratigraphic Unit</b>	Nicosia		
	<b>Lithology</b>	Calcareenite		



**Sample 124 – Calcareenite, Nicosia Formation**



 <b>smooth</b>		<b>Dry</b>	<b>Water Saturated</b>	<b>units</b>
	<b>Diffusivity x 10<sup>-6</sup></b>	1.02	1.08	m <sup>2</sup> /s
	<b>Thermal Conductivity</b>	1.72	2.06	W/mK
	<b>Specific Heat Capacity x 10<sup>-3</sup></b>	0.66	0.80	J/K kg
	<b>Density x 10<sup>-6</sup></b>	2.57	2.39	kg/m <sup>3</sup>
	<b>Absorption/ Moisture</b>	5.12		%
	<b>Formation/Stratigraphic Unit</b>	Nicosia		
	<b>Lithology</b>	Calcareenite		



**Sample 125 – Calcareenite, Nicosia Formation**



 <p><b>smooth</b></p>		<b>Dry</b>	<b>Water Saturated</b>	<b>units</b>
	<b>Diffusivity x 10<sup>-6</sup></b>	0.72	0.72	m <sup>2</sup> /s
	<b>Thermal Conductivity</b>	1.08	1.39	W/mK
		0.65	0.94	J/K kg
	<b>Density x 10<sup>-6</sup></b>	2.32	2.06	kg/m <sup>3</sup>
	<b>Absorption/ Moisture</b>	10.44		%
	<b>Formation/Stratigraphic Unit</b>	Nicosia		
	<b>Lithology</b>	Calcareenite		

**Sample 126 - Sandy Marl, Nicosia Formation**




 <p><b>smooth</b></p>		<b>Dry</b>	<b>Water Saturated</b>	<b>units</b>
	<b>Diffusivity x 10<sup>-6</sup></b>	0.37	0.56	m <sup>2</sup> /s
	<b>Thermal Conductivity</b>	0.56	0.88	W/mK
	<b>Specific Heat Capacity x 10<sup>-3</sup></b>	0.89	0.96	J/K kg
	<b>Density x 10<sup>-6</sup></b>	1.65	1.67	kg/m <sup>3</sup>
	<b>Absorption/ Moisture</b>	2.51		%
	<b>Formation/Stratigraphic Unit</b>	Nicosia		
	<b>Lithology</b>	Sandy Marl		



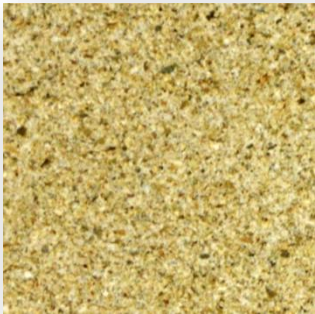
**Sample 127 – Calcarenite, Pachna Formation**



		<b>Dry</b>	<b>Water Saturated</b>	<b>units</b>
	<b>Diffusivity x 10<sup>-6</sup></b>	0.68	0.72	m <sup>2</sup> /s
	<b>Thermal Conductivity</b>	1.18	1.45	W/mK
	<b>Specific Heat Capacity x 10<sup>-3</sup></b>	0.78	0.96	J/K kg
	<b>Density x 10<sup>-6</sup></b>	2.23	2.09	kg/m <sup>3</sup>
	<b>Absorption/ Moisture</b>	5.98		%
	<b>Formation/Stratigraphic Unit</b>	Pachna		
	<b>Lithology</b>	Calcarenite		


**Sample 128 – Calcarenite, Pachna Formation**



		<b>Dry</b>	<b>Water Saturated</b>	<b>units</b>
	<b>Diffusivity x 10<sup>-6</sup></b>	0.60	0.69	m <sup>2</sup> /s
	<b>Thermal Conductivity</b>	1.03	1.33	W/mK
	<b>Specific Heat Capacity x 10<sup>-3</sup></b>	0.74	0.92	J/K kg
	<b>Density x 10<sup>-6</sup></b>	2.33	2.10	kg/m <sup>3</sup>
	<b>Absorption/ Moisture</b>	9.05		%
	<b>Formation/Stratigraphic Unit</b>	Pachna		
	<b>Lithology</b>	Calcarenite		


**Sample 129** – Calcarenite, Pachna Formation



		<b>Dry</b>	<b>Water Saturated</b>	<b>units</b>
	<b>Diffusivity x 10<sup>-6</sup></b>	0.87	0.77	m <sup>2</sup> /s
	<b>Thermal Conductivity</b>	1.43	1.49	W/mK
	<b>Specific Heat Capacity x 10<sup>-3</sup></b>	0.75	0.92	J/K kg
	<b>Density x 10<sup>-6</sup></b>	2.21	2.12	kg/m <sup>3</sup>
	<b>Absorption/ Moisture</b>	3.51		%
	<b>Formation/Stratigraphic Unit</b>	Pachna		
	<b>Lithology</b>	Calcarenite		


**Sample 130 – Chalk, Pachna Formation**



 <b>smooth</b>		<b>Dry</b>	<b>Water Saturated</b>	<b>units</b>
	<b>Diffusivity x 10<sup>-6</sup></b>	0.43	0.59	m <sup>2</sup> /s
	<b>Thermal Conductivity</b>	0.69	1.17	W/mK
	<b>Specific Heat Capacity x 10<sup>-3</sup></b>	0.89	1.23	J/K kg
	<b>Density x 10<sup>-6</sup></b>	1.80	1.62	kg/m <sup>3</sup>
	<b>Absorption/ Moisture</b>	16.59		%
	<b>Formation/Stratigraphic Unit</b>	Pachna		
	<b>Lithology</b>	Chalk		


**Sample 131 – Calcarenite, Nicosia Formation**



		<b>Dry</b>	<b>Water Saturated</b>	<b>units</b>
	<b>Diffusivity x 10<sup>-6</sup></b>	-----	0.67	m <sup>2</sup> /s
	<b>Thermal Conductivity</b>	0.42	1.03	W/mK
	<b>Specific Heat Capacity x 10<sup>-3</sup></b>	-----	0.92	J/K kg
	<b>Density x 10<sup>-6</sup></b>	2.01	1.70	kg/m <sup>3</sup>
	<b>Absorption/ Moisture</b>	21.56		%
	<b>Formation/Stratigraphic Unit</b>	Nicosia		
	<b>Lithology</b>	Calcarenite		

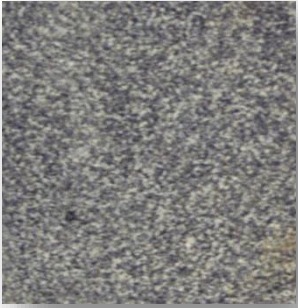
**Sample 132 - Reef Limestone, Pachna Formation (Koronia Member)**



 <p><b>smooth</b></p>		<b>Dry</b>	<b>Water Saturated</b>	<b>units</b>
	<b>Diffusivity x 10<sup>-6</sup></b>	1.09	1.02	m <sup>2</sup> /s
	<b>Thermal Conductivity</b>	2.11	2.18	W/mK
		0.77	0.86	J/K kg
	<b>Specific Heat Capacity x 10<sup>-3</sup></b>			
	<b>Density x 10<sup>-6</sup></b>	2.52	2.48	kg/m <sup>3</sup>
	<b>Absorption/ Moisture</b>	1.00		%
	<b>Formation/Stratigraphic Unit</b>	Pachna (Koronia Member)		
	<b>Lithology</b>	Reef Limestone		


**Sample 133** – Diabase, Volcanic Sequence (Basal Group)



 <b>smooth</b>		<b>Dry</b>	<b>Water Saturated</b>	<b>units</b>
	<b>Diffusivity x 10<sup>-6</sup></b>	1.18	1.16	m <sup>2</sup> /s
	<b>Thermal Conductivity</b>	2.32	2.21	W/mK
	<b>Specific Heat Capacity x 10<sup>-3</sup></b>	0.72	0.72	J/K kg
	<b>Density x 10<sup>-6</sup></b>	2.71	2.68	kg/m <sup>3</sup>
	<b>Absorption/ Moisture</b>	0.67		%
	<b>Formation/Stratigraphic Unit</b>	Volcanic Sequence (Basal Group)		
	<b>Lithology</b>	Diabase		

**Sample 134** – Calcareenite, Marine Terrace





		<b>Dry</b>	<b>Water Saturated</b>	<b>units</b>
	<b>Diffusivity x 10<sup>-6</sup></b>	0.66	0.73	m <sup>2</sup> /s
	<b>Thermal Conductivity</b>	1.07	1.40	W/mK
<b>smooth</b>	<b>Specific Heat Capacity x 10<sup>-3</sup></b>	0.68	0.92	J/K kg
	<b>Density x 10<sup>-6</sup></b>	2.37	2.07	kg/m <sup>3</sup>
	<b>Absorption/ Moisture</b>	11.63		%
	<b>Formation/Stratigraphic Unit</b>	Marine Terrace		
	<b>Lithology</b>	Calcareenite		





**Sample 135 – Calcarenite, Nicosia Formation**



 <p><b>smooth</b></p>		<b>Dry</b>	<b>Water Saturated</b>	<b>units</b>
	<b>Diffusivity x 10<sup>-6</sup></b>	0.78	1.01	m <sup>2</sup> /s
	<b>Thermal Conductivity</b>	1.08	1.55	W/mK
	<b>Specific Heat Capacity x 10<sup>-3</sup></b>	0.55	0.66	J/K kg
	<b>Density x 10<sup>-6</sup></b>	2.50	2.32	kg/m <sup>3</sup>
	<b>Absorption/ Moisture</b>	5.48		%
	<b>Formation/Stratigraphic Unit</b>	Nicosia		
	<b>Lithology</b>	Calcarenite		



**Sample 136** – Calcarenite, Aeolian deposits



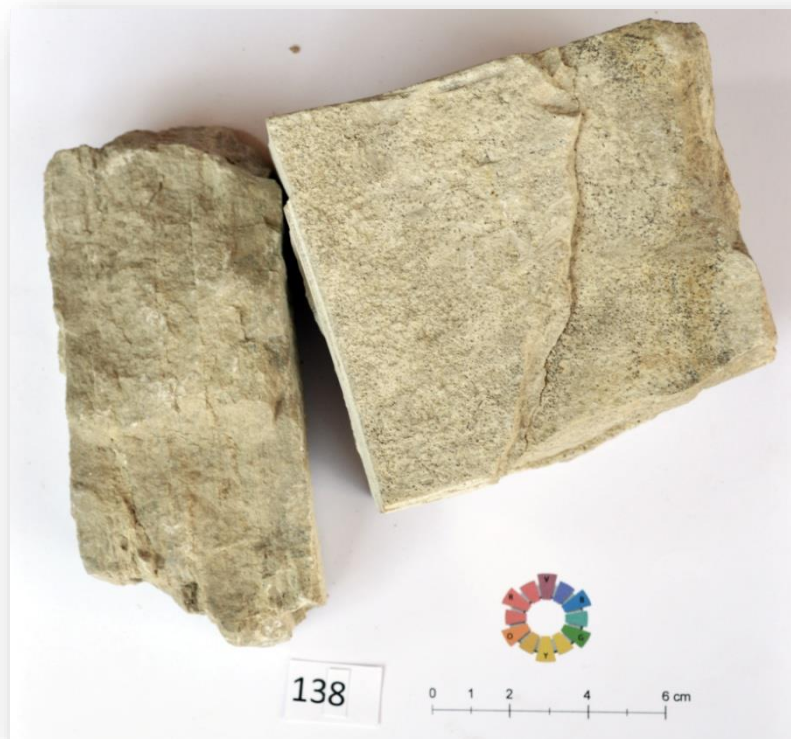
 <b>smooth</b>		<b>Dry</b>	<b>Water Saturated</b>	<b>units</b>
	<b>Diffusivity x 10<sup>-6</sup></b>	0.79	0.86	m <sup>2</sup> /s
	<b>Thermal Conductivity</b>	1.29	1.58	W/mK
		0.68	0.86	J/K kg
	<b>Density x 10<sup>-6</sup></b>	2.40	2.13	kg/m <sup>3</sup>
	<b>Absorption/ Moisture</b>	10.08		%
	<b>Formation/Stratigraphic Unit</b>	Aeolian deposits		
	<b>Lithology</b>	Calcarenite		

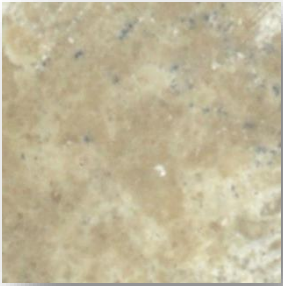
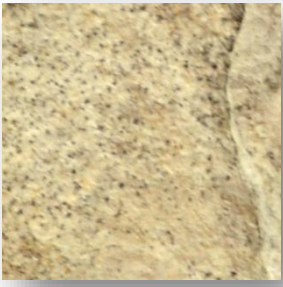
**Sample 137** – Calcarenite, Aeolian deposits



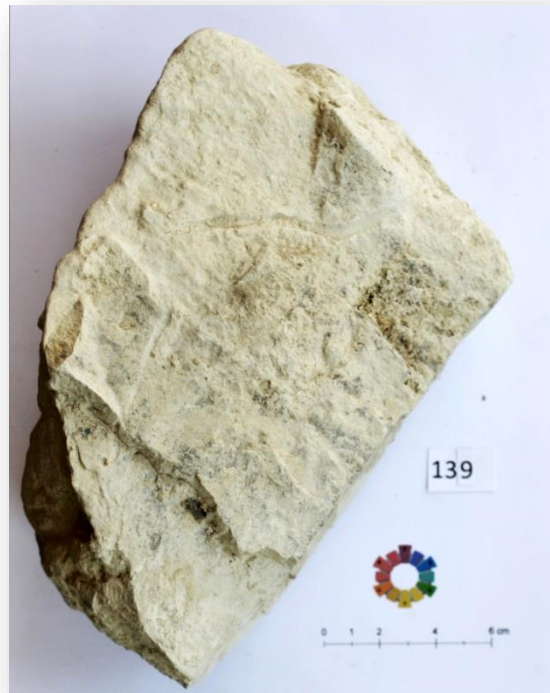
 <p><b>smooth</b></p>		<b>Dry</b>	<b>Water Saturated</b>	<b>units</b>
	<b>Diffusivity x 10<sup>-6</sup></b>	0.47	0.74	m <sup>2</sup> /s
	<b>Thermal Conductivity</b>	0.68	1.30	W/mK
	<b>Specific Heat Capacity x 10<sup>-3</sup></b>	0.60	0.92	J/K kg
	<b>Density x 10<sup>-6</sup></b>	2.37	1.93	kg/m <sup>3</sup>
	<b>Absorption/ Moisture</b>	20.20		%
	<b>Formation/Stratigraphic Unit</b>	Aeolian deposits		
	<b>Lithology</b>	Calcarenite		

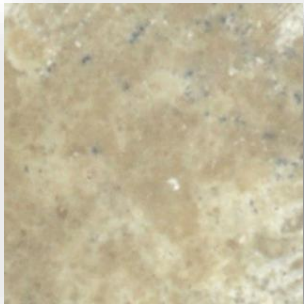

**Sample 138 – Limestone, Lapatsa Formation**



 <p><b>smooth</b></p>		<b>Dry</b>	<b>Water Saturated</b>	<b>units</b>
	<b>Diffusivity x 10<sup>-6</sup></b>	0.99	----	m <sup>2</sup> /s
	<b>Thermal Conductivity</b>	1.61	----	W/mK
	<b>Specific Heat Capacity x 10<sup>-3</sup></b>	0.58	----	J/K kg
	<b>Density x 10<sup>-6</sup></b>	2.75	---	kg/m <sup>3</sup>
	<b>Absorption/ Moisture</b>	---		%
	<b>Formation/Stratigraphic Unit</b>	Lapatsa		
	<b>Lithology</b>	Limestone		



**Sample 139 – Chalks, Lapatsa Formation**



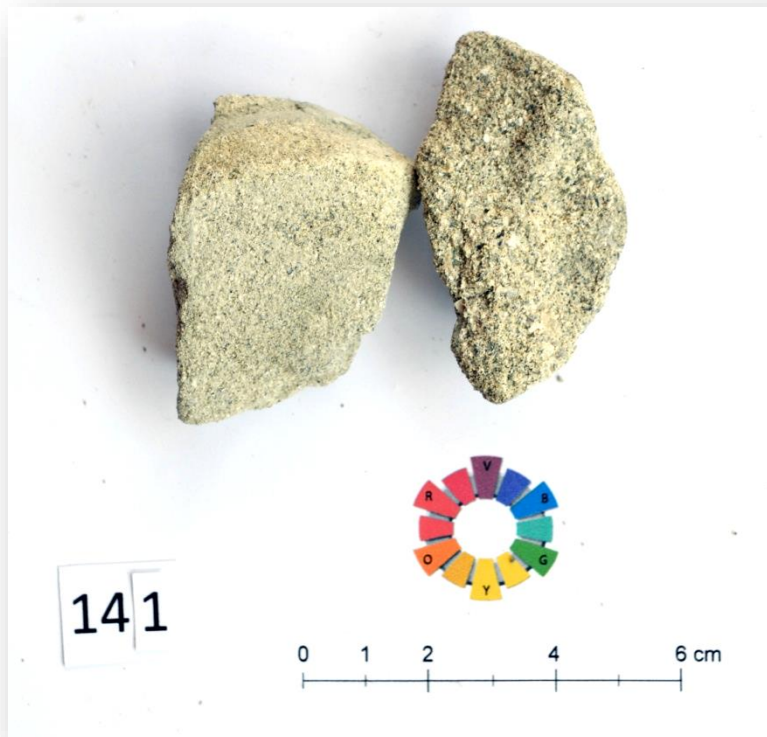
		<b>Dry</b>	<b>Water Saturated</b>	<b>units</b>
	<b>Diffusivity x 10<sup>-6</sup></b>	1.34	----	m <sup>2</sup> /s
	<b>Thermal Conductivity</b>	1.92	----	W/mK
	<b>Specific Heat Capacity x 10<sup>-3</sup></b>	1.45	----	J/K kg
<b>smooth</b>				
	<b>Density x 10<sup>-6</sup></b>	2.40	---	kg/m <sup>3</sup>
	<b>Absorption/ Moisture</b>	----		%
	<b>Formation/Stratigraphic Unit</b>	Lapatsa		
	<b>Lithology</b>	Chalks		



**Sample 140 - Chalky Marls, Lapatsa Formation**



 <p><b>smooth</b></p>		<b>Dry</b>	<b>Water Saturated</b>	<b>units</b>
	<b>Diffusivity x 10<sup>-6</sup></b>	0.54	----	m <sup>2</sup> /s
	<b>Thermal Conductivity</b>	0.75	----	W/mK
	<b>Specific Heat Capacity x 10<sup>-3</sup></b>	0.70	----	J/K kg
	<b>Density x 10<sup>-6</sup></b>	1.97	----	kg/m <sup>3</sup>
	<b>Absorption/ Moisture</b>	----		%
	<b>Formation/Stratigraphic Unit</b>	Lapatsa		
	<b>Lithology</b>	Chalky Marls		

**Sample 141 – Sandstone, Kythrea Formation**



 <b>smooth</b>		<b>Dry</b>	<b>Water Saturated</b>	<b>units</b>
	<b>Diffusivity x 10<sup>-6</sup></b>	0.39	----	m <sup>2</sup> /s
	<b>Thermal Conductivity</b>	0.54	----	W/mK
		0.73	----	J/K kg
	<b>Density x 10<sup>-6</sup></b>	1.90	----	kg/m <sup>3</sup>
	<b>Absorption/ Moisture</b>	----		----
	<b>Formation/Stratigraphic Unit</b>	Kythrea		
	<b>Lithology</b>	Sandstone		

**Sample 142 – Marls, Kythrea Formation**

<p>No photo available.</p> <p>The sample was very small and was dissolved during the experiments.</p>		<b>Dry</b>	<b>Water Saturated</b>	<b>units</b>
	<b>Diffusivity x 10<sup>-6</sup></b>	0.61	----	m <sup>2</sup> /s
	<b>Thermal Conductivity</b>	0.87	----	W/mK
	<b>Specific Heat Capacity x 10<sup>-3</sup></b>	0.67	----	J/K kg
	<b>Density x 10<sup>-6</sup></b>	2.12	----	kg/m <sup>3</sup>
	<b>Absorption/ Moisture</b>	----		%
	<b>Formation/Stratigraphic Unit</b>	Kythrea Formation		
	<b>Lithology</b>	Marls		

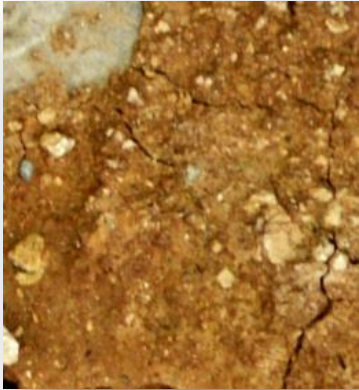
**Sample 143 – Marls, Kythrea Formation**

<p>No photo available.</p> <p>The sample was very small and was dissolved during the experiments.</p>		<b>Dry</b>	<b>Water Saturated</b>	<b>units</b>
	<b>Diffusivity x 10<sup>-6</sup></b>	0.52	----	m <sup>2</sup> /s
	<b>Thermal Conductivity</b>	0.78	----	W/mK
	<b>Specific Heat Capacity x 10<sup>-3</sup></b>	0.69	----	J/K kg
	<b>Density x 10<sup>-6</sup></b>	2.18	----	kg/m <sup>3</sup>
	<b>Absorption/ Moisture</b>	----		%
	<b>Formation/Stratigraphic Unit</b>	Kythrea Formation		
	<b>Lithology</b>	Marls		





**Sample 144 - Silicified Sand and Gravel, Colluvium (Apalos Formation)**



		<b>Dry</b>	<b>Water Saturated</b>	<b>units</b>
	<b>Diffusivity x 10<sup>-6</sup></b>	---	0.56	m <sup>2</sup> /s
	<b>Thermal Conductivity</b>	0.32	0.90	W/mK
	<b>Specific Heat Capacity x 10<sup>-3</sup></b>	not possible to be calculated (no density value)		
<b>Soil and small gravel</b>				
	<b>Density x 10<sup>-6</sup></b>	not possible to be calculated as the samples are not homogeneous but are composed of different materials in different stages and lithologies (soil and gravels)		
	<b>Absorption/ Moisture</b>	---	---	%
	<b>Formation/Stratigraphic Unit</b>	Colluvium (Apalos Formation)		
	<b>Lithology</b>	Silt. sand and small gravel		



**Sample 145 - Silicified Sand and Gravel,, Alluvium**



 <p><b>Soil and small gravel</b></p>		<b>Soil and small gravel</b>		<b>Gravel</b>		
		<b>Dry</b>	<b>Water Satur.</b>	<b>Dry</b>	<b>Water Satur.</b>	<b>units</b>
	<b>Diffusivity x 10<sup>-6</sup></b>	0.28	0.66	1.51	1.31	m <sup>2</sup> /s
	<b>Thermal Conductivity</b>	0.36	1.35	2.2	1.98	W/mK
	<b>Specific Heat Capacity x 10<sup>-3</sup></b>	not possible to be calculated (no density value)				
 <p><b>gravel</b></p>	<b>Density x 10<sup>-6</sup></b>	not possible to be calculated as the samples are not homogeneous but are compose of different materials in different stages and lithologies (soil and gravels)				
	<b>Absorption/ Moisture</b>	---		---		%
	<b>Formation/ Stratigraphic Unit</b>	Alluvium				
	<b>Lithology</b>	Silt. sand and gravel				



**Sample 146 - Silicified Sand and Gravel, Fanglomerate**



		<b>Soil and small gravel</b>		<b>Gravel</b>		
		<b>Dry</b>	<b>Water Satur.</b>	<b>Dry</b>	<b>Water Satur.</b>	<b>units</b>
	<b>Diffusivity x 10<sup>-6</sup></b>	---	---	0.98	0.93	m <sup>2</sup> /s
	<b>Thermal Conductivity</b>	0.11	0.59	1.12	1.23	W/m K
<b>Soil and gravel</b>	<b>Specific Heat Capacity x 10<sup>-3</sup></b>	not possible to be calculated (no density value)				
	<b>Density x 10<sup>-6</sup></b>	not possible to be calculated as the samples are not homogeneous but are compose of different materials in different stages and lithologies (soil and gravels)				
	<b>Absorption/Moisture</b>	---	---	---	---	%
	<b>Formation/Stratigraphic Unit</b>	Fanglomerate				
	<b>Lithology</b>	Silt. sand and gravels				



**Sample 147 - Silicified Sand and Gravel, Fanglomerate**



 <p><b>Soil and small gravel</b></p>		<b>Soil and small gravel</b>		<b>Gravel</b>		
		<b>Dry</b>	<b>Water Satur.</b>	<b>Dry</b>	<b>Water Satur.</b>	<b>units</b>
	<b>Diffusivity x 10<sup>-6</sup></b>	0.22	0.62	0.87	0.87	m <sup>2</sup> /s
	<b>Thermal Conductivity</b>	0.29	1.13	1.10	1.25	W/mK
	<b>Specific Heat Capacity x 10<sup>-3</sup></b>	not possible to be calculated (no density value)				
 <p><b>gravel</b></p>	<b>Density x 10<sup>-6</sup></b>	not possible to be calculated as the samples are not homogeneous but are compose of different materials in different stages and lithologies (soil and gravels)				
	<b>Absorption/ Moisture</b>	---	---		%	
	<b>Formation/ Stratigraphic Unit</b>	Fanglomerate				
	<b>Lithology</b>	Silt. sand and gravel				

**Sample 148 - Silicified Sand and Gravel, Alluvium**

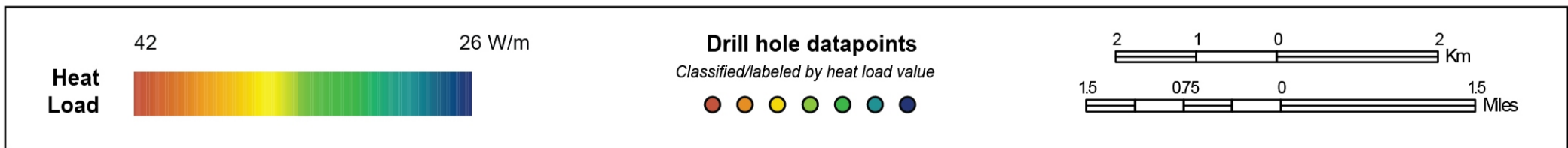
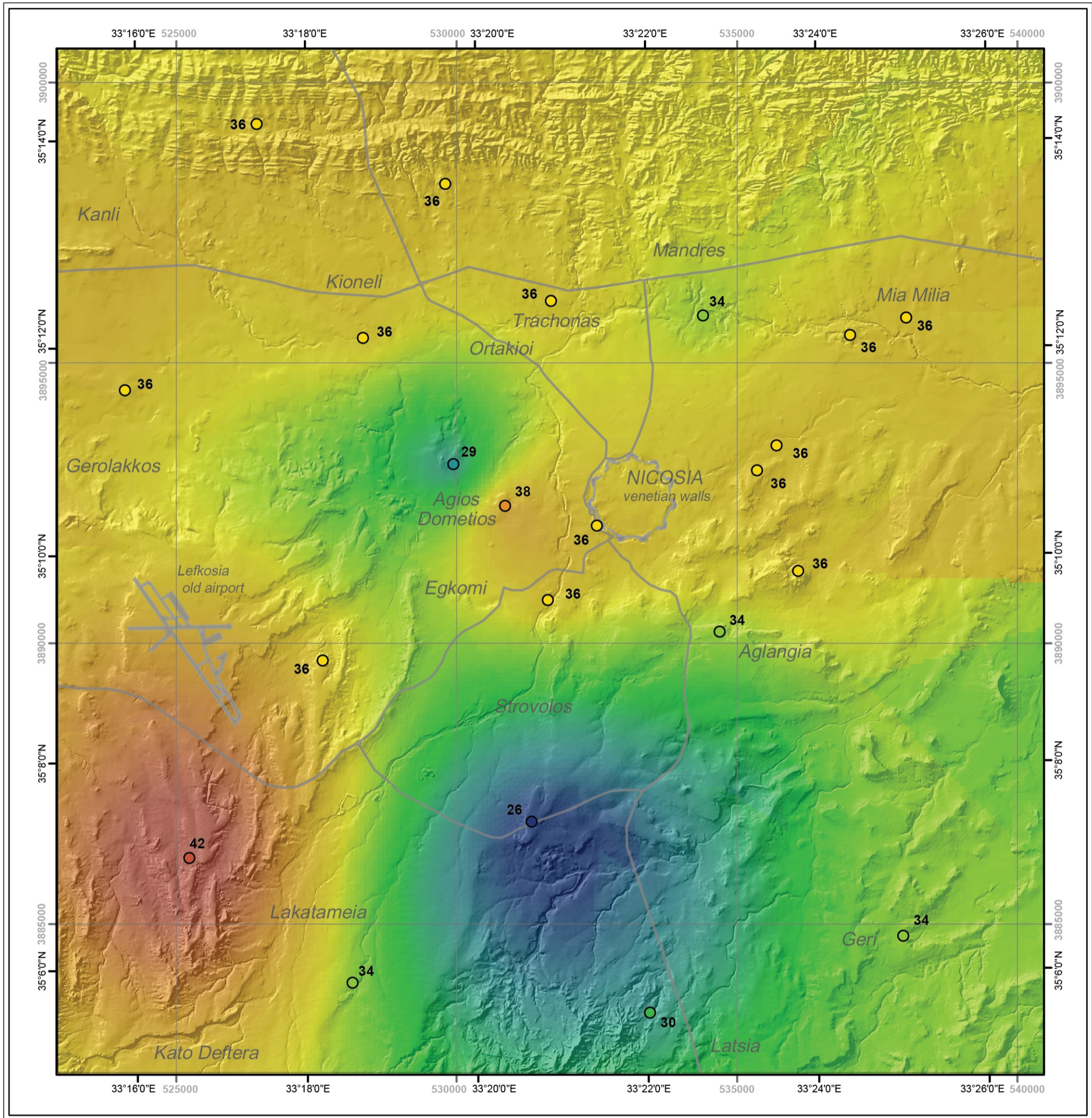


		<b>Soil and small gravel</b>		<b>Gravel</b>		
		<b>Dry</b>	<b>Water Satur.</b>	<b>Dry</b>	<b>Water Satur.</b>	<b>units</b>
	<b>Diffusivity x 10<sup>-6</sup></b>	0.26	0.54	1.02	1.59	m <sup>2</sup> /s
	<b>Thermal Conductivity</b>	0.38	1.08	1.25	2.23	W/mK
<b>Soil and small gravel</b>	<b>Specific Heat Capacity x 10<sup>-3</sup></b>	not possible to be calculated (no density value)				
	<b>Density x 10<sup>-6</sup></b>	not possible to be calculated as the samples are not homogeneous but are composed of different materials in different stages and lithologies (soil and gravels)				
	<b>Absorption/ Moisture</b>	---		---		%
	<b>Formation/ Stratigraphic Unit</b>	Alluvium				
	<b>Lithology</b>	Silicified Sand and Gravel				
<b>gravel</b>						

## APPENDIX IV

# DESIGN LOAD MAP OF GROUND HEAT EXCHANGERS FOR THE GREATER NICOSIA AREA, CYPRUS

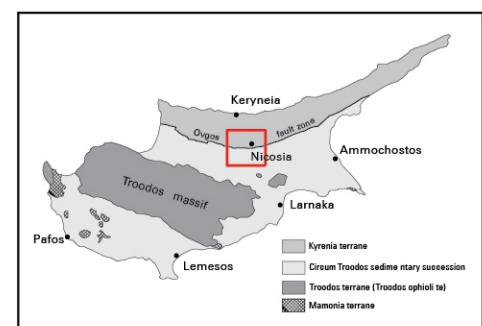
by Iosifina I. Stylianou



Map presents the performance of Vertical Ground Heat Exchangers up to 100 m depth, after 24 hours of operation in cooling mode. Calculated data present the heat load per meter depth that can be transferred to the ground in each borehole of the greater Nicosia area.

Map was compiled with the use of Geographic Information System (GIS). Small areas with dense data surrounded by wide areas containing sparse data are characteristic of the heat load map. As such, the user should keep in mind that the heat loss map is well constrained in areas of dense data and more interpretive in areas of sparse data.

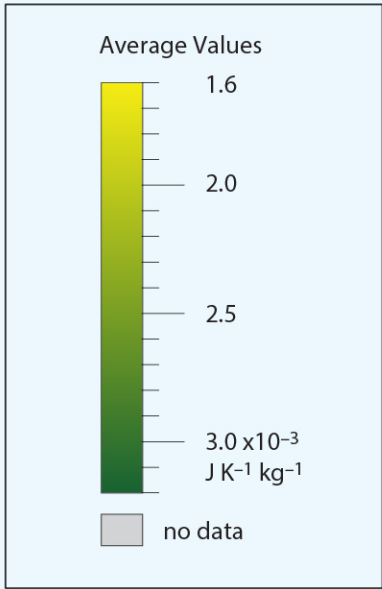
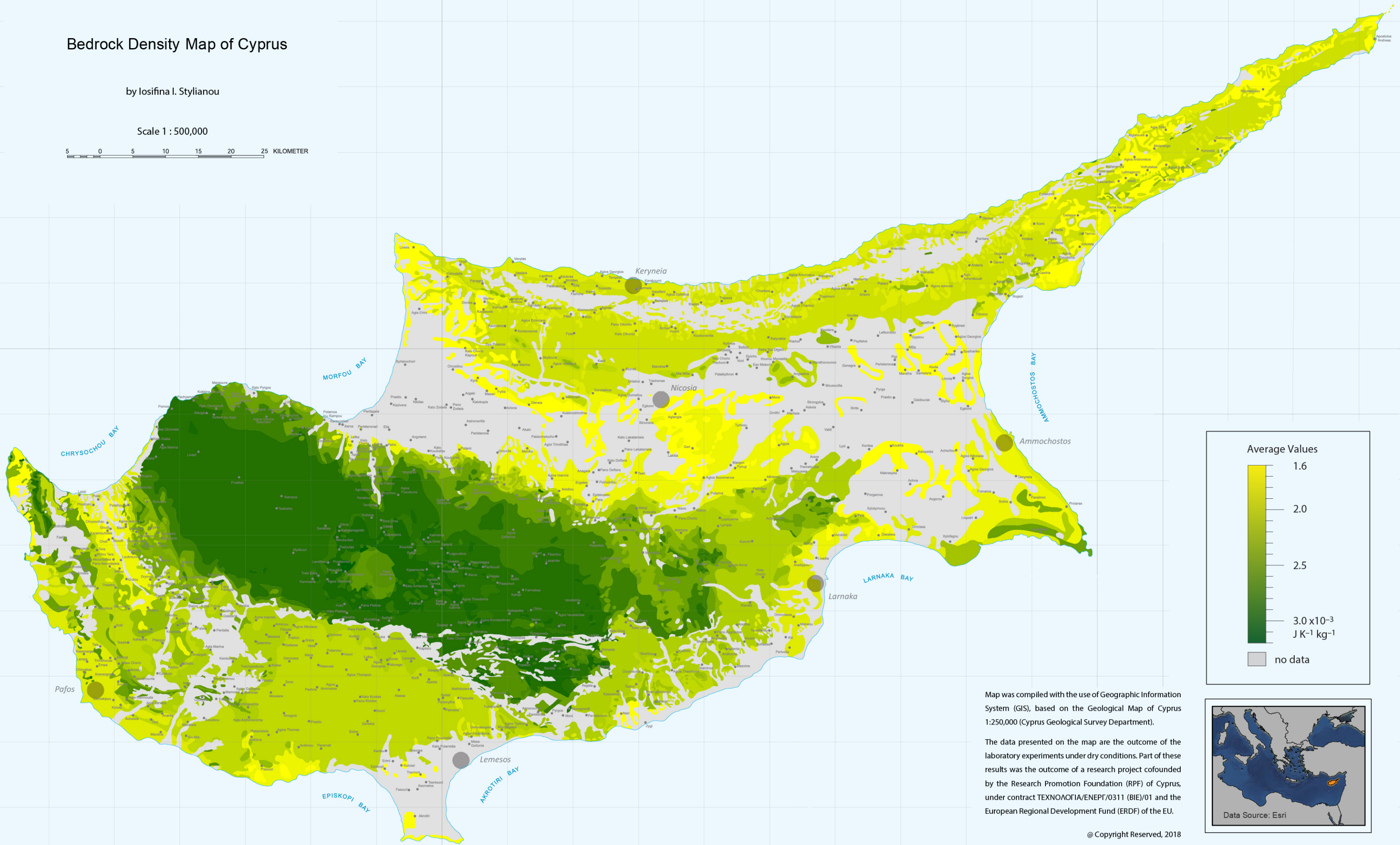
The digital elevation model presented on the background of the map was supplied by the Cyprus Geological Survey Department.



# Bedrock Density Map of Cyprus

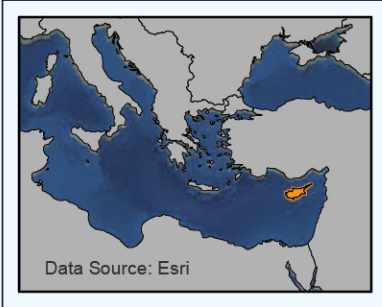
by Iosifina I. Stylianou

Scale 1 : 500,000



Map was compiled with the use of Geographic Information System (GIS), based on the Geological Map of Cyprus 1:250,000 (Cyprus Geological Survey Department).

The data presented on the map are the outcome of the laboratory experiments under dry conditions. Part of these results was the outcome of a research project cofounded by the Research Promotion Foundation (RPF) of Cyprus, under contract TEXNOAOFIA/ENEPT/0311 (BIE)/01 and the European Regional Development Fund (ERDF) of the EU.



@ Copyright Reserved, 2018

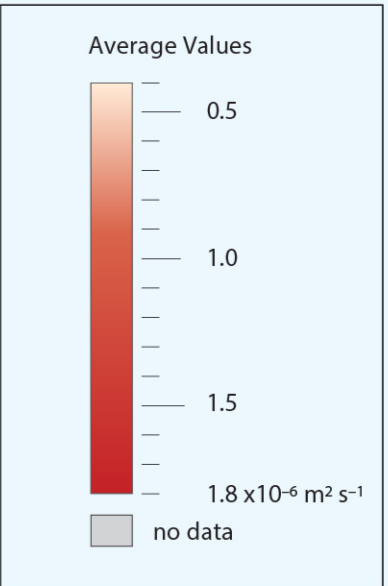
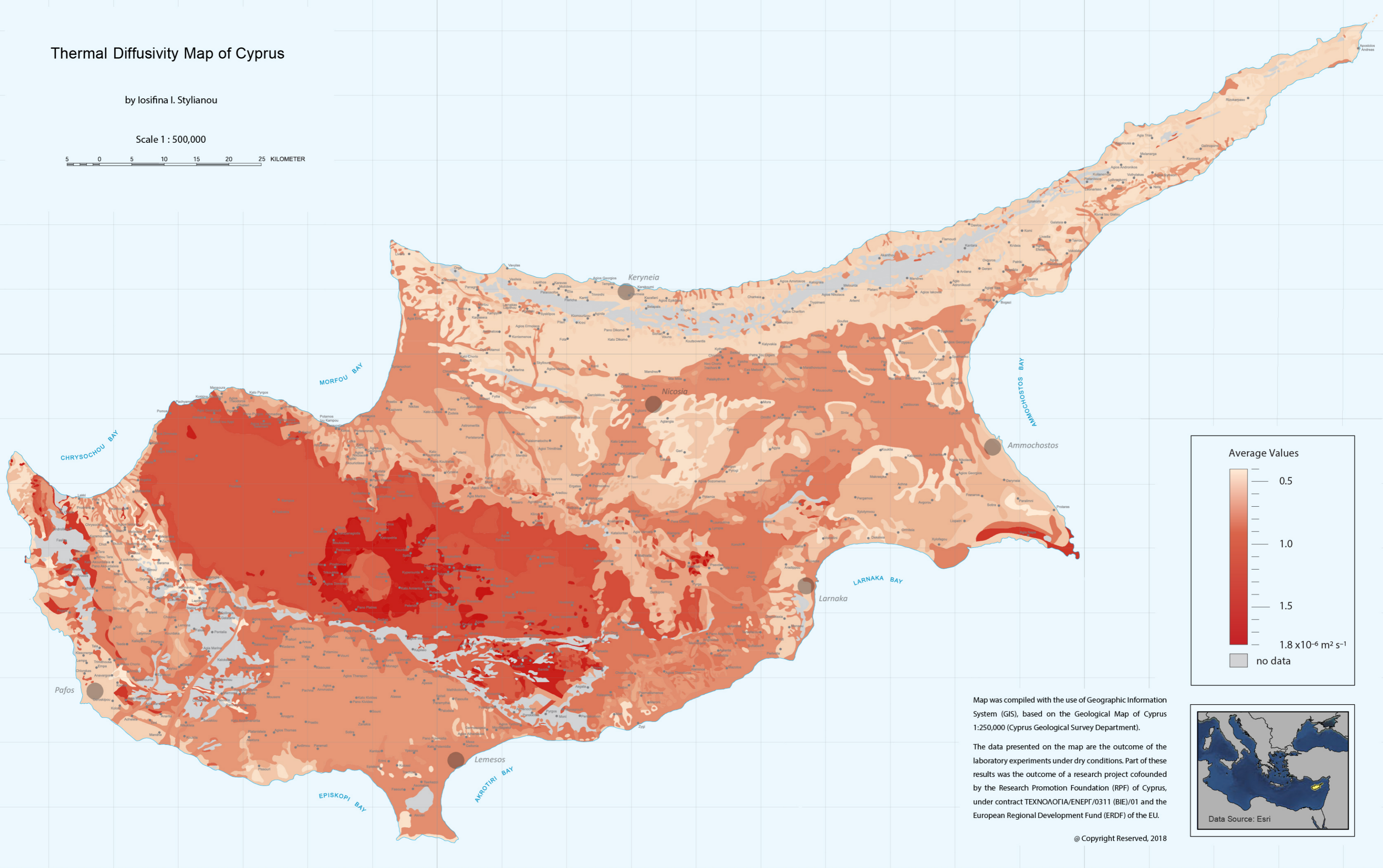


# Thermal Diffusivity Map of Cyprus

by Iosifina I. Stylianou

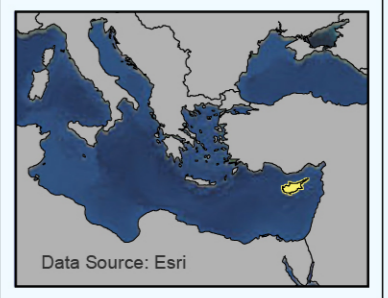
Scale 1 : 500,000

5 0 5 10 15 20 25 KILOMETER



Map was compiled with the use of Geographic Information System (GIS), based on the Geological Map of Cyprus 1:250,000 (Cyprus Geological Survey Department).

The data presented on the map are the outcome of the laboratory experiments under dry conditions. Part of these results was the outcome of a research project cofunded by the Research Promotion Foundation (RPF) of Cyprus, under contract TEXNOΛΟΓΙΑ/ΕΝΕΡΓ/0311 (BIE)/01 and the European Regional Development Fund (ERDF) of the EU.

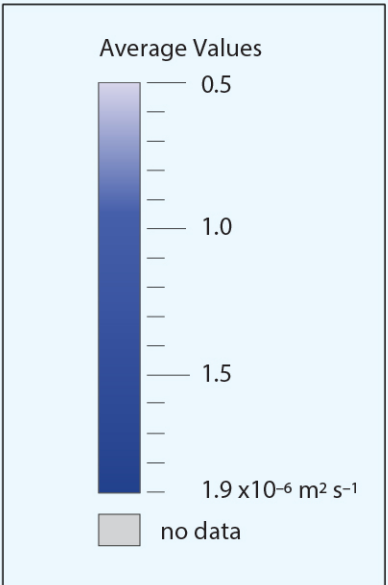
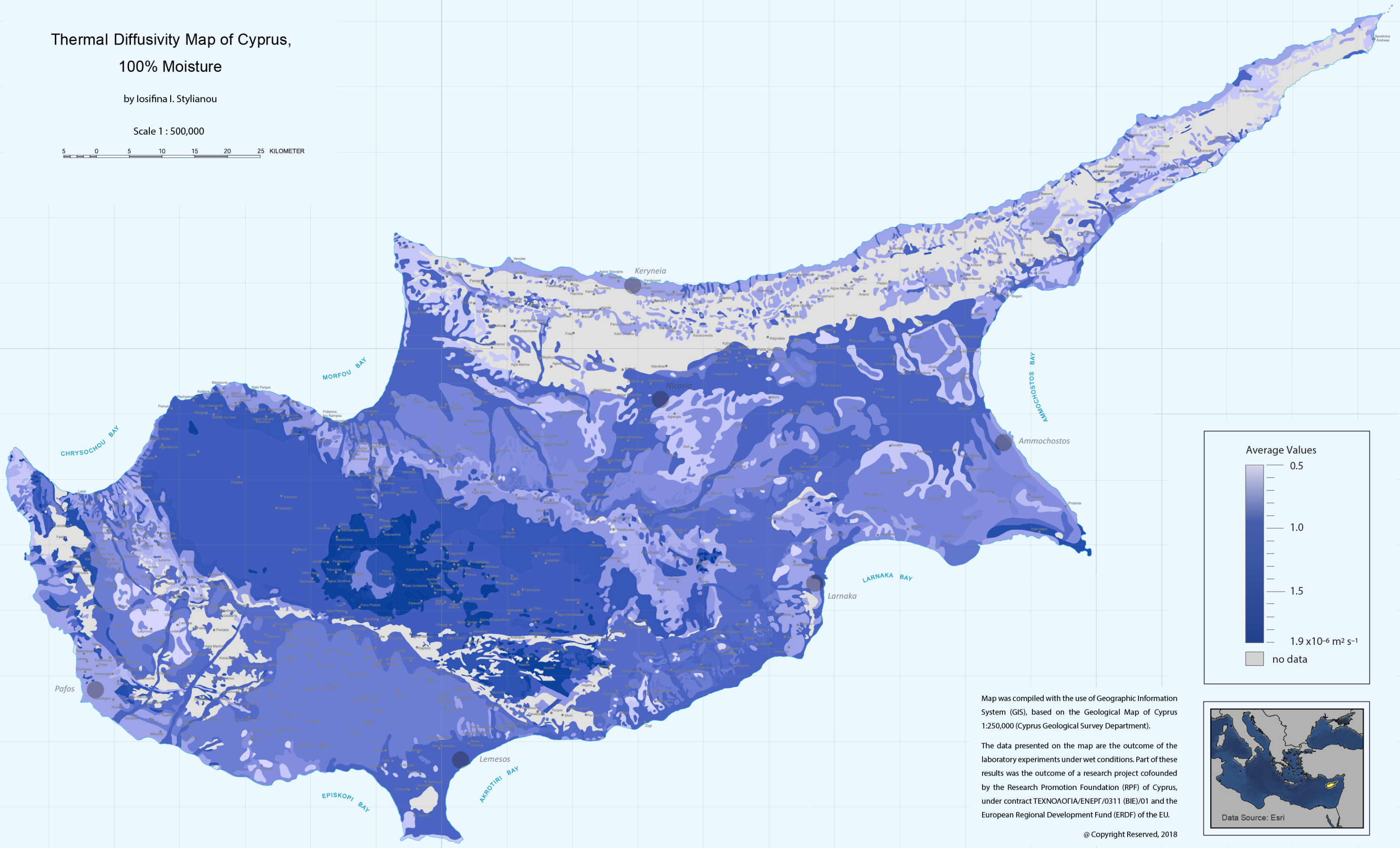


@ Copyright Reserved, 2018

# Thermal Diffusivity Map of Cyprus, 100% Moisture

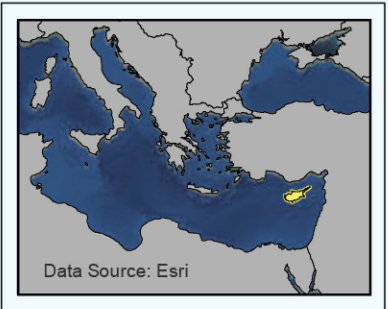
by Iosifina I. Stylianou

Scale 1 : 500,000



Map was compiled with the use of Geographic Information System (GIS), based on the Geological Map of Cyprus 1:250,000 (Cyprus Geological Survey Department).

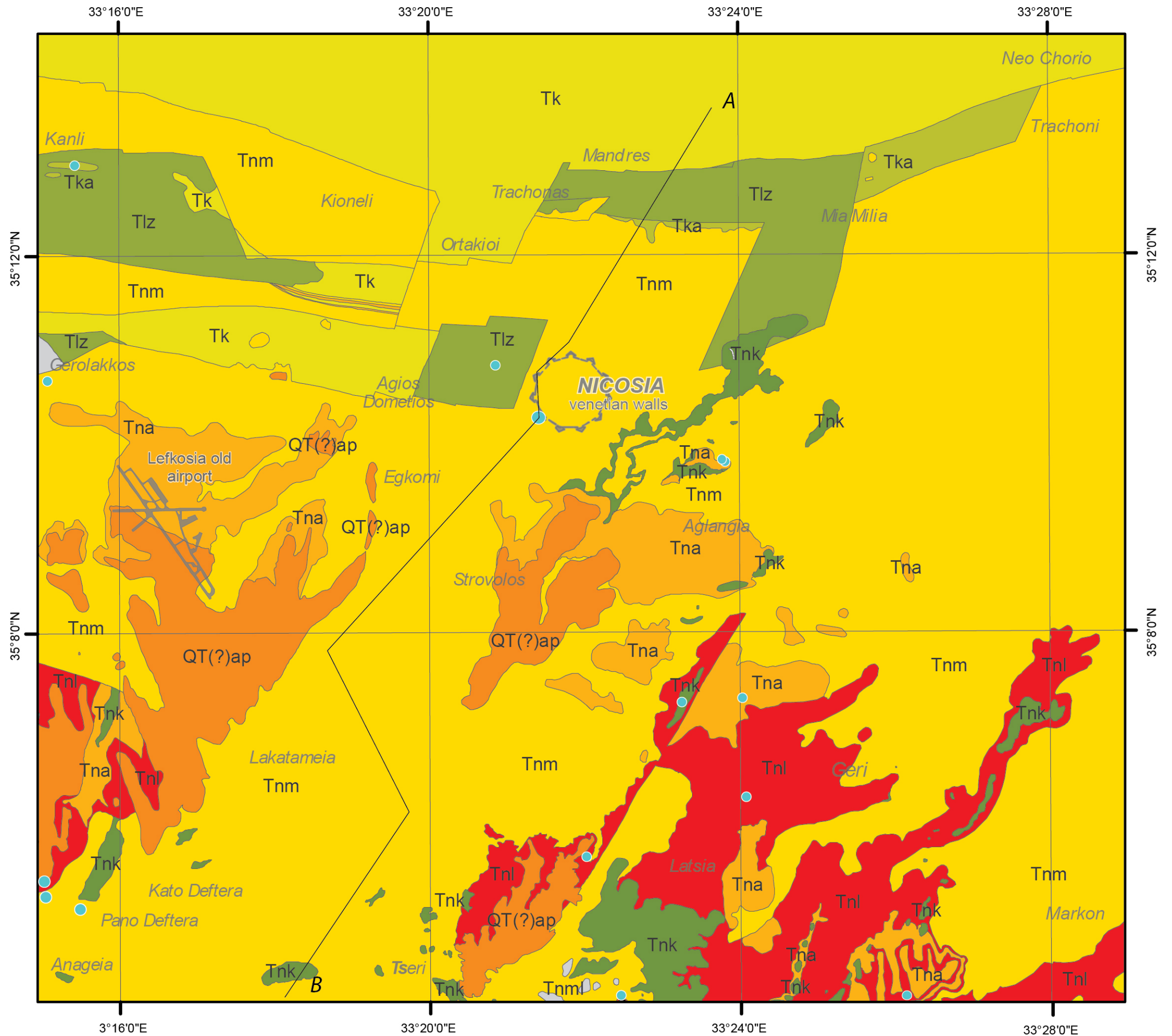
The data presented on the map are the outcome of the laboratory experiments under wet conditions. Part of these results was the outcome of a research project cofunded by the Research Promotion Foundation (RPF) of Cyprus, under contract ΤΕΧΝΟΛΟΓΙΑ/ΕΝΕΡΓ/0311 (BIE)/01 and the European Regional Development Fund (ERDF) of the EU.



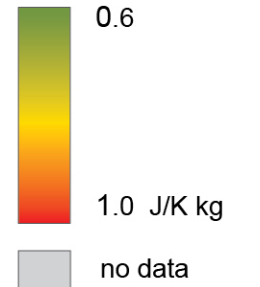
@ Copyright Reserved, 2018

# Specific Heat Capacity Map of the Greater Nicosia Area

by Iosifina I. Stylianou



## Specific Heat Capacity

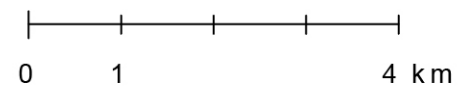


## Geological Features

- Qt(?)ap Apalos Formation
- Tn Nicosia Formation
  - Tnml Marine Littoral Member
  - Tnml Aspropamboulos Memb.
  - Tnl Lithic Sand Member
  - Tna Athalassa Member
  - Tnk Kephales Member
  - Tnm Marl Member
  - Tnbc Basal Conglom. Memb.
- Tka Kalavassos Formation
- Tlz Lapatza Formation
- Tk Kythrea Formation
- Tp Pakhna Formation
- TKl Lefkara Formation
- Km Moni Formation

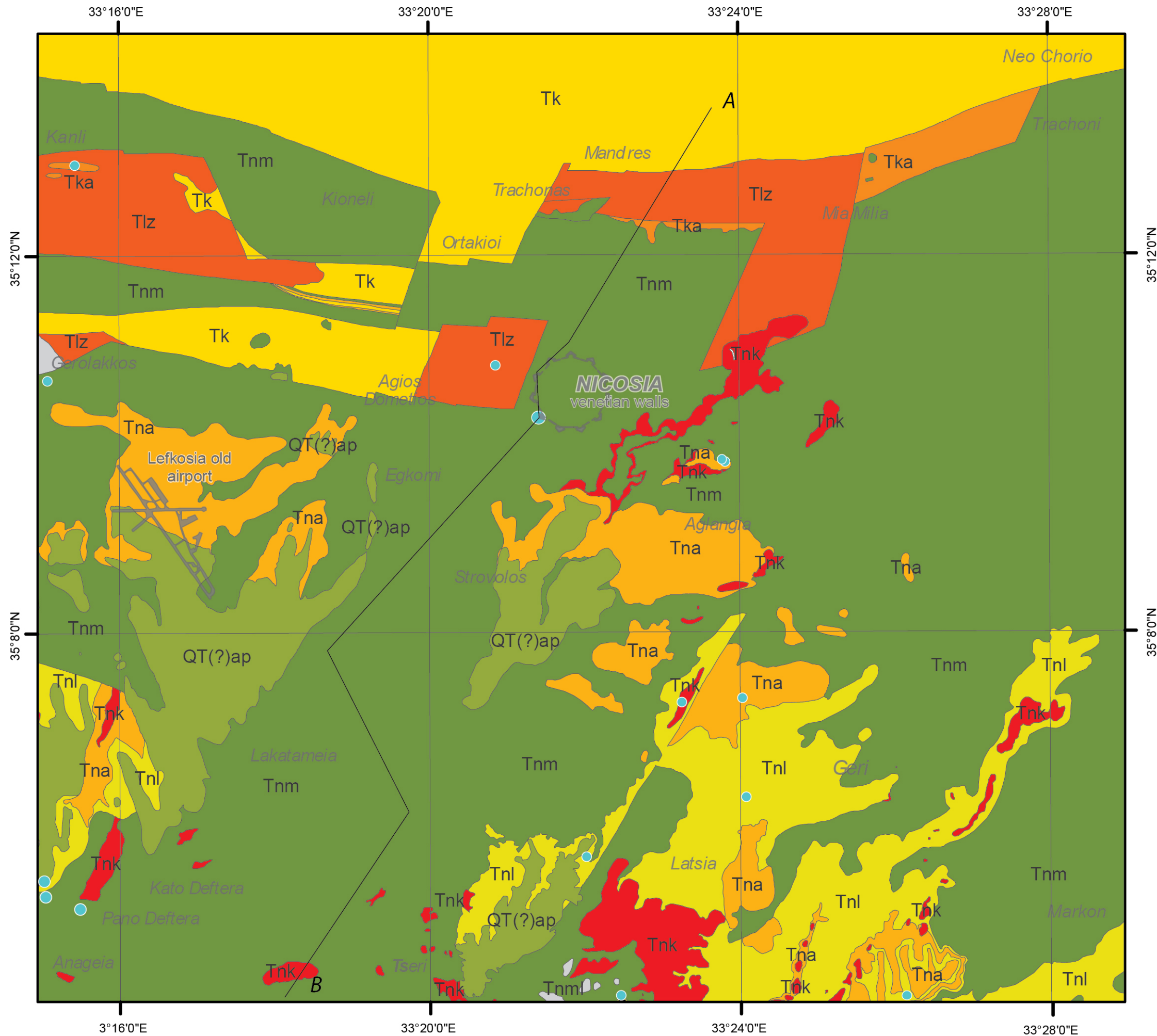
## Other Features

- Sampling Point
- A — B Cross Section Line
- Geri** Built-up areas

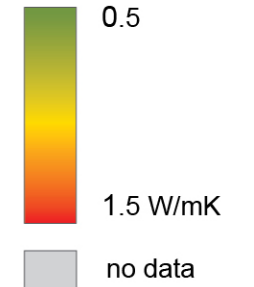


# Thermal Conductivity Map of the Greater Nicosia Area

by Iosifina I. Stylianou



## Thermal Conductivity

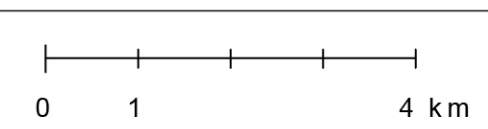


## Geological Features

- Qt(?)ap Apalos Formation
- Tn Nicosia Formation
  - Tnml Marine Littoral Member
  - Tnml Aspropamboulos Memb.
  - Tnl Lithic Sand Member
  - Tna Athalassa Member
  - Tnk Kephales Member
  - Tnm Marl Member
  - Tnbc Basal Conglom. Memb.
- Tka Kalavassos Formation
- Tlz Lapatza Formation
- Tk Kythrea Formation
- Tp Pakhna Formation
- Tkl Lefkara Formation
- Km Moni Formation

## Other Features

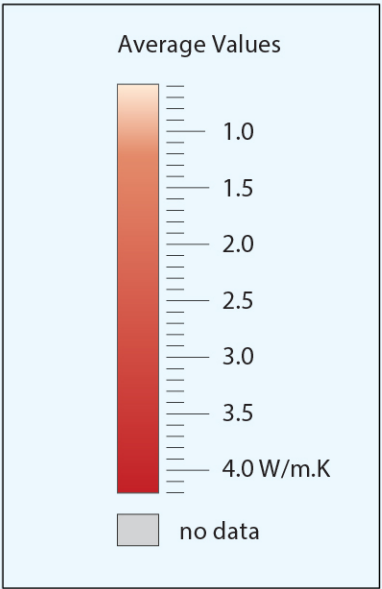
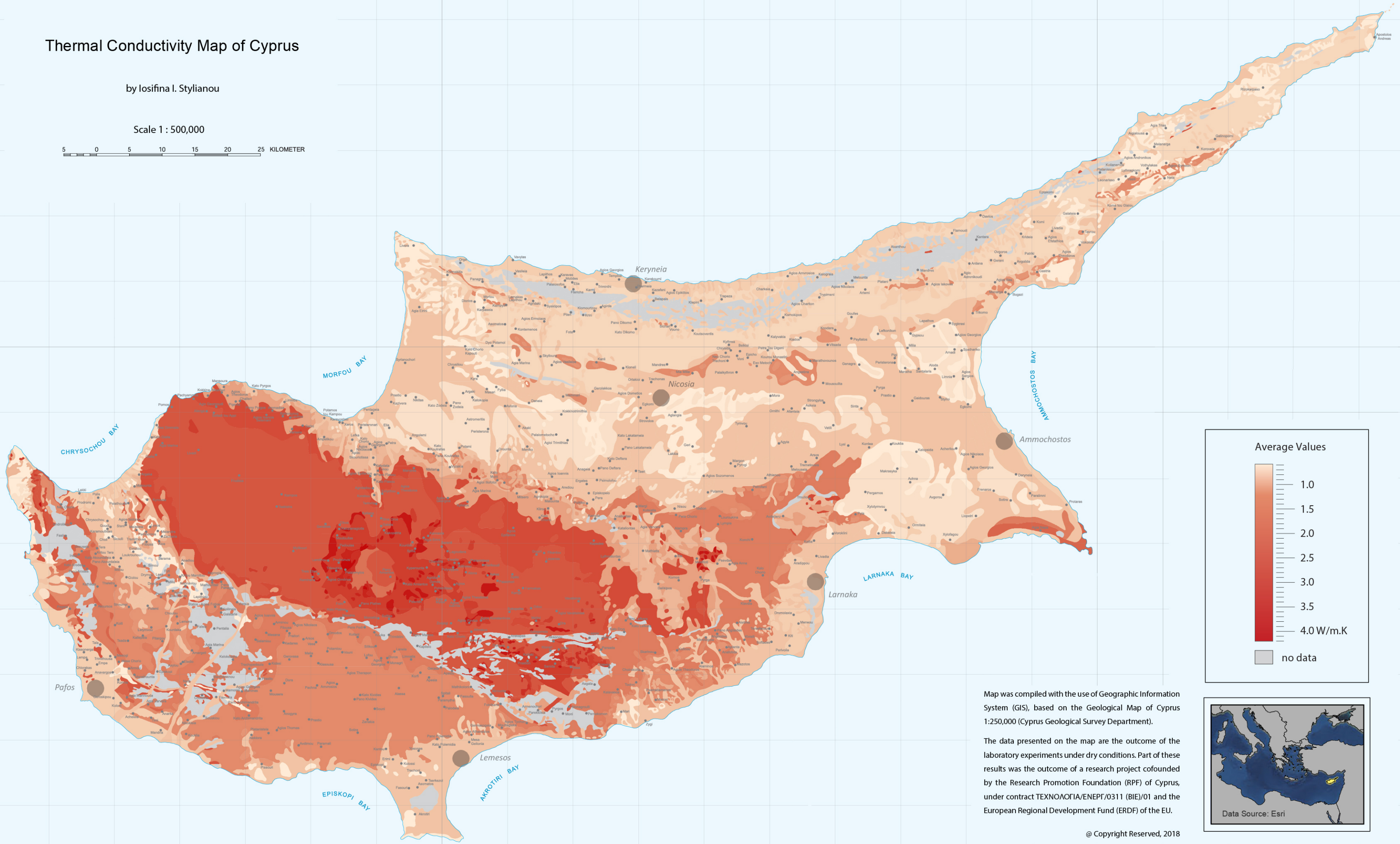
- Sampling Point
- A — B Cross Section Line
- Ger** Built-up areas



# Thermal Conductivity Map of Cyprus

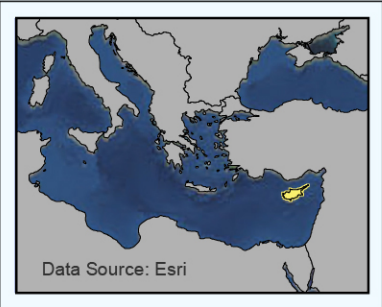
by Iosifina I. Stylianou

Scale 1 : 500,000



Map was compiled with the use of Geographic Information System (GIS), based on the Geological Map of Cyprus 1:250,000 (Cyprus Geological Survey Department).

The data presented on the map are the outcome of the laboratory experiments under dry conditions. Part of these results was the outcome of a research project cofounded by the Research Promotion Foundation (RPF) of Cyprus, under contract ΤΕΧΝΟΛΟΓΙΑ/ΕΝΕΡΓ/0311 (BIE)/01 and the European Regional Development Fund (ERDF) of the EU.

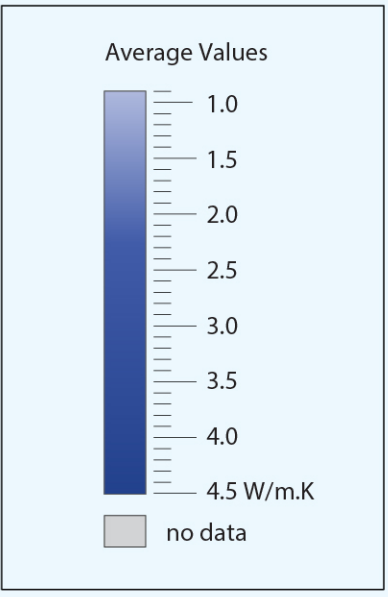
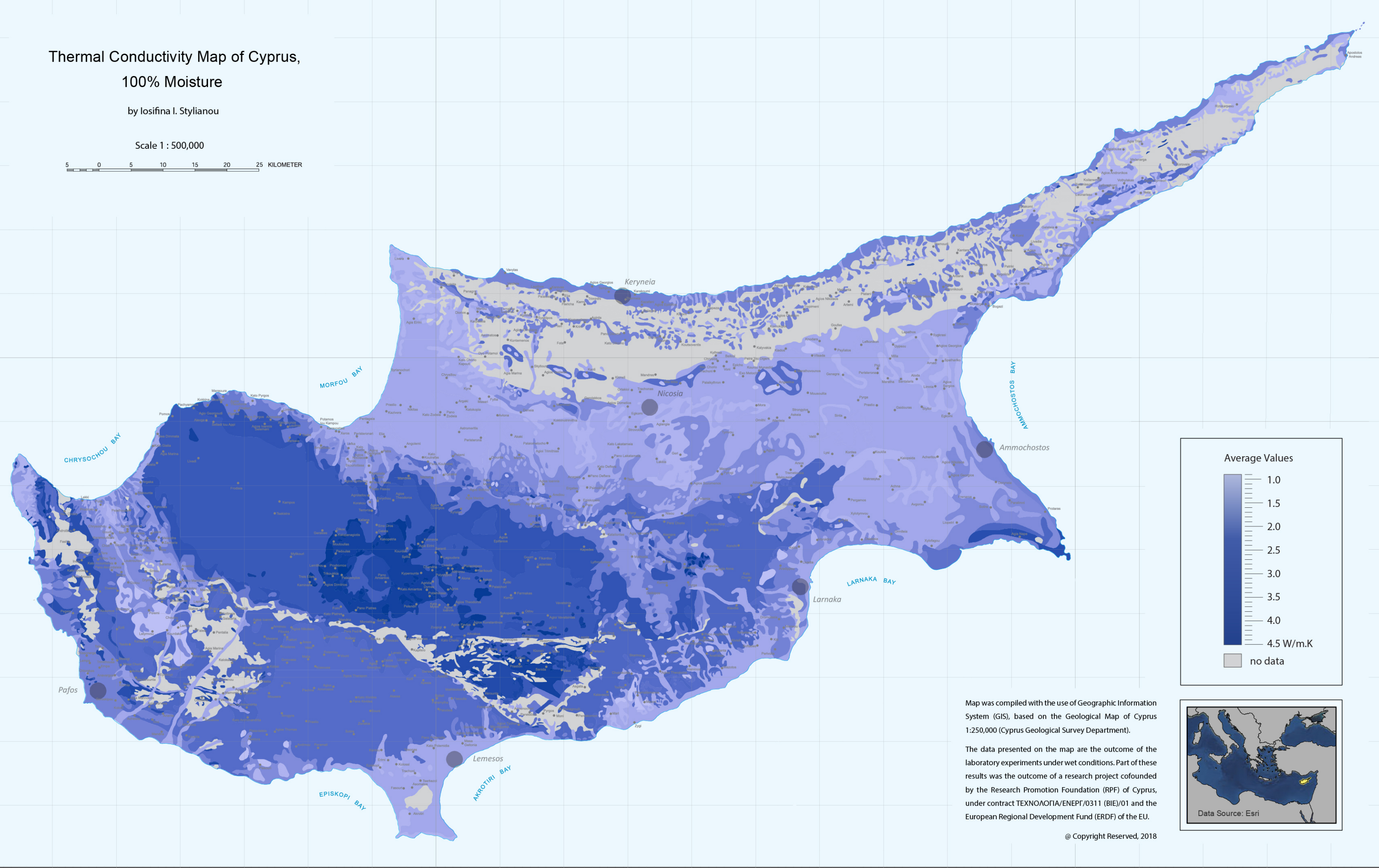
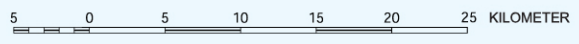


@ Copyright Reserved, 2018

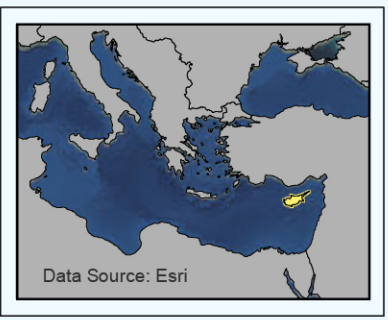
# Thermal Conductivity Map of Cyprus, 100% Moisture

by Iosifina I. Stylianou

Scale 1 : 500,000



Map was compiled with the use of Geographic Information System (GIS), based on the Geological Map of Cyprus 1:250,000 (Cyprus Geological Survey Department).  
The data presented on the map are the outcome of the laboratory experiments under wet conditions. Part of these results was the outcome of a research project cofounded by the Research Promotion Foundation (RPF) of Cyprus, under contract ΤΕΧΝΟΛΟΓΙΑ/ΕΝΕΡΓ/0311 (BIE)/01 and the European Regional Development Fund (ERDF) of the EU.



@ Copyright Reserved, 2018